Exploring the Role of Sulphur Compounds derived from Broccoli on Prostate Cancer Metabolism

Gemma Louise Beasy

Quadram Institute Bioscience

A thesis submitted for the degree of Doctor of Philosophy to the University of East Anglia

March 2023

Dedication

To those lost to cancer

“Nothing in life is to be feared, it is only to be understood. Now is the time to understand more, so that we may fear less”

– Marie Curie

Acknowledgements

I would like to thank my primary and secondary supervisors, Dr. Paul Kroon and Dr. Maria Traka, for all of their support and guidance during my PhD. I thank them for giving me the opportunity to develop as a researcher, and for sharing their knowledge.

I would like to thank all of the Kroon and Traka group members for their invaluable experience, support and time; without them it would have been impossible.

I would like to give a massive thank you to Dr. Perla Rey for the support and advice with the transcriptomic analysis.

I am thankful to Dr. Marianne Defernez for the support and guidance with the metabolomic analysis.

For teaching me with her incredible scientific knowledge of the LC MS/MS and her calmness, I am grateful to Dr. Shikha Saha.

For their unwavering support, I am grateful to Dr. Priscilla Day-Walsh, Dr. Jennifer Ahn-Jarvis and Dr. Antonietta Hayhoe.

I am grateful to the BigC Cancer Charity and Biotechnology and Biological Science Research Council for providing funding for the project.

Finally, I would like to thank my family especially my mum and dad, my friends, and my partner Toby; you challenge and inspire me to be the best version of myself. I would not be the person I am today without their endless emotional support, encouragement and love. I am forever grateful.

Keep smiling.

Abstract

While diets rich in cruciferous vegetables such as broccoli have been shown to reduce prostate cancer risk and progression potentially due to the presence of sulfur-containing compounds, the role of the sulfur-containing compound S-methyl-L-cysteine sulfoxide (SMCSO) in cancer metabolism is relatively unexplored. A recent human study observed consumption of broccoli soups reduced fasting plasma glucose in men on active surveillance, however this was independent of the glucosinolate content. Since others have shown that SMCSO beneficially affects glucose metabolism in rodent models, it seems it is likely that SMCSO in the broccoli soups caused the observed reduction in fasting plasma glucose in the human study.

The overall aim of the research presented in this thesis was to investigate the effects of SMCSO and its metabolite S-methyl methanethiosulfonate (MMTSO) on prostate cancer energy metabolism, using cultured DU145 prostate cancer cells. This was explored through the use of the Seahorse Bioanalyser, RNA-sequencing and untargeted/targeted metabolomic analyses that observed changes in real-time mitochondrial energetics, gene expression, and global metabolomic profile respectively.

MMTSO and to a lesser extent SMCSO reduced mitochondrial metabolism, increased fatty acid dependency, upregulated gene expression of pathways associated with immune function and apoptosis including interleukin-2 signal transducer and activator of transcription-5 (IL2-STAT5), increased metabolite changes relating to the tricarboxylic acid (TCA) cycle, and decreased concentration of key non-essential amino acids. In addition, since there have been no randomised controlled trials that have investigated the potential effects of SMCSO on prostate cancer progression, products that could be suitable for future cancer human trials were assessed and characterised.

Overall, the evidence presented in this thesis demonstrated SMCSO and MMTSO are capable of modulating mitochondrial, transcriptomic and metabolomic profiles of DU145 prostate cancer cells, and may contribute to the reduction observed in prostate cancer progression following consumption of a broccoli-rich diet.

Contents

Table of Contents

List of Figures

List of Tables

Chapter One.

General Introduction

Chapter One: General Introduction

1.1 The Prostate

The prostate is a walnut sized exocrine gland found in men that surrounds the urethra and is located at the base of the bladder. The prostate is divided into three zones: transitional (5-10 % normal prostate volume), central (25 % normal prostate volume), and peripheral (over 70 % normal prostate volume) (1). The transitional zone surrounds the urethra, the central zone surrounds the ejaculatory ducts, and the peripheral zone surrounds both the central and transitional zones. The transitional zone is the most common site for benign prostatic hyperplasia; while peripheral zone is the most common zone for prostate cancer and accounts for 70-80 % of all prostate cancers (2). The primary function of the prostate is to secrete an alkaline fluid, semen, that contains proteolytic enzymes that protect and nourish sperm (3). The alkaline nature of the prostatic fluid aids the neutralisation of the acidic environment of the vaginal tract which helps prolong the lifespan of the sperm (4). The prostate produces a protease called prostate-specific antigen (PSA) which makes the secreted fluid more liquefied by catalysing the hydrolysis of larger peptides found in the semen (5). The level of PSA in the blood serum is used as a marker to help prostate cancer diagnosis, however there are limited markers that can distinguish between the severity and grade of cancer (6).

1.2 Prostate Cancer: Incidence and Diagnosis

Prostate cancer has become the most common form of cancer in men, and the fifth leading cause of cancer-related death worldwide especially in elderly men > 65 years of age (7, 8). In the United Kingdom, prostate cancer accounts for 27 % of all new cancer cases with over 50,000 new cases every year (9). The highest rates of prostate cancer are seen across Western countries including Europe, America and New Zealand, with the lowest rates seen in South Central Asia (10). While there is variation in incidence geographically, this cannot be justified alone by the known risk factors of ethnicity, age and family history (7, 11), and could point to increased capacity for diagnosis as well as environmental factors such as exercise and dietary patterns (12-14). A few studies have reported an increased risk for prostate cancer with western dietary pattern of higher intake of red and processed meats, and high-fat foods compared to those on a diet with a higher intake of vegetables (15, 16). More recently, dietary patterns were evaluated on prostate cancer in the CAPLIFE study; they reported an unhealthy diet was associated with

higher chances of prostate cancer particularly for cases graded 1 or 2 and localised to the prostate (17). Thus, whilst there is currently limited evidence on how to prevent prostate cancer, dietary and lifestyle modifications could lead to reduced risk and development of prostate cancer.

Men aged between 45 and 75 and over are highly recommended for screening for prostate cancer through PSA measurement (18, 19). However, PSA levels can be raised for several reasons including presence of urinary tract infection or benign tissues, and ejaculation (20), leading to further unnecessary invasive procedures including magnetic resonance imaging (MRI). Whilst MRI scanning is worthwhile in identifying questionable nodules within the prostate, it misses 1 in 4 of clinically significant malignancies (21). After at least two elevated PSA values and MRI testing, a prostate tissue biopsy would give the prostate cancer diagnosis. Previously, biopsies were taken through transrectal ultrasound (TRUS) guided approach, although due to failure to biopsy all prostate zones, the transperineal prostate biopsy (TPB) is now used. A TPB is performed through insertion of sterile ultrasound probe into the rectum for needle guidance and visualisation of the prostate, alongside a template to aid placement of biopsy needle and sample all prostate zones with, depending on prostate size, approximately 25 samples taken for analysis (22). If prostate cancer is diagnosed, depending on the grade and stage of the cancer, the most appropriate treatment or management will be selected. For example, if a low-grade, low-stage localised prostate cancer is diagnosed, patients may be recommended active surveillance. Active surveillance monitors prostate cancer closely through repeat biopsies and PSA testing (23). Dietary interventions with individuals on active surveillance are becoming increasingly more attractive as a potential mechanism for reducing prostate cancer development and progression (24-26).

1.3 Metabolic Profiles and Tricarboxylic Acid (TCA) Metabolism Unique to Prostate Cancer

The prostate has a unique metabolic profile compared to other organs (27, 28), summarised in Table 1.1. It accumulates and secretes large concentrations of citrate through the truncated tricarboxylic (TCA) cycle to either be used in seminal fluid production and maintain male fertility (29) or for lipid synthesis through conversion back to acetyl-CoA (30). Prostate cells accumulate high levels of zinc that inhibits mitochondrial aconitase enzyme reducing citrate oxidation in the TCA cycle and facilitating citrate accumulation and secretion (31), summarised in Figure

1.1A. The citrate accumulation is very energy inefficient, consequently prostate cells implement other metabolic pathways to survive and pursue function including utilising fatty acids via beta oxidation, incorporating aspartate and glutamine in the TCA cycle, and they are highly glycolytic (32).

Table 1.1. Unique Metabolic Profile of Normal Prostate Cells and Prostate Cancer Cells

Pathway/Molecule	Normal Prostate Cells	Prostate Cancer Cells
Oxidative Phosphorylation	Inactive	Active
The TCA Cycle	Inactive	Active
Glycolysis	Highly Active	Reduced
Glucose	Used	Used
Citrate	Secreted	Used

In the malignant transformation to prostate cancer, the cells alter their central metabolism in order to meet the high energy demands of cancer proliferation, migration and invasion (33-35). During the transformation, there is reprogramming of citrate metabolism where concentrations of zinc decrease leading to activation of mitochondrial aconitase enzyme and flux through the TCA cycle to produce the ATP required for proliferation (36), summarised in Figure 1.1B. This leads to decreased zinc and citrate levels in cancer tissue compared to normal tissue (37), and increased aerobic glycolysis, glutaminolysis and oxidative phosphorylation (32). Prostate cancers also exhibit increased fatty acid oxidation and lipogenesis that alter central carbon metabolism to maintain the heightened energetic demands of the rapid tumour growth (38). Studies have reported that prostate cancer cells display a raised uptake of fatty acids (39) with prostate tumours having higher levels of TCA intermediates including malate, fumarate and succinate, compared to normal tissues (40).

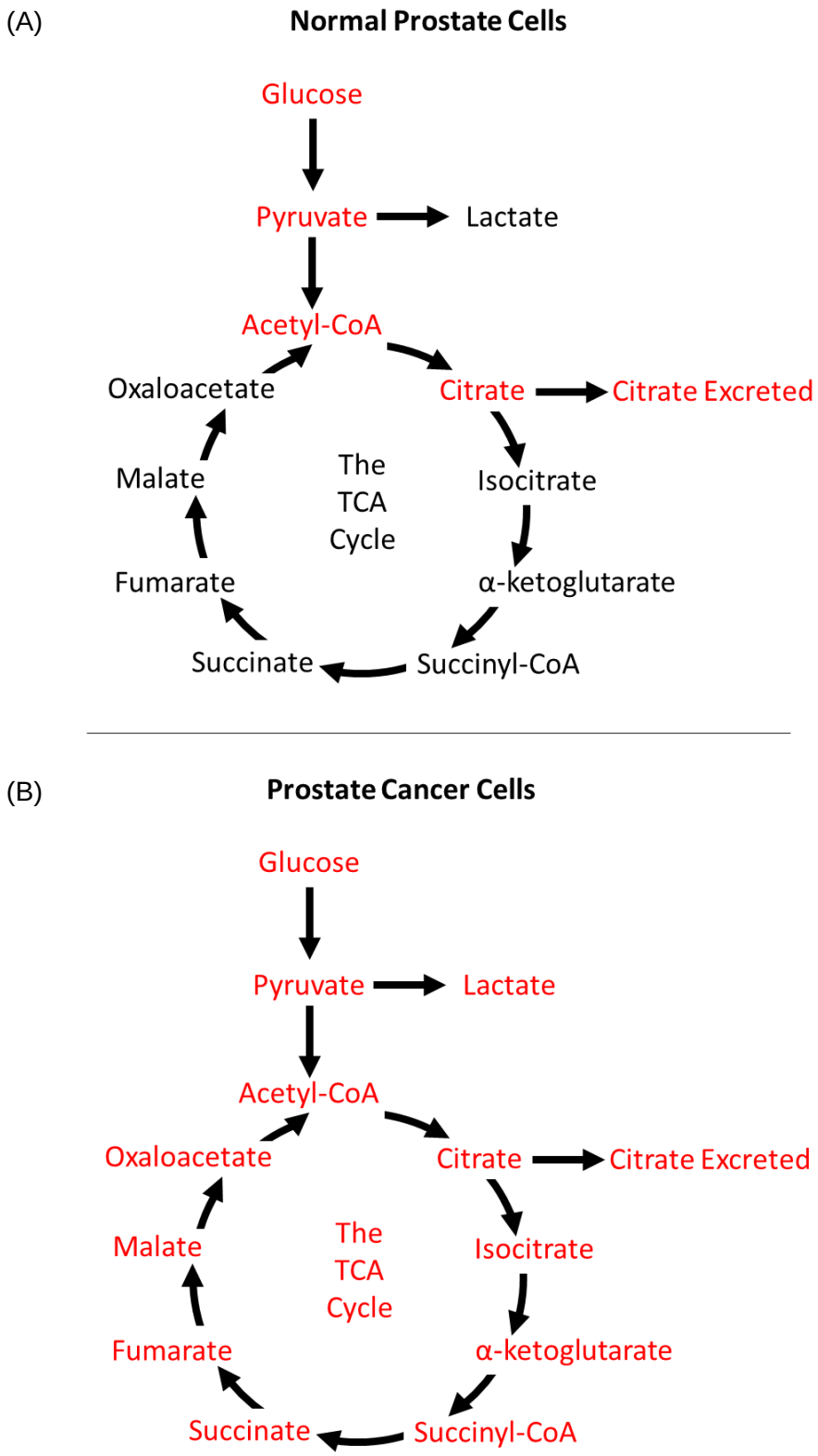

Figure 1.1. Snapshot of the metabolism transformation of normal prostate to prostate cancer. (A) Normal prostate cells demonstrate a truncated tricarboxylic acid (TCA) cycle that results in increased citrate that is excreted (highlighted by red text). (B) During transformation to prostate cancer, the intracellular concentrations of zinc decrease leading to inhibition of aconitase enzyme and increased flux through TCA cycle (highlighted by red text).

1.4 Immune Regulation and Prostate Cancer

Immune regulation is key for effective immune responses and removal of pathogens to protect the body from infections (41). The immune system plays a key role in cancers including prostate cancer, through multiple immune evasion mechanisms, and are able to actively suppress and evade antitumour immune responses (42). These include decreased inflammatory immune cell interaction, inhibition of antigen presentation, defective T cell responses and an enhanced immunosuppressive tumour microenvironment (43-45). Numerous cancers including prostate are capable of epithelial immune cell-like transition through expressing a range of cytokines, immune transcription factors, and immune checkpoint molecules that suppress anti-cancer immune activity (46, 47). The prostate tumour microenvironment contains several immune cells including tumour-associated macrophages, tumour-associated neutrophils, T regulatory cells and myeloid-derived suppressor cells. These cells, through direct interaction or indirect interaction through cytokine secretion (48, 49), have been reported to play a key role in the progression and development of the prostate cancer, although the mechanisms by which these cells modulate and promote tumorigenesis remain unclear. It is key to explore the immune regulation of prostate cancer as this could identify potential key genes, metabolites, and signalling pathways facilitating prostate cancer progression that could be targeted through therapeutic development (50, 51).

Tumour-associated macrophages and neutrophils have been reported to promote prostate tumourgenesis and modulate the tumour microenvironment (52). Tumour-associated macrophages can be divided into classical activation (M1 type) macrophages and alternative activation (M2 type) macrophages (53). In the tumour microenvironment, there is a higher abundance of M2 type macrophages than M1 type macrophages; M1 type macrophages stimulate inflammation whilst M2 type macrophages exert immune suppression and promote tumorigenesis (53, 54). One study reported that prostate cancer patients with a higher abundance of tumour-associated macrophages were correlated with poor prognosis with M2 type macrophages significantly linked with the progression and invasion of the cancer (55). An additional study reported CCN3, a key cytokine in regulating cell signalling from the extracellular matrix and linked with tumour-associated macrophages, is overexpressed in prostate cancer cell lines (56). A further study reported the upregulation of CCN3 induced VEGF production and regulated angiogenesis in

prostate cancer microenvironment (57). Tumour-associated neutrophils are immune cells with a controversial role in tumour progression. One study reported tumour-associated neutrophils had both tumour-promoting and anti-tumour effects through transforming growth factor-beta (TGF-β) where a tumour-promoting phenotype was associated with TGF-β induction and anti-tumour effects were caused by blockage of TGF-β (58). Tumour associated neutrophils have been reported to activate angiogenesis through inducing MMP-9 in aggressive prostate cancer (59). More recently, a study reported that neutrophils infiltrated prostate tumour in bone of metastatic prostate cancer patients and induced apoptosis of prostate cancer cells facilitated through inhibition of the signal transducer and activator of transcription 5 (STAT5), known to support prostate cancer progression (60).

There have been multiple studies highlighting the capacity of T regulatory cells with a CD4+ and FOXP3+ phenotype to modulate immune tolerance of the tumour microenvironment (61, 62). One study conducted on 22 patients with prostate cancer reported that the quantity of FOXP3+ T regulatory cells was negatively associated with overall survival rate of the prostate cancer participants (63). An additional study with 102 men diagnosed with localised prostate cancer reported a significant increase in prostate cancer risk in men expressing epithelial CD4+ T regulatory with a positive association of CD4+ FOXP3+ T regulatory cells in normal prostate tissue with Gleason scores and stage of tumour progression (64). T regulatory cells also facilitated immunosuppressive effects including CD80/CD86 interaction on antigen-presenting cells through the surface cytotoxic T lymphocyte-associated antigen 4 resulting in inhibition of the T cell function (65).

The presence of myeloid-derived suppressor cells including immature macrophages and dendritic cells in the tumour microenvironment has been reported to promote metastasis and proliferation of the cancer cells through immunosuppressive effects (66). In vitro studies conducted on myeloid-derived suppressor cells demonstrated increased production of interleukin-10 (IL-10) and decreased interleukin-6 (IL-6) and TNF-α where increased IL-6 directly regulated myeloid-derived suppressor cell IL-10, promoting metastasis (67). Myeloid-derived suppressor cells encouraged the development of prostate cancer through the CD40-CD40L interaction with mast cells leading to increased expression of ARG1, NOS2 and STAT3 in transgenic adenocarcinoma of the mouse prostate (TRAMP) mouse model (68). One study reported increased myeloid-derived suppressor cells

in the blood of prostate cancer patients were associated with poor prognosis (69). Myeloid-derived suppressor cells were reported to influence the phosphoinositide 3-kinase (PI3K)/PTEN/AKT signalling pathway in prostate cancer mouse models (70), although the importance of myeloid-derived suppressor cells and PTEN loss in prostate cancer patients remains unknown.

Cellular components of the innate immune response including cytokines TGF-β, IL-6 and IL-10 play a key role in cancer progression, angiogenesis and immunosuppression (49). Interestingly, IL-6 mediates activation of several signalling pathways that have been shown to be involved in increasing prostate cancer cell proliferation including the PI3K/AKT pathway, the Janus kinase (JAK)/STAT pathway, and the extracellular signal-regulated kinase 1 and 2 (ERK1/2)-mitogen activated protein kinase (MAPK) pathway (49). IL-6 has been reported to increase prostate cancer aggressiveness by mediating epithelial-to-mesenchymal transition, and through interaction of IL-6 receptor and activation of STAT3 modulating prostate cancer growth (71, 72), indicating a key role of IL-6 in prostate cancer progression.

1.5 Mitochondria, Reactive Oxygen Species (ROS) and Prostate Cancer

Reactive oxygen species (ROS) are highly reactive, oxygen-containing molecules including hydrogen peroxide and free radicals, that promote pathogenesis of several diseases including cancer (73). Studies have demonstrated that elevated levels of ROS in prostate cancer cells can cause oxidative damage to DNA, proteins and lipids, mitochondrial dysfunction, increased glucose metabolism and activation of NADPH oxidases, all of which contribute to prostate cancer progression (74-76). Mitochondria are key players in tumorigenesis being involved in energetic capabilities of cancer cells supporting not only cell proliferation but the malignant transformation of prostate cancer (77). Composed of complex I, II, III, IV and ATP synthase, the mitochondrial electron transport chain stimulates oxidative phosphorylation to produce ATP with ROS as a damaging by-product (78). One study reported elevated levels of mutations in mitochondrial complex I-encoding genes were associated with 70 % reduction in NADH-pathway capacity and increased ROS levels in the high-grade prostate cancer tissue samples (79). Interestingly, recent studies have reported glutamate oxaloacetate transaminase 1 (GOT 1) was upregulated in prostate cancer tissue samples compared to normal tissue samples (80, 81). GOT 1 converts aspartate to oxaloacetate, increasing production of NADPH inhibiting ROS, regulating redox balance and promoting

prostate cancer progression (82). Thus, ROS-mediated pathways in prostate cancer could be targets for developing cancer prevention therapies.

1.6 Dietary Patterns and Prostate Cancer

Dietary patterns play an important role in prostate cancer risk and development with a diet high in dairy products, animal fat and red meat associated with increased risk and a diet high in fish, legumes, fruit and vegetables linked with reduced risk (83, 84). Epidemiological evidence of bioactive compounds found in fruits and vegetables have shown a negative association with prostate cancer progression (85, 86). These include sulfur-containing compounds from cruciferous and alliaceous vegetables, polyphenols from berries, pomegranate, dark chocolate, and red wine, and carotenoids from tomatoes and carrots (87). These bioactive compounds have different visual and taste properties for example, the sulfur-containing compounds give cruciferous vegetables the pungent smell and bitter taste which can be released during food preparation and chewing (88) whereas the polyphenols give the foods red, purple and blue colour and some are astringent (89). A report of a dietary intervention in which patients with localised prostate cancer consumed either an oral capsule of a mixture of pomegranate, green tea, broccoli and turmeric or an identical placebo for 6 months provided evidence of a significant reduction in median PSA rise in the treated group (14.7 %) compared to the placebo group (78.5 %) (90), indicating that food bioactives in combination have the potential to reduce prostate cancer risk. However, to what extent each compound contributed to this reduced risk would need to be evaluated with each bioactive separately.

1.7 Glucosinolates and Isothiocyanates from Cruciferous Vegetables

The chemopreventive effects of cruciferous vegetables such as broccoli, sprouts and cabbage, have been associated with the presence of a particular group of sulfur-containing compounds, the glucosinolates (91, 92). The most abundant glucosinolate in broccoli is glucoraphanin that predominately accumulates in the florets and is hydrolysed to the isothiocyanate sulforaphane (93). More than 130 types of glucosinolate structures had been determined with only a small percentage present in the human diet (94). These can be divided into three groups dependent on the amino acid precursor: aliphatic, such as glucoraphanin and sinigrin, aromatic, such as glucotropaeolin, or indole, such as glucobrassicin (95). In the European Prospective Investigation into Cancer and Nutrition (EPIC) human

study, dietary intake of 2121 participants was assessed. They reported the mean total glucosinolate intake estimated at 14.2 ± 1.1 mg/day for men and 14.8 ± 1.3 mg/day for women with broccoli, Brussel sprouts and cauliflower as the main contributors to total glucosinolate intake (96).

With the health benefits of diets rich in glucosinolates such as glucoraphanin being highlighted repeatedly in epidemiological studies and with supporting data from in vitro studies, high-glucoraphanin F_1 broccoli hybrids from the wild plant *Brassica villosa* were developed (93). After 11 back crosses, the hybrids contained 2.5 to 3 times more glucoraphanin than standard broccoli, and this has been commercialised as Beneforté® broccoli (97). More recently, a very high glucoraphanin containing F_1 broccoli hybrid has been developed with fewer integrations, and this is named 1086 (98). A series of randomised control trials have utilised these high glucoraphanin products in the form of broccoli soups to investigate the effect of glucosinolates/isothiocyanates on health and disease (24, 25, 99).

Largely, glucosinolates themselves do not exhibit biological effects. However, they are enzymatically hydrolysed either through (i) the breaking of cells which can occur due to chewing or via processing such as chopping or blending which releases the plant myrosinase (a thioglucosidase enzyme) to hydrolyse the glucosinolates, or (ii) by microbial thioglucosidases present in the gut microbiota. Hydrolysis of glucosinolates by thioglucosidases removes the glucose moiety to yield an unstable intermediate which rapidly breaks down to give several derivates including indoles, thiocyanates and isothiocyanates. The most studied isothiocyanate is sulforaphane which is derived from glucoraphanin. The derivates can be absorbed and reach the peripheral circulation (100). The processes involved in the conversion of glucoraphanin to sulforaphane are summarised in Figure 1.2. In plants, myrosinase enzymes breakdown glucosinolates and the breakdown products are thought to be produced as a defence mechanism against insects and pathogens (95). In humans, once ingested the glucosinolates are somewhat absorbed through the gastrointestinal mucosa with a large proportion metabolised in the gut lumen (101). In the proximal region of the gastrointestinal tract, specific gut microbes hydrolyse the glucosinolates and cause the release of the various breakdown products including isothiocyanates. There is an extensive literature showing that isothiocyanates modulate various pathways and enzymes including xenobiotic-metabolising and phase II detoxification enzymes and thereby

give protection from DNA damage (102). Interestingly, the phase II enzyme GSTP1, a member of the glutathione-S-transferase (GST) family is silenced by CpG island DNA hypermethylation in 90-95 % of prostate cancers (103).

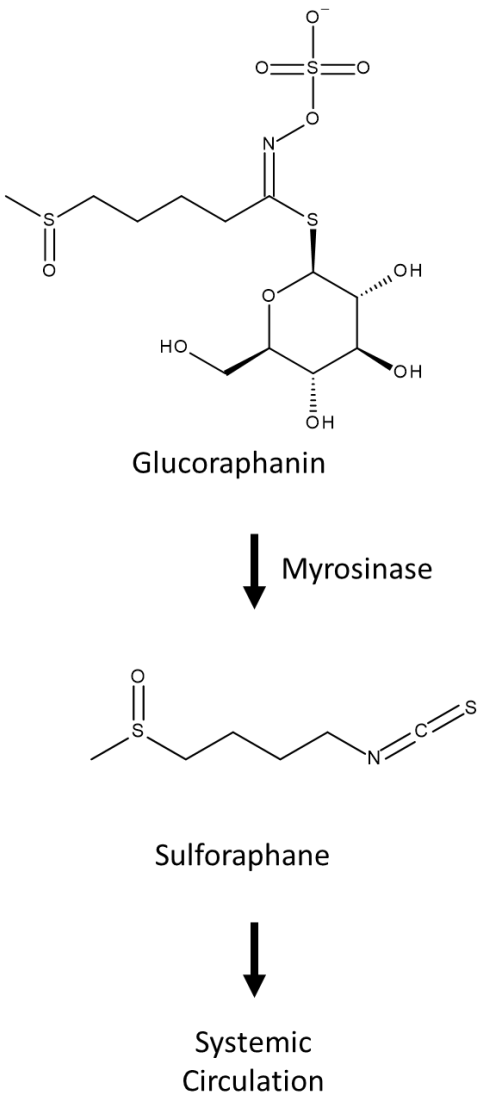

Figure 1.2. Metabolism of Glucoraphanin. The glucosinolate, glucoraphanin, is hydrolysed by myrosinase enzyme to the active compound sulforaphane that is released as free sulforaphane into systemic circulation. Adapted from Livingstone et al., 2019.

Isothiocyanates, including phenethyl isothiocyanate (PEITC) found in water cress, benzyl isothiocyanate (BITC) found in cabbage, and sulforaphane ([1-isothioyanato-4-(methyl-sulfinyl) butane]) found in broccoli, have been reported to exert cancer protective activities including causing growth arrest and cell death (104-107). Brassica vegetables also contain epithiospecifier proteins that can influence in hydrolysis of glucosinolates and, depending on the conditions, can convert intermediate sulfur compounds into nitriles such as sulforaphane-nitrile.

Studies have indicated nitriles to be less potent at inducing phase II detoxification enzymes than isothiocyanates (108, 109) Thus, optimising the hydrolysis of glucoraphanin such that production of the isothiocyanate sulforaphane is favoured over the other breakdown products is expected to increase the potential chemoprotective effects of broccoli.

A key transcription factor important in regulating antioxidant and phase II detoxification enzymes and modulates cancer progression is nuclear factor-erythroid 2-related factor-2, Nrf2 (110). Nrf2, a basic leucine zipper (bZIP) protein, regulates numerous cell survival responses and repress oncogenic signalling pathways including suppression of nuclear factor-kappaB (NF-$_{K}$B) (111). PEITC, BITC and sulforaphane act as potent regulators of Nrf2 and NF-$_{K}$B. When exposed to these sulfur compounds, the Nrf2-Kelch-like ECH-associated protein 1 (Keap1) loses its ability to target Nrf2 for degradation, resulting in accumulation and nuclear translocation of Nrf2, increasing antioxidant and anti-inflammatory activity (112). PEITC was shown to suppress the expression of c-Myc in the LNCaP and 22Rv1 human prostate cancer cell lines, with 10 mg PEITC exposure 4 times/day for 1-week in TRAMP mice associated with a significant decrease in plasma lactate and pyruvate levels which was linked with suppression of glycolysis (104, 113). BITC exposure to CRW-22Rv1 and PC3 human prostate cancer cell lines induced ROS generation, and suppressed growth by affecting DNA fragmentation, causing loss of mitochondrial membrane potential and activating caspase 3/7 (114). TRAMP mice fed broccoli sprouts rich in sulforaphane was associated with decreased histone deacetylase 3 protein expression in the prostate and reduced prostate cancer incidence and progression to invasive cancer (115).

1.8 S-methyl-L-Cysteine Sulfoxide (SMCSO) and its Metabolites from Cruciferous and Alliaceous Vegetables

Much of the current evidence regarding the health benefits for cruciferous and alliaceous vegetable consumption have been associated with the hydrolysis product of glucoraphanin, sulforaphane. However, the secondary metabolite S-methyl-L-cysteine sulphoxide (SMCSO; methiin) present in cruciferous and alliaceous vegetables, may also give health benefits and contribute to the protective effects of a broccoli-rich diet. Interestingly, SMCSO is often found in greater concentrations (1 – 4 % dry weight) in comparison to glucosinolates (typically 0.1 – 0.6 % dry weight) in Brassica vegetables (116). SMCSO is metabolised by microbial or plant cysteine conjugate β lyases to produce a range

of biologically active compounds including S-methyl methanethiosulphinate (MMTSI) and S-methyl methanethiolsulphonate (MMTSO) (117), and potentially further undetermined compounds; summarised in Figure 1.3. The full mechanism for SMCSO metabolism in humans remains unclear, although gut microbiota could play a part as the conversion of SMCSO to the reduced analogue, S-methyl cysteine, was reported to be via bacterial-mediated reduction reactions (118, 119).

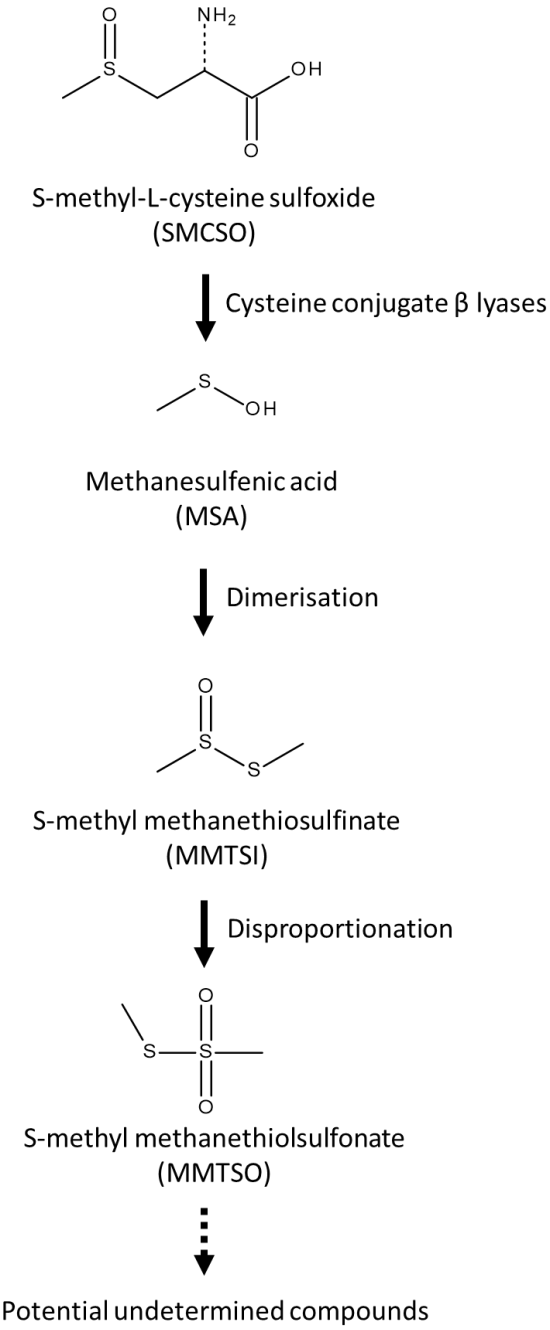

Figure 1.3. Metabolism of S-methyl-L-cysteine sulfoxide (SMCSO). Initially, SMCSO is broken down by cysteine conjugate β lyases to secondary bioactive compounds through dimerisation and disproportionation reactions to generate S-methyl methanethiolsulfonate (MMTSO) and potential undetermined compounds. Adapted from Livingstone et al., 2019.

There are only a few reports from studies of the absorption, metabolism and biological activities of SMCSO and its metabolites, MMTSI and MMTSO with only a few studies available that are concerned with effects on cancer progression. Thiosulphinates, such as S-methyl methanethiosulfinate (MMTSI), have been reported to inhibit the proliferation of human prostate and colon cancer cell lines through both caspase-dependent and caspase independent apoptosis pathways (120-122). An additional study demonstrated that exposure of HepG2 human liver cancer cells to MMTSO and MMTSI, more so than SMCSO, reduced mitochondrial potential, particularly at the high glucose environment. The study also demonstrated upregulated pathways relating to immune responses including IL-6/JAK/STAT3 and TGF-β signalling, and downregulated common dysregulated cancer-related pathways including angiogenesis, KRAS signalling and hedgehog signalling (123), suggesting bioactivity of the sulfur compounds in cancer cells. Further to this, another study reported SMCSO exposure for 24-hour to prostate cancer cell lines demonstrated no changes to mitochondrial or glycolytic function, with no significant change in ROS or redox status of PTEN in normal prostate epithelial cells (124). To note, the tissue-specific metabolism of SMCSO metabolites, MMTSI or MMTSO, were not investigated, thus further studies are required to elucidate the role of SMCSO metabolites in prostate cancer development. Of the in vivo evidence from animal studies, SMCSO and some of the metabolites when fed to rats, were reported to inhibit chemically induced tumourgenesis (125-128), potentially due to the presence of thio-sulphinate and thiol functional groups in the breakdown products of SMCSO (106). In addition to cancer, SMCSO consumption by diabetic rats led to lipid-controlling and blood glucose-controlling effects (117, 129-131), suggesting SMCSO may have other health benefits related to glucose modulation and metabolism. At present, there are no established routes by which humans can synthesise SMCSO, making the origin of SMCSO likely from diet (25). Thus, the use of dietary intervention to explore the role of SMCSO in human health and disease seems the most plausible route.

1.9 Sulfur-Containing Compounds and Glucose Metabolism

Glucose plays a key role in cancer development. It has been widely reported that cancer has an altered glucose metabolism phenotype relying on both glucose and glutamine to provide additional energy which supports the tumour growth; this is known as the Warburg effect (132). Epidemiological studies have indicated that

high blood glucose (hyperglycaemia) and high insulin levels increase the risk, prevalence and growth of cancers including pancreatic, bladder and breast by promoting proliferation and migration of the tumours (133, 134). Glucose transporters (GLUTs), that facilitate glucose uptake, are usually over-expressed in cancer cells; GLUT1 in prostate cancer is found in the most aggressive tumours and prevents cell death of cancer cells (135). A study found under glucose deprivation, prostate cancer cells overexpressing GLUT1 sustained mitochondrial activity, significantly increased production of reduced glutathione and induced necrotic cell death (135) suggesting a role of glucose metabolism in prostate cancer progression. In addition, a cell based study indicated that insulin stimulated prostate cancer progression, migration and invasion through upregulation of Forkhead transcription factor 2, which is commonly involved in angiogenesis (136), implicating a role of insulin metabolism in prostate cancer growth. Even though it has been observed that diabetic men have a lower risk of prostate cancer compared to non-diabetic men (137), the role of hyperglycaemia remains uncertain in prostate cancer.

There are limited reports of the effects of sulfur-containing compounds on glucose metabolism and regulation. One study reported that 2.5 mg/kg sulforaphane intraperitoneally three times per week over 15 weeks prevented glucose intolerance development in high-diet and high-fructose diet rats, with fasting blood glucose significantly reduced in rats given sulforaphane compared to not-treated rats (138). A study found administration of 10 mg/kg sulforaphane to diabetic mice decreased fasting blood glucose and serum lipopolysaccharide levels, and increased liver antioxidant capacities (139), suggesting a protective anti-diabetic effect of sulforaphane. A further study investigated the effects of non-toxic sulfur and methylsulfonylmethane on human monocytes and reported the sulfur-containing compounds prevented high glucose induced inflammation by regulating NF-$_K$B through reactive oxygen species and protein kinase C-dependent pathways (140). A few animal studies have indicated that SMCSO consumption by diabetic rats led to lipid-controlling and blood glucose-controlling effects (129-131). A recent animal study reported that daily gavage of 200 mg/kg SMCSO for 30 days reduced blood glucose, triglycerides and very-low-density-lipoprotein levels. This was associated with improved liver glycogen, ameliorated damage to the pancreatic islets and increased activity of IL-10 cytokine which was linked with antioxidant activity (141). Another animal study with 26 rats that were divided into three groups (control, diabetic and diabetic + 200 mg/kg SMCSO) for 30 days, processed and

assessed duodenum samples using histopathological and immunohistochemical tests. SMCSO administration decreased hyperglycaemia, prevented the structural changes of the duodenum caused by diabetes, and decreased NF-$_K$B expression (142). These studies suggest that consumption of SMCSO could modulate glucose metabolism, mitigate oxidative stress and encourage immunomodulation.

1.10 Sulfur-Containing Compounds and Prostate Cancer Metabolism: Evidence from Human Studies

Sulfur-containing compounds are a group of secondary metabolites found in cruciferous and alliaceous vegetables such as broccoli and garlic. Epidemiological studies have highlighted these compounds for their health benefits and reduced risk of prostate cancer (26, 143). However, regardless of this evidence there have been limited human intervention studies which demonstrate the effect of diets rich sulfur-metabolites and prevention of prostate cancer development. One meta-analysis was conducted to assess the link between intake of cruciferous vegetable and prostate cancer risk. In the systematic literature search, that included 6 population based case control studies and 7 cohort studies, there was a significant decrease in prostate cancer risk and cruciferous vegetables consumption (144). Although due to the limited study number, further studies are needed. On the other hand, a further study recruited 20 men with recurrent prostate cancer consuming 200 µmoles/day of sulforaphane-rich extracts for a maximum of 20-weeks. Of the 20 participants, only one had a significant reduction in PSA level with seven participants observing smaller non-significant reductions (145), thus further studies delineating the role of sulforaphane as a preventative compound in tissues are warranted.

One double-blind randomised control study recruited 98 men scheduled for prostate biopsy and were assigned to either 200 µmoles/day broccoli sprout extract or matched placebo for 4 to 6 weeks prior to their biopsy. From the RNA-sequencing analysis of prostate tissue, they reported 40 differentially expressed genes associated with broccoli sprout extract including downregulation of genes previously reported in prostate cancer development (146). The study also reported increased accumulation of sulforaphane and metabolites in both plasma and urine in the broccoli sprout extract supplementation compared to matched placebo (146).

One pharmacokinetics study, the Bioavailability of Sulforaphane from Broccoli Soups (BOBS) study explored the appearance of sulfur-containing compounds in blood and urine samples from a three-phase, double blinded, randomised

crossover trial involving 10 healthy participants. The participants consumed 300 g broccoli soups with different glucoraphanin enrichment: low: 84 ± 2.8 μmoles glucoraphanin/300 g soup; intermediate: 280 ± 8.8 μmoles glucoraphanin/300 g soup; high: 452 ± 10.6 μmoles glucoraphanin/300 g soup . The study reported a threefold increase in the intermediate level soup and fivefold increase in the high level soup of sulforaphane in plasma, with 2 to 15 % excretion yield (mole percent from glucoraphanin) (99). In the plasma samples, the sulforaphane and metabolite concentrations peaked between 6 to 8 hours which was in contrast to SMCSO that peaked much earlier, between 1.5 to 2 hours (99). The later peak absorption of sulforaphane is consistent with a requirement for gut microbiota-dependent (colonic) hydrolysis of glucoraphanin to generate sulforaphane. Similar broccoli soups to those used in the BOBS pharmacokinetics study were used in the Effect of Sulforaphane on Prostate Cancer Prevention (ESCAPE) study. This study utilised a three-arm parallel design to investigate the effects of once-a-week consumption of one of the three broccoli soups on health parameters in 49 men on active surveillance for prostate cancer. The study reported, in the control arm, several hundred changes in gene expression in the prostate tissue with increased expression of potentially oncogenic-related pathways such as epithelial-mesenchymal transition and inflammatory processes (24). These gene expression changes were mitigated in a glucoraphanin dose-dependent manner with those on the high glucoraphanin broccoli soup indicating the largest suppression (24). This study contributes to the mechanistic understanding of how cruciferous vegetable consumption could reduce risk and progression of prostate cancer.

Whilst there has been in vitro and in vivo studies on the effect of SMCSO and its breakdown products on human cell lines and in rats (117), there is limited human interventional studies that have explored the role of SMCSO in humans. One study evaluated the effect of SMCSO and S-carboxymethyl-L-cysteine sulphoxide (SCMCSO) in four healthy males for fourteen days through administration of radiolabelled SMCSO and radiolabelled SCMCSO. Following the administration, the radiolabelled compounds had completely degraded to sulphate, with the urine being the major path for excretion (96 % in 14 days) (147). A further study utilised a four-week parallel single blinded design with a three-times-a-week high-dose glucoraphanin broccoli soup to men scheduled for a TPB. They reported accumulation of SMCSO within the prostate tissue as well as sulphate and ADP, and also detected SMCSO within urine samples linked with that in the prostate tissue (25). Although SMCSO role in humans remains relatively unknown, this

study suggests a potential mechanism for SMCSO in cancer cell metabolism. Considering the abundance and distribution of SMCSO in a wide range of vegetables, the role of the sulfur metabolites in prostate cancer progression still remains unknown, thus further studies are warranted.

1.11 Sulfur-Containing Compounds, Glucose and Prostate Cancer Metabolism: Evidence from Human Studies

Men with diabetes have a lower overall risk of prostate cancer (137), however the role of high blood glucose is unclear. Very few studies have focused on the effect of high blood glucose in the context of prostate cancer and these provide conflicting evidence; some report a shielding effect of high blood glucose and prostate cancer whilst others suggest an increased risk of advanced prostate cancer in men with high blood glucose (148). The association between diabetes and prostate cancer risk was investigated in men from the Health Professionals Follow-Up Study which ran between 1986 and 2004. During that time, 4,511 new prostate cancer cases were diagnosed with prostate cancer risk lowered for men diagnosed for 1-6 years and the risk further lowered for men who had been diagnosed for 6-15 years, suggesting that diabetes is linked with reduced prostate cancer risk (149). On the other hand, of the 1,663 men diagnosed with prostate cancer on the Finnish Randomized Study of Screening for Prostate Cancer (FinRSPC), 808 had normal blood glucose levels, 454 were in the pre-diabetes range and 401 were in the diabetes range. Those who had blood glucose in the diabetes range, but not the pre-diabetes range, had an increased risk of prostate cancer (150). To add, from the long term use of antidiabetic drugs this risk association is removed, suggesting that diabetic fasting blood glucose could be a prostate cancer risk factor. Thus, further human studies are warranted to further decipher the link further between impaired glucose metabolism and cancer progression through potential dietary interventions, to prevent the development of such conditions.

Cruciferous vegetable consumption has been negatively associated with the development of metabolic diseases such as diabetes (138, 151, 152). One study investigated the pharmacogenomic effects of Prostaphane that contains sulforaphane on prostate tumour cells, PNT1A, 22RV1 and DU145. They reported a dose effects for 2 transcripts for 22RV1, 9 transcripts for PNT1A and 6 for DU145, highlighting an oncogene that expression was reduced in PNT1A and 22RV1 after exposure to Prostaphane (153). A few studies have explored the role on broccoli consumption and glucose metabolism. One study investigated the effects of

broccoli sprout powder rich in sulforaphane in 81 type-2 diabetic patients with random allocation to either 10 g/day of broccoli sprout powder, 5 g/day of broccoli sprout powder or matched placebo for 4 weeks. The study reported that 10 g/day broccoli sprout powder led to a reduction in fasting glucose (1.9 mmol/l), and a significant reduction in serum insulin concentration (0.85 mU/l) (154). Another study evaluated the effects of broccoli sprout powder in an obese type 2 diabetic cohort and demonstrated that 5 g/day broccoli sprout extract containing 5410 ppm of sulforaphane, reduced fasting blood glucose by 0.7 mM and reduced glycated haemoglobin (HbA1c) by 4 mmol/mol (138). Interestingly, the ESCAPE study also observed that all 3 variants of broccoli soup reduced fasting plasma glucose compared with baseline: low-glucoraphanin; 0.51 mmol/l, intermediate-glucoraphanin; 0.25 mmol/l and high-glucoraphanin: 0.67 mmol/l (24). It could be suggested that as all 3 broccoli soups decreased glucose levels, other phytochemicals present in the broccoli such as SMCSO could be responsible for this decrease in fasting plasma glucose in prostate cancer cohort. As the study did not have a control soup that contained no glucoraphanin, a no-glucoraphanin soup should be included as a key control arm in future human interventions.

The majority of clinical trials investigating the link between bioactive compounds and prostate cancer have shown the beneficial effects of a diet rich in cruciferous and alliaceous vegetables and reduced risk of prostate cancer, although some have indicated no effect. The inconsistency in the results could possibly be due to study type or sample size assessed. This warrants additional human intervention trials to delineate the role of the dietary compounds further with larger cohorts and cross-over studies.

1.12 Exposure of Prostate Tissue to Sulfur-Containing Compounds

From the epidemiological evidence, it is evident that there is an association between consumption of sulfur-containing compounds and reduced risk of prostate cancer. However, it remains unclear how and to what extent the prostate tissue is exposed to sulfur-containing compounds. Within the existing literature, a few mechanisms have been proposed including exposure of dietary compounds to the prostate tissue through urinary reflux, through the systemic circulation or as a consequence of microbial influence.

The concept of urinary reflux involves the passage of urine from the urethra into the prostatic ducts (155). Urinary reflux to the prostate tissue was first reported in

1982 with a human study involving 10 men with prostatitis receiving an intra-vesicle instillation of carbon particles. Of the prostate tissue samples removed through transurethral resection of the prostate, 70 % contained the carbon particles (155), suggesting urinary reflux as a route of infection or inflammatory process in prostatitis. Consistent with this, another study reported higher concentrations of urate and creatinine, common waste products from urine, in prostate secretions from men with prostatitis (156). One study involving the assessment of the prostate glands from 27 men who had previously received bladder cancer treatment with intravesical Bacillus Calmette-Guerin, showed that the peripheral zone of the prostate is the most likely area to be exposed to urine due to the ductal anatomy (2). However, another study investigated the incidence of granulomatous prostatitis in prostate tissue removed from 472 patients who endured transurethral resection of the prostate after bladder cancer treatment with intravesical Bacillus Calmette-Guerin and had benign prostate hyperplasia. The study found granuloma formation occurred throughout the prostate gland (157), indicating urinary reflux may not be zone specific but instead results in exposure of the whole prostate. Although much of the evidence has been from studies of urinary reflux in patients with disease including prostatitis, it seems likely that exposure of the prostate tissue to plant-derived bioactive compounds including sulfur-containing compounds found in urine also occurs in healthy people. As several studies have reported the presence of sulfur-containing compounds in urine samples (24-26, 99), it seems likely that the sulfur-containing compounds are exposed to the prostate through a urinary reflux mechanism and as a consequence these compounds could contribute to reductions in prostate cancer progression.

The exposure of dietary bioactive compounds to the prostate could also occur through systemic circulation. A pharmacokinetics study following consumption of broccoli soups reported the appearance of the dietary sulfur-containing compounds, sulforaphane and SMCSO, in plasma of healthy individuals (99). A more recent human study (Norfolk ADaPt) recruited men scheduled for a trans-perineal prostate biopsy and utilised a randomised, double-blinded, 2 × 2-factorial design to test the effects of broccoli and garlic dietary supplements in a four-week intervention study. Of the 39 men who completed, they reported sulforaphane and alliin were found in both the peripheral and transitional zone of the prostate tissue samples (26). With the exposure being higher in specific zones and the complex arterial network via the prostatic arteries (158), this makes systemic circulation a plausible mechanism of exposure of dietary sulfur-containing compounds to the

prostate. Although due to further metabolism such as sulphation, glucuronidation and methylation (99, 159), this could reduce the biological activity of the compounds leading to lower concentration of delivery through systemic circulation to the prostate.

There has been recent evidence of specific microbes being associated with the prostate tissue and urinary tract as well as prostate cancer pathogenesis (160, 161). A recent study reported the presence of five specific anaerobic bacteria in the urine of patients with higher prostate cancer risk (162). It has also been reported that *Escherichia* isolated from faecal samples of 5 participants were found to metabolise glucosinolates and SMCSO to their reduced compounds (119). These studies suggest a link between specific bacteria present in the prostate, prostate cancer risk and progression and microbial breakdown of sulfur metabolites, suggesting a role of the microbiome in delivery of dietary compounds to the prostate.

1.13 Thesis Hypotheses and Objectives

This thesis reports the results of studies of the effects of the sulfur-containing compounds, SMCSO and its metabolite MMTSO, on prostate cancer metabolism, which was investigated in vitro using cultured DU145 prostate cancer cells.

The two hypotheses of this thesis were:

1. The sulfur-containing compounds SMCSO and/or MMTSO reduce prostate cancer risk/progression by beneficially altering energy metabolism in prostate cancer cells.
2. The sulfur-containing compounds SMCSO and/or MMTSO affect the energy metabolism phenotype of prostate cancer cells by changing the expression of genes and metabolite profiles involved in energy metabolism and metabolic pathways.

These hypothesis were addressed by:

- Investigating the effects of treatments with SMCSO and MMTSO on real-time mitochondrial energetics of DU145 prostate cancer cells, using the Seahorse Bioanalyser (Chapter 2).
- Determining the effects of treatments with SMCSO and MMTSO on the gene expression profiles of DU145 prostate cancer cells, using the next generation sequencing technology, RNA-sequencing (Chapter 3).
- Evaluating the effects of treatments with SMCSO and MMTSO on the global metabolomic profile of DU145 prostate cancer cells, using untargeted and targeted metabolomic analyses (Chapter 4).

In addition, since there have been no randomised controlled trials that have specifically investigated the potential effects of SMCSO consumption on prostate cancer progression, and a key limitation has been the lack of a suitable SMCSO-rich food product and an appropriate SMCSO-free placebo food product, a further objective of the research was to develop and characterise products that could be suitable for future cancer human trials (Chapter 5).

Chapter Two.

In vitro analysis of SMCSO and MMTSO on prostate mitochondrial energetics and metabolism

Chapter Two: In vitro analysis of SMCSO and MMTSO on prostate mitochondrial energetics and metabolism

2.1 Introduction

Cruciferous vegetables such as broccoli accumulate sulfur-containing compounds. These compounds are responsible for the characteristic pungent taste of the vegetables and have been associated with many beneficial effects including anti-diabetic and chemopreventative. Whilst much of the beneficial effects of these sulfur-containing compounds have been linked with the hydrolytic product of glucoraphanin, sulforaphane (SFN), S-methyl cysteine sulfoxide (SMCSO) and potentially its metabolite, S-methyl methanethiolsulphonate (MMTSO) have been poorly studied. Considering the abundance and distribution of SMCSO in a wide range of cruciferous and alliaceous vegetables (117), the role of SMCSO and MMTSO in prostate cancer energy metabolism remains unknown.

The potential chemopreventative role of SMCSO and MMTSO has been virtually overlooked with only a few in vitro studies investigating their effect on energy metabolism in cancer cells. One cell based study reported SMCSO treatment to prostate cancer cell lines demonstrated no changes to mitochondrial or glycolytic function, with no significant change in ROS or redox status of PTEN in normal prostate epithelial cells (124). Another cell based study demonstrated that exposure of MMTSO and MMTSI to human liver cancer cells (HepG2) decreased mitochondrial potential, upregulated pathways relating to immune response including IL-6/JAK/STAT3 signalling, and downregulation commonly dysregulated cancer-related pathways including angiogenesis and KRAS signalling (123).

Whilst there is limited evidence from animal studies have reported the anti-diabetic and lipid-controlling effect of SMCSO in diabetic rats (129-131, 142), only a few mouse studies have explored the effect of SMCSO and MMTSO in vivo on cancer progression and metabolism. Doses of 0.5 mmol/kg SMCSO and 0.05 mmol/kg MMTSO administered to ICR mice significantly inhibited induced genotoxicity, with severe toxic effects of 0.5 and 1.0 mmol/kg MMTSO (125). Another animal study reported 5 mg/kg MMTSO alongside azoxymethane for five weeks to rats reduced aberrant crypt foci, precursor lesions of colorectal cancer, and decreased numerous biomarkers of cell proliferation (126). MMTSO was explored on large bowel cancer progression, where they found a protective and potential chemopreventative ability for liver neoplasms, and indicated antioxidant activity

against oxidative degradation of lipids in tests with rabbit erythrocyte membrane and rat hepatocytes (128), potentially due to the presence of thio-sulphinate and thiol functional groups (117, 163). These studies suggest that MMTSO could be a potential chemopreventive agent in vivo and that further studies to investigate this are warranted.

To date, there have been two human studies that have explored SMCSO in humans: one investigating the excretion and one the accumulation in the prostate tissue. One study reported fourteen days after administration of [35S]-SMCSO and [35S]-SCMCSO to 4 healthy males, the radiolabelled compounds had completely degraded to sulphate, with the urine being the major path for excretion (96 % in 14 days) (147). The other study reported that SMCSO accumulated in the prostate tissue as well as sulphate and ADP, with the supplemented exhibiting a higher SMCSO concentration in both the prostatic tissues and urine (25). Further cell-based assays demonstrated SMCSO affected ATP present in cells (25). These studies could suggest that SMCSO and/or its metabolites may have biological properties that remain unidentified, and that they may play a role in the effect of a broccoli-rich diet.

Unlike normal cells, prostate cancer cells rewire their central metabolism in order to meet the high energy demands of the cancer proliferation, migration and invasion (39). Normal prostate cells are citrate-focused and aim to utilise glucose and aspartate through glycolysis to generate citrate for secretion. However, prostate cancer cells have a unique metabolic profiling that drives oxidative phosphorylation and utilise more fatty acids via beta-oxidation to feed into the citric acid (TCA) cycle to generate ATP and support the cancer growth (36, 164). Androgen-signalling in prostate cancer promotes TCA cycle functions including amino acid metabolism, and this plays a vital role in prostate cancer progression (36). Studies have reported that prostate cancer cells display a raised uptake of extracellular fatty acids (165) with prostate tumours having elevated levels of TCA intermediates including malate, fumarate and succinate, compared to normal tissues (40). Interestingly, recent studies have reported a role of glutamine and glutamate metabolism in the redox balance of prostate cancer progression via glutamate oxaloacetate transaminase 1 (GOT1) (81). There is a gap in the current literature of the biological effects of these dietary sulfur compounds, SMCSO and MMTSO, on central energy metabolism in prostate cancer. Evaluating the mitochondrial metabolism in prostate cancer cells following exposure to SMCSO

and MMTSO, will give a better understanding of their effect on energy metabolism in prostate cancer progression.

This chapter investigates SMCSO and its metabolite, MMTSO, through molecular techniques to investigate their influence on DU145 prostate cancer cell metabolism. This data provides the first evidence of the metabolic role of MMTSO in DU145 prostate cancer cells. In combination with transcriptomic and metabolomic analysis (Chapter 3 and 4) this gives a comprehensive understanding of prostate cancer metabolism and the effect of exposure to dietary sulfur metabolites, which could lead to better therapeutic responses.

2.2 Aims

Investigate effects of sulfur-containing compounds, SMCSO and MMTSO, on cell viability and metabolism in DU145 prostate cancer cell line:

- To characterise the effect of SMCSO and MMTSO on cell viability to select a non-toxic and potentially physiologically relevant concentration for further mitochondrial energy assessment.
- To investigate the effects of SMCSO and MMTSO individually and in combination on mitochondrial metabolism in prostate cancer cells.
- To evaluate the effects of SMCSO and MMTSO on ATP production and maximal respiration, using Seahorse XFp and XFe96 Bioanalyser.
- To perform analyses on other metabolic pathways such as glycolysis, glutamine and fatty acid metabolism using appropriate Seahorse assays.

2.3 Materials and Methods

2.3.1 Cell Culture

Human prostate adenocarcinoma cell line, DU145 (Cat. HTB-81), was purchased from the American Type Culture Collection (ATCC®); human normal prostate epithelial cells, PNT1A (Cat. 95012614) were purchased from the European Collection of Authenticated Cell Cultures (ECACC). DU145 cells were cultured in EMEM media (ATCC®), PNT1A cells were cultured in RPMI-1640 (Merck®) media; both media were supplemented with 10% Fetal bovine serum (FBS, ThermoFisher®) and 1% penicillin/streptomycin (ThermoFisher®). All cells were cultured to 70% confluence and grown as adherent monolayers maintained at 37°C in a humidified atmosphere containing 5% CO_2 and cultured under standard glucose environment of 5.5 mM unless stated otherwise. The high glucose treatments were delivered in DMEM media (Merck®) supplemented with 1 mM sodium pyruvate (ThermoFisher®) and 10 mM glucose solution (ThermoFisher®) to mimic an intermediate glucose environment or 25 mM glucose solution (ThermoFisher®) to mimic a high glucose environment.

2.3.2 Treatment with SMCSO or MMTSO

After the cells were cultured in standard conditions, the appropriate treatment or vehicle control was added in triplicate, unless stated otherwise, diluted in medium for a further 24-hour incubation. S-methyl L-cysteine sulfoxide (SMCSO) was purchased from LKT Laboratories (CAS 6858-87-8, purity >98%). S-methyl methanethiosulfonate (MMTSO) was purchased from Merck® (CAS 2949-92-0, purity 97%). Both SMCSO and MMTSO were dissolved in water to create a 10 mM stock solution that was diluted to the final treatment concentrations. Both were used in parallel with a water control.

2.3.3 WST-1 Assay

The WST-1 colorimetric assay assesses the cleavage of tetrazolium salt WST-1 ((4-[3-(4-Iodophenyl)-2-(4-nitro-phenyl)-2H-5-tetrazolio]-1,3-benzene sulfonate) to formazan by mitochondrial enzymes of metabolically active viable cells. WST-1 cell proliferation kit (Merck®) was used according to the manufacturer's specifications. Briefly, the cells were seeded at 1.25 x 10^5 cells/ml in 96-well plates in a final volume of 200 µl/well. Cells were cultured under standard conditions for 24-hours. After 24-hours, the media was removed, and cells were treated with a combination

of SMCSO and MMTSO diluted in medium for 24 hours. Ten microliters of WST-1 reagent were added to each well and incubated in standard culture conditions. WST-1 cleavage was measured after 30-min or 1-hour at 450 nm (sample) and 650 nm (background) using the FLUOstar Omega microplate reader (BMG Technologies). Medium plus WST-1 served as a blank, which was deducted from all values. WST Activity (% relative to control) were calculated by the equation: (WST-1 value/Control value) x 100.

2.3.4 Cell Viability Assay

DU145 cells were seeded at 2.5 x 10^5 cells/ml in 12-well plates in a final volume of 1 ml/well and cultured under standard conditions for 48-hours. After 48-hours, the media was removed, the wells were washed with 1x phosphate-buffered saline (PBS, Gibco®) and cells were treated with SMCSO or MMTSO diluted in medium for 24-hours. The treatment was removed, and all wells were washed with 1x PBS before the addition of 250 µl of 0.25 % trypsin (Gibco®) to each well. Cells were incubated for 10-minutes under standard conditions. To neutralise the trypsin, 500 µl of medium was added to each well. Cells were diluted 1:1 with trypan blue (ThermoFisher). Images of the cells were taken, and cell viability was measured by Countess™ II Automated Cell Counter (ThermoFisher).

2.3.5 Seeding Seahorse Cell Culture Miniplate

The Seahorse Bioanalyser was chosen to measure oxygen consumption rate (OCR) and extra-cellular acidification rate (ECAR). Assays are run in real-time and selected based on pathway assessment. In this chapter, cell mito stress test (166), glycolysis stress test (167), real-time ATP test (168), and mito fuel flex test (169) were used, representing rates of mitochondrial metabolism, glycolysis, real-time ATP measurement and fuel dependency respectively. The compounds used within each assay has been optimised and standardised by Agilent for each test. For example, with the cell mito stress test, fCCP is the second injection which is a mitochondrial membrane uncoupler and allows for the quantification of maximal respiration (166).

By use of the Seahorse XFp and Seahorse XFe96 Bioanalysers (Agilent®), assessment of mitochondrial respiratory rate (oxygen consumption rate, OCR) and non-mitochondrial respiratory rate (extracellular acidification rate, ECAR) in live cells through fluorescent technology activated by the presence of oxygen and protons in the cell culture medium was conducted. The Seahorse XFp Bioanalyser

(Agilent®) allowed the assessment of 6-samples (Figure 2.1A); the Seahorse XFe96 Bioanalyser (Agilent®) allowed for the assessment of up to 92-samples (Figure 2.1B).

For both Bioanalysers, DU145 cells were grown to 70-80 % confluency and seeded at 3 x 10^4 cells/well in a total volume of 200 µl in the central wells of Seahorse cell culture plates (Agilent®). For the XFp the two outer wells acted as the assay controls; for the XFe96, the four corner wells acted as the assay controls, all contained media only. The surrounding moats or empty wells were filled with sterile 1xPBS (Gibco®). The cells were cultured under standard conditions for 24-hours prior to treatment.

2.3.6 Preparation of Seahorse Sensor Cartridge

At least 8-hours prior to the assay run, the appropriate sensor cartridge for the correct Bioanalyser was selected (Figure 2.1C and 2.1D) and hydrated with 200 µl/well of XF Calibrant solution (Agilent®). For the XFp sensor cartridges, an additional 400 µl was added in each of the surrounding moats. The cartridge was placed in a 37 °C non-CO_2 incubator until required. The sensor cartridge contains four injection ports that the metabolic inhibitor compounds are added into on the day of the assay and a probe in the centre of each injection port. The compounds are released from the injection ports into the medium over the course of the assay, and the probes are lowered into the medium at regular intervals during the assay which measure the OCR and ECAR.

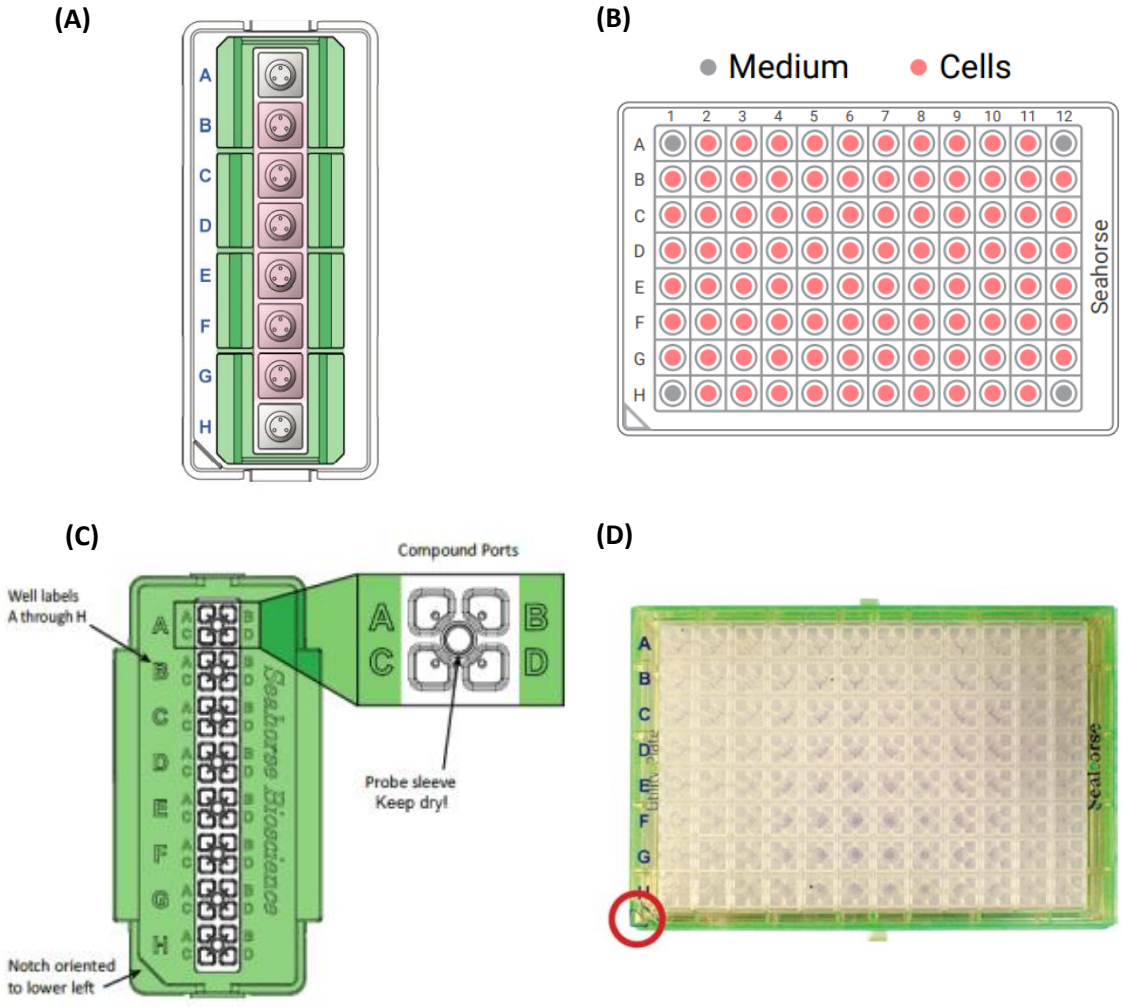

Figure 2.1. Seahorse plates (A) XFp cell culture miniplates **(B)** XFe96 cell culture miniplates, highlighting the four corners used for blank (contain medium only) **(C)** XFp sensor cartridge with compound injection ports. **(D)** XFe96 sensor cartridge with compound injection ports. For the XFp cell culture miniplates, the central 6 wells (B-G) were seeded with cells in medium, the two outer wells (A and H) contained media without cells. For the XFe96 cell culture plates, up to 92 wells were seeded with cells in medium, the four corner wells (A1, A12, H1 and H12) contained media without cells. For the sensor cartridges, at least 8-hours prior to assay, the appropriate sensor cartridge was selected and hydrated with XF Calibrant solution. The cartridge contains injection ports to add the compounds and probes to measure the OCR and ECAR per well. For the XFe96 plate, the triangular notch (circled in red) should be at the bottom left-hand corner. Source: Agilent®.

2.3.7 Preparation of Seahorse Cell Culture plate

After treatment with SMCSO or MMTSO, as described in section 2.3.2, the media was removed and the cells were washed and incubated with 180 µl of warmed assay medium: Agilent® XF base DMEM, pH 7.4, supplemented with 2 mM L-glutamine (Merck®), 2 mM pyruvate (ThermoFisher®) and 10 mM glucose (ThermoFisher®) for 1-hour in a 37°C non-CO_2 incubator. For glyco stress assay, the Agilent® XF base DMEM, pH 7.4, medium was supplemented with just 2 mM L-glutamine (Merck®).

2.3.8 Loading of Seahorse XFp Sensor Cartridge

Once the cell culture plate was added to the 37°C non-CO_2 incubator, the sensor cartridge was loaded with the compounds for the appropriate test. For the mitochondrial stress test, oligomycin, FCCP, rotenone and antimycin A were required; for the glycolysis stress test glucose, oligomycin, and 2-deoxy-D-glucose were required. For the XFp analysis, all compounds, apart from the glucose (ThermoFisher®), were purchased from Merck®. The compounds were diluted in DMSO to generate 10 mM stock solutions, which were stored at -20°C until required. On the day of the assay, the working solutions of the compounds were generated by dilution in warmed assay medium (Table 2.1 and Table 2.2) and inserted into the sensor cartridge into the correct port. Once the compounds had been inserted, the sensor cartridge was loaded into the Seahorse XFp Extracellular Analyser and calibrated. After calibration, the cell culture miniplate was loaded into the Seahorse XFp Analyser and the assay commenced.

Table 2.1. Template for loading injection ports of the sensor cartridge for mito stress assay

Port Designation	Injection Volume	Port Concentration	Well Concentration
A – Oligomycin	20 µl	10 µM	1.0 µM
B – FCCP	22 µl	5.0 µM	0.5 µM
C – Rotenone/ Antimycin A	25 µl	5.0 µM	0.5 µM

Table 2.2. Template for loading injection ports of the sensor cartridge for glyco stress test

Port Designation	Injection Volume	Port Concentration	Well Concentration
A – Glucose	20 µl	100 mM	10 mM
B – Oligomycin	22 µl	10 µM	1.0 µM
C – Deoxy-D-glucose	25 µl	500 mM	50 mM

2.3.9 Loading of Seahorse XFe96 Sensor Cartridge

Once the cell culture plate was added to the 37°C non-CO_2 incubator, the sensor cartridge was loaded with the compounds for the appropriate test. For the real-time ATP test, oligomycin and, rotenone and antimycin A were required; for the mito fuel flex test, UK5099, etomoxir and BPTES were required. For the XFe96 analysis, all compounds were purchased from Agilent® from the appropriate test kit. The compounds were stored at room temperature. On the day of the assay, the compounds were prepared and diluted in assay medium as per the manufacturer's instructions to generate working solutions of the compounds. The final compound added also contained 1:1000 dilution of Hoechst dye (20 mM, Thermo Fisher®) to allow for normalisation. All compounds were inserted into the XFe96 plate using a multi-channel pipette. Once the compounds had been inserted, the sensor cartridge was loaded into the Seahorse XFe96 Extracellular Analyser and calibrated. After calibration, the cell culture plate was loaded into the Seahorse XFe96 Analyser, and the assay commenced.

2.3.10 Cell Mito Stress Assay using Seahorse XFp Bioanalyser

The mitochondrial stress assay was conducted according to manufacturer's instructions. Measurements were taken approximately every 7-minutes for a total of approximately 80-minutes. Oligomycin was injected at 14-minutes, FCCP was injected at 35-minutes and Rotenone/Antimycin A was injected at 54-minutes from the start of the assay. The ATP production and maximal respiration can be estimated from the outputs from the pre-set template (Figure 2.2).

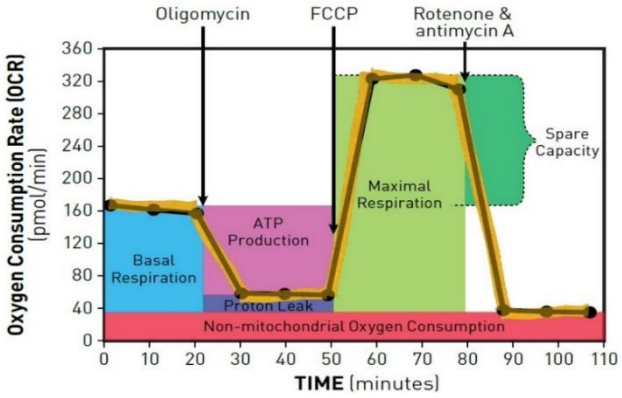

Figure 2.2. Seahorse Cell Mito Stress Profile. The pre-set template for the Cell Mito Stress Test assay allows for estimates of basal respiration, ATP production and proton leak after Oligomycin addition, maximal respiration after FCCP addition and Spare capacity and non-mitochondrial oxygen consumption after Rotenone & Antimycin A addition. Source: Agilent®.

2.3.11 Glyco Stress Test using Seahorse XFp Bioanalyser

The glyco stress test was conducted according to manufacturer's instructions. Measurements were taken approximately every 7-minutes for a total of approximately 80-minutes. Glucose was injected at 14-minutes, oligomycin was injected at 35-minutes and 2-deoxy-D-glucose was injected at 54-minutes from the start of the assay. The glycolysis can be estimated from the outputs from the pre-set template (Figure 2.3).

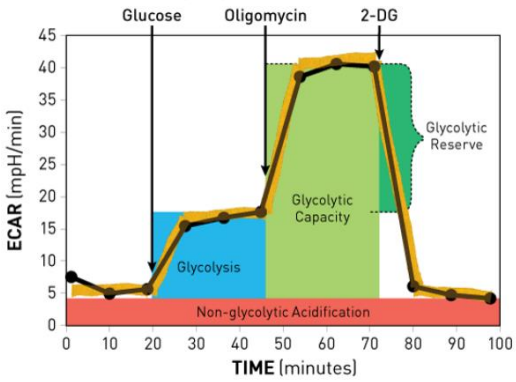

Figure 2.3. Seahorse Glyco Stress Test Profile. The pre-set template for the Glycolysis Stress Test allows for estimates of glycolysis after glucose addition, glycolytic capacity after oligomycin addition and glycolytic reserve after 2-deoxy-D-glucose (2-DG) addition. Source: Agilent®.

2.3.12 Real-time ATP Test using Seahorse XFe96 Bioanalyser

The real-time ATP test was conducted according to manufacturer's instructions. Measurements were taken approximately every 7-minutes for a total of approximately 60-minutes. Oligomycin was injected at 14-minutes, Rotenone/Antimycin A was injected at 35-minutes from the start of the assay. The total ATP production rate from glycolytic and mitochondrial ATP production rate, and the % oxidative phosphorylation can be estimated from the outputs from the pre-set template (Figure 2.4).

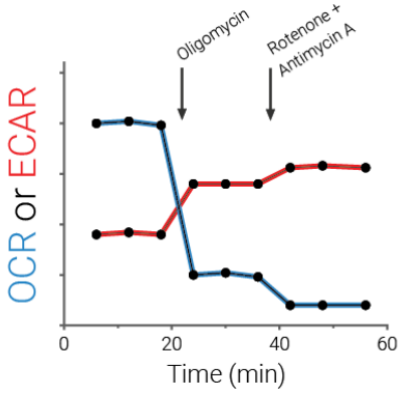

Figure 2.4. Seahorse Real-time ATP test. The pre-set template for the real-time ATP test allows for estimates of total ATP production and % of oxidative phosphorylation after oligomycin and rotenone/antimycin A addition. Source: Agilent®.

2.3.13 Mito-Fuel Flex Test using Seahorse XFe96 Bioanalyser

The mito-fuel flex test was conducted according to manufacturer's instructions. Measurements were taken approximately every 7-minutes for a total of approximately 90-minutes. The first injection was injected at 14-minutes, followed by the second injection at 54-minutes from the start of the assay (Table 2.3). This test allows for estimates of multiple assessments to evaluate the dependency of glutamine, fatty acids and glucose from the outputs from the pre-set template.

Table 2.3. Template for injections timings for mito-fuel flex test

Assessment	First Injection	Second Injection
Glutamine dependency	BPTES	UK5099 + Etomoxir
Fatty acid dependency	Etomoxir	UK5099 + BPTES
Glucose dependency	UK5099	Etomoxir + BPTES

2.3.14 Normalisation using Total Protein using BCA Assay for XFp

After the Seahorse XFp assay, protein was extracted from each well and quantified. The assay medium was removed, and 1x cell lysis buffer (Cell Signaling Technologies) was added to each well. The wells were scraped, and the lysate placed into Eppendorf tubes. The samples were briefly vortexed and vortexed every 5-minutes whilst incubated on ice for a total of 15-minutes. The samples were centrifuged at 14,000 rpm for 10-minutes at 4°C and the supernatant was taken for quantification by bicinchoninic (BCA) protein assay (Merck®). Briefly, bovine serum albumin (BSA, Merck®) was diluted in 50 mM sodium phosphate buffer, pH 6.0, to generate stocks ranging from 0–1000 µg/ml. BCA working reagent was made by the ratio 50:1 of BCA Reagent A (bicinchoninic acid) (Merck®) to BCA Reagent B (copper II sulphate) (Merck®). Twenty-five microlitres of each protein standard and samples were added to a 96-well plate before the addition of 200 µl of BCA working reagent. The plate was placed in a 37°C non-CO_2 incubator for 30-minutes. The absorbance was measured at 565 nm using the FLUOstar Omega microplate reader (BMG Technologies) and total protein concentration was calculated and each well normalised. Data are presented as pmol/min/µg protein.

2.3.15 Normalisation using Hoechst Staining for XFe96

Prior to the XFe96 assay, the CLARIOstar® Plus microplate reader (BMG LABTECH) was setup with the following instrument settings stated in Table 2.4.

Table 2.4. Instrument settings for Normalisation using Hoechst Staining

Optic settings	Fluorescence intensity, endpoint – Top read	
	Monochromator settings	Hoechst pre-set Ex 355-20 Em 455-30
	Gain and focus	1400 / 2.1 mm
General settings	Number of flashes	2
	Settling time	0 s
Well scan	Matrix scan	15 x 15 (3mm)
Incubation Temperature	37°C	

As previously mentioned in section 2.3.8, Hoechst dye was mixed with the last compound. Due to the automatic insertion of the dye with the last compound to the cells, the plate was ready to be taken to the CLARIOstar® Plus plate reader (BMG LABTECH) at the end of the Seahorse assay, where the fluorescence of each well was read. The fluorescence produced was proportional to the number of cells in each well. For quantification, the average signal of each well was divided by the averaged blanks (four corner wells) to give the signal/blank ratio. This ratio was exported into excel and imported into the Seahorse Wave software where the data were normalised. Data are presented as pmol/min/Norm. Unit.

2.3.16 Statistical analysis

All statistical analysis were performed in Prism using GraphPad Software. Where appropriate either one-way ANOVA followed by Tukey's honest statistical hypothesis test for multiple comparisons, or unpaired two-way T-test were used. A $p < 0.05$ with a 95 % confidence interval was defined to be statistically significant; n.s. $p > 0.05$; no significance present, *$p \leq 0.05$, **$p \leq 0.01$, ***$p \leq 0.001$, ****$p \leq 0.0001$. Data are expressed as mean ± standard deviation.

2.4 Results

2.4.1 SMCSO did not affect WST-1 activity under all glucose environments

To access the effect of SMCSO on cell viability, WST-1 assay was used. Briefly, DU145 cells were cultured for 24 hours allowing adherence and treated for a further 24 hours with the compounds before the addition of the WST-1 reagent. WST-1 activity (% relative to control) was measured as: (WST-1 value/Control value) x 100. SMCSO elicited no effect on WST-1 activity in basal (5.5 mM), intermediate (10 mM) and high (25 mM) glucose environments (Figure 2.5A – C).

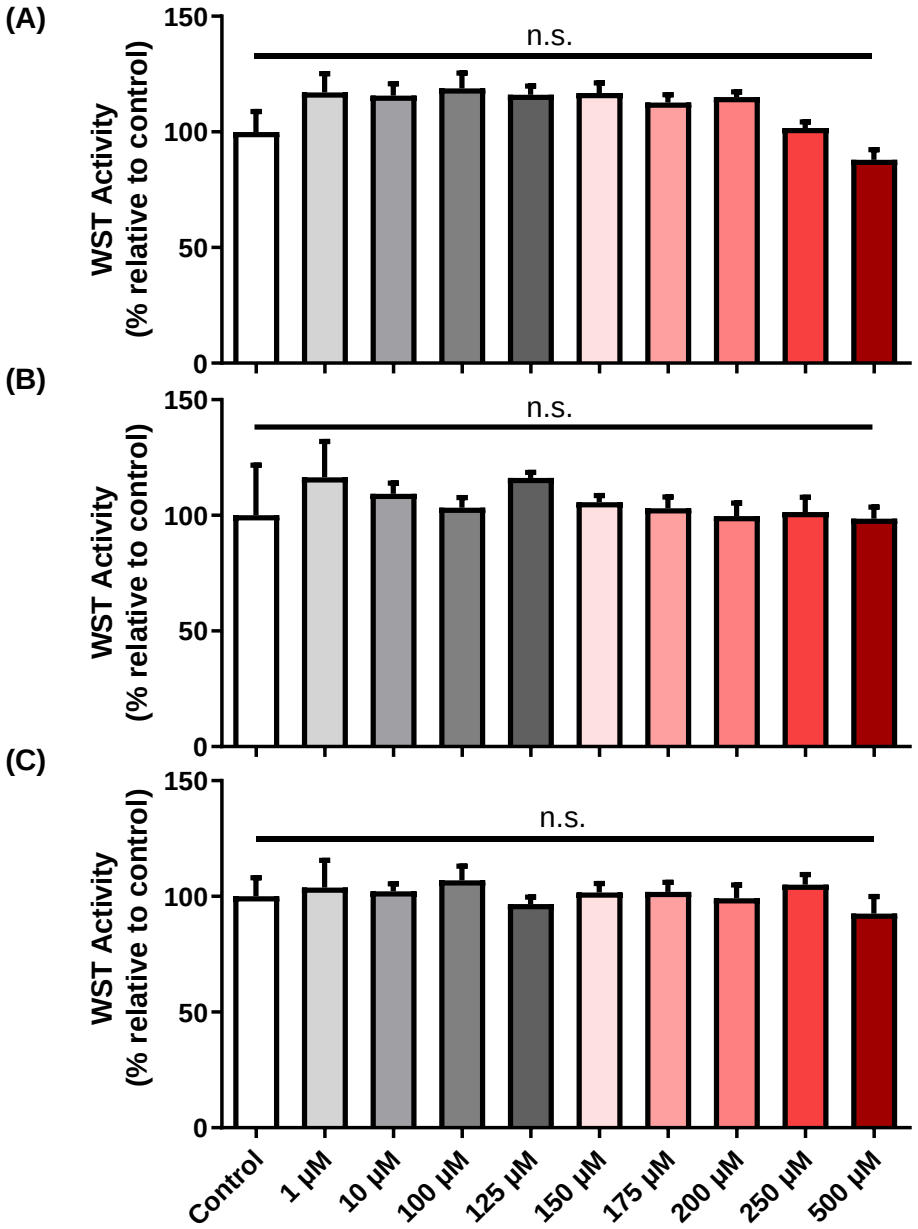

Figure 2.5. WST-1 activity of DU145 cells with SMCSO treatments. Briefly, the cells were cultured for 24-hours and treated for a further 24-hours with 0 µM – 500 µM concentrations of SMCSO before the addition of WST-1 reagent and absorbance measured. Cells were either treated in glucose concentrations of (A) basal, 5.5 mM, (B) intermediate, 10 mM, or (C) high 25 mM. SMCSO did not affect WST-1 activity in all glucose concentrations. n.s. = not significant.

2.4.2 High concentrations of MMTSO reduced WST-1 activity under all glucose environments

Further to the WST-1 assays with SMCSO, the WST-1 assay was used to assess the metabolic activity of DU145 cells when treated with MMTSO. As before, the same method was employed with increasing dosage of the compound. MMTSO caused a decrease in WST-1 activity in high concentrations; concentrations greater than 250 µM in basal and intermediate glucose environment (Figure 2.6A and 2.6B), and 175 µM and greater in high glucose environment (Figure 2.6C).

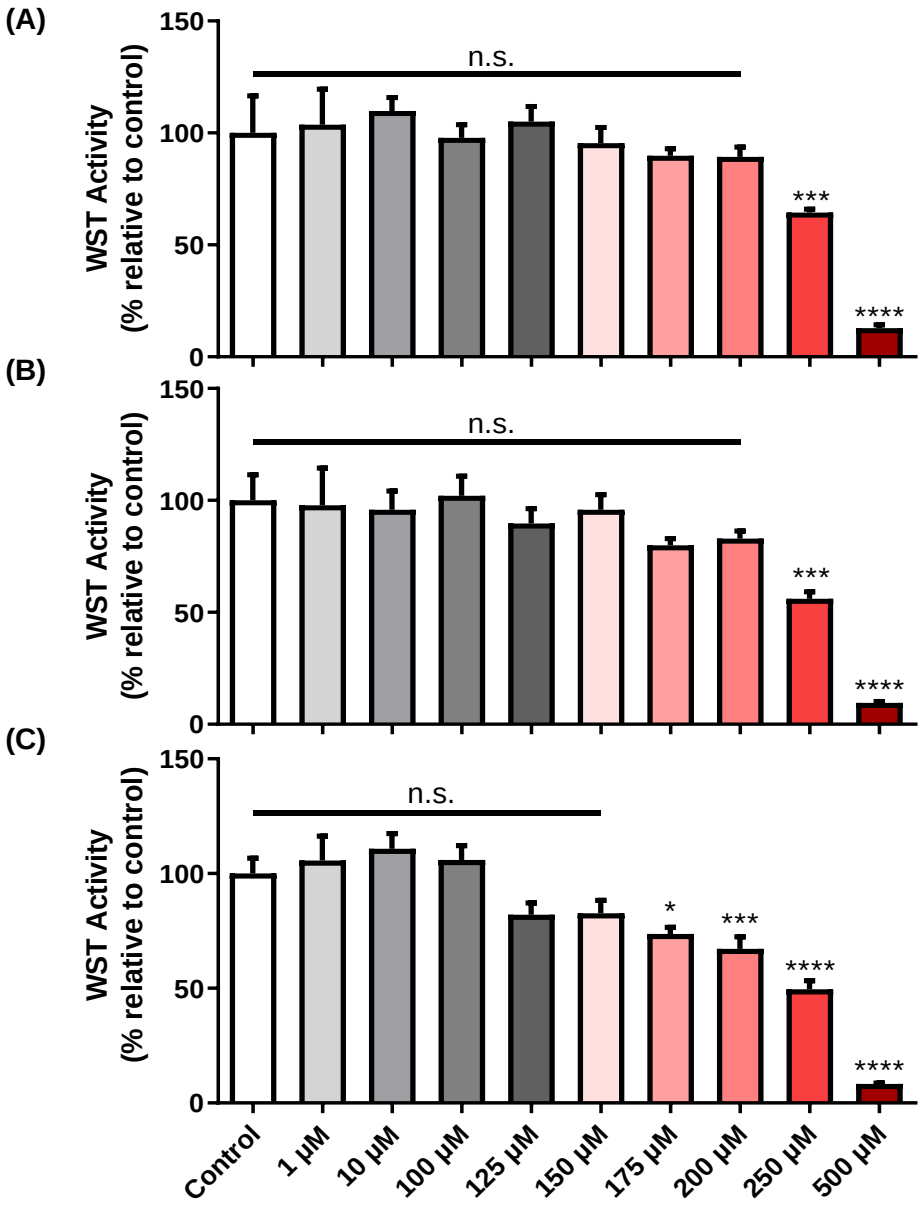

Figure 2.6. WST-1 activity of DU145 cells with MMTSO treatments. Briefly, the cells were cultured for 24-hours and a treated for a further 24-hours with 0 µM – 500 µM concentrations of MMTSO before the addition of WST-1 reagent and absorbance measured. Cells were either treated in glucose concentrations of (A) basal, 5.5 mM, (B) intermediate, 10 mM, or (C) high 25 mM. High concentrations of MMTSO did affect WST-1 activity in all glucose concentrations. n.s. = not significant; ** = $p < 0.01$; *** = $p < 0.001$; **** = $p < 0.0001$.

2.4.3 SMCSO did not affect cell viability; at 500 µM MMTSO reduced cell viability

To further evaluate the effect of the sulfur compounds, SMCSO and MMTSO, on cell viability, cell staining, and quantification were used. Briefly, DU145 cells were cultured for 24 hours allowing adherence and a treated for a further 24 hours with the compounds at increasing concentrations: 0, 10, 100 and 500 µM in basal glucose environment. The cells were trypsinised, mixed with trypan blue at 1:1 ratio, and added to a Countess cell counting slide. The slide was inserted into the Countess imager and the cells were counted, and live cell percentage was evaluated. Paralleling the result seen in WST-1, SMCSO had no effect on cell viability as seen by no difference in the increased compound concentrations (Figure 2.7A). However, MMTSO treatment at 500 µM did affect cell viability as seen by the significant decrease in live cell percentage (Figure 2.7B).

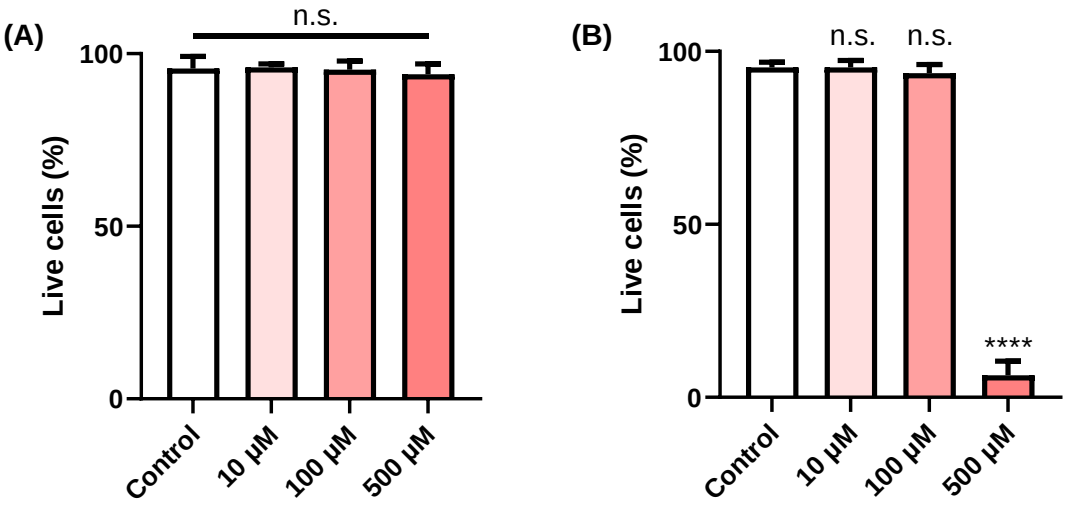

Figure 2.7. Cell viability of DU145 cells with treatments of SMCSO and MMTSO. Briefly, the cells were cultured for 24-hours and a treated for a further 24-hours with 0, 10, 100 and 500 µM concentrations of SMCSO and MMTSO under basal (5.5 mM) glucose environment, before the cells were trypsinised and cell viability assessed using Countess cell imager. Live cell percentage was assessed for SMCSO (A) and MMTSO (B) treatments. SMCSO did not affect cell viability, but MMTSO did affect cell viability at 500 µM. n.s. = not significant; **** = $p < 0.0001$.

2.4.4 DU145 have a higher mitochondrial metabolism compared to PNT1A

To assess the mitochondrial metabolism of human prostate cancer cells compared to normal human prostate epithelial cells, the Seahorse XFp Bioanalyser was used. Briefly, prostate cancer cells, DU145, were cultured for 24 hours allowing adherence and treated for a further 24 hours with vehicle (water) in basal (5.5 mM) glucose environment before the cell mitochondrial stress test was used. Prostate cancer cells (DU145) have higher mitochondrial metabolism compared to normal prostate epithelial cells (PNT1A), Figure 2.8A. Although not significant, DU145 cells have higher ATP production and maximal respiration, when compared to PNT1A cells (Figure 2.8B and 2.8C).

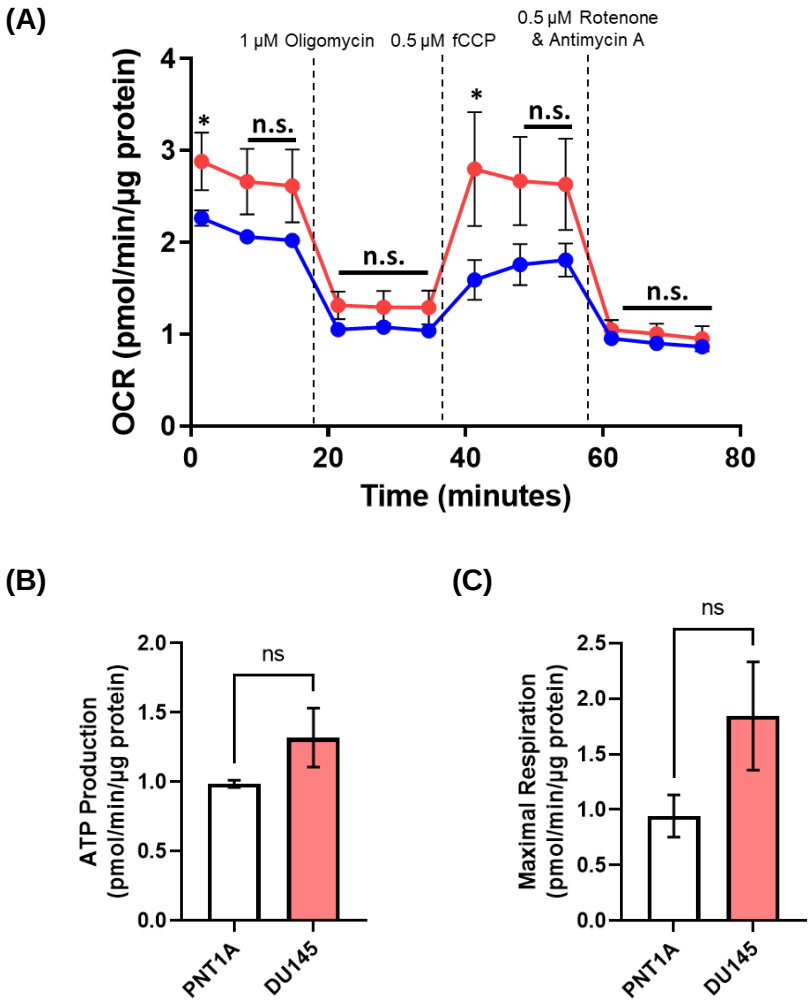

Figure 2.8. Mitochondrial stress tests with PNT1A and DU145 cells. Briefly, the cells were cultured for 24-hours and treated for a further 24-hours with vehicle under glucose concentrations of basal before the cell mitochondrial stress test was used on the Seahorse XFp Bioanalyser. (A) DU145 cells have higher mitochondrial metabolism compared to PNT1A. Although not significant, DU145 have higher ATP production (B) and maximal respiration (C), when compared to PNT1A . n.s. = not significant; * = $p < 0.1$.

2.4.5 SMCSO exposure for 24-hours had no effect on mitochondrial metabolism

To assess prostate mitochondrial metabolism, the Seahorse XFp Bioanalyser was used. From a previous dietary intervention involving consumption of broccoli soups, SMCSO was reported in urine up to concentrations ~100 µM (25). Due to potential urinary reflux of SMCSO, treatment of 100 µM SMCSO was selected for the following experiments. Briefly, DU145 cells were cultured for 24 hours allowing adherence and a treated for a further 24 hours with either the vehicle (water) or 100 µM SMCSO in three glucose environments: basal (5.5 mM, Figure 2.9A), intermediate (10 mM, Figure 2.9B) or high (25 mM, Figure 2.9C) before the cell mitochondrial stress test was used. Compared to the control, SMCSO had no significant effect on mitochondrial metabolism (red lines in Figure 2.9A – 2.9C).

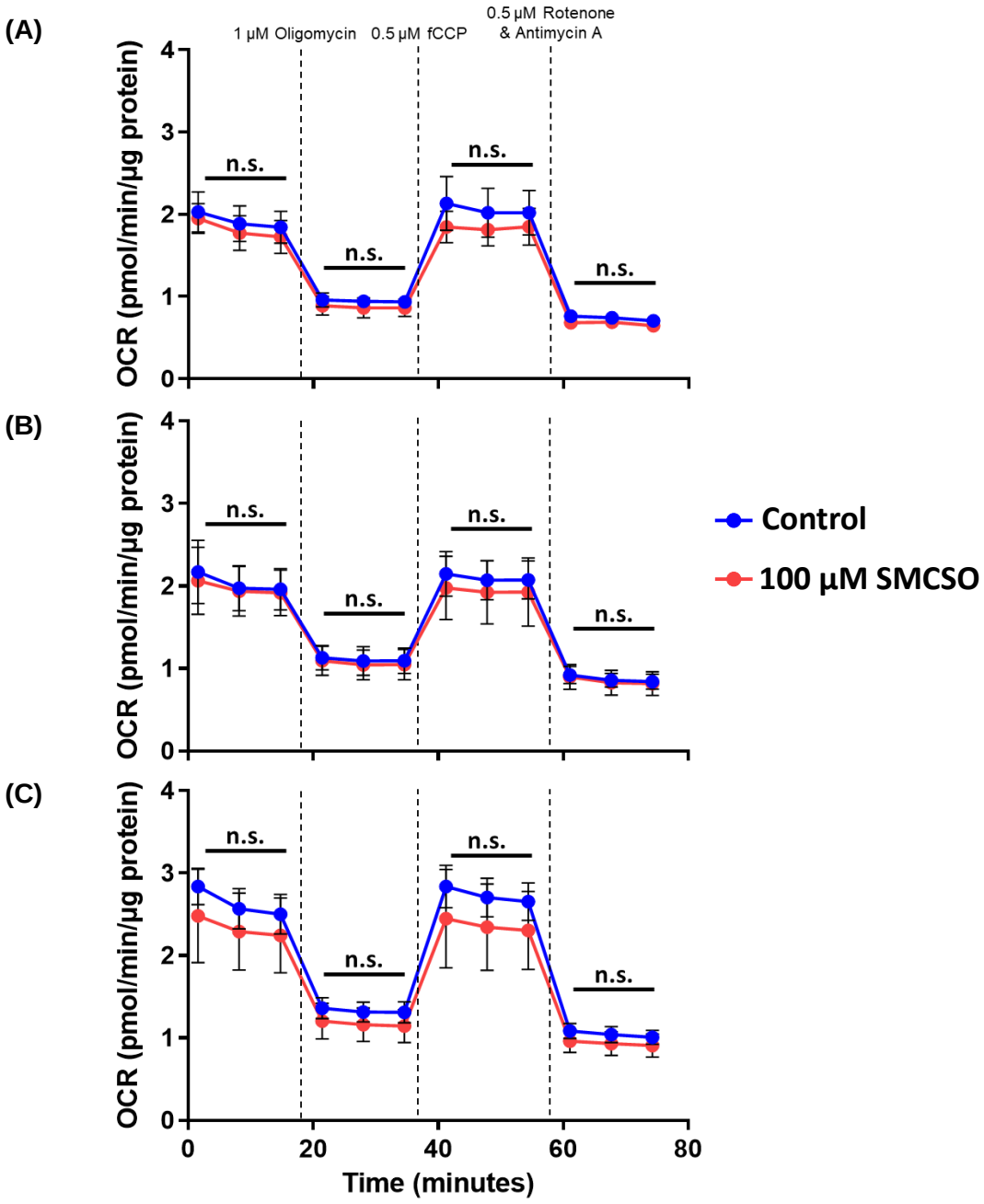

Figure 2.9. Mitochondrial stress tests with SMCSO treatments. Briefly, the cells were cultured for 24-hours and a treated for a further 24-hours with vehicle or 100 µM SMCSO under glucose concentrations of (A) basal, 5.5 mM, (B) intermediate, 10 mM, or (C) high, 25 mM before the cell mitochondrial stress test was used on the Seahorse XFp Bioanalyser. SMCSO exposure for 24-hours had no effect on mitochondrial metabolism. n.s. = not significant.

2.4.6 SMCSO exposure for 24-hours had no effect on ATP production or maximal respiration in DU145 cells

From the cell mitochondrial stress test (Figure 2.9), ATP production and maximal respiration was assessed. Briefly, ATP production is calculated from the decrease in OCR upon injection of oligomycin (ATP synthase inhibitor) compared to basal respiration; maximal respiration is calculated from the increase in OCR upon injection of fCCP (electron uncoupler) to mimic the maximum rate of respiration of the cells. Compared to the control, SMCSO had no significant effect on ATP production in basal (5.5 mM, Figure 2.10A), intermediate (10 mM, Figure 2.10B) or high (25 mM, Figure 2.10C) glucose environments, or on maximal respiration in basal (5.5 mM, Figure 2.10D), intermediate (10 mM, Figure 2.10E) or high (25 mM, Figure 2.10F) glucose environments.

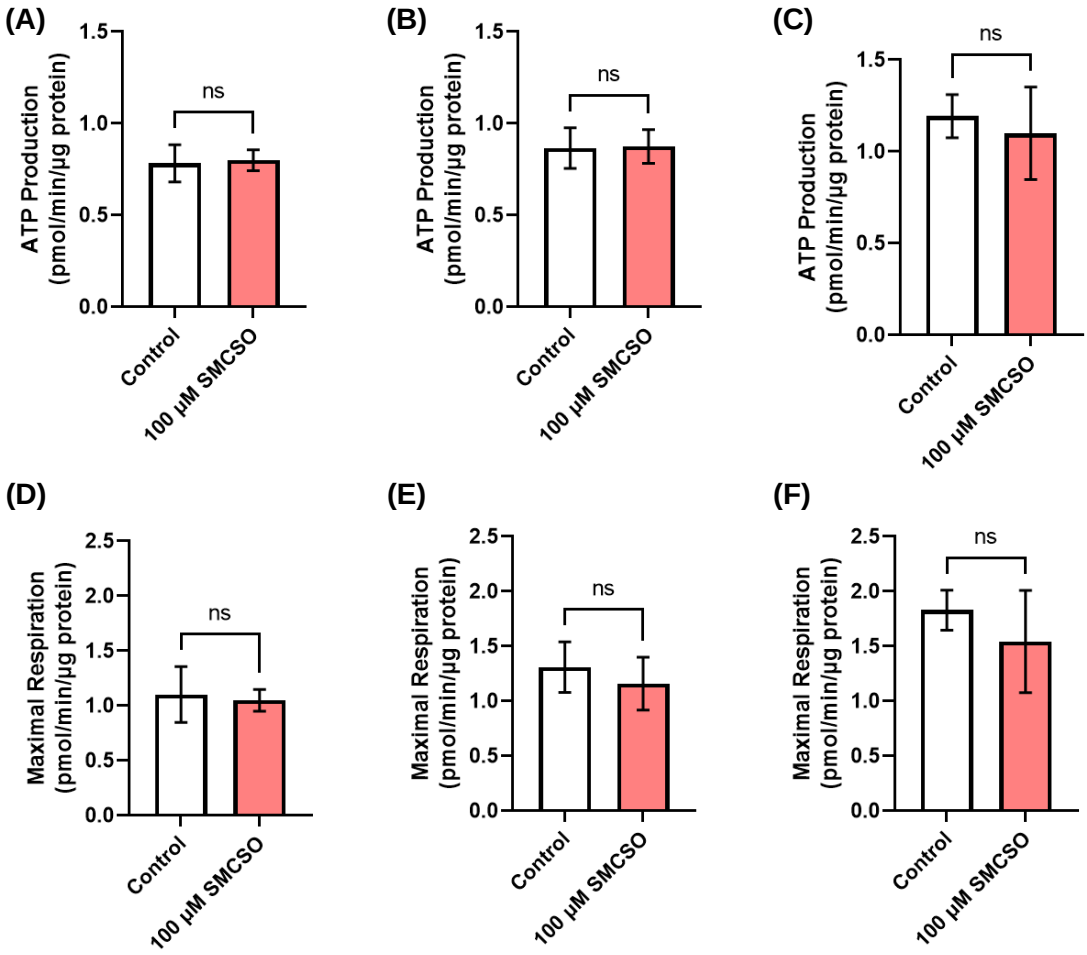

Figure 2.10. Assessment of ATP production and maximal respiration from 100 µM SMCSO exposure. Briefly, the cells were cultured for 24-hours and a treated for a further 24-hours with vehicle or 100 µM SMCSO under glucose concentrations of (A and D) basal, 5.5 mM, (B and E) intermediate, 10 mM, or (C and F) high 25 mM before the cell mitochondrial stress test was used on the Seahorse XFp Bioanalyser. SMCSO exposure for 24 hours had no effect on ATP production (A-C) or maximum respiration (D-F) in DU145 cells. n.s. = not significant.

2.4.7 Ten micromolar MMTSO exposure for 24-hours reduced mitochondrial metabolism under high glucose environment

To further assess the effect of non-glucosinolate sulfur metabolites on prostate mitochondrial metabolism, MMTSO was investigated using the Seahorse XFp Bioanalyser. To date, no previous human study has investigated the physiological concentration of MMTSO. For experiments with MMTSO, 10 µM and 100 µM concentrations were selected.

As described above, DU145 cells were cultured for 24 hours allowing adherence and treated for a further 24 hours with either the vehicle (water) or 10 µM in three glucose environments: basal (5.5 mM, Figure 2.11A), intermediate (10 mM, Figure 2.11B) or high (25 mM, Figure 2.11C) before the cell mitochondrial stress test was used. Ten micromolar MMTSO, compared to the control, did not affect mitochondrial metabolism in basal and intermediate glucose environments (Figure 2.11A and 2.11B), but reduced mitochondrial metabolism in high glucose environment (red line in Figure 2.11C).

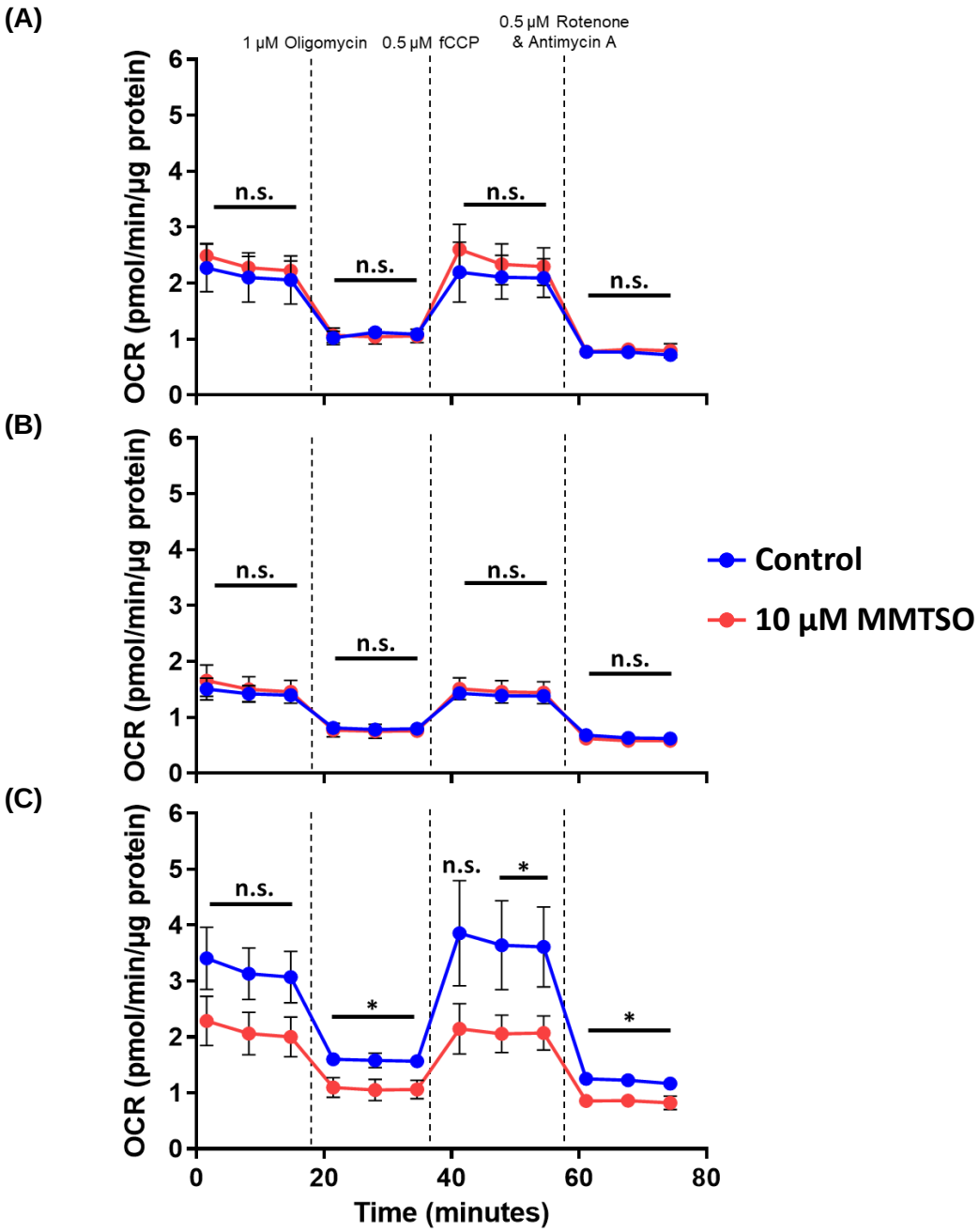

Figure 2.11. Mitochondrial stress tests with 10 µM MMTSO treatment. Briefly, the cells were cultured for 24-hours and a treated for a further 24-hours with vehicle, or 10 µM MMTSO under glucose concentrations of (A) basal, 5.5 mM, (B) intermediate, 10 mM, or (C) high, 25 mM, before the cell mitochondrial stress test was used on the Seahorse XFp Bioanalyser. MMTSO under high glucose environment reduced mitochondrial metabolism. n.s. = not significant; * = $p < 0.1$; ** = $p < 0.01$; **** = $p < 0.0001$.

2.4.8 Ten micromolar MMTSO exposure for 24-hours reduced ATP production and maximal respiration in high glucose environment

To further assess the effect of MMTSO on prostate energy metabolism, ATP production and maximal respiration were assessed using the Seahorse XFp Bioanalyser, as previously described in section 2.4.6. Compared to the control, 10 µM MMTSO had no effect on ATP production or maximal respiration in basal (5.5 mM, Figure 2.12A and 2.12D) and intermediate (10 mM, Figure 2.12B and 2.12E) but reduced ATP production and maximal respiration in high (25 mM, Figure 2.12C and 2.12F) glucose environment.

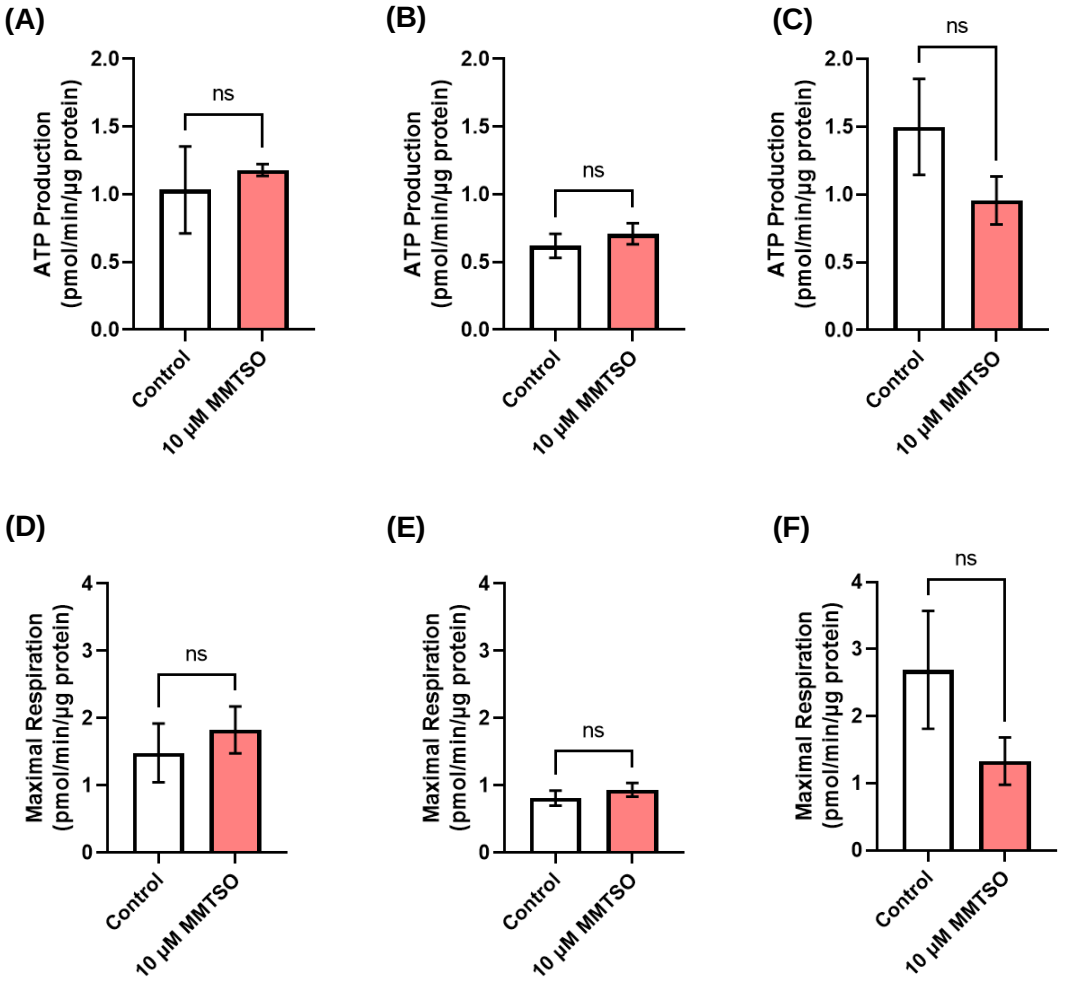

Figure 2.12. Assessment of ATP production and maximal respiration from 10 µM MMTSO exposure. Briefly, the cells were cultured for 24-hours and a treated for a further 24-hours with vehicle or 10 µM MMTSO under glucose concentrations of (A and D) basal, 5.5 mM, (B and E) intermediate, 10 mM, or (C and F) high 25 mM before the cell mitochondrial stress test was used on the Seahorse XFp Bioanalyser. MMTSO exposure for 24 hours reduced ATP production (A-C) and maximal respiration (D-F) in high glucose environment, although not significant. n.s. = not significant.

2.4.9 One hundred micromolar MMTSO exposure for 24-hours reduced mitochondrial metabolism in all glucose environments

To further assess the effect of non-glucosinolate sulfur metabolites on prostate mitochondrial metabolism, 100 µM MMTSO was investigated using the Seahorse XFp Bioanalyser. Briefly, the DU145 cells were cultured for 24-hours and a treated for a further 24-hours with vehicle or 100 µM MMTSO under glucose concentrations of basal (5.5 mM, Figure 2.13A), intermediate (10 mM, Figure 2.13B), or high (25 mM, Figure 2.13C), before the cell mitochondrial stress test was used. MMTSO exposure at 100µM for 24 hours reduced mitochondrial metabolism in all glucose environments (red lines in Figure 2.13).

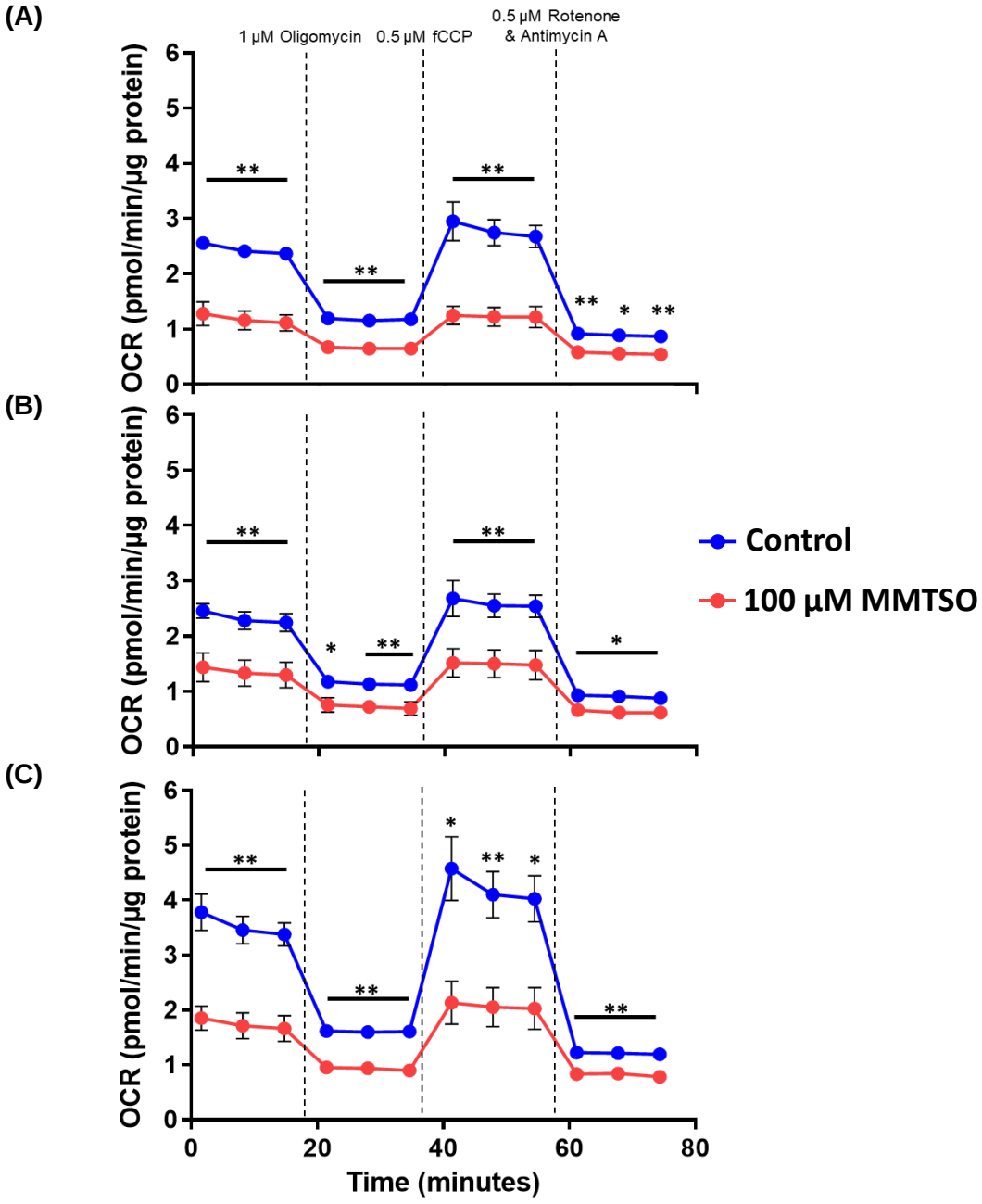

Figure 2.13. Mitochondrial stress tests with 100 µM MMTSO treatments. Briefly, the cells were cultured for 24-hours and a treated for a further 24-hours with vehicle or 100 µM MMTSO under glucose concentrations of (A) basal, 5.5 mM, (B) intermediate, 10 mM, or (C) high 25 mM before the cell mitochondrial stress test was used on the Seahorse XFp Bioanalyser. MMTSO exposure reduced mitochondrial metabolism. * = $p < 0.1$, ** = $p < 0.01$.

2.4.10 One hundred micromolar MMTSO exposure for 24-hours significantly reduced ATP production and maximal respiration in all glucose levels

To further assess the effect of MMTSO on prostate energy metabolism, ATP production and maximal respiration were assessed using the Seahorse XFp Bioanalyser, as previously described in section 2.4.6. Compared to the control, 100 µM MMTSO significantly reduced ATP production and maximal respiration in all glucose environments (Figure 2.14A – 2.14F); with a 2-fold decrease in ATP production and maximal respiration in the high glucose environment (Figure 2.14C and 2.14F respectively).

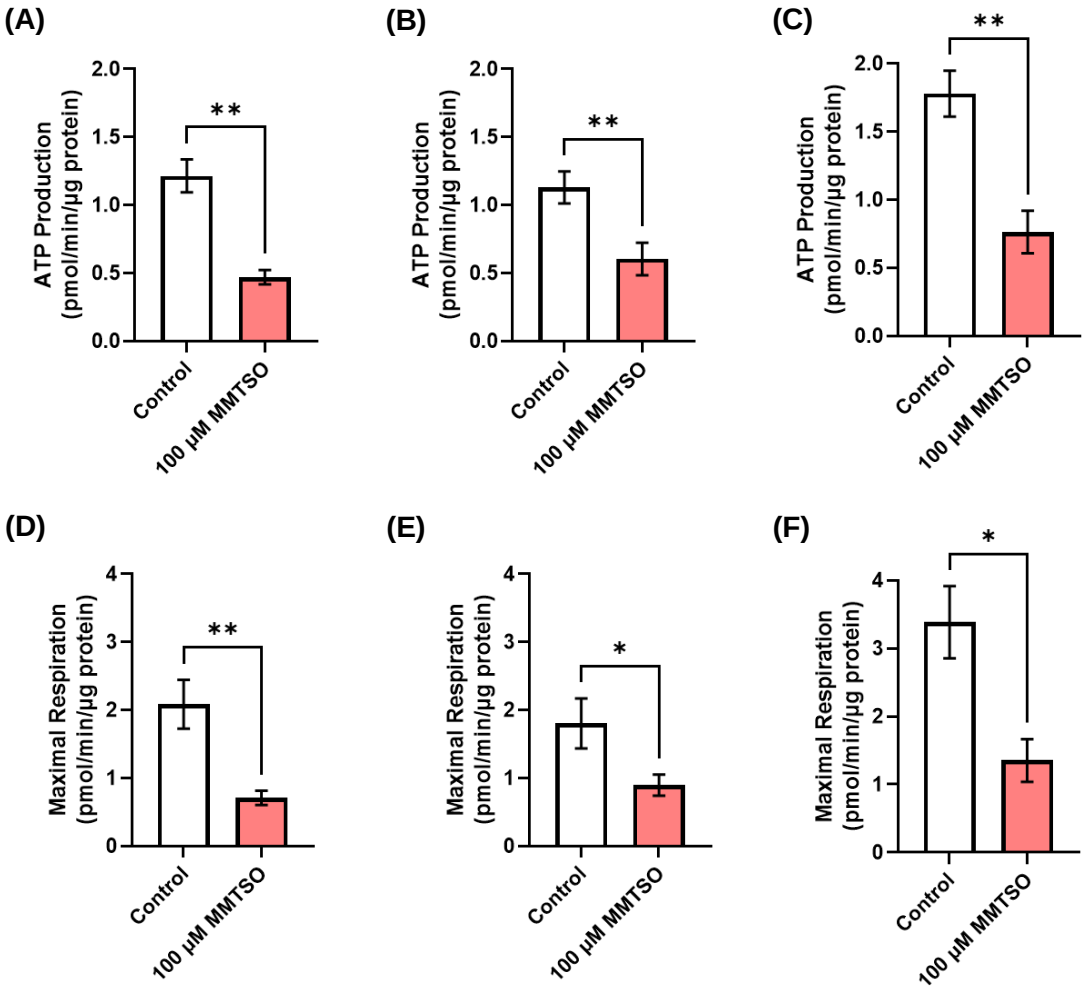

Figure 2.14. Assessment of ATP production and maximal respiration from 100 µM MMTSO exposure. Briefly, the cells were cultured for 24-hours and a treated for a further 24-hours with vehicle or 100 µM MMTSO under glucose concentrations of (A and D) basal, 5.5 mM, (B and E) intermediate, 10 mM, or (C and F) high 25 mM before the cell mitochondrial stress test was used on the Seahorse XFp Bioanalyser. 100 µM MMTSO caused significant reduction in ATP production (A-C) and maximal respiration (D-F) in DU145 cells. * = $p < 0.1$, ** = $p < 0.01$.

2.4.11 Combination of SMCSO and MMTSO both at 100 µM for 24-hours significantly reduced mitochondrial metabolism

To further evaluate the effect of sulfur-metabolites on prostate metabolism, the combination of SMCSO and MMTSO was assessed using the Seahorse XFp Bioanalyser, mimicking the environment if SMCSO and MMTSO were both present. Briefly, the DU145 cells were cultured for 24-hours and a treated for a further 24-hours with vehicle, 100 µM SMCSO and 10 µM MMTSO (Figure 2.15A and 15B) or 100 µM SMCSO and 100 µM MMTSO (Figure 2.15C and 2.15D) under either basal (5.5 mM) or high (25 mM) glucose environments, before the cell mitochondrial stress test was used. SMCSO (100 µM) and MMTSO (10 µM) combined elicited no significant effect (Figure 2.15A and 2.15B). The combination of SMCSO (100 µM) and MMTSO (100 µM) significantly reduced mitochondrial metabolism in both basal and high glucose environments (red lines in Figure 2.15C and 2.15D), where the compounds combined gave a much greater reduction compared to MMTSO alone suggesting a potential synergistic effect.

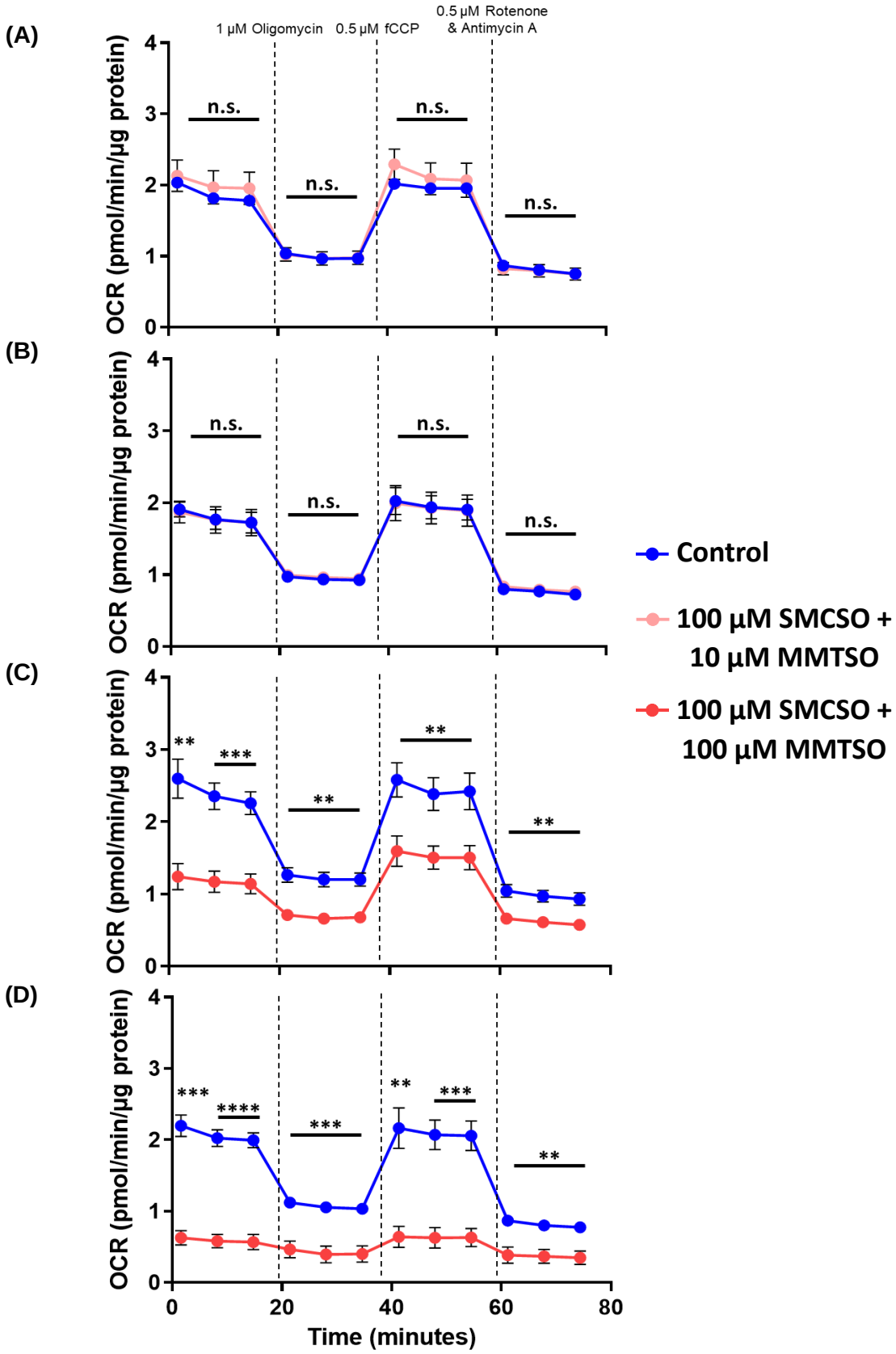

Figure 2.15. Mitochondrial stress tests with SMCSO and MMTSO combination treatments. Briefly, the cells were cultured for 24-hours and a treated for a further 24-hours with vehicle or 100 µM SMCSO + 10 µM MMTSO, or 100 µM SMCSO + 100 µM MMTSO under glucose concentrations of (A and B) basal, 5.5 mM, or (C and D) high 25 mM before the cell mitochondrial stress test was used on the Seahorse XFp Bioanalyser. SMCSO and MMTSO combined both at 100 µM exposure reduced mitochondrial metabolism; when MMTSO reduced 10-fold to 10 µM elicited no significant difference compared to control. n.s. = not significant, ** = $p < 0.01$, *** = $p < 0.001$, **** = $p < 0.0001$.

2.4.12 Combination of SMCSO and MMTSO both at 100 µM for 24-hours significantly reduced ATP production and maximal respiration

To further consider the effect of MMTSO on prostate energy metabolism, ATP production and maximal respiration were assessed using the Seahorse XFp Bioanalyser, as previously described in section 2.4.6. Compared to the control, the combination of SMCSO (100 µM) and MMTSO (100 µM) significantly reduced ATP production and maximal respiration in basal and high glucose environments (Figure 2.16); more so in the high glucose environment (Figure 2.16B and 2.16D).

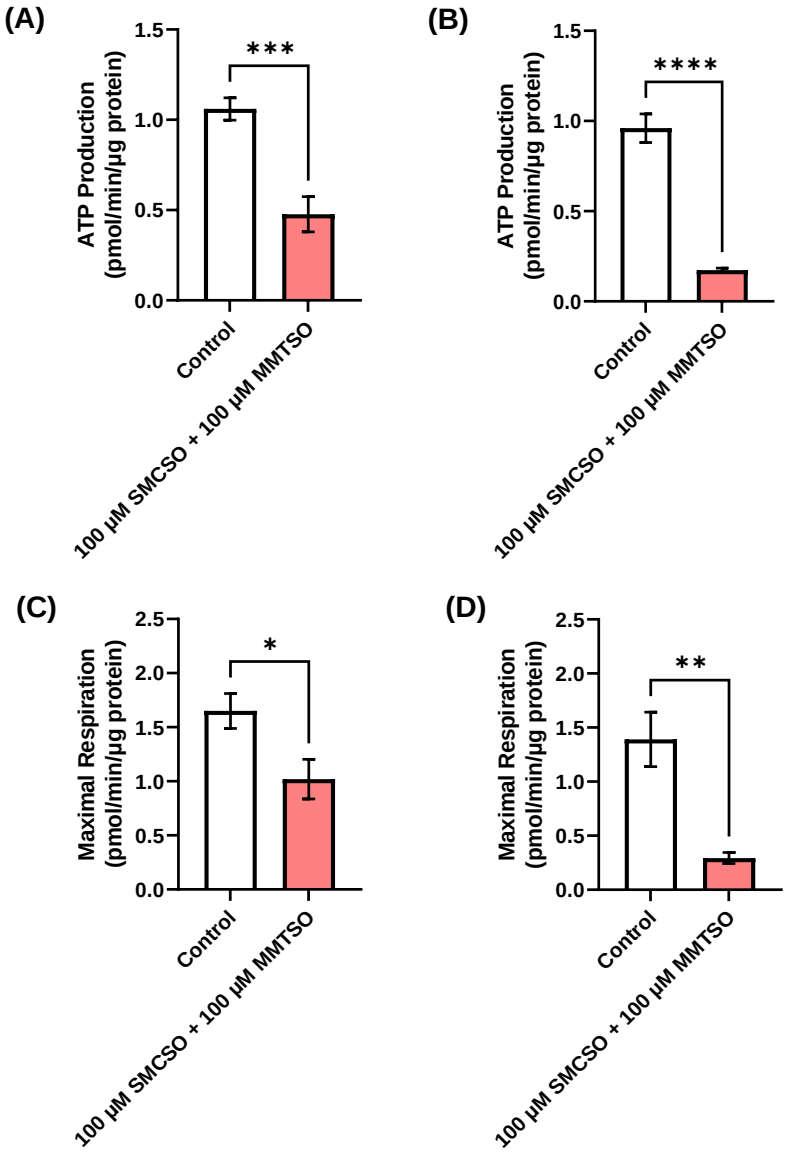

Figure 2.16. Assessment of ATP production and maximal respiration from SMCSO and MMTSO combination treatments. Briefly, the cells were cultured for 24-hours and a treated for a further 24-hours with vehicle or 100 µM SMCSO + 100 µM MMTSO under glucose concentrations of (A and C) basal, 5.5 mM, or (B and D) high, 25 mM before the cell mitochondrial stress test was used on the Seahorse XFp Bioanalyser. Combination of 100 µM SMCSO and 100 µM MMTSO caused significant reduction in ATP production (A-B) and maximal respiration (C-D) in DU145 cells. * = $p < 0.1$, ** = $p < 0.01$, *** = $p < 0.001$, **** = $p < 0.0001$.

2.4.13 MMTSO reduced mitochondrial ATP and percentage oxidative phosphorylation in a dose-dependent manner

To further consider the effect of MMTSO on prostate metabolism, total ATP production (sum of glycolytic ATP and mitochondrial ATP) and oxidative phosphorylation (%) were assessed using the Seahorse XFe96 Bioanalyser. Briefly, DU145 cells were cultured for 24-hours and a treated for a further 24-hours with vehicle, or 20, 40, 60, 80 or 100 µM MMTSO under basal 5.5 mM or high 25 mM glucose, before the real-time ATP test was used on the Seahorse XFe96 Bioanalyser. There is a reduction in OCR kinetic profile, following 100 µM MMTSO treatment compared to the control in both basal and high glucose environment (Figure 2.17). MMTSO had no significant effect on total ATP over all concentrations (Figure 2.18A), and on glycolytic ATP at 100 µM MMTSO in basal and high glucose (Figure 2.18B). however, did significantly reduce mitochondrial ATP at 100 µM MMTSO in the high glucose environment, Figure 2.18C (ii). MMTSO also reduced the percentage of oxidative phosphorylation in a dose-dependent manner in basal and high glucose (Figure 2.18D).

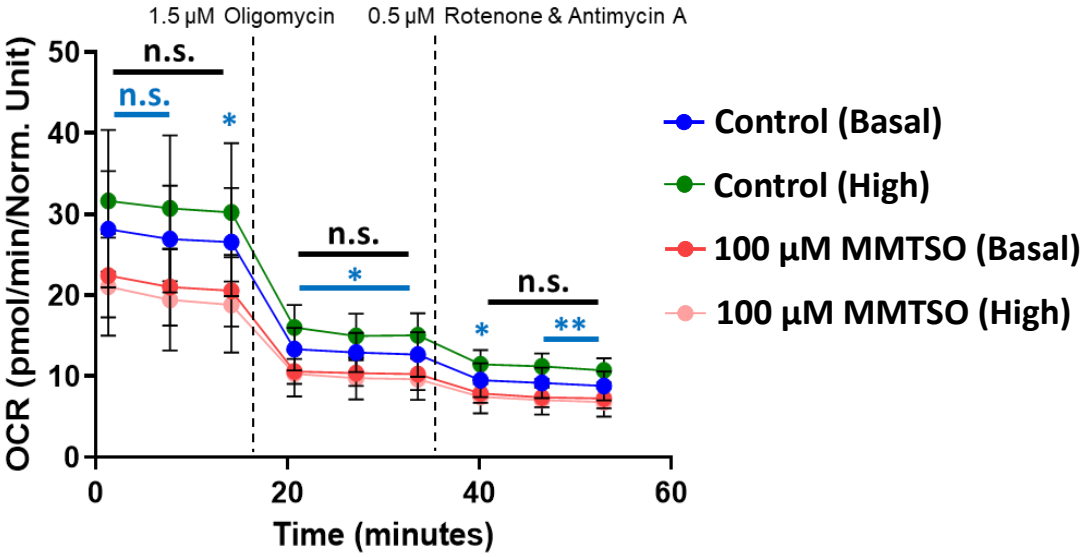

Figure 2.17. Real-time ATP kinetic profile with MMTSO treatments. Briefly, the cells were cultured for 24-hours and a treated for a further 24-hours with vehicle, or MMTSO under basal 5.5 mM and high 25 mM glucose, before the real-time ATP test was used on the Seahorse XFe96 Bioanalyser. Following MMTSO treatment, there is a reduction in the kinetic profile in both the basal (red line) and high glucose (pink line) in comparison to the controls (blue line and green line respectively). Black significant values correspond to the comparison with control and 100 µM MMTSO in basal glucose; the light blue significant values correspond to the comparison with control and 100 µM MMTSO in high glucose. n.s. = not significant, * = $p < 0.1$, ** = $p < 0.01$.

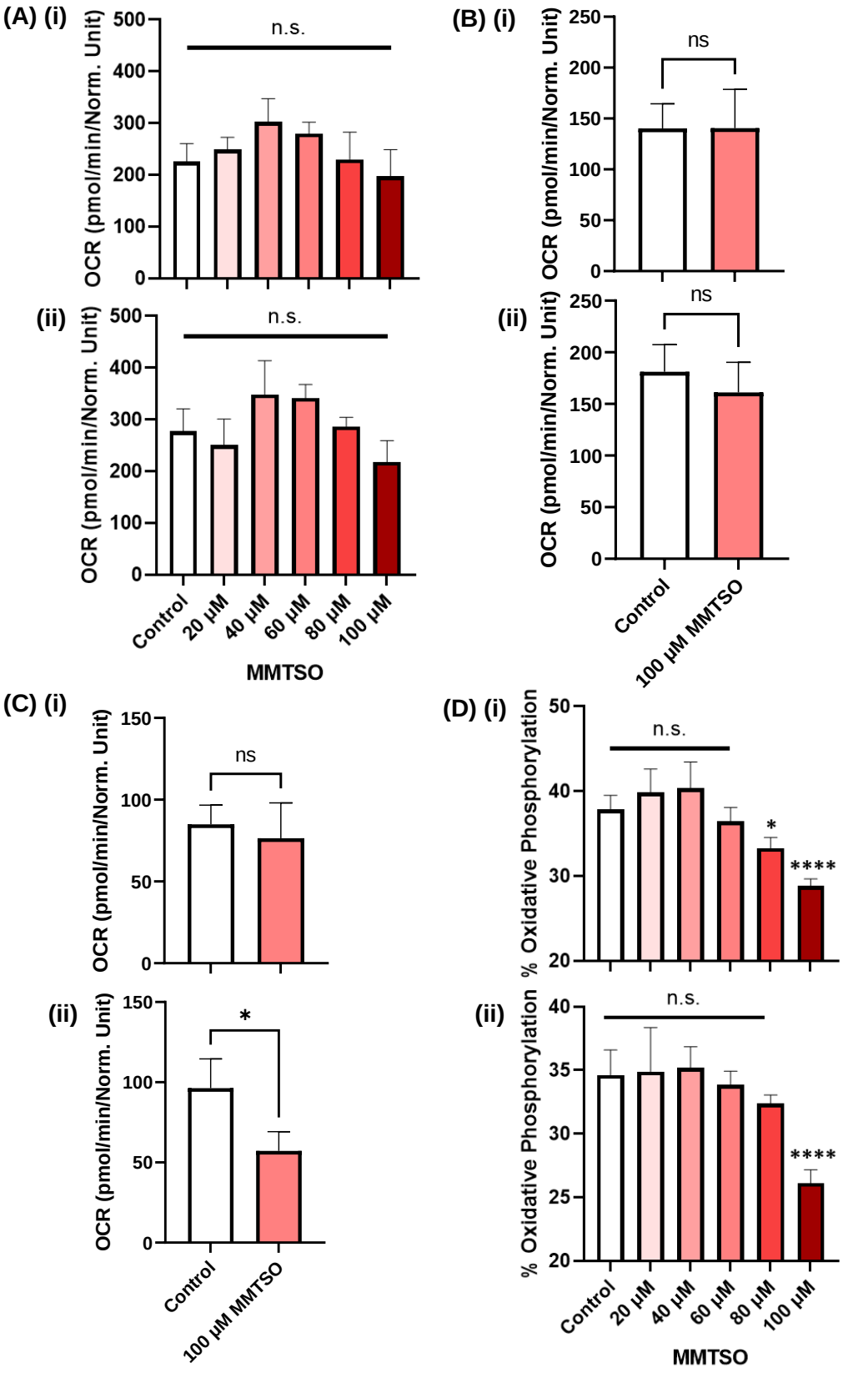

Figure 2.18. Real-time ATP test with MMTSO treatments. Briefly, the cells were cultured for 24-hours and a treated for a further 24-hours with vehicle, or MMTSO under basal 5.5 mM and high 25 mM glucose, before the real-time ATP test was used on the Seahorse XFe96 Bioanalyser. (A) Total ATP in (i) basal and (ii) high glucose, (B) Glycolytic ATP in (i) basal and (ii) high glucose, (C) Mitochondrial ATP in (i) basal and (ii) high glucose, (D) % oxidative phosphorylation in (i) basal and (ii) high glucose. Following 100 µM MMTSO treatment, there is a reduction in mitochondrial ATP and % oxidative phosphorylation compared to control. n.s. = not significant, * = $p < 0.1$, **** = $p < 0.0001$.

2.4.14 SMCSO and MMTSO reduced glycolysis under high glucose environment

To consider other metabolic pathways such as glycolysis on prostate metabolism, the glyco stress test was employed using the Seahorse XFp Bioanalyser. Briefly, DU145 cells were cultured for 24-hours and a treated for a further 24-hours with vehicle, or 100 µM SMCSO (Figure 2.19A), or 100 µM MMTSO (Figure 2.19B) under high 25 mM glucose environment, before the glycolysis stress test was used on the Seahorse XFp Bioanalyser. SMCSO and MMTSO exposure reduced glycolysis of DU145 cells compared to control, although only significant at 54 minutes in MMTSO treatment (Figure 2.19).

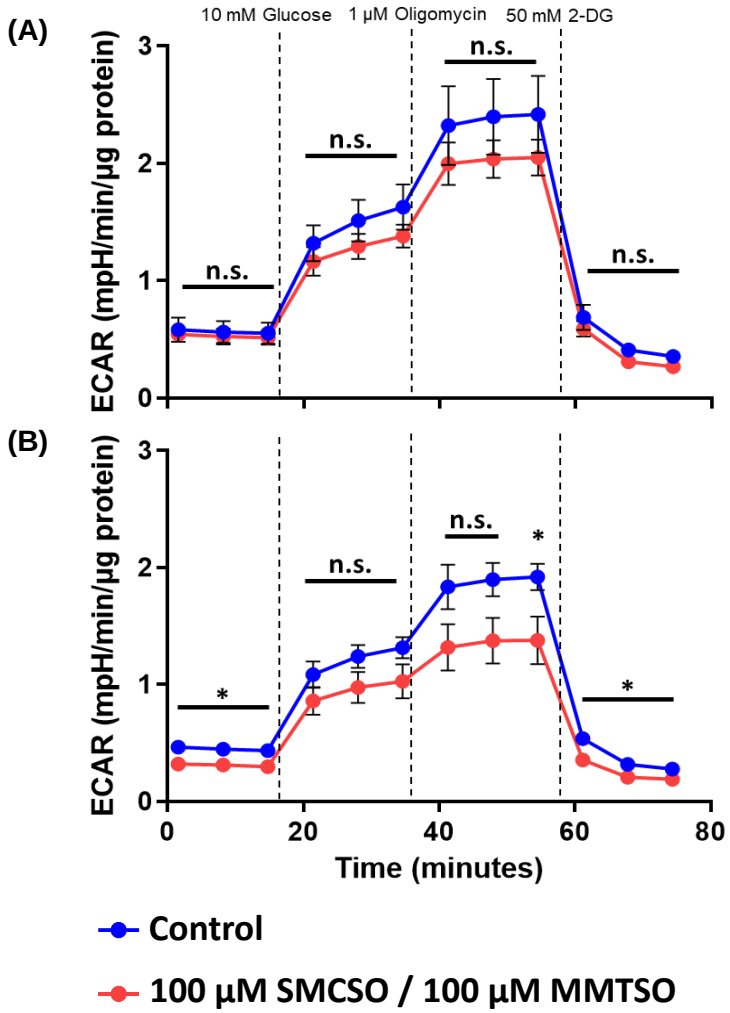

Figure 2.19. Glycolysis stress tests with SMCSO and MMTSO treatments. Briefly, the cells were cultured for 24-hours and a treated for a further 24-hours with vehicle, or 100 µM SMCSO or 100 µM MMTSO under high 25 mM glucose, before the glycolysis stress test was used on the Seahorse XFp Bioanalyser. SMCSO (A) and MMTSO (B) exposure reduced glycolytic ability, although only significant at 54 minutes in MMTSO treatment. n.s. = not significant, * = $p < 0.1$.

2.4.15 MMTSO increased fatty acid dependency but not glutamine or glucose dependency compared to control

To further consider other metabolic pathways such as glutamine and fatty acid metabolism, the mito fuel flex kit was utilised using the Seahorse XFe96 Bioanalyser. Briefly, DU145 cells were cultured for 24-hours and a treated for a further 24-hours with vehicle, or 100 µM MMTSO under basal 5.5 mM glucose, before the mito fuel flex test was used on the Seahorse XFe96 Bioanalyser. The measurement of cells' reliance on glutamine, fatty acid or glucose pathways to maintain baseline respiration (dependency) was assessed. Following 100 µM MMTSO treatment, there was a reduction in OCR kinetic profile in glutamine (Figure 2.20A), fatty acid (Figure 2.20B) and glucose (Figure 2.20C) pathways, compared to the control. There is no difference with glutamine and glucose dependency (Figure 2.20D and 2.20F respectively), however, there is an increased dependency with fatty acid pathway to maintain baseline respiration following MMTSO treatment (Figure 2.20E).

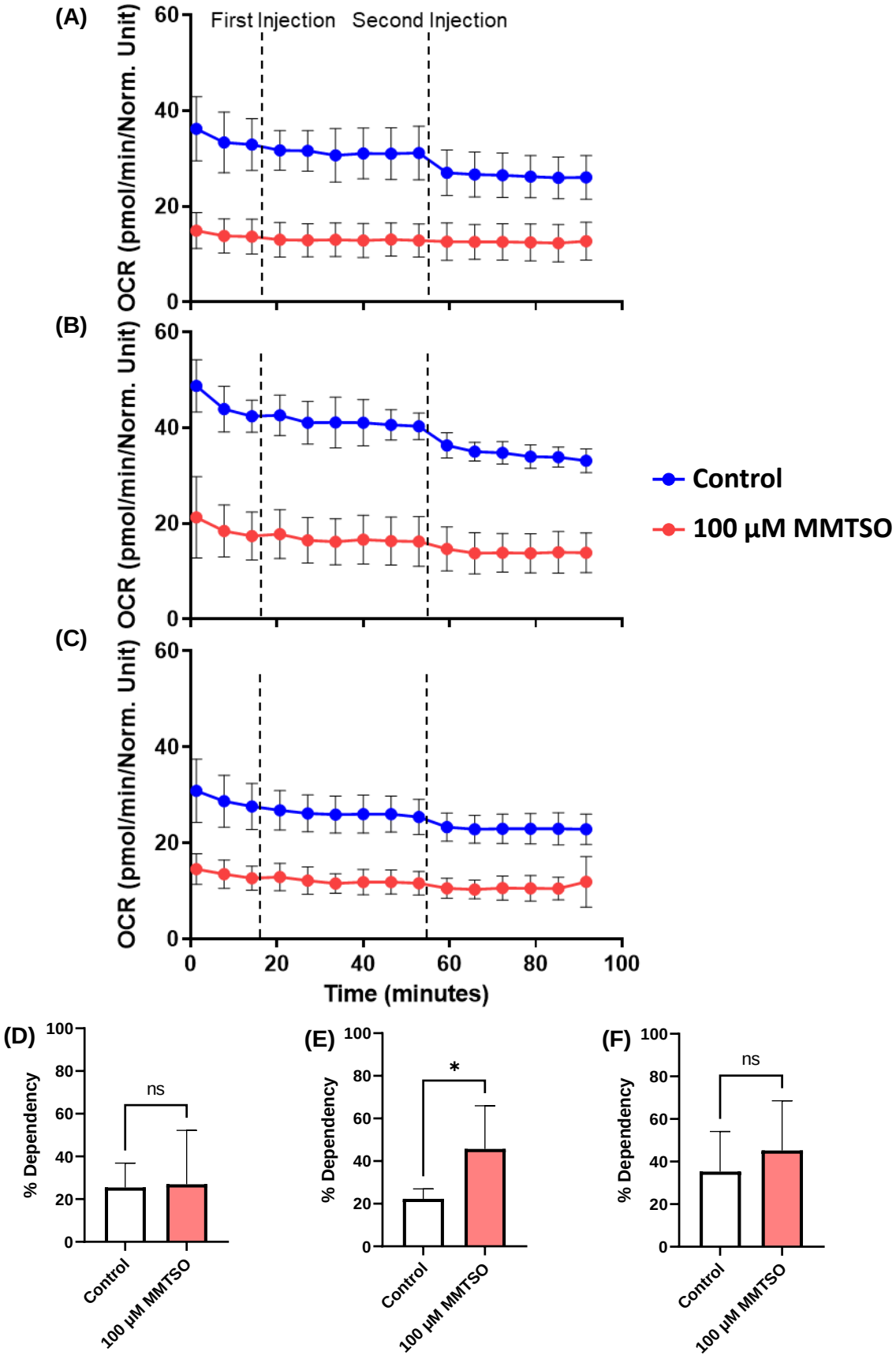

Figure 2.20. Mito fuel flex tests with MMTSO treatments. Briefly, the cells were cultured for 24-hours and a treated for a further 24-hours with vehicle, or 100 µM MMTSO under basal 5.5 mM glucose, before the mito fuel flex was used on the Seahorse XFp Bioanalyser. Kinetic profile and % dependency of (A and D) glutamine, (B and E) fatty acid, (C and F) glucose. MMTSO compared to control, leads to increased dependency with fatty acid pathway. n.s. = not significant, * = $p < 0.1$.

2.5 Discussion

Whilst epidemiological studies have indicated a negative association between consumption of cruciferous vegetables and cancer metabolism (85, 86, 91, 170-172), much of this evidence has focused on sulforaphane, with very little evidence of the potential molecular effects of S-methyl cysteine sulfoxide (SMCSO) and its metabolite S-methyl methanethiosulfonate (MMTSO). Here, SMCSO and MMTSO were administered to DU145 prostate cancer cells to evaluate the molecular effects of these bioactive compounds on prostate cancer energy metabolism.

With limited molecular research, careful consideration was taken with the design of the in vitro experiments, especially concerning the concentrations of the compounds. Due to the location of the prostate and potential exposure from urinary reflux, urine concentration could be the most appropriate approximation for physiological concentration of SMCSO and MMTSO (155). Regarding SMCSO, a previous dietary intervention involving consumption of broccoli soups, was reported in urine up to concentrations ~100 μM and due to potential urinary reflux of SMCSO to the prostate (25), treatment of 100 μM SMCSO was selected. Regarding MMTSO, despite the ongoing development of detection methods for bioactive compounds, there is currently no published quantification method for MMTSO, and so it has not been measured in urine, plasma or tissue samples. Thus, the physiologically relevant concentration of MMTSO remains speculative, and concentrations used within this chapter (10 μM and 100 μM) did not affect cell viability and allow for proof-of principle analysis of the metabolite.

Another consideration to experimental design concerned the glucose environment of cultured cells. Since high glucose supports tumour progression through increased cell proliferation, promotes inflammation and increased oxidative stress (133), increasing levels of glucose concentration were explored in combination with the sulfur compounds: basal (5.5 mM), intermediate (10 mM) and high (25 mM). Pharmacokinetic analysis reported SMCSO concentration peaked in plasma at 1.5 hours post broccoli soup consumption (99). A similar peak is seen in postprandial glucose spike after a meal (173), thus combining the sulfur metabolites and different glucose environments could be physiologically relevant in a normal dietary response to consumption of a meal with cruciferous vegetables.

Cell viability assessment was conducted to select a non-toxic and potentially physiologically relevant concentration for further mitochondrial energy assessment. From this assessment, there was no effect of SMCSO on WST-1 assay or on percentage of live cells, however MMTSO elicited a significant decrease at doses over 250 µM in the basal and intermediate glucose and over 175 µM in the high glucose environment. We could hypothesise that SMCSO may not demonstrate bioactivity on its own and it is the breakdown compound of SMCSO, MMTSO, that elicits the effect. This hypothesis has been suggested previously within published literature (117, 123). Assessment of mitochondrial metabolism between normal PNT1A cells and cancer DU145 cells reported higher OCR for DU145 cells compared to PNT1A, similar studies have reported this increased energy turnover of cancerous cells (77). There is emerging evidence that mitochondria play a key role in tumour progression, cell proliferation, and metastatic ability of prostate cancer (77, 174). With mitochondrial stress testing, MMTSO at 100 µM, not SMCSO, significantly reduced mitochondrial metabolism, particularly in the high glucose environment (2-fold decrease compared to control). This reduction could be explained as thiosulfonic compounds (like MMTSO) have been shown to bind strongly and selectively to STAT3-SH2 domain and showed modest antiproliferative and cytotoxic effect on the colon cancer cell line, HCT-116 (175). Thus, suggesting the STAT3-SH2 interaction with MMTSO, associated with mitochondrial pyruvate metabolism and activation of target genes (175, 176), leads to the reduced mitochondrial function, reduced cell proliferation and increased apoptosis.

From assessment of metabolic pathways, MMTSO not SMCSO reduced mitochondrial ATP, percentage of oxidative phosphorylation, reduced glycolysis in the high glucose environment, suggesting MMTSO is reducing the metabolic capacity of the DU145 prostate cancer cells leading to potential metabolism reprogramming. The evidence observed with SMCSO is in agreement with one cell-based study that also demonstrated SMCSO treatment led to no significant changes to mitochondrial or glycolytic function in prostate cancer cell lines (124). Different outcomes were demonstrated when different cell lines were used. For example, another cell based study demonstrated that exposure of MMTSO to human liver cancer cells (HepG2) decreased mitochondrial potential (123). These studies and the evidence presented in this chapter demonstrate MMTSO modulates energy metabolism in prostate cancer cells.

Previous studies have indicated that inhibition of mitochondria ATP synthase leads to reduced prostate cancer growth in prostate stromal cells (174), thus further investigation of whether MMTSO is acting on specific proteins is warranted. Whilst there is limited existing evidence of the biological activity of SMCSO and MMTSO, these were not specific to prostate cancer and much of this research focused on antidiabetic effects in rats (129-131, 142) and MMTSO as a potential chemopreventative agent in human liver tumours in rats (128). This is the first evidence that the metabolite of SMCSO, MMTSO, could have biological activity and demonstrate a dynamic shift in mitochondrial metabolism in DU145 prostate cancer cells. This is explored further at a gene and metabolite level in Chapter 3 and 4.

An increased dependency of fatty acid metabolism in DU145 prostate cancer cells following MMTSO treatment was observed. With the unique prostate cancer metabolism, it is able to utilise more fatty acids via beta-oxidation to feed into the TCA cycle to produce more ATP in order to meet the high energy demands (36), and fatty acids are commonly upregulated in prostate cancer (164). Thus, suggesting that in the presence of MMTSO, the DU145 cells become more dependent on fatty acid regulation to maintain baseline respiration. Although limited to in vitro analysis, this chapter investigated potential fundamental and molecular effects these compounds may have in vivo.

Thiosulphinates isolated from the garlic chive, including S-methyl methanethiosulfinate (MMTSI, the precursor compound before disproportionation to MMTSO), reported to have promising inhibitory effects on proliferation of human prostate and colon cancer cell lines through both caspase-dependent and caspase independent apoptosis pathways (120-122). Interestingly, allicin another organosulfur compound with a similar structure to MMTSO exhibited inhibition of MMP-2 and MMP-9 expression leading to inhibition of cell proliferation and induced apoptosis (177). These studies provide evidence that similar compounds to MMTSO act on pathways relating to cell proliferation and apoptosis, suggesting MMTSO could also have similar properties and further studies are warranted.

Seahorse Bioanalysers and standardised kits offer key advantages for understanding of how dietary compounds influence metabolic analysis in real-time, live cell metabolism. The Seahorse XFp and XFe96 Bioanalysers were both used in this chapter (166-169). A major limitation of the XFp is the limited number of wells in the cell culture miniplate; out of the 8 wells in total, 2 are used for

background, allowing for comparison of one control and one treatment in triplicates. Whereas a major benefit of using the XFe96, allows for multiple comparisons on the same plate with more replicates; out of 96 wells in total, 4 are used for background, leaving 92-wells. One major benefit of using XFp, is that optimisation of certain compounds used such as fCCP, or cell number seeding would be more cost-effective on this machine, rather than running a full XFe96 plate that could be quite costly. Overall, it is beneficial to have the use of both machines as this allows for cost-effective optimisation and assessment of a single treatment on the Seahorse XFp; and more in-depth analysis of metabolic pathways with more compounds or more concentrations of one compound on the Seahorse XFe96.

2.6 Conclusion

This chapter gives a valuable insight into the molecular effects of SMCSO and MMTSO on prostate cancer metabolism, highlighting MMTSO (100 µM), not SMCSO (100 µM), significantly reduced mitochondrial metabolism, mitochondrial ATP and glycolytic rate, and increased fatty acid dependency, particularly in the high glucose environment, after a 24-hour treatment in DU145 prostate cancer cell line. The Seahorse Bioanalysers are useful for understanding of dietary metabolite and real-time metabolism interaction in prostate cancer cells. The Seahorse XFe96 has a major advantage over the XFp for increased number of wells (92 to 6) allowing for comparison of many treatments. Further work is needed to put context into these findings with transcriptomic and metabolomic profiling, to give a wider view of how these dietary compounds act within the cell.

Chapter Three.

Effects of SMCSO and MMTSO on global gene expression profiles of prostate cancer cells

Chapter Three: Effects of SMCSO and MMTSO on global gene expression profiles of prostate cancer cells

3.1 Introduction

The data presented in Chapter 2 provides the first direct evidence that the SMCSO metabolite MMTSO has potentially important biological activity; MMTSO, not SMCSO, elicited mitochondrial and metabolic effects in cultured DU145 prostate cancer cultured cells. This Chapter builds on the evidence presented in Chapter 2 and explores the role of SMCSO and MMTSO on gene expression profiles and key pathways in DU145 prostate cancer cells using next generation RNA-sequencing.

Over the last several decades, the use of omics approaches have made significant progress, for example in the ease with which omics approaches can be done, the quality of the generated data, and in terms of the costs. RNA-sequencing has become the dominant tool for transcriptome profiling especially within cancer research (178). The use of RNA-sequencing in cancer research has wider implications, not only giving evidence on differential gene expression analysis but also in detection of cancer biomarkers and therapeutic targets (178). For example, a potential prostate-specific biomarker, the androgen-reduced long noncoding RNA, PSLNR, was identified by RNA-sequencing (179).

The impact of sulfur-containing compounds on global gene expression of human cells has been reported across numerous cell lines including breast, colorectal and prostate (180-183), and also in tissues (24, 146, 184). These reports describe altered gene expression in cells and tissues exposed to sulforaphane and demonstrated that sulforaphane regulated genes involved in oxidative stress responses, metabolic processes and apoptosis (24, 146, 180-184). One recent human study (the ESCAPE study) investigated the effect of glucoraphanin on the transcriptomic profile of human prostate biopsies of men on active surveillance following a one-a-week broccoli soup consumption with increasing levels of glucoraphanin (low, intermediate and high) for 12-months (24). The authors used RNA-sequencing with prostate biopsies, and reported a significant suppression of cancer-related pathways including apoptosis, inflammatory response, and angiogenesis, and these changes were dose-dependent in line with the glucoraphanin content of the broccoli (24). A more recent human study (the Norfolk ADAPT study) provided evidence that the sulfur-metabolites, sulforaphane and alliin, were detected in prostate biopsies (26), and it was shown separately that

both metabolites altered the transcriptional pathways associated with prostate cancer and immune regulation (185). Interestingly, the SAP study reported that SMCSO was detected in the prostate tissue for both control and supplemented groups, and postulated that it may have come from the background western diet (25). To date there are limited published reports concerned with the potential biological activities of SMCSO and its major human metabolite MMTSO, on cancerous prostate cells, particularly for MMTSO.

There is one published report concerned with the possible effect of SMCSO on gene expression (186). The study reported that SMCSO did not affect the expression of genes that are induced by Nrf-2 in human liver cancer cells (HepG2) or mouse primary hepatocytes (186). There are currently no published reports of studies aimed to explore whether or not SMCSO or its metabolite, MMTSO, affect global gene expression in cancerous prostate cells which have a distinct metabolic phenotype compared to non-cancerous prostate cells. However, there is some evidence from in vitro studies that suggest they could influence transcription factors. Thiosulfonic derivates including MMTSO were able to interact with key transcription factor STAT3, bind strongly to the STAT3-SH2 domain, and cause cytotoxicity in cultured HCT-116 colon cancer cells (175), and it would seem likely that these effects would be associated with at least some changes in gene expression. A report of an in vitro study that investigated the effect of SMCSO and its metabolites on the transcriptomic profile of PNT1A (normal prostate epithelial cells), provided evidence that SMCSO and MMTSO treatments caused transcriptional changes in PNT1A cells, although only a small number of changes were significant (SMCSO treatment, 14 upregulated and 19 downregulated genes; MMTSO treatment, 9 upregulated and 7 downregulated genes) (123). The 33 genes differentially expressed in PNT1A cells in response to SMCSO treatment were further assessed by the authors using database and gene ontology analysis and this identified cellular response to oxidative stress and cellular response to oxidation-reduction processes as significantly altered processes (123). Despite this evidence, the transcriptomic effect of SMCSO and its metabolite MMTSO has not been explored in prostate cancer cells.

Use of RNA-sequencing to investigate difference between normal and cancerous prostate tissue has identified a huge number of mutations in tumours that are associated with and are likely the cause of the uncontrolled gene expression (187). Of particular interest were mutations in and dysregulation of the phosphatase and

tensin homolog gene (PTEN). PTEN, a tumour suppressor gene located on chromosome 10q23, is the most frequent deleted or mutated gene found present in prostate cancer cases (188). Interestingly deletion at the 10q23 locus is the most common form of PTEN inactivation (189), leading to the hyperactivation of the PI3K/AKT/mTORC1 signalling pathway and promoting cancer proliferation (190). Recent in vitro studies reported sulforaphane (2 and 5 μM) and SMCSO (20, 50 and 100 μM) pre-treatment prior to hydrogen peroxide exposure did not protect PTEN redox status against oxidative stress, nor significantly change mitochondrial reactive oxygen species (ROS) production in PNT1A cells (124). These data suggest evidence of no significance of a protective or antioxidative effect from SMCSO in normal prostate epithelial cells. However, no studies have reported on prostate cancer cell lines, and there are no reports of the effects of MMTSO. Since it has been shown that MMTSO (but not SMCSO) has the capacity to alkylate thiols (191-193), it increases the likelihood that MMTSO may have specific effects on cellular antioxidant networks and oxidative stress, and further justifies the need for studies of the effects of MMTSO on gene expression and other important cellular processes.

3.2 Aims

The overall aim was to explore the effects of sulfur-containing compounds SMCSO and MMTSO on the transcriptomic profile of human prostate cancer cells:

- To quantify the effects of SMCSO and MMTSO treatments on the global transcriptional profile of DU145 prostate cancer cells in different glucose conditions.
- To determine the effects of SMCSO and MMTSO treatments and glucose conditions on cellular and metabolic pathways by interrogating the transcription profiling data with the Hallmark database.
- To assess the interplay between glucose environment and responses of DU145 human prostate cancer cells to SMCSO and MMTSO treatments.

3.3 Materials and Methods

3.3.1 Cell Treatments

DU145 cells were cultured in standard conditions for 48-hours to allow for adherence and growth to 70-80 % confluency. Once the cells reached the required confluency, the appropriate treatment or vehicle control was added (previously described in 2.3.1 and 2.3.2, Chapter 2). The appropriate treatment or vehicle control were added in replicates of five diluted in cell culture medium either under basal glucose environment of 5.5 mM, or high glucose environment of 25 mM for a further 4-hour or 24-hour incubation, Figure 3.1.

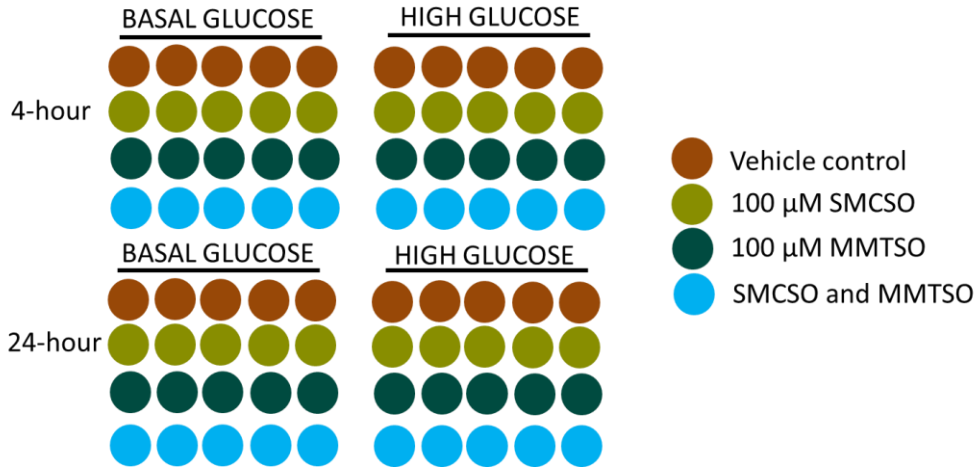

Figure 3.1. Treatment template for transcriptomic analysis. Briefly, cells were cultured for 48-hours under standard conditions before a further 4-hour or 24-hour incubation with the vehicle control (water, brown circles), or appropriate treatment: 100 µM SMCSO (olive circles), 100 µM MMTSO (dark green circles) or 100 µM SMCSO + 100 µM MMTSO (blue circles) in replicates of five.

3.3.2 RNA extraction from DU145 cells

The treatment medium was removed from the DU145 cells, and 700 µl of QIAzol lysis reagent (Qiagen) was added to each well. Each well was scraped with a cell scraper and the cell lysate transferred to an RNAse free Eppendorf tube. All tubes were stored at -80 °C until the day of extraction. Total RNA was extracted from all samples on the same day using Qiagen RNeasy mini kit and QIAzol extraction protocol according to the manufacturer's instructions. Total RNA concentration and quality was assessed using Nanodrop™ spectrophotometer (ThermoFisher®) to determine the RNA yield and 260/280 ratio. All samples were stored at -80 °C until day of submission.

3.3.3 RNA-Sequencing of DU145 cells

The prepared samples were sent to Macrogen Europe. Once at the facility, the samples were checked for quality and quantity with only suitably high quality RNA samples sent for sequencing i.e. only samples with an RNA integrity number (RIN) value of > 7 and quantity of 1 µg were carried forward for sequencing. All eighty samples were sent for TruSeq Stranded mRNA Library Preparation poly(A) selection sequencing, performed on an Illumina NovaSeq 2x using 150 base paired-end reads generating 30 million paired-end reads per sample.

3.3.4 Data Processing and Filtering

The data processing was performed with support from QIB bioinformation Dr. Perla Rey following the protocol for the 'New Tuxedo' (194) and using the high performance computing environment (195), that provided tools for alignment of reads to the reference genome, assembly of transcripts and quantification of gene expression.

The RNA-Sequencing analysis comprised of three main processes: (I) processing the raw RNA-sequencing reads to give an approximation of gene counts, (II) relative analysis of the gene counts to give quantification of the differentially expressed genes, and (III) functional analysis using gene set enrichment analysis of the differentially expressed genes, Figure 3.2.

The first process involved the raw reads being assessed for quality using FASTQC (version 0.11.9) before removal of adapter sequences, low quality reads <30, and reads shorter than 60 bp using FASTP (version 0.23.1). The high-quality reads were mapped to the human reference genome using HISAT2, (version 2.1.0), and further assembled into full length transcripts using StringTie (version 1.2.2), to estimate the expression levels of all known genes. After the initial assembly, the transcripts were merged to create a set of transcripts for all samples, and these were compared to the reference human annotation using gffcompare (version 0.9.8). The merged transcripts were used to create gene counts for further analyses. In the second process, the gene counts were scale transformed, further filtered for outliers and low expressed genes were removed. This reduced the memory size of the data and increased the speed of the subsequent analysis. The gene counts were taken for analysis of differential gene expression using R Studio (version 4.2.1), and the DESeq2 package (version 1.24.0) (196). The gene expression data contained 60,617 genes, which included all genes in the assembly

such as protein coding genes and non-coding genes. A filter was applied to keep only genes with a minimum of 10 counts for at least 5 samples. In the final process, the differentially expressed genes were ranked and taken forward for gene set enrichment analysis (GSEA) of enriched pathways.

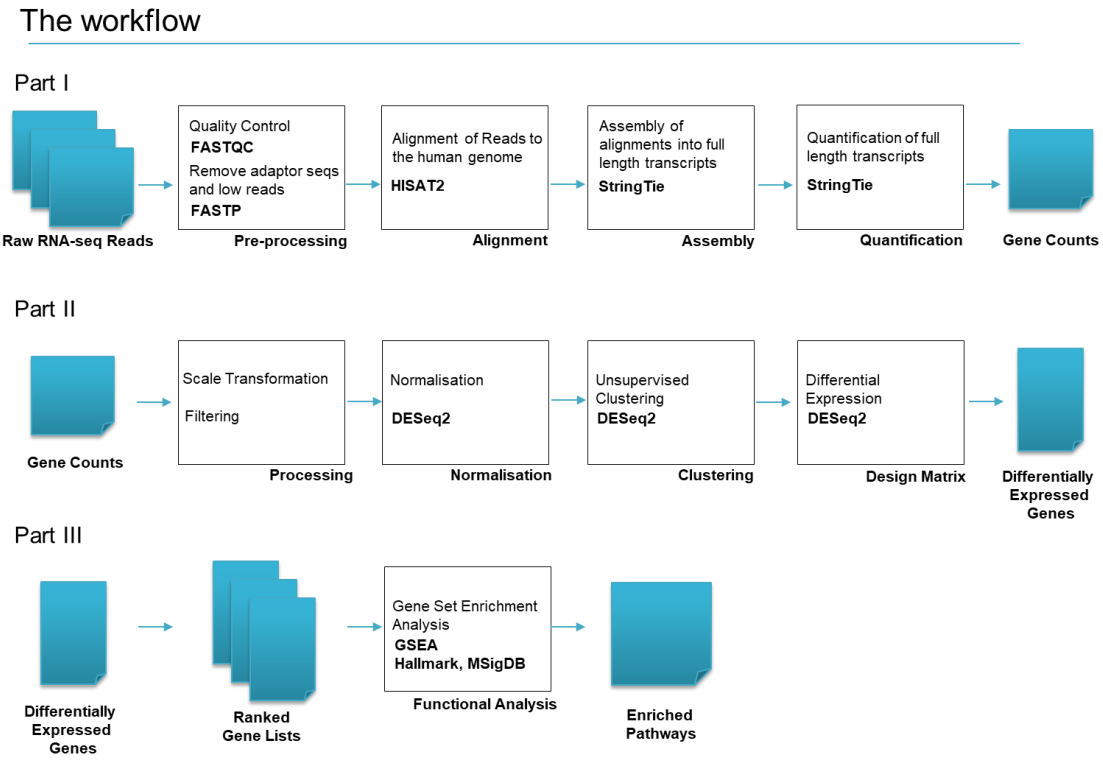

Figure 3.2. The workflow used for RNA-Sequencing data analysis. Briefly, Part I allowed the assessment of gene counts from the raw RNA-sequencing reads, Part II generated the differentially expressed genes from the gene counts, Part III produced enriched pathway analysis from the differentially expressed genes.

3.3.5 Exploratory Analysis of Gene Expression

To visualise similarities and differences between samples, principal component analysis (PCA) and Poisson plots were used. For the PCA plots, each data point represented the expression profile of each sample examined onto the first few components to visualise distribution between samples in an unsupervised manner using VST transformed data (197). Poisson plots allowed for visual distances between samples, taking the raw gene counts and measuring the dissimilarity between the samples. The Poisson dissimilarity matrix is calculated using the Poisson Distance function from the library PoiClaClu version 1.0.2.1 (198).

3.3.6 Differential Gene Expression Analysis

Differential expression analysis, using DESeq2, used the input of unnormalised gene expression data where each point indicated the number of reads mapped to a gene in each sample (196). Each time point was inputted separately to test for the main effect of the treatments SMCSO and MMTSO on transcriptional profiles.

The Wald test was used to estimate differentially expressed genes between the individual treatment groups (SMCSO, MMTSO) with the design: = ~treatA + treatB, where ~treatA specified the effect of MMTSO, comparing samples treated with MMTSO vs. non-MMTSO, and treatB specified the effect of SMCSO, comparing samples treated with SMCSO vs. non-SMCSO. The Likelihood Ratio Test was used to estimate the differentially expressed genes between SMCSO and MMTSO and to assess any significant interactions between SMCSO and MMTSO with the design = ~treatA + treatB + treatA:treatB. SMCSO and MMTSO in combination increased the power of the study and allowed for treatment vs. non-treatment comparison. The statistically significant genes were corrected for multiple testing and for false discovery rates through the Benjamini Hochberg correction.

The differential expression analysis generated $\log_2$ fold change (Log_2FC) values to visualise fold changes and assess the degree of gene expression changes of treatment groups. A negative Log_2FC value demonstrated a gene downregulated by the treatment; a positive value demonstrated a gene upregulated by the treatment. This data was used to generate mean average (MA) plots. Briefly, the MA plots are scatter plots that plot log fold change on vertical axis and log of the mean of normalised expression counts of all samples on the horizontal axis. They allowed the visualisation, identification and degree of gene expression changes. Genes with no significant difference in expression clustered around the 0 value, genes with significant difference clustered away from the 0 value and indicate the degree of genes downregulated (below 0) or upregulated (above 0) from the treatment.

3.3.7 Functional Gene Expression Analysis

The functional analysis of differential gene expression was conducted. The differential gene expression data were ranked using the rank-rank geometric overlap algorithm to attain a rank metric score for each gene (199). The genes were ranked from taking the log fold change multiplied by the log10-transformed p-value. The ranked genes inputted into gene set enrichment analysis (GSEA)

software (version 4.2.3) (200), using the Hallmark gene set collections (version 2022) within the Molecular Signature Database (MSigDB) (201). GSEA generated normalised enrichment scores (NES) for each pathway; the NES reported the distribution of gene ontology across the ranked genes. The Hallmark database was selected as it represents well known biological pathways influenced in cancer. Statistical significance was defined as FDR-adjusted p-value (adj. p-value) of < 0.05, according to the Benjamini-Hochberg correction.

3.4 Results

3.4.1 Quality Control Statistics of RNA-sequencing reads

The RNA-sequencing reads were filtered, processed and aligned to the human reference genome before further subsequent analysis was conducted. This indicated good quality and alignment to the reference genome. Summary of percentage passed filter and overall alignment at 4-hour and 24-hour time points is shown in Figure 3.3.

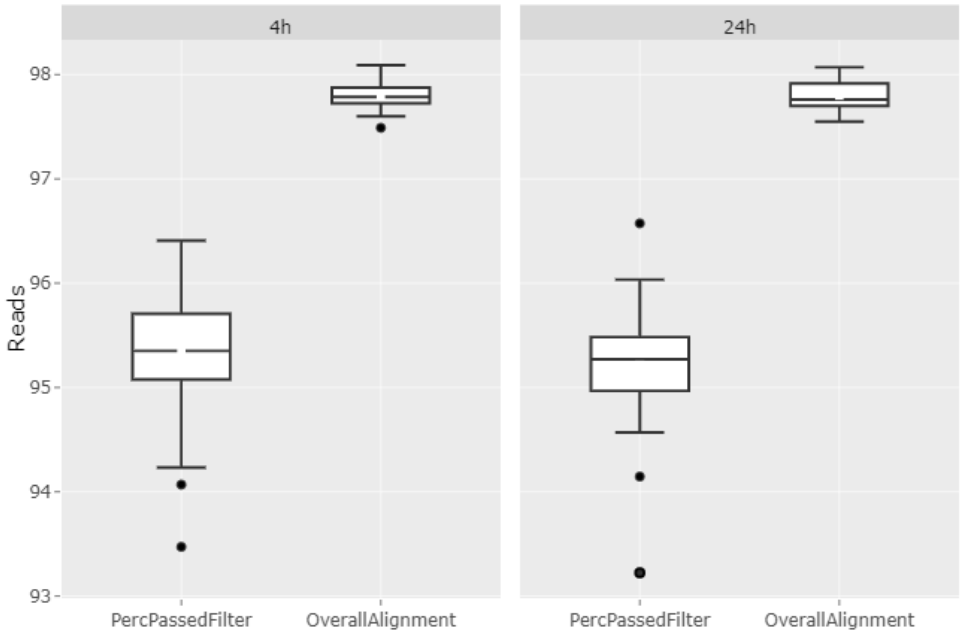

Figure 3.3: Quality Control Statistics. Briefly, the raw RNA-sequencing reads were taken for quality control, removal of adaptor sequences and low reads prior to alignment to the human reference genome. Summary of percentage that passed filter and percentage of overall alignment for 4-hour and 24-hour indicated good quality reads and good alignment to reference genome.

3.4.2 Distance analysis revealed similarities between 4-hour samples and 24-hour samples

To evaluate the sample distance between control and treatments, Poisson heatmaps were utilised. Poisson plots assess overall similarity between samples using sample-to-sample distances (198). Poisson distances use raw gene counts to assess the measure of dissimilarity between them. Within the plot, each sample is compared in a symmetrical manner. The dark clusters of samples (top left and bottom right in Figure 3.4) indicate similarities between gene expression in the samples although from multiple treatment groups.

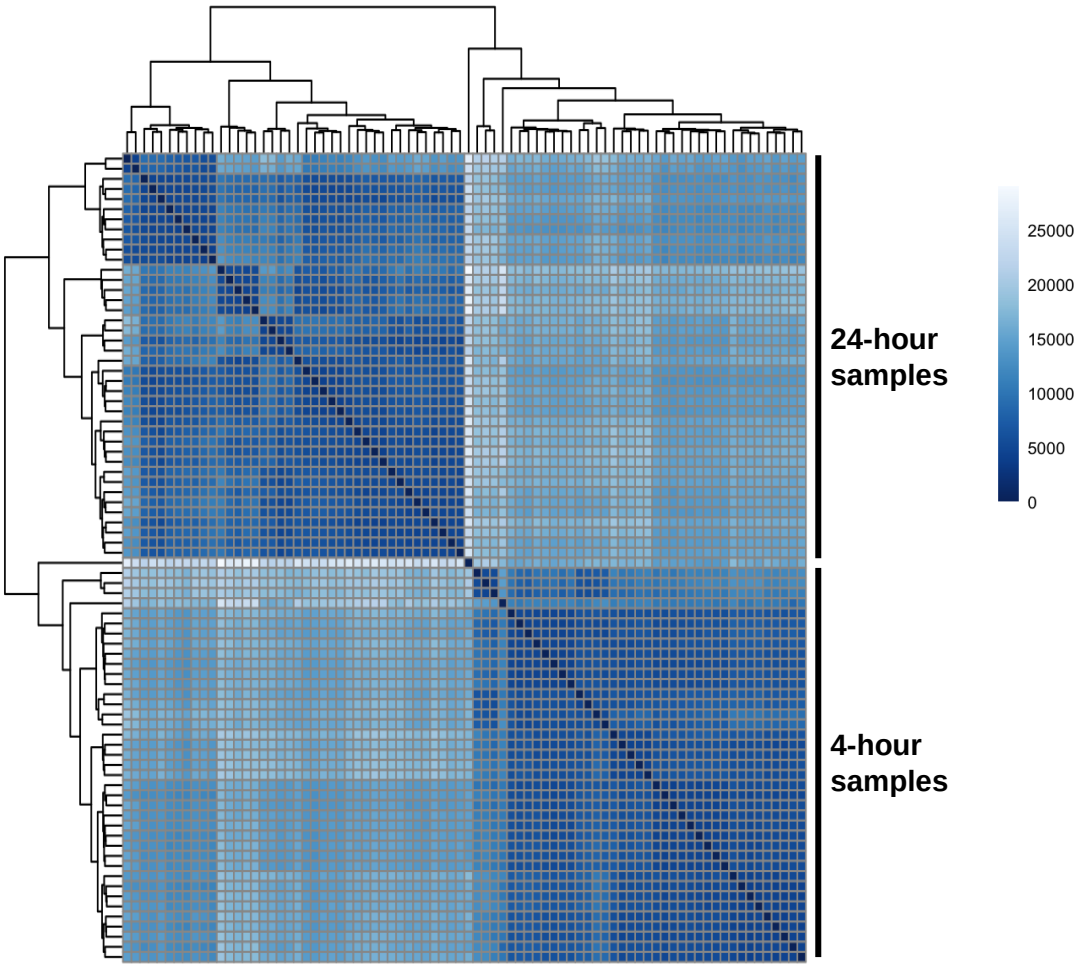

Figure 3.4: Heatmap of sample distribution using Poisson distances of all samples. The dark blue represents a low dissimilarity between samples; the light blue represents a large dissimilarity. In this case, the dark clusters of samples (top right and bottom right) indicate similarities between gene expression in the samples although from multiple treatment groups.

3.4.3 MMTSO treated samples clustered separately from non-MMTSO treated samples

To explore whether there was gene clustering between MMTSO and non-MMTSO samples, PCA plots were utilised. PCA plots also visualise sample-to-sample distances where likeness and variance between samples are demonstrated in an unsupervised manner, using the VST transformed data to ensure there is equal contribution from all genes (197). There was distinct clustering with MMTSO samples in basal glucose conditions at 4-hour (Figure 3.5A) and at 24-hour (Figure 3.5B), and in high glucose at 4-hour (Figure 3.6A) and at 24-hour (Figure 3.6B), compared to non-MMTSO treated samples. There was particularly tight clustering in the MMTSO samples in high glucose at 24-hour (Figure 3.6B). PCA plots were also employed to assess gene clustering between SMCSO and non-SMCSO samples, however there was no clear clustering with SMCSO samples compared to non-SMCSO samples at all time-points and under all glucose environments (Figure 3.7 and 3.8).

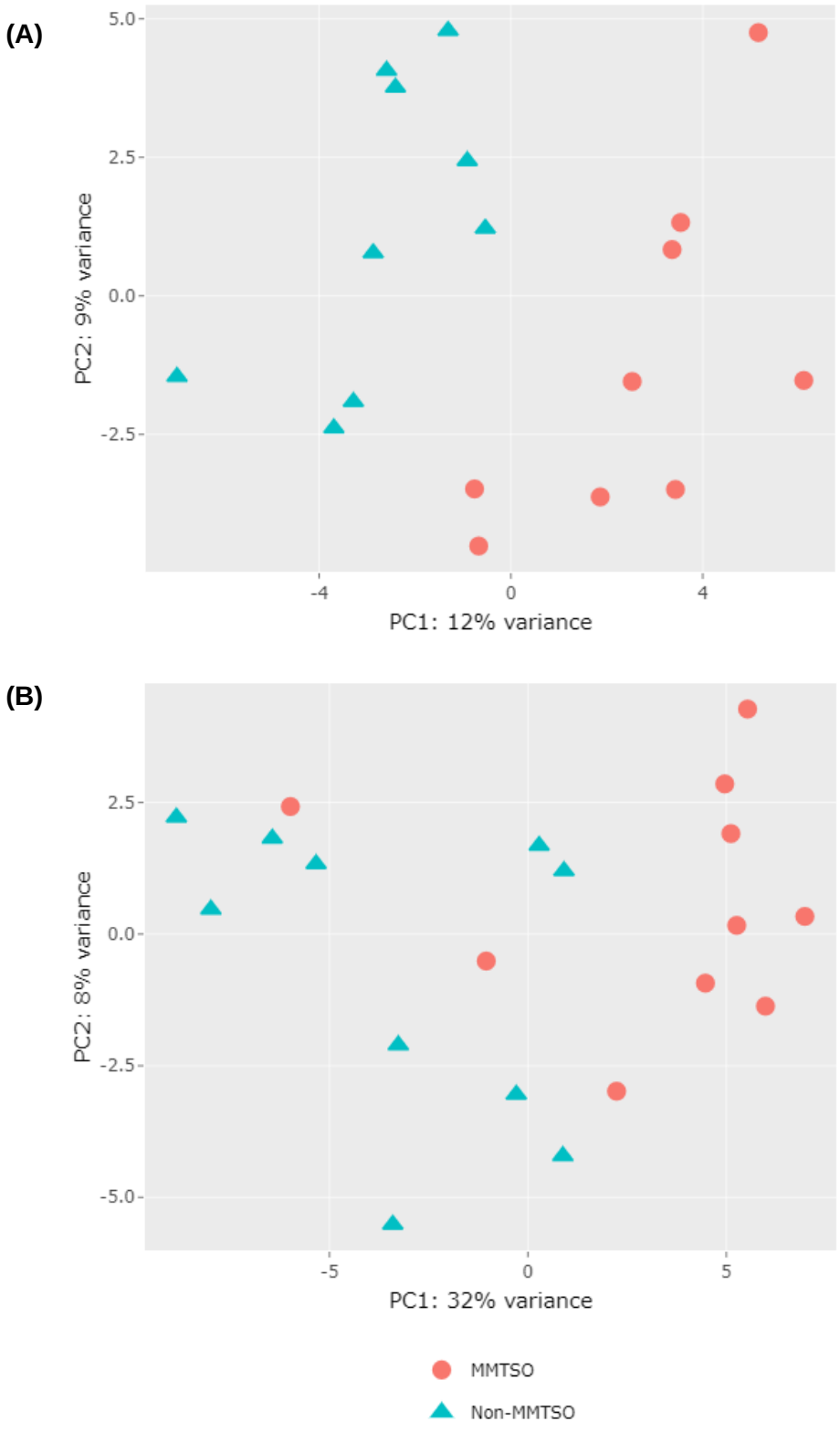

Figure 3.5. Principal component analysis (PCA) plots for MMTSO vs. non-MMTSO samples in basal glucose. Clustering is demonstrated in the MMTSO treatment (red circles) vs. non-MMTSO (blue triangles) in both time points at 4-hours (A) and 24-hours (B).

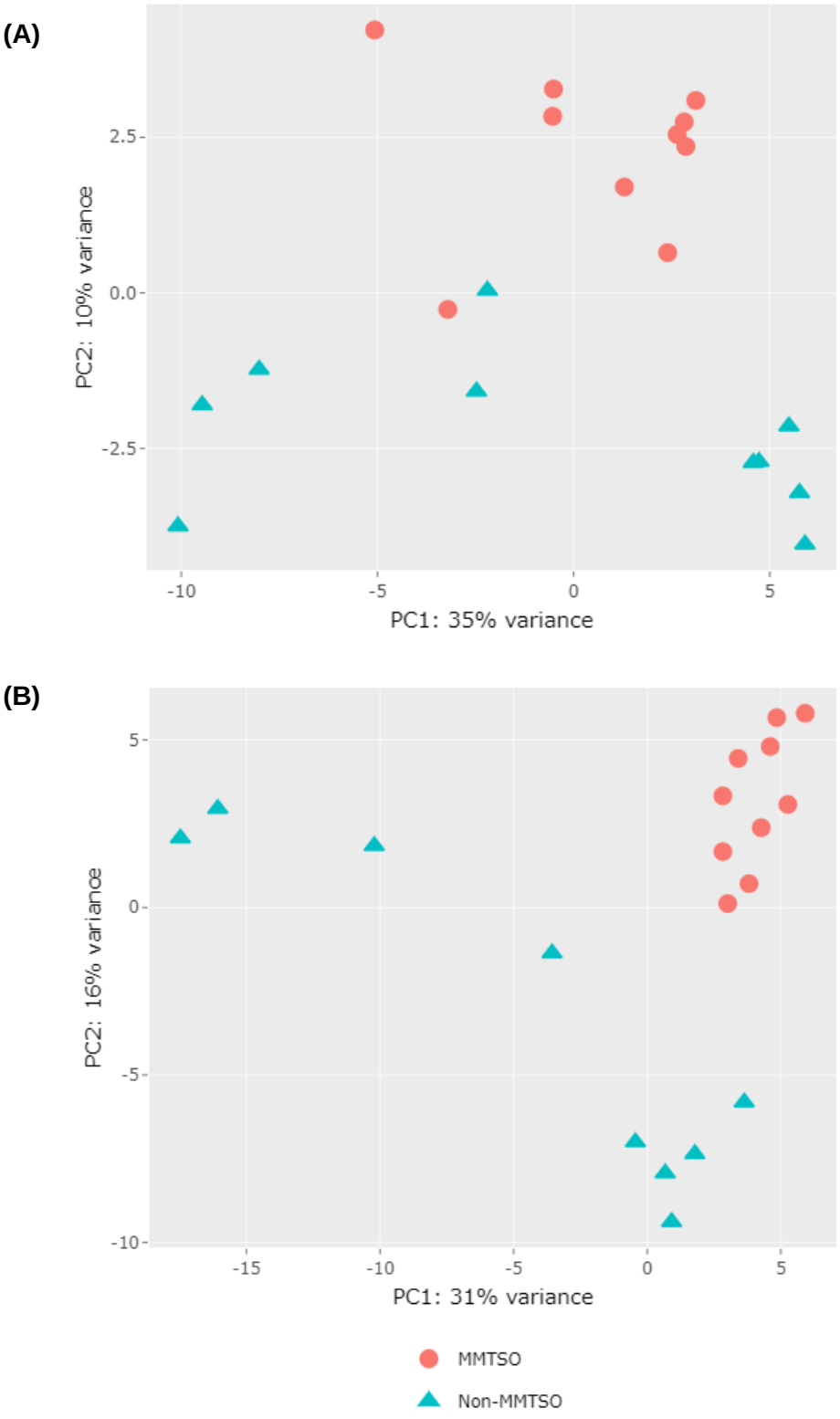

Figure 3.6. Principal component analysis (PCA) plots for MMTSO vs. non-MMTSO samples in high glucose. Clustering is demonstrated in the MMTSO treatment (red circles) vs. non-MMTSO (blue triangles) at 4-hours (A) and 24-hours (B); with particularly tight clustering demonstrated with MMTSO samples at 24-hour time point (B).

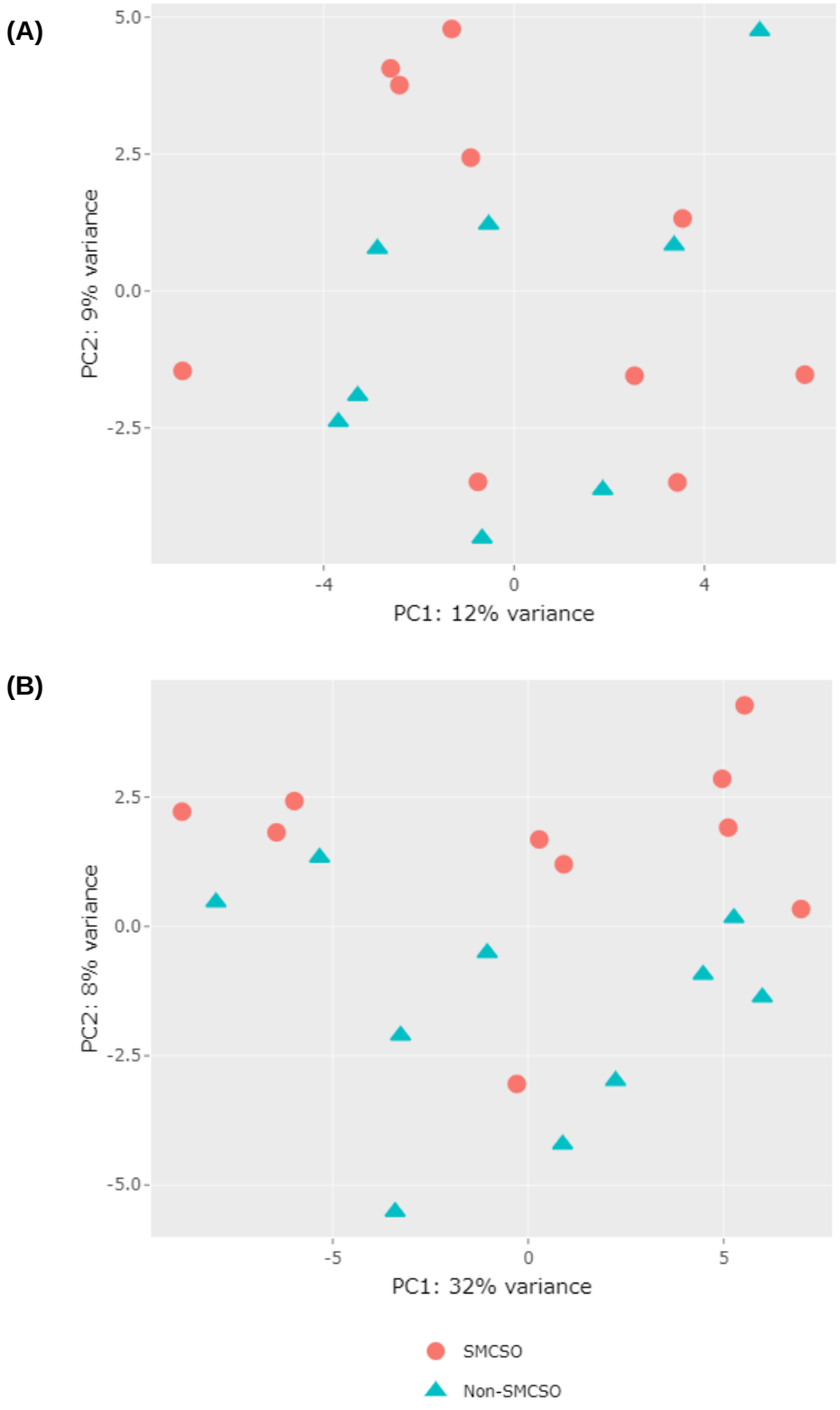

Figure 3.7. Principal component analysis (PCA) plots for SMCSO vs. non-SMCSO samples in basal glucose. No clear clustering is demonstrated in the SMCSO treatment (red circles) vs. non-SMCSO (blue triangles) at 4-hours (A) and 24-hours (B).

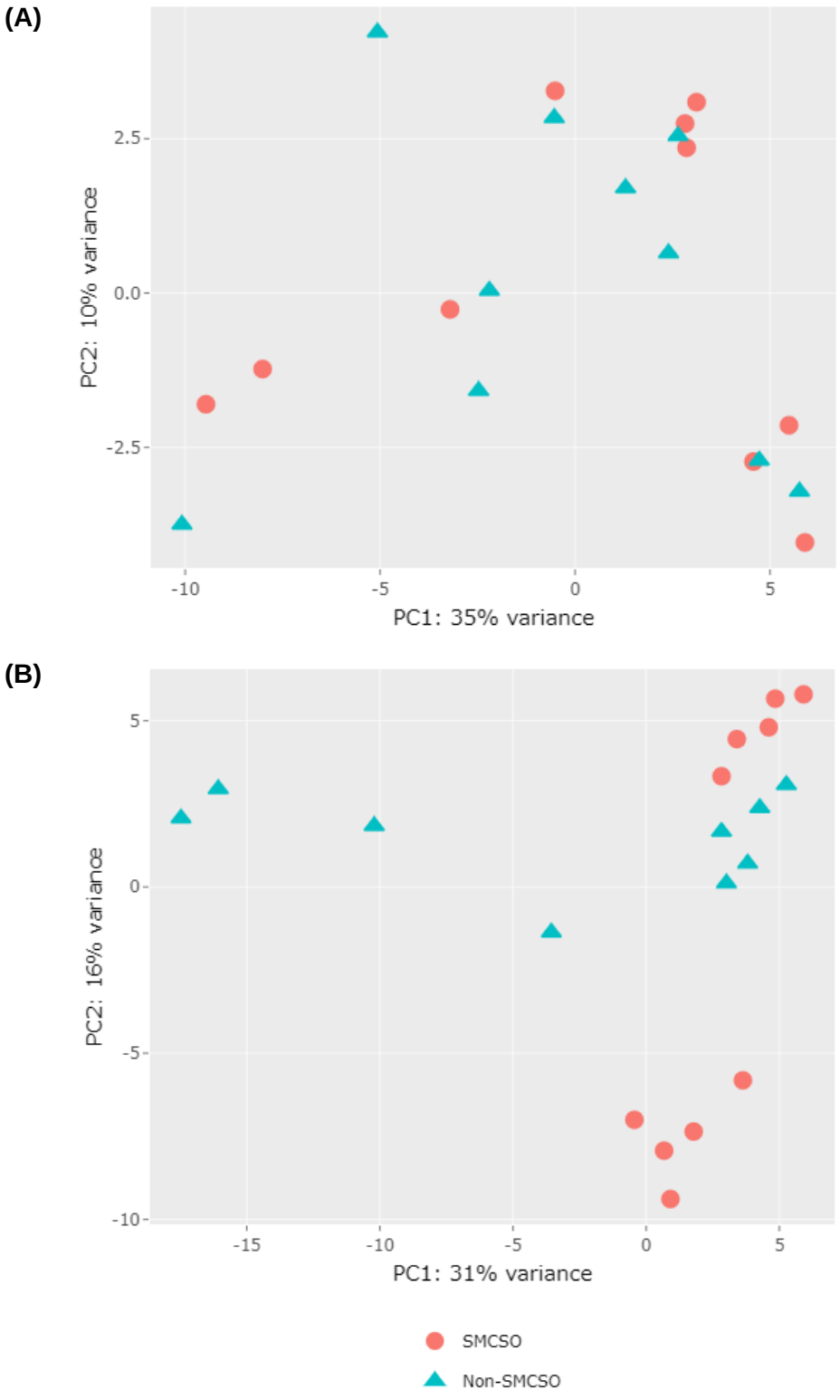

Figure 3.8. Principal component analysis (PCA) plots for SMCSO vs. non-SMCSO samples in high glucose. No clear clustering is demonstrated in the SMCSO treatment (red circles) vs. non-SMCSO (blue triangles) at 4-hours (A) and 24-hours (B).

3.4.4 MMTSO treatment gave rise to more differentially expressed genes

Differential gene expression analysis was conducted to explore gene expression changes between the treatment groups. Briefly, a MA plot was used to visualise the changes in gene expression in terms of log fold change (Y-axis), and the log of the mean of normalised expression counts over the samples (X-axis) where each blue dot represents the statistically significant differentially expressed genes (FDR-adjusted p-value < 0.05). Of the genes that passed Wald testing at 4-hours (19,418 in basal; 19,208 in high), MMTSO treatment, compared to non-MMTSO samples, resulted in a large number of differentially expressed genes in both glucose conditions (Table 3.1, Figure 3.9A and 3.9C). SMCSO treatment, compared to non-SMCSO samples, resulted in no differentially expressed genes in both glucose conditions (Figure 3.9B and 3.9D).

Table 3.1. Number of genes differentially expressed in response to MMTSO (compared to non-MMTSO) at 4-hours in basal and high glucose environment

FDR-adjusted p-value	MMTSO, Basal	MMTSO, High
≤ 0.1	3074 (↑1603 ↓1471)	3219 (↑1592 ↓1627)
≤ 0.05	2339 (↑1255 ↓1084)	2360 (↑1148 ↓1212)

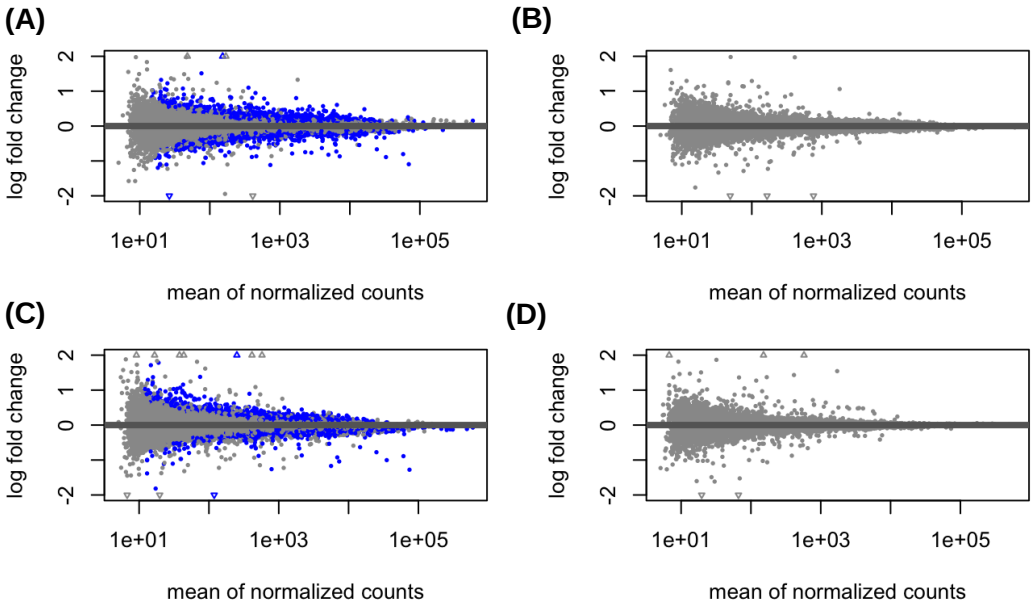

Figure 3.9. MA plots for differential expression at 4-hours for MMTSO and SMCSO treatment. (A) MMTSO vs non-MMTSO in basal glucose, (B) SMCSO vs non-SMCSO in basal glucose, (C) MMTSO vs non-MMTSO in high glucose, (D) SMCSO vs non-SMCSO in high glucose. The grey dots represent the genes; the blue dots represent the statistically significant differentially expressed genes correct to Benjamini-Hochberg. The triangles represent the genes that fall out of the y-axis. MMTSO treatment (compared to non-MMTSO) influences differentially expressed genes; SMCSO does not.

Of the genes that passed Wald testing at 24-hours (19,522 in basal; 19,504 in high), MMTSO treatment resulted in more differentially expressed genes in comparison to SMCSO, with substantially more in the high glucose environment (Table 3.2). At 24-hours, MMTSO treatment, compared to non-MMTSO samples in basal (Figure 3.10A) and high (Figure 3.10C) glucose demonstrated a large proportion of differentially expressed genes; SMCSO treatment, compared to non-SMCSO samples, in basal glucose (Figure 3.10B) had very few differentially expressed genes of significance (Table 3.2); however, in the high glucose (Figure 3.10D), there was significantly more differentially expressed genes.

Table 3.2. Number of genes differentially expressed in response to MMTSO and SMCSO (compared to non-MMTSO and non-SMCSO respectively) at 24-hours

FDR-adjusted p-value	MMTSO, Basal	MMTSO, High
≤ 0.1	3401 (↑1737 ↓1664)	8328 (↑4253 ↓4075)
≤ 0.05	2578 (↑1314 ↓1264)	7085 (↑3585 ↓3500)
	SMCSO, Basal	SMCSO, High
≤ 0.1	7 (↑4 ↓3)	3548 (↑1653 ↓1895)
≤ 0.05	7 (↑4 ↓3)	2237 (↑1004 ↓1233)

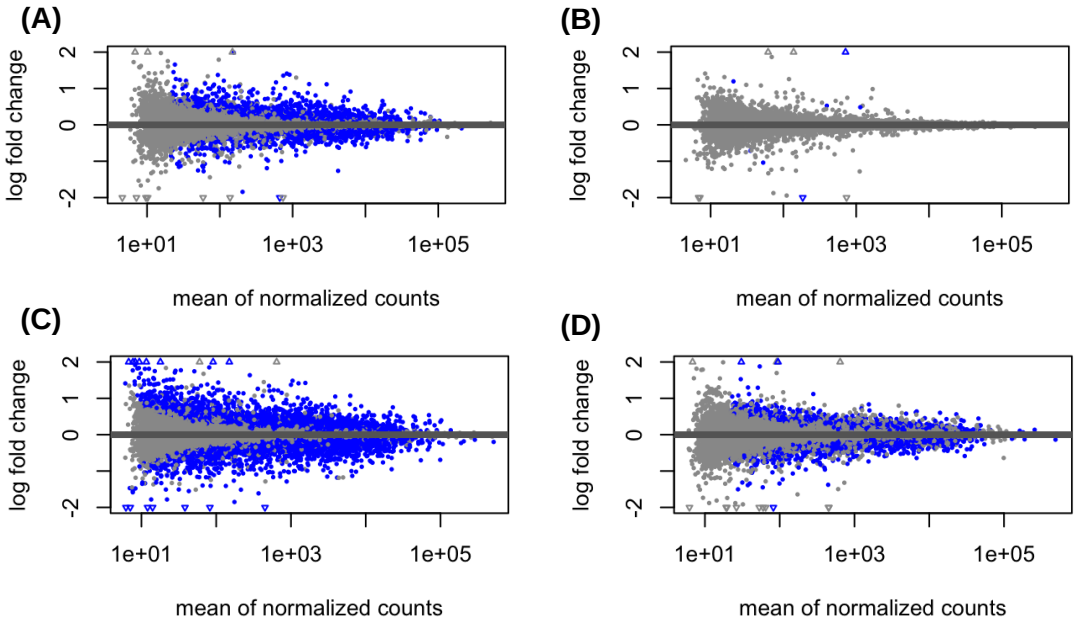

Figure 3.10. MA plots for differential expression at 24-hours for MMTSO and SMCSO treatment. (A) MMTSO vs non-MMTSO in basal glucose, (B) SMCSO vs non-SMCSO in basal glucose, (C) MMTSO vs non-MMTSO in high glucose, (D) SMCSO vs non-SMCSO in high glucose. The grey dots represent the genes; the blue dots represent the statistically significant differentially expressed genes correct to Benjamini-Hochberg. The triangles represent the genes that fall out of the y-axis. MMTSO treatment (compared to non-MMTSO) in basal and high glucose and SMCSO in high glucose demonstrate a significant number of differentially expressed genes.

Figures 3.9 and 3.10 highlight two observations; one that MMTSO samples appear to have a greater impact on the differential expression of genes than SMCSO samples; and the other that the high glucose environment led to more differentially expressed genes, especially with MMTSO treatment, compared to basal glucose environment.

3.4.5 MMTSO and to a lesser extent SMCSO significantly affected biological pathways

Gene set enrichment analysis (GSEA) using the Hallmark database was used to assess whether SMCSO or MMTSO treatment influenced biological pathways in DU145 cells. Initially, enrichment plots were generated to assess the profiles of the gene sets in response to the treatment and glucose environment, Figure 3.11.

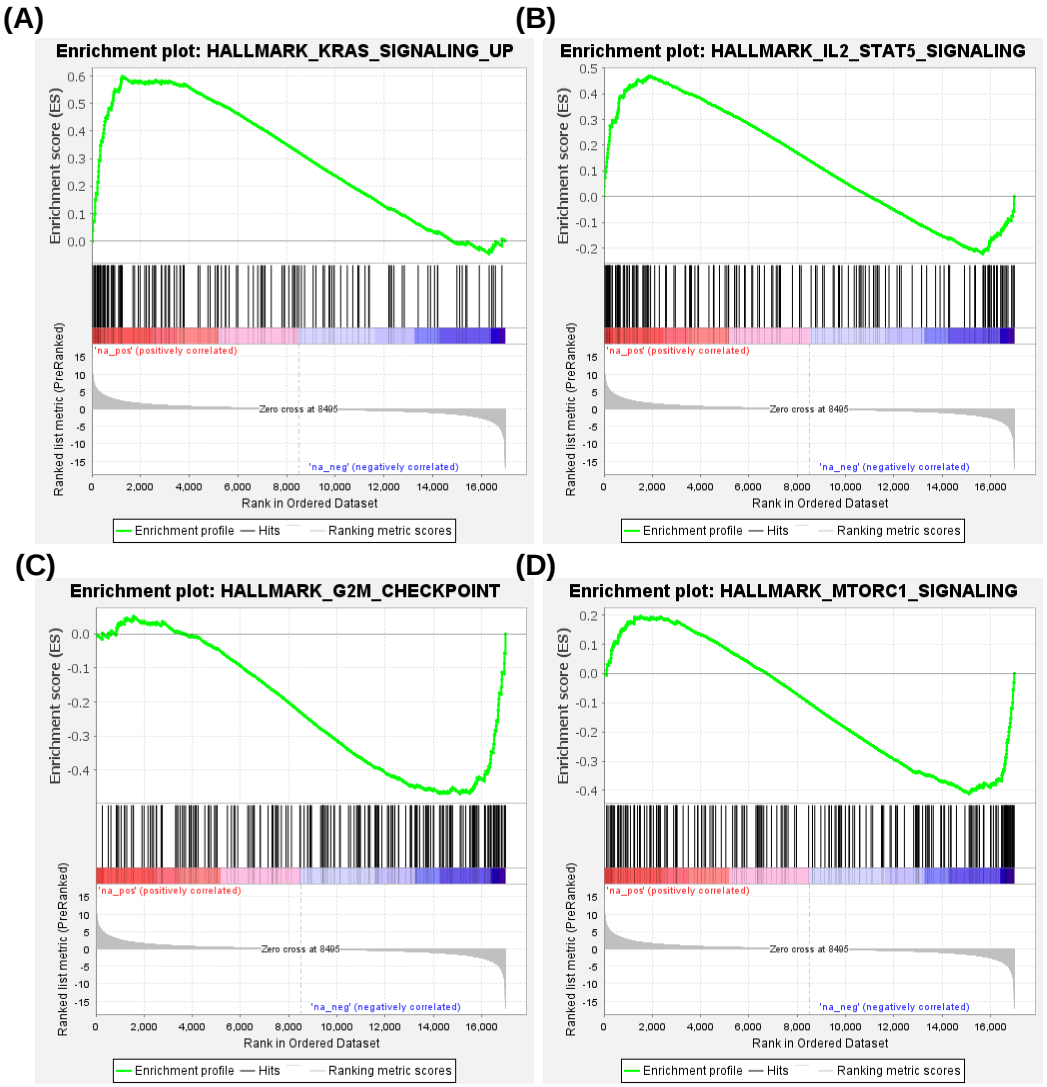

Figure 3.11: Enrichment plot examples. The black lines represent specific genes in the gene set; green line is the enrichment profile. KRAS (A) and IL-2STAT5 (B) signalling were upregulated (positive enrichment scores); G2M checkpoint (C) and mTORC1 (D) signalling were downregulated (negative enrichment scores) following MMTSO treatment for 24-hour in basal glucose environment.

The enrichment analysis gave an indication of how each treatment influenced the profiles of gene sets within biological pathways. From this normalisation was conducted to generated normalised enrichment scores (NES); a positive enrichment score indicated upregulation and a negative enrichment score indicated downregulation. Evaluation of the NES scores was conducted.

There were fewer significant gene sets following MMTSO treatment in basal glucose at 4-hour compared to 24-hour (7 and 21 gene sets respectively, Figure 3.12). Both 4-hour and 24-hour MMTSO treatment, led to upregulation of four signalling pathways: epithelial mesenchymal transition (EMT), interleukin-2-signal transducer and activator of transcription 5 (IL2-STAT5), tumour necrosis factor alpha via nuclear factor kappa B (TNFα via NF_KB) and KRAS. Interestingly, MMTSO treatment at 4-hour led to upregulation of interleukin-6-janus kinase-signal transducer and activator of transcription 3 (IL6-JAK-STAT3) signalling (Figure 3.12A), whilst MMTSO treatment at 24-hour also led to the downregulation of cell cycle regulation and growth pathways including G-phase to M-phase (G2M) checkpoint and E2 Factor (E2F) targets and mammalian target of rapamycin complex 1 (mTORC1/mTOR) (Figure 3.12B).

Comparing SMCSO treatment in basal and high glucose at 24-hour, there were fewer significant gene sets following SMCSO treatment in basal glucose compared to in high glucose (8 and 22 gene sets respectively, Figure 3.13). Both basal and high glucose SMCSO treatment, led to downregulation of three signalling pathways: cholesterol homeostasis, fatty acid metabolism, and mTORC1/mTOR.

Notably, SMCSO and MMTSO treatment in high glucose showed a similar NES response in 6 gene sets (Figure 3.14), indicating downregulation of four signalling pathways including mTORC1/mTOR, and upregulation of two signalling pathways.

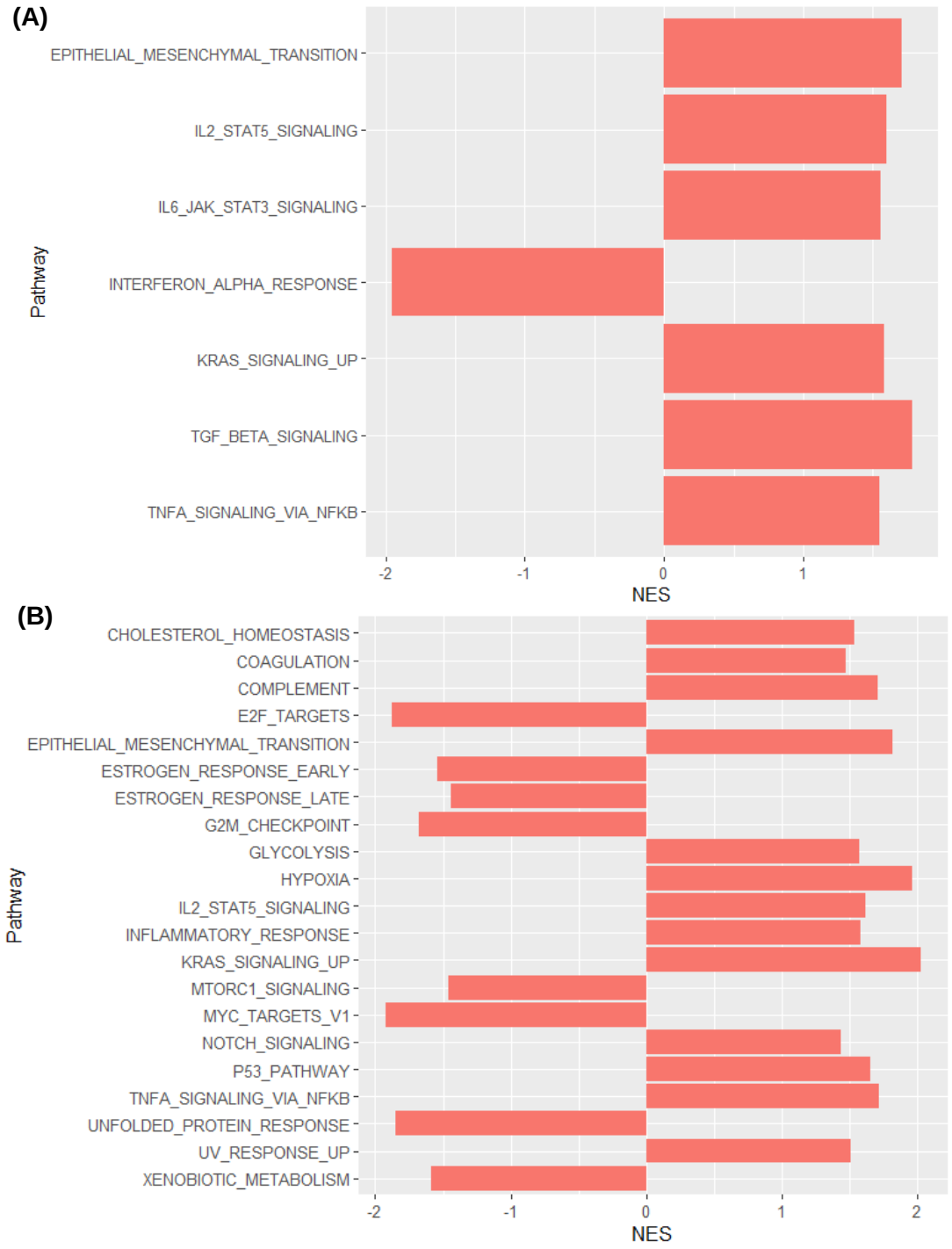

Figure 3.12: Pathway assessment of 4-hour and 24-hour MMTSO treatment in basal glucose environment. Pathway analysis was conducted using GSEA software and the Hallmark database. Demonstrated are the 7 gene sets at 4-hour (A) and 21 gene sets at 24-hour (B) significant to q-value ≤0.05. NES, normalised enrichment score; IL2, interleukin 2; IL6, interleukin 6; JAK, Janus kinase; STAT3 or 5, Signal transducer and activator of transcription 3 or 5; KRAS UP, genes upregulated by KRAS signalling; TGF, transforming growth factor; TNFA, tumour necrosis factor alpha; E2F, E2 Factor; G2M, G2 phase to M phase; mTORC1, mammalian target of rapamycin complex 1 (mTOR pathway); MYC, family of regulator genes; P53, tumour protein p53; UV, ultraviolet.

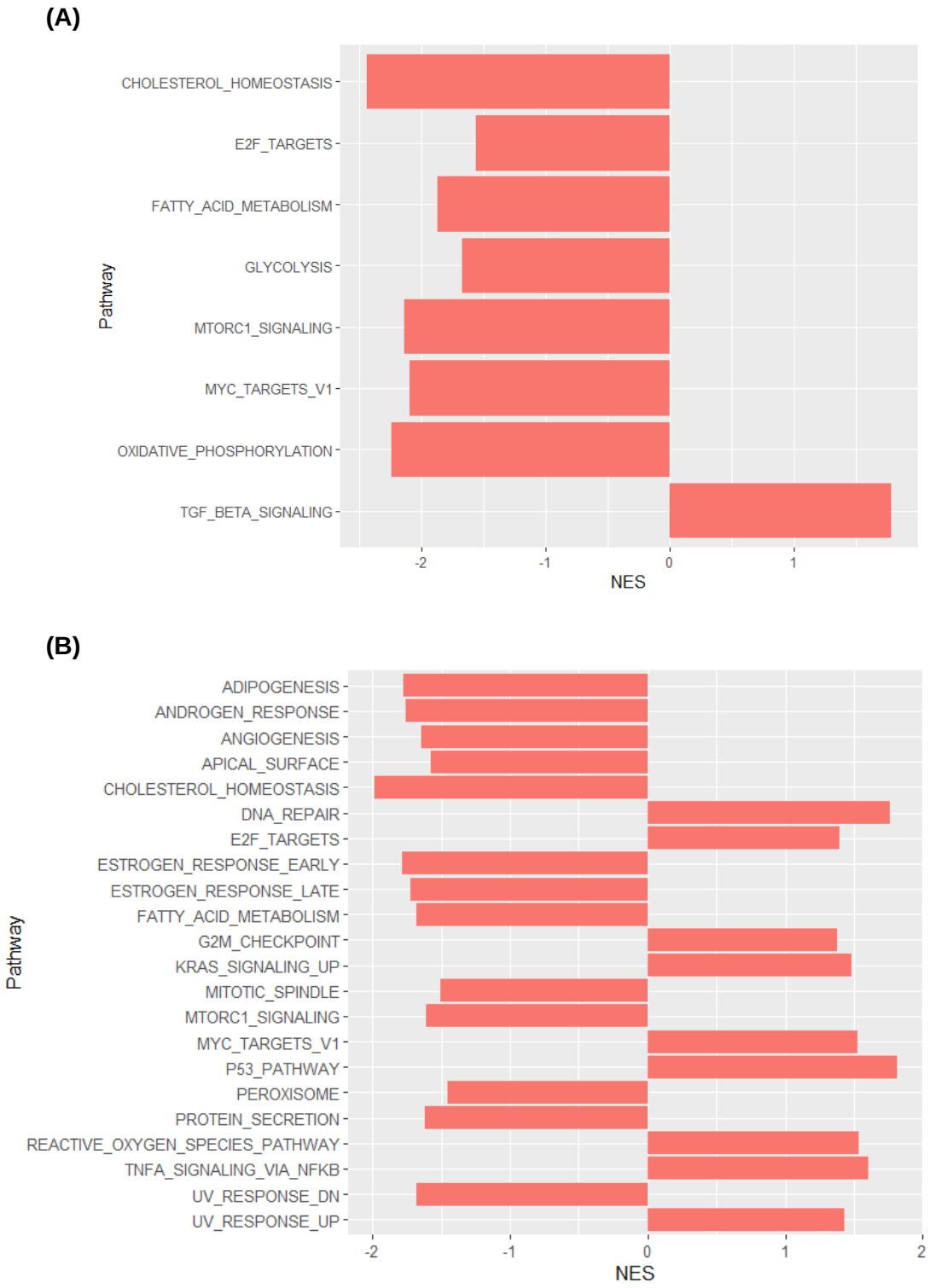

Figure 3.13: Pathway assessment of 24-hour SMCSO treatment in basal and high glucose environment. Pathway analysis was conducted using GSEA software and the Hallmark database. Demonstrated are the 8 gene sets for basal glucose (A) and 22 gene sets for high glucose (B) significant to q-value ≤0.05. NES, normalised enrichment score; E2F, E2 Factor; G2M, G2 phase to M phase; KRAS UP, genes upregulated by KRAS signalling; mTORC1 (mTOR pathway), mammalian target of rapamycin complex 1; MYC, family of regulator genes; P53, tumour protein p53; UV, ultraviolet.

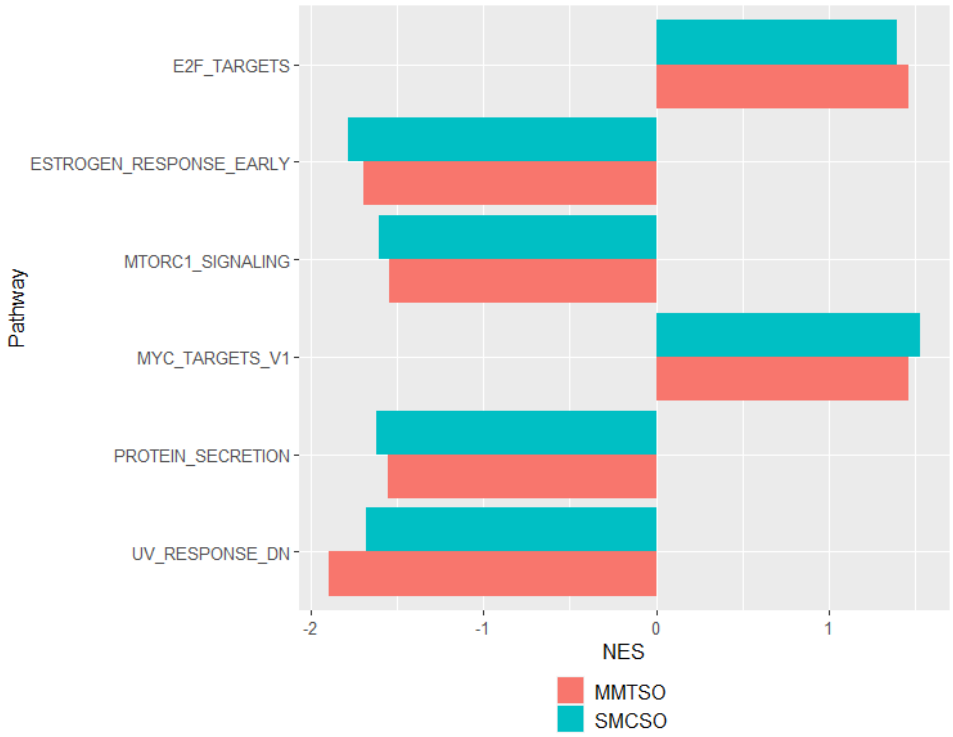

Figure 3.14: Pathway assessment of 24-hour treatment of MMTSO and SMCSO in high glucose environment. Pathway analysis was conducted using GSEA software and the Hallmark database. Demonstrated are the 6 gene sets for MMTSO (pink) and SMCSO (blue) in high glucose significant to q-value ≤0.05. NES, normalised enrichment score; E2F, E2 Factor; mTORC1, mammalian target of rapamycin complex 1 (mTOR pathway); MYC, family of regulator genes; UV, ultraviolet.

3.4.6 MMTSO treatment altered expression of multiple gene sets

Assessment of the enriched genes from the Hallmark pathway analysis (section 3.4.5) was conducted using the GSEA data and differentially expressed gene lists, in order to further assess SMCSO and MMTSO influence on functional biological pathways. Briefly, the Log_2FC of the top 15 enriched genes from the Hallmark analysis with an FDR-adjusted p-value of < 0.05 were selected and plotted on bar plots; a Log_2FC more than 0 indicated an increase in gene expression (upregulation), a Log_2FC less than 0 indicated a decrease in gene expression (downregulation). SMCSO did not reach statistical significance for any of the genes whereas MMTSO did reach statistical significance for all the genes assessed. Following MMTSO treatment at 4-hour, the top genes from IL6-JAK-STAT3 pathway indicated that key genes in cell immune signalling including JUN were upregulated (Figure 3.15), whereas key genes in the TGF-β pathway including TFB1 were downregulated (Figure 3.16). Following MMTSO treatment at 24-hour, the top genes from G2M checkpoint indicated key genes in cell cycle regulation including BCL3 were downregulated (Figure 3.17), and key genes from the p53 pathways including SOCS1 were upregulated (Figure 3.18).

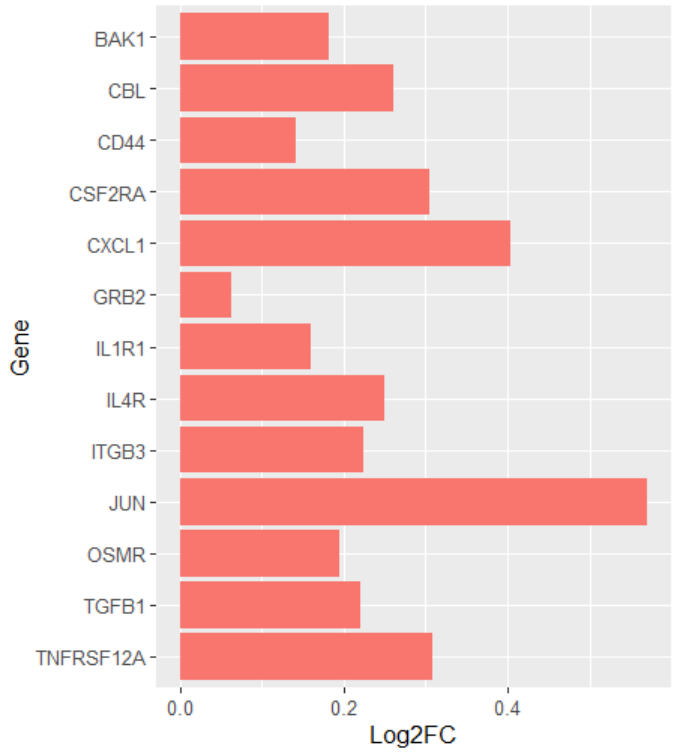

Figure 3.15. Top enriched differentially expressed genes from IL6-JAK-STAT3 gene set by MMTSO treatment in basal glucose at 4-hour. Key genes in cell immune signalling including JUN were upregulated. All genes are significant to q-value ≤0.05.

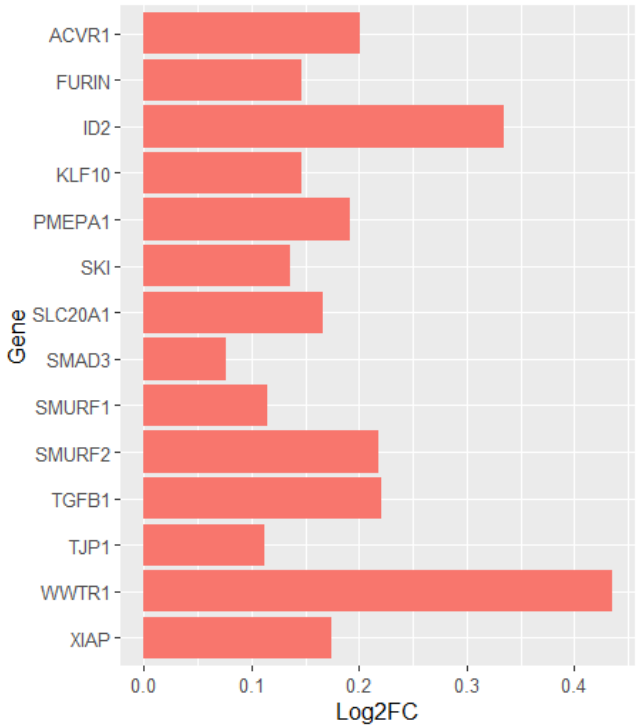

Figure 3.16. Top enriched differentially expressed genes from TGF-β gene set by MMTSO treatment in basal glucose at 4-hour. Key genes in cell immune signalling including TGFB1 were upregulated. All genes are significant to q-value ≤0.05.

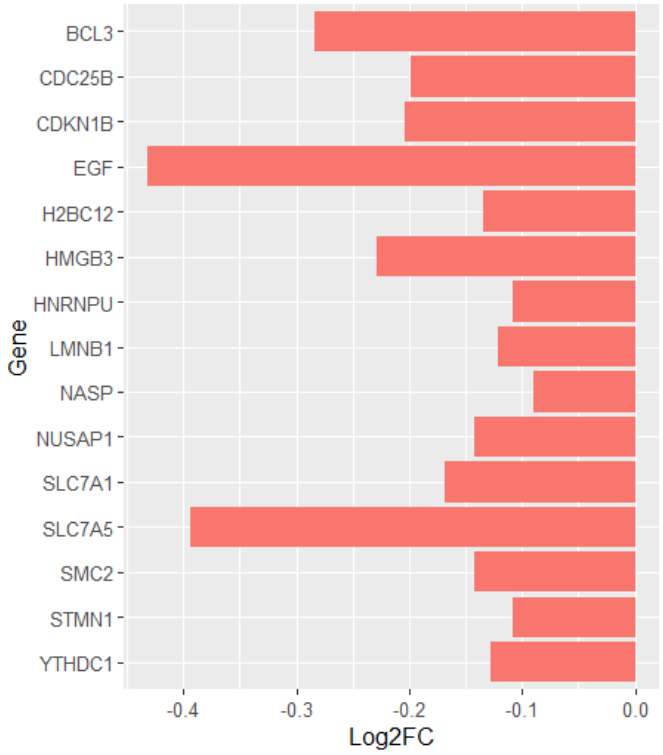

Figure 3.17. Top enriched differentially expressed genes from G2M Checkpoint gene set by MMTSO treatment in basal glucose at 24-hour. Key genes in cell cycle regulation including BCL3 were downregulated. All genes are significant to q-value ≤0.05.

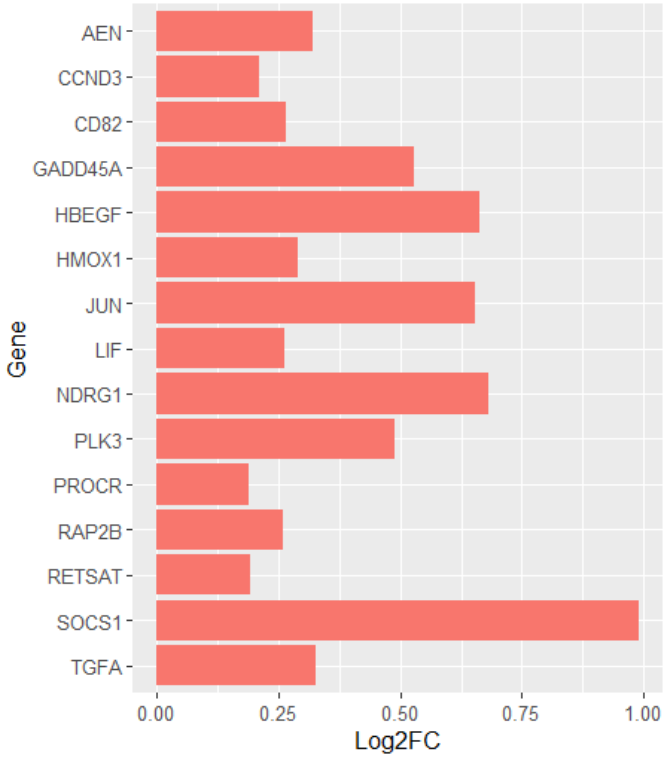

Figure 3.18. Top enriched differentially expressed genes from p53 pathway gene set by MMTSO treatment in basal glucose at 24-hour. Key genes in cell cycle regulation including SOCS1 were upregulated. All genes are significant to q-value ≤0.05.

In response to MMTSO treatment, the IL-2-STAT5 signalling pathway gene sets were upregulated in both 4-hour and 24-hour samples (Figure 3.12). The top 15 enriched genes were selected and the Log_2FC of the commonly expressed were plotted on bar plots. Of the top 15 enriched genes in the IL-2-STAT5 signalling pathway, one of the four pathways upregulated by MMTSO at both 4-hour and 24-hour, there were 7 genes that were upregulated in both: CCND3, CDCP1, HK2, KLF6, LIF, PNP and SPRY4 (Figure 3.19).

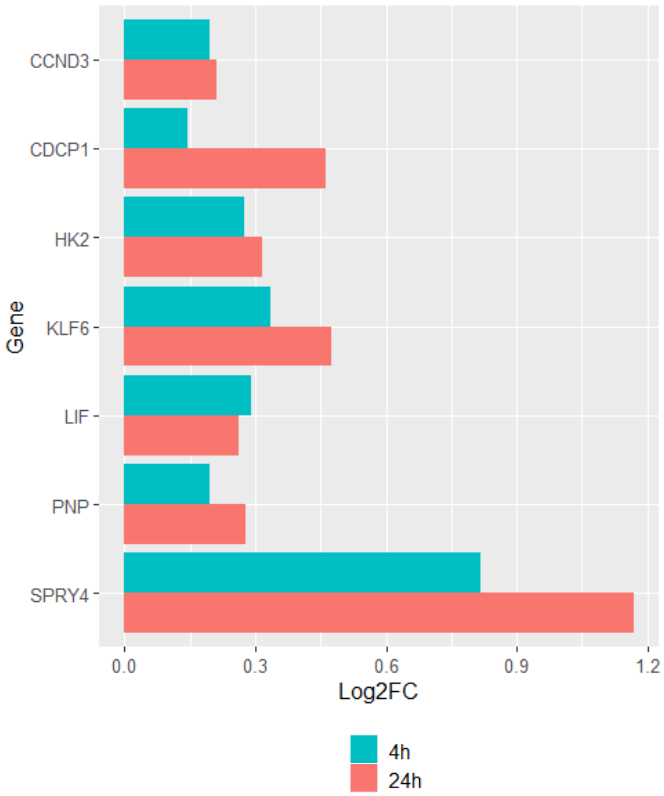

Figure 3.19. Seven of the genes from IL-2-STAT5 gene set were upregulated at both time points under MMTSO treatment. Of the 7 genes (CCND3, CDCP1, HK2, KLF6, LIF, PNP and SPRY4), the 24-hour Log_2FC are more than the 4-hour, indicating more upregulation at this time point. All genes are significant to q-value ≤0.05.

Following MMTSO treatment, the mTORC1/mTOR signalling pathway gene sets were downregulated in both basal and high glucose at 24-hour (Figure 3.12). The top 15 enriched genes were selected and the Log_2FC of the commonly expressed genes were plotted on bar plots. Of the top 15 enriched genes in the mTORC1/mTOR signalling pathway, there were 11 genes that were downregulated following MMTSO treatment in basal and high glucose conditions: ACACA, ACSL3, ATP2A2, EPRS1, GCLC, GSR, NUPR1, PHGDH, SHMT2, WARS1, and XBP (Figure 3.20). The high glucose condition indicated higher abundance of transcripts from all genes when compared to basal glucose condition, indicating more stronger downregulation within this glucose environment. Notably, the mTORC1/mTOR signalling pathway was downregulated by four treatment environments all at 24-hours: MMTSO treatment in basal glucose and in high glucose, SMCSO treatment in basal glucose and in high glucose.

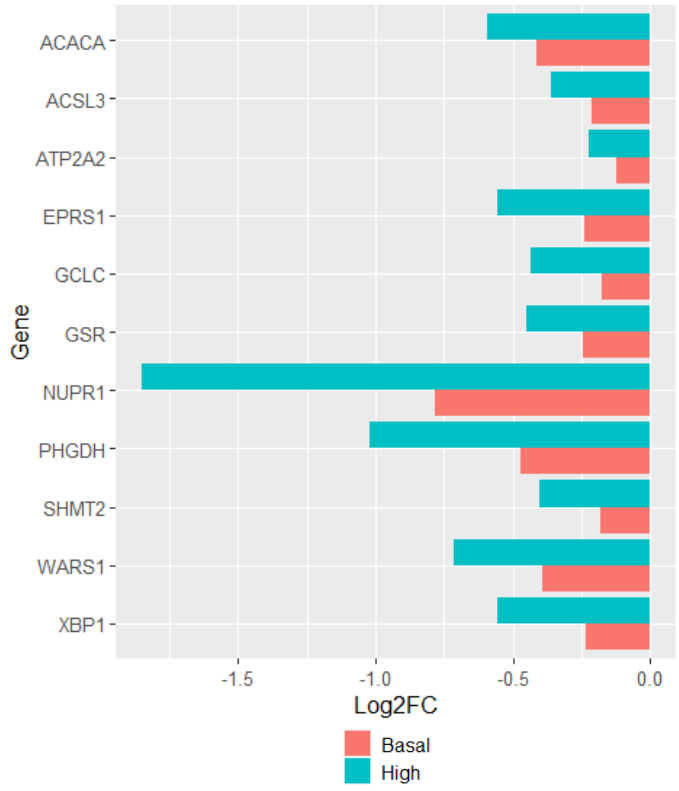

Figure 3.20. Eleven of the genes from the mTORC1/mTOR gene set were downregulated at 24-hour by MMTSO treatment in both glucose environments. Of the 11 genes (ACACA, ACSL3, ATP2A2, EPRS1, GCLC, GSR, NUPR1, PHGDH, SHMT2, WARS1, and XBP), the high glucose Log_2FC are more than the basal glucose, indicating more downregulation at this glucose environment. All genes were significant to q-value ≤0.05.

3.4.7 MMTSO treatment induced regulation of antioxidant and apoptosis related genes

Examination of the effects of treatments on key metabolism-related genes including those related with apoptosis and antioxidant metabolism was conducted using the differentially expressed gene lists. Genes known to be related to these pathways were selected and those with an FDR-adjusted p-value of < 0.05 were taken forward for visual representation of the Log_2FC values. SMCSO treatment did not reach statistical significance for this set of genes but, in contrast, MMTSO treatment did reach statistical significance for all the genes assessed.

Following MMTSO treatment for 24-hour, the antioxidant related genes were downregulated in both basal and high glucose environments. There were 6 genes that were downregulated following MMTSO treatment in basal and high glucose: GCLC, GPX8, GSR, NQO1, SLC6A9 and SRXN1 (Figure 3.21). The high glucose Log_2FC (blue lines) are larger for all genes when compared to basal glucose Log_2FC (pink lines), indicating there was greater downregulation within this glucose environment. Of these antioxidant genes GCLC, GSR and NQO1 were all downregulated following MMTSO exposure for 4-hour and 24-hour under basal and high glucose (Figure 3.22).

Interestingly, the observed downregulation of antioxidant genes with MMTSO treatment is opposite to what is observed with sulforaphane treatment (202). In the context of broccoli soups, sulforaphane and MMTSO could be produced at different transit times with sulforaphane production much earlier than MMTSO, potentially suggesting the sulforaphane upregulates antioxidant response then MMTSO downregulates the response.

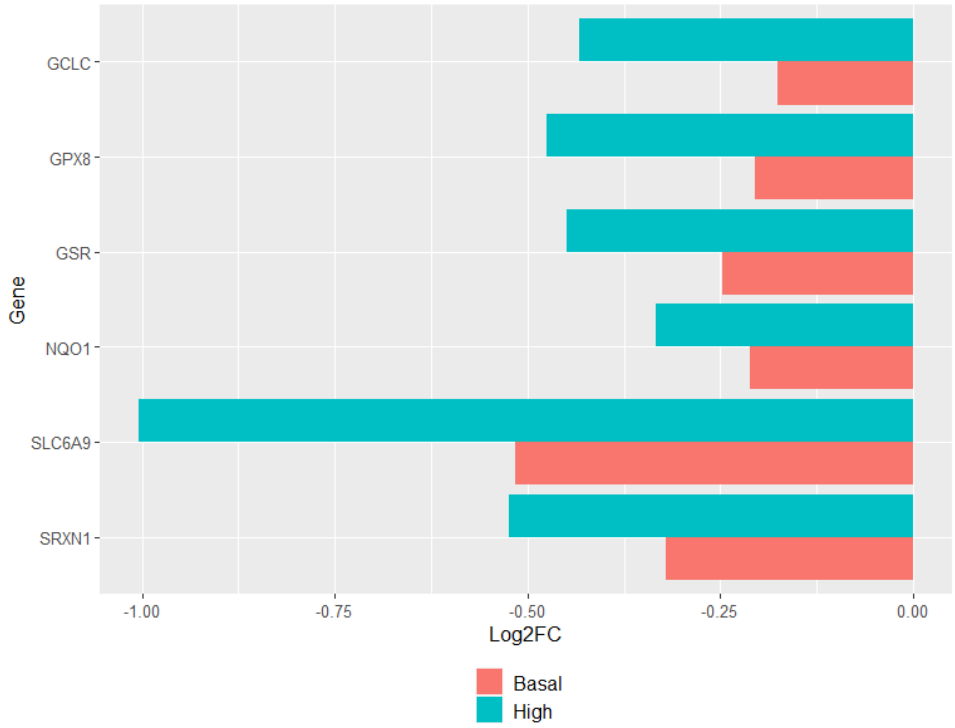

Figure 3.21. Six of the genes associated with antioxidant effects were downregulated at 24-hour by MMTSO treatment in both glucose environments. Of the six genes (GCLC, GPX8, GSR, NQO1, SLC6A9 and SRXN1), all genes are downregulated and significant to q-value ≤0.05.

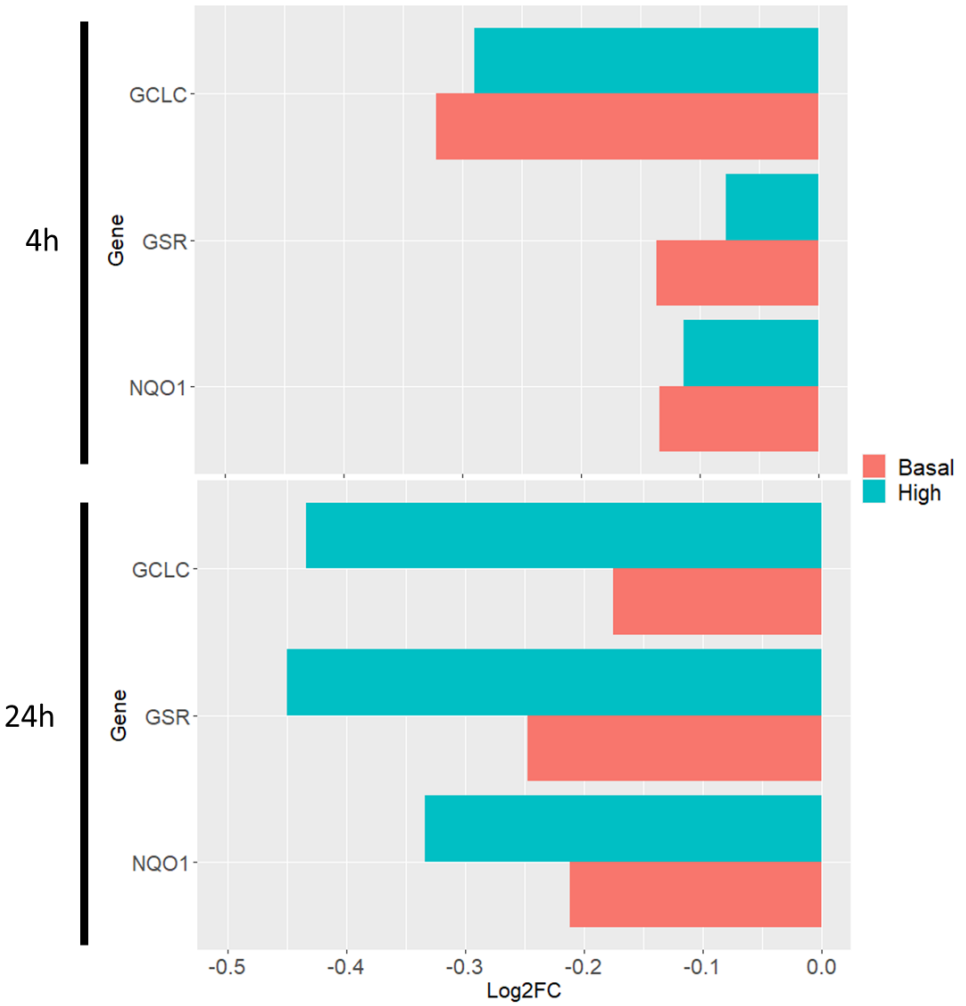

Figure 3.22. Three of the genes associated with antioxidant effects were downregulated by MMTSO treatment at both time-points and in both glucose environments. GCLC, GSR and NQO1 were all downregulated following MMTSO exposure for 4-hour and 24-hour under basal and high glucose environments. All genes are significant to q-value ≤0.05.

Following MMTSO treatment for 24-hour, four apoptotic related genes were upregulated (BAK1, CARD19, FADD, and TNFAIP8) in both basal and high glucose environments (Figure 3.23). The high glucose Log_2FC (blue lines) were generally higher for all genes when compared to basal glucose Log_2FC (pink lines), apart from TNFAIP8, indicating greater upregulation at this glucose environment.

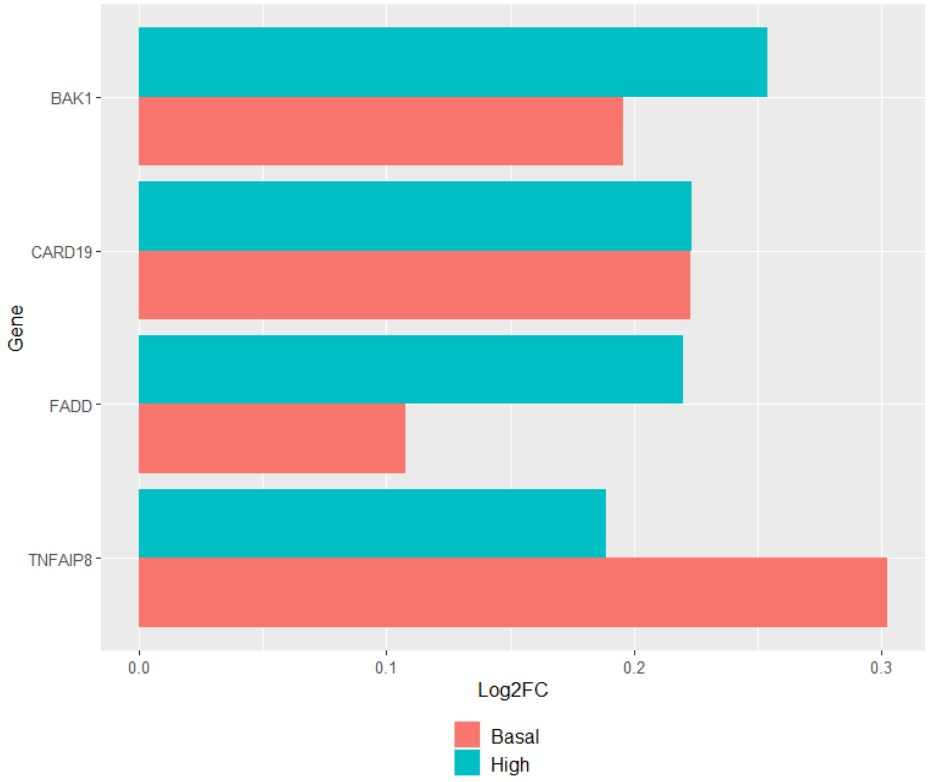

Figure 3.23. Four of the genes associated with apoptotic effects were influenced by MMTSO treatment at 24-hour under both glucose environments. BAK1, CARD19, FADD, and TNFAIP8 were upregulated in basal and high glucose conditions. All genes are significant to q-value ≤0.05.

3.5 Discussion

The effect of regular consumption of broccoli on the transcriptomic profile of prostate tissue from prostate cancer patients has been previously reported (24, 185), and suggested there was a positive effect of sulfur-containing compounds on the expression of cancer-related genes. However, the transcriptomic effects of the sulfur metabolites, SMCSO and MMTSO, in prostate cancer cells has not been previously explored.

Data presented in this Chapter provides the first evidence of the effects of the sulfur-containing compounds SMCSO and MMTSO on metabolic and cancer related pathways which was conducted using gene set enrichment analysis (GSEA) and the Hallmark database. The data presented in this Chapter reported that MMTSO more strongly affects global gene expression than SMCSO and revealed the key cellular pathways that were significantly influenced by MMTSO exposure. The evidence presented in Chapter 2 reported MMTSO, but not SMCSO, affected key metabolic pathways. The gene expression data presented in this Chapter reported key regulation and metabolic genes and pathways were significantly influenced by MMTSO and to a lesser extent SMCSO and provides a potential explanation for the result observed in Chapter 2. Of note, the high glucose environment elicited greater effects on gene expression and cellular pathways compared to basal glucose. This is in agreement with previously published reports in other cancer cells lines that reported high glucose increased key signalling pathways through modulating AMPK/mTOR/S6 and MAPK pathways in endometrial cancer cells (203) and increased DNA damage and expression of DNA damage response genes in breast cancer cells (204). Although a few reports have highlighted the effects of high glucose on gene expression profiles in cancer cell lines, this remains unexplored in prostate cancer cells. This Chapter gave insights into the effects of the glucose environment of the DU145 prostate cancer cells on their response to treatment with dietary sulfur metabolites.

The tumour suppressor gene, p53, is commonly mutated in about 50% of human prostate cancers (205). Downregulation of p53 promotes tumour cell proliferation and survival (206), however with MMTSO exposure this gene set was upregulated, suggesting potential activation of p53 key genes. This finding is consistent with previous evidence from the ESCAPE study that indicated sulfur metabolites may be able to suppress known oncogenic pathways in prostate cancer (24). Of note from the top enriched genes of p53 pathway following MMTSO exposure, there

was upregulation of key regulatory genes including the suppressor of cytokine signalling 1 (SOCS1), cyclin D3 (CCND3), and the Growth Arrest and DNA Damage-inducible 45 (GADD45). SOCS1 is usually repressed in prostate cancer by the microRNA miR30d, with upregulation leading to inhibited invasion and migration of prostate cancer cells (207). Upregulation of CCND3 was reported to bind to and diminish androgen receptor activity in prostate cancer cells and as a consequence a reduction in the rate of cell proliferation (208). GADD45-alpha and GADD45-beta have been described as potential therapeutic target genes in chemo-resistant prostate cancer (209, 210). High levels of the GADD45-beta enhanced chemosensitivity and promoted apoptosis via mitogen-activated protein kinase (MAPK) pathway in prostate cancer cell lines, DU145 and 22RV1 (209). Interestingly, STAT proteins play an important role in regulating p53 (211). There is evidence p53 decreases STAT3 phosphorylation and DNA-binding ability in prostate cancer cells (212), leading to decreased tumour-suppression ability. Moreover, accumulation of mutated p53 along with loss of function could encourage STAT3-assocaited tumour cell proliferation (205).

Like other cancers, prostate cancer can develop immune mechanisms to support evasion from specific immune responses and regulation in the body (50). These mechanisms include modifying the microenvironment of the tumour to a more immunosuppressive environment, ineffective T cell responses and reduced antigen presentation (213). The gene sets significantly upregulated relating to immune regulation (TGF-β, IL-6-JAK-STAT3 and IL2-STAT5) following MMTSO treatment suggest that MMTSO can influence immune regulation in the prostate cancer cells and may be a means of evading cancer development.

The gene set TGF-β and IL-6-JAK-STAT3 signalling was significantly upregulated following MMTSO treatment at 4-hour. TGF-β signalling and EMT gene sets were both upregulated at 4-hour following MMTSO treatment; this could suggest TGF-β is inhibiting proliferation and inducing apoptosis. Dysregulated TGF-β plays a role in immunosuppression, evasion of immune surveillance, epithelial to mesenchymal transition (EMT) and promoting tumour progression (214, 215). SMAD3 was one of the top enriched genes in the TGF-β signalling gene set. It has been reported that the targeted deletion of SMAD3 in a mouse model of tumorigenesis and prostate cancer cells induced EMT through TGF-β1, suggesting a role of SMAD3 deletion in prostate cancer metastasis (216). Activated SMAD cascade led to G1-arrest and up-regulation of cyclin-dependent kinase inhibitors (217) and

downregulation of Myc associated genes (218) in prostate cancer cells, suggesting SMAD upregulation, as seen following MMTSO treatment at 4-hour, could promote apoptosis-related pathways. Interestingly, thiosulfonic derivates such as MMTSO and allicin were able to interact with STAT3 and cause cytotoxic activity in a colon cancer cell line (175) and suppress cell proliferation of chemo-resistant malignant tumours (cholangiocarcinoma) via STAT3 signalling (219). The upregulation of IL-6-JAK-STAT3 gene set following MMTSO exposure, suggests that MMTSO might be interacting with or acting on STAT3 leading to cell cycle regulation.

The gene set IL2-STAT5 was significantly upregulated following MMTSO treatment at 4-hour and 24-hour. IL-2 is a cytokine approved for advance renal cell carcinoma and metastatic melanoma immunotherapy (220) and is considered a promising candidate for prostate cancer targeting and immune recognition (221). Recent reports found serum levels of IL-2 to be three times higher in patients with prostate cancer than those with prostatic hyperplasia (222). Prostate cancers are known to accumulate T-regulatory cells leading to the inhibition of tumour hybrid cells (THCs) and depleting them of IL-2. Increased levels of IL-2 promotes a pro-inflammatory phenotype and a less favourable immune environment for the progression of the prostate cancer (221). Interestingly, a human study demonstrated patients with prostate cancer treated with a standard treatment of zoledronate and IL-2 for 12-months had significantly increased survival rate compared to those just treated with zoledronate alone (223). Further, sulfur metabolites present in garlic (including allicin with a similar chemical structure to MMTSO) have been shown to cause upregulation of the IL-2 immune regulation pathway (224). Similar upregulation is observed following MMTSO treatment; which may relate to the presence of thiol groups that are present in both MMTSO and allicin (117). The observation that MMTSO causes an upregulation in IL-2 signalling gene sets provides evidence that MMTSO could play a role in immunomodulatory effects of prostate cancer.

The association of prostate cancer progression and oxidative stress has been linked with an increase of reactive oxygen species (ROS), although the mechanisms by which ROS and antioxidant response contribute to prostate cancer development remains uncertain (225). The prostate cancer cell lines PC3, DU145 and LNCaP, were reported to have increased ROS generation compared to normal prostate epithelium cells. This increased ROS influenced the activity of key regulatory cascades including extracellular signal-regulated kinase (ERK)1/ERK2

and caused cyclin B-dependent G2M cell cycle arrest, while inhibition of ROS activity led to decreased matrix metalloproteinase 9 (MMP-9) activity and reduced mitochondrial potential in prostate cancer cells (226), providing further evidence that decreased production of ROS leads to reduced prostate cancer development. The antioxidant system comprises of various enzymes including those involved in glutathione metabolism (glutamate-cysteine ligase (GCLC) and glutathione reductase (GSR)), and phase II detoxing enzymes such as NAD(P)H dehydrogenase quinone 1 (NQO1) which plays a key role in ROS regulation and protecting cells from gene damage (225, 226). GCLC (involved in glutathione biosynthesis from glutamate), GSR (involved in the conversion of oxidised glutathione to reduced glutathione), and NQO1 (involved in the reduction of quinones to hydroquinones), have all been reported to be overexpressed in many types of cancer including renal, lung and prostate cancers (227, 228). The prostate cancer cell line DU145 was reported to have high NQO1 and GCLC levels compared to normal and other cancer cell lines (229). The inhibition of NQO1 decreased ROS and p53 levels and suppressed NF-$_{K}$B interaction modulating inflammatory response associated with prostate cancer progression (230). The observation that MMTSO caused a downregulation of GCLC, GSR and NQO1 genes provides evidence that MMTSO could play a role in oxidative stress and antioxidant effects of prostate cancer. It is worth mentioning that the reported downregulation of antioxidant genes with MMTSO treatment in this study is opposite to what is observed with sulforaphane treatment in other studies (202). However, there is some overlap from this study with other studies including the Norfolk ADaPt study (185) and a previous broccoli soup intervention (231) also indicated an upregulation of immune signalling pathways associated with carcinogenesis in the prostate such as TGF-β signalling.

The initiation of intrinsic and extrinsic apoptotic pathways are key for chemoprevention of prostate cancer. The intrinsic apoptotic pathway involves disruption of mitochondrial membrane integrity, while the extrinsic apoptotic pathway is activated by pro-apoptotic receptor and ligand interaction at the cell surface (232). Dietary compounds, such as the sulfur compound sulforaphane have been linked with cell cycle arrest and apoptosis in numerous cancer models (85, 233), however the effects of MMTSO on apoptosis remain unclear. Interestingly, the extrinsic apoptotic pathway is initiated by the binding of ligands to cell surface death receptors associated with Fas-associated death domain (FADD), whereby upregulated FADD initiates the caspase cascade resulting in

programmed cellular destruction and apoptosis (234). Upregulation of FADD was shown following MMTSO treatment, suggesting increased apoptosis in the presence of this treatment. BCL-2 antagonist killer (BAK1) is a serine/threonine kinase that acts as a pro-apoptotic regulator in the intrinsic apoptotic pathway (235). BAK1 suppression was linked with induction of androgen-independent prostate cancer cell growth (236), suggesting that the upregulation of BAK1 promotes apoptosis. Here, it was reported that BAK1 was upregulated following MMTSO treatment. The sulfur compound with a similar structure to MMTSO, allicin, activated caspase cascades through up-regulating BAX and down-regulating BCL-2 regulation for induction of apoptosis in cholangiocarcinoma (219). The observation that MMTSO caused upregulation of apoptotic related genes provides evidence that MMTSO could play a role in inducing apoptosis in prostate cancer.

While there is limited literature concerned with studies exploring the molecular mechanisms by which SMCSO and MMTSO may influence cellular processes using model systems, there is a complete lack of human interventions investigating the bioactivity of these compounds. Data presented here does highlight the potential biological effects of SMCSO and MMTSO on prostate cancer gene regulation, these are limited to a cultured cell line, and the observations need to be verified with data from a human dietary intervention study designed to test the effects of an SMCSO/MMTSO treatment versus a suitable control. The first step would be to identify or develop a suitable food product that was rich in SMCSO/MMTSO that could subsequently be used in a human intervention. The obvious participants for such as trial would be prostate cancer patients who are on active surveillance via prostate biopsies as this would allow access to prostate tissue samples that could be used to investigate effects of treatment versus control on transcriptomic profile.

RNA-sequencing, depending on sample size, can be costly, time-consuming on sample preparation and data analysis, and limited by software, tools and database used (237). Despite this it has become a popular technique used to quantify and characterise the transcriptome of cells and tissues, allowing assessment from multiple treatment groups under different environments. Future work could use single cell multiomics in prostate cancer to identify cell mutations within the cancer microenvironment to identify potential targets within the cancer and determine correct treatment on an individual to individual basis to reduce cancer growth.

3.6 Conclusion

The data presented in this Chapter provides evidence that treating DU145 prostate cancer cells with MMTSO, and to a lesser extent SMCSO, causes changes in the transcriptional profile of the cells. MMTSO, but not SMCSO, treatment to DU145 prostate cancer cells influenced key immune and regulatory signalling pathways including IL-2-STAT5, IL-6-JAK-STAT3 and TGF-β, and key antioxidant genes including GCLC, GSR and NQO1, and apoptotic-related genes including BAK1 and FADD. These effects are similar to the transcriptional changes observed in the prostate tissue of patients in the ADAPT and ESCAPE human dietary intervention studies and suggest that the changes in these studies could have been caused by SMCSO/MMTSO as well as glucoraphanin/sulforaphane present.

Chapter Four.

Effects of SMCSO and MMTSO treatments in different glucose environments on the metabolite profiles of prostate cancer cells

Chapter Four: Effects of SMCSO and MMTSO treatments in different glucose environments on the metabolite profiles of prostate cancer cells

4.1 Introduction

Chapter 2 provided evidence that the sulfur-metabolites exposure to DU145 prostate cancer cells led to reduced mitochondrial capacity and glycolytic ability, and increased of fatty acid dependency; Chapter 3 gave evidence that the sulfur-metabolites exposure to DU145 prostate cancer cells led to regulation of key cellular and potentially cancer-related genes and pathways including up regulation of genes associated with inflammatory response and apoptosis and downregulation of genes associated with antioxidant capacity. Collectively from the mitochondrial energetics assessment discussed in Chapter 2 and assessment of key genes and pathways discussed in Chapter 3, this Chapter further evaluates the influence of SMCSO and MMTSO on DU145 prostate cancer cells by assessment of metabolite profiles and metabolic pathways using untargeted and targeted metabolomic analysis.

Metabolomics is an evolving field in dietary epidemiology that allows measurement and comparison of large numbers of small compounds including fatty acids, sugars and amino acids in a biological sample (238). It provides a real-time snapshot of the physiological metabolism of the biological sample at a given time-point as the measured metabolite concentrations reflect biochemical alterations. There are numerous clinical applications from the use of metabolomics including examining the association of metabolites in samples and cancer risk and development to biomarker identification (239). Global metabolomics analyses have been used to screen a number of dietary compounds for potential chemopreventive combination treatments. For example, modulation of cancer cell metabolism, alterations in STAT3, mTORC1, AMPK signalling, reduced ATP levels and induction of apoptosis in mouse and human prostate cancer cell lines have been reported (240). It can be extremely useful to apply large scale metabolomics analyses to biological samples to identify metabolites that might prompt malignant transformation of normal prostate epithelial cells to cancerous cells.

The prostate is known to display a unique metabolite profile (241, 242). A normal prostate relies on glucose oxidation for ATP production with low citrate metabolism in the tricarboxylic acid (TCA) cycle leading to accumulation of citrate (243).

However, when normal prostate epithelial cells undergo malignant transformation into cancerous cells there is metabolic reprogramming leading to activation of the TCA cycle which is driven by reductions in zinc levels and the abundance/activity of zinc-dependent enzymes which affects lipid and energy metabolism (239). Even though prostate cancer cells do not exhibit the Warburg effect, they produce lactate which facilities immune evasion, angiogenesis and cancer development (244). The use of metabolomics in prostate cancer has identified key metabolite differences compared to normal prostate epithelial cells, such as greater levels of metabolites including choline and sarcosine associated with cancer progression (245). Interestingly, a recent review found key metabolites to be consistently altered in prostate cancer tissue and urine samples across a range of different studies, which these 'signature' metabolites including valine, taurine, leucine and citrate (243). This indicates these metabolites may be useful biomarkers for prostate cancer and tumour aggressiveness that can be assessed in multiple biological samples.

Previous human studies have conducted global metabolite profiling on biological samples to assess potential biomarkers in cancer development. Metabolomic analysis of baseline serum samples in conjunction with dietary assessment of participants in the Prostate, Lung, Colorectal, and Ovarian (PLCO) Cancer Screening Trial, identified 412 known metabolites of which 39 dietary biomarkers were identified. They reported correlations between S-methyl cysteine and consumption of beans, tryptophane betaine and peanut intake, and trigonelline and quinate with coffee (246). The Alpha-Tocopherol, Beta-Carotene Cancer Prevention (ATBC study) conducted metabolomic analysis of serum samples from 523 cases of lethal prostate cancer with matched controls and identified 860 known compounds including 34 metabolites that were significantly associated with lethal prostate cancer. Higher levels of thioproline, cystine and cysteine (amino acids involved in redox metabolism) were correlated with reduced risk of lethal prostate cancer, while increased levels of several lipids including ketone bodies and fatty acids were associated with metastatic cases (247, 248). These studies highlight the impact of metabolite profiling of prostate cancer tissue and other biological samples.

Global metabolite profiling from participants recruited onto broccoli soup interventions has given an insight into the role of sulfur-containing compounds on the metabolite profile of biological samples such as urine, plasma, prostate and adipose tissue. Analysis of prostate, adipose and urine from participants recruited

on the SAP study showed there were higher levels of tryptophane betaine, trigonelline and quinate in the non-intervention arm (124), metabolites potentially linked with habitual dietary associations such as those individuals who drank coffee. Further analyses allowed the identification of differences in metabolic pathways between the study arms in steroid hormone biosynthesis and caffeine metabolism, with those in the broccoli soup arm reported as having higher levels of SMCSO in the urine and of ADP in the prostate (124). Analysis of prostate tissue that was absent of cancer foci from men recruited onto the ESCAPE study, a three-arm broccoli soup intervention with low, intermediate and high levels of glucoraphanin, also reported that whilst 448 metabolites were detected, there were no significant differences in metabolites across the three broccoli soup arms (24). Interestingly, there was increased glutathione metabolites related with redox status (glutathione-reduced, S-methyl glutathione and cysteine-glutathione disulphide) across all three broccoli soup arms (unpublished data), suggesting the increase may not be connected to glucoraphanin content in the soups and may instead be due to other sulfur-containing compounds present such as SMCSO or MMTSO. This observation in particular indicates it is key to investigate the effect of other sulfur-containing compounds on metabolomic profile of prostate cancer cells.

4.2 Aims

The overall aim was to assess the effects of treatments with the sulfur-containing compounds SMCSO and MMTSO on metabolite profile of DU145 cultured prostate cancer cells:

- To use untargeted global metabolite profiling to assess the effects of treatments on the metabolite profiles of prostate cancer cells exposed to SMCSO and MMTSO.
- To undertake functional analyses of the metabolite changes to identify metabolic pathways that are significantly altered by treatments compared to controls.
- To investigate how difference in the glucose environment affect changes in metabolite profiles in response to treatments with SMCSO and MMTSO.
- To use quantitative targeted analyses to explore the effects of SMCSO and MMTSO treatments on the concentrations of metabolites of interest such as amino acids.

4.3 Materials and Methods

4.3.1 Cell Treatments

DU145 cells were cultured in standard conditions in T-75 flasks until 80 % confluent. Once confluent, the appropriate treatment or vehicle control was added (previously described in 2.3.1 and 2.3.2, Chapter 2). The appropriate treatment or vehicle control were added in replicates of five diluted in cell culture medium either under standard glucose environment of 5.5 mM, or high glucose environment of 25 mM for a further 24-hour incubation (Figure 4.1). Cell pellets and supernatants were collected from each flask.

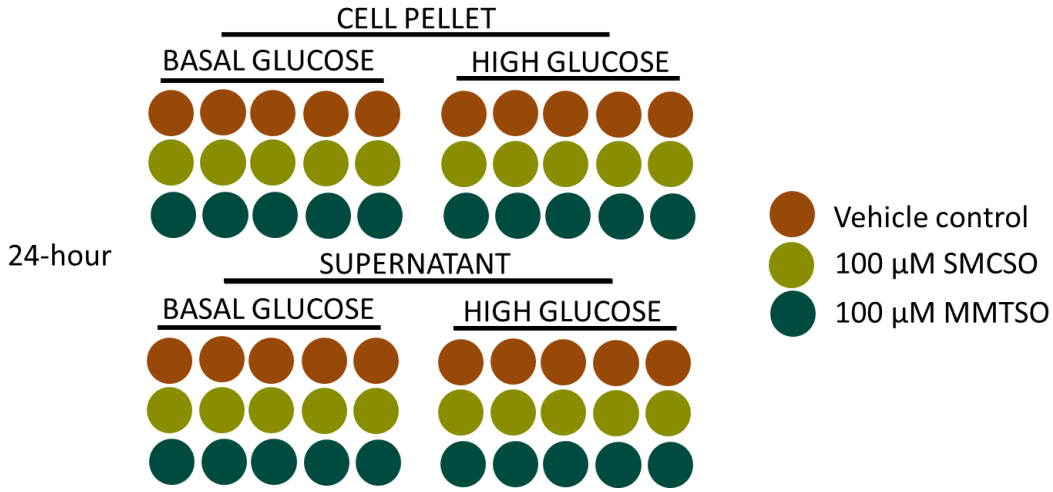

Figure 4.1. Treatment template for metabolomic analysis. Briefly, cells were cultured under standard conditions until 80 % confluent before a further 24-hour incubation with the vehicle control (water, brown circles), or appropriate treatment: 100 µM SMCSO (olive circles) or 100 µM MMTSO (dark green circles) in replicates of five.

4.3.2 Cell Pellet Preparation

Once the supernatant was removed and collected (described in 4.3.3, Chapter 4), the cells in the flasks were washed with cold 0.9 % NaCl solution which was then removed. One millilitre of cold 0.9 % NaCl solution was added to each flask and the cells were scraped off the flask surfaces using a cell scraper. All cells were transferred to the appropriately barcoded tubes and mixed well. Cells were counted using the Countess cell counter (ThermoFisher®) and centrifuged at 2000 rpm for 5-minutes at 4 °C to pellet the cells (approximately 100-150 µl volume of cell pellet was required for the metabolomics analyses). The supernatant was removed and discarded from the cells, and the cell pellets were immediately frozen at -80 °C. All

samples were stored at -80 °C prior to submission for untargeted global metabolomics analysis to Metabolon.

4.3.3 Supernatant Preparation

The supernatant was collected, transferred to a 50 ml falcon tube, and centrifuged at maximum speed for 5-minutes at 4 °C, to eliminate dead cells and debris. Three hundred microlitres of the supernatant was transferred to the appropriately barcoded tubes and immediately frozen at -80 °C. All samples were stored at -80 °C prior to submission for untargeted global metabolomics analysis to Metabolon.

4.3.4 Sample Preparation

Once received by Metabolon, samples were prepared using the automated MicroLab STAR system from Hamilton Company. A number of recovery standards were added prior to the first step in the extraction process for quality control (QC) purposes. Proteins were precipitated and removed with methanol under vigorous shaking for 2-minutes (Glen Mills GenoGrinder 2000) followed by centrifugation. The resulting extract was divided into five fractions: two for analysis by two separate reverse phase (RP)/UPLC-MS/MS methods with positive ion mode electrospray ionisation (ESI), one for analysis by RP/UPLC-MS/MS with negative ion mode ESI, one for analysis by HILIC/UPLC-MS/MS with negative ion mode ESI, and one sample was kept for backup. Samples were placed briefly on a TurboVap® (Zymark) to remove the organic solvent. The sample extracts were stored overnight under nitrogen before preparation for analysis.

4.3.5 Quality Assurance

A number of controls were analysed in conjugation with the experimental samples: a pooled matrix made by taking small volumes of each experimental sample served as technical replicates throughout the data set; extracted water samples served as process blanks; a QC mix of standards was added to every sample being analysed. The compounds in the QC mix were selected to not interfere with the measurement of endogenous compounds and allowed instrument performance monitoring and aided chromatographic alignment. The experimental samples were randomised across the platform run with QC samples spaced evenly among the injections.

4.3.6 Ultra-high Performance Liquid Chromatography (UPLC)- Tandem Mass Spectroscopy

All methods used a Waters ACQUITY ultra-performance liquid chromatography (UPLC) and a Thermo Scientific Q-Exactive high resolution/accurate mass spectrometer interfaced with a heated electrospray ionisation (HESI-II) source and Orbitrap mass analyser operated at 35,000 mass resolution. The sample extract was dried then reconstituted in solvents compatible to each of the four methods. Each reconstitution solvent contained a mixture of standards at fixed concentrations to ensure injection and chromatographic consistency. One aliquot was analysed using acidic positive ion conditions, chromatographically optimised for more hydrophilic compounds. In this method, the extract was gradient eluted from a C18 column (Waters UPLC BEH C18-2.1x100 mm, 1.7 µm) using water and methanol, containing 0.05% perfluoropentanoic acid (PFPA) and 0.1% formic acid (FA). Another aliquot was also analysed using acidic positive ion condition; however it was chromatographically optimised for more hydrophobic compounds. In this method, the extract was gradient eluted from the same afore mentioned C18 column using methanol, acetonitrile, water, 0.05% PFPA and 0.01% FA and was operated at an overall higher organic content. Another aliquot was analysed using basic negative ion optimised conditions using a separate dedicated C18 column. The basic extracts were gradient eluted from the column using methanol and water, however with 6.5mM Ammonium Bicarbonate at pH 8. The fourth aliquot was analysed via negative ionisation following elution from a HILIC column (Waters UPLC BEH Amide 2.1x150 mm, 1.7 µm) using a gradient consisting of water and acetonitrile with 10mM ammonium formate, pH 10.8. The MS analysis alternated between MS and data-dependent MS^n scans using dynamic exclusion. The scan range varied slighted between methods but covered 70-1000 m/z.

4.3.7 Bioinformatics

The informatics system consisted of four major components: the Laboratory Information Management System (LIMS), the data extraction and peak-identification software, data processing tools for QC and compound identification, and a collection of information interpretation and visualisation tools for data analysts. The hardware and software for this informatics were the LAN backbone and a database server running Oracle 10.2.0.1 Enterprise Edition.

4.3.8 Data Extraction and Compound Identification

Raw data were extracted, peaks identified, and QC processing done using Metabolon's hardware and software. Metabolites were identified by comparison to library entries of purified standards or recurrent unknown entities. Metabolon use a library based on authenticated standards that contains the retention time/index (RI), mass to charge ratio (*m/z*), and chromatographic data (including MS/MS spectral data) on all compounds present in the library. In addition to this, biochemical identifications were based on three criteria: retention index within a narrow RI window of the proposed identification; accurate mass match to the library +/- 10 ppm; and the MS/MS forward and reverse scores between the experimental data and authentic standards. The MS/MS scores are based on a comparison of the ions present in the experimental spectrum to the ions present in the library spectrum. While there may be similarities between these molecules based on one of these factors, the use of all three data points can be utilised to distinguish and differentiate biochemicals. More than 3300 commercially available purified standard compounds have been acquired and registered into LIMS for analysis on all platforms for determination of their analytical characteristics.

4.3.9 Metabolite Quantification and Data Normalisation

Peaks were quantified using area-under-the-curve and allocated into several biologically relevant classes: amino acids, carbohydrates, vitamins, tricarboxylic acid cycle (energy), lipids, nucleotides, peptides, and xenobiotics. Cell samples were normalised to total protein as determined by Bradford assay to account for differences in metabolite levels due to difference in the amount of material present in each sample. Supernatant samples were not normalised. One of the control replicates in high glucose conditions was removed before further analysis because it was shown the cells had not reached the 80 % confluency threshold that all the other replicates had reached.

4.3.10 Functional Analysis

The normalised raw LCMS/MS values with their corresponding Human Metabolome Database (HMDB) ID, Kyoto Encyclopaedia of Genes and Genomes (KEGG) ID or name itself were entered into MetaboAnalyst 5.0 online platform for principal component analysis (PCA), and pathway analysis. No filters were applied, the data were log transformed and underwent global testing with relative-betweenness centrality. If a single HMDB ID was given by Metabolon, this ID was

used; when no HMDB ID was available, but a KEGG ID was, the KEGG ID was used. In the 35 cases where there were multiple HMDB IDs were given, one of these IDs were selected based on biological context such as selection of the L-form rather than the D-form of amino acids including proline. Otherwise, the compound name itself provided by Metabolon was used. Pathway associated metabolites were selected from the small molecule pathway database (SMPDB) which contains detailed analysis on human metabolic pathways and metabolite signalling pathways with more than 30,000 small molecules found in humans (249, 250).

4.3.11 Targeted Amino Acid Extraction and Quantification

Supernatants and cell fractions that had been stored -80 °C were thawed and cell fractions were washed once with cold 0.9 % NaCl solution. Metabolite extraction buffer consisting of 50 % methanol, 30 % acetonitrile and 20 % MilliQ water was made and kept at -20 °C until required. To the cells, 500 µl of the metabolite extraction buffer per million cells was added and incubated at -80 °C for 24-hours before the cells were scraped off at 4 °C and the insoluble material was transferred into pre-cooled Eppendorf tubes. The supernatant samples were thawed, centrifuged at maximum speed for 5-minutes at 4°C before 80 µl of each sample was transferred to pre-cooled Eppendorf tubes containing 400 µl of metabolite extraction buffer. Both the cell and supernatant samples were vortexed at 1400 rpm for 15-minutes at 4 °C using Eppendorf ThermoMixer. Samples were centrifuged at maximum speed for 20-minutes at 4 °C before 80 µl of each sample were transferred to pre-cooled vials. The vials were placed into a vacuum centrifuge drier for 30-minutes before resuspension with 90 µl of 60 % acetonitrile in water. For calibration curve, 17 amino acids in 0.1 M hydrochloric acid (79248-5X2ML, Supelco) were diluted in 60 % acetonitrile in water to give 2.5 mM stock. The stock was diluted further from 0 µM to the highest concentration of 1 mM in fivefold concentrations. All standards were made prior to each run. Into separate vials, 90 µl of each concentration was added. All samples had 10 µl of 2.5 mM stable isotope-labelled canonical amino acid mix (MSK-CAA-1, Cambridge Isotope Laboratories) was added, and each vial was crimped and vortexed thoroughly.

A model Agilent 6490 Triple Quadrupole LC/MS system equipped with a binary pump, cooled autosampler, degasser, column oven and diode array detector, was used. A mobile phase A of 10 mM ammonium formate (Sigma-Aldrich®) in acetonitrile containing 0.15 % formic acid, a mobile phase B of 10 mM ammonium

formate (Sigma-Aldrich®) in MilliQ water containing 0.15 % formic acid. The amino acids were analysed using HILIC column and detected by multiple reaction monitoring (MRM) mode using positive electrospray ionisation. The injection volume was 1 µl per sample. The source conditions were as follows: dry gas temperature 200 °C; dry gas flow 16 L/min; nebuliser pressure 50 psi; capillary voltage 3500 V; sheath gas temperature 300 °C; sheath gas flow 11 L/min; nozzle voltage 1000 V; high pressure RF 150 V; and low pressure RF 60 V, as previously described by Perez-Moral and colleagues (251). Quantification was performed by calculating the peak area ratio of the analyte in the sample to that for the internal standard and using this value to calculate the concentration from a calibration curve generated with calibration standards and the same quantity of internal standard that were run alongside samples.

4.3.12 Statistical Analysis

Generation of graphs and statistical analyses were performed in Prism using GraphPad Software or MatLab were appropriate. As appropriate, either unpaired two-way T-tests, hypergeometric comparison tests, or one-way ANOVAs followed by Tukey's honest statical hypothesis testing for multiple comparisons were used. Data are reported as mean ± standard deviation with a $p < 0.05$ (95 % confidence interval) defined to be statistically significant, n.s. $p > 0.05$.

4.4 Results

4.4.1 Data from the untargeted global metabolomics analysis achieved the necessary quality assurance criteria

The instrument variability was determined by calculating the median relative standard deviation for the internal standards added to each sample prior to injection into the mass spectrometers. The overall process variability was determined by calculating the median relative standard deviation of all endogenous metabolites present in all of the matrix samples for multiple technical replicates of pooled samples. The percentages for instrument and process variability met Metabolon's acceptance criteria attaining quality assurance criteria, Table 4.1.

Table 4.1. Instrument and process variability percentages for sample analysis by Metabolon

Quality Control Sample	Measurement	Median Relative Standard Deviation	
		Cell	Supernatant
Internal Standards	Instrument Variability	6 %	4 %
Endogenous Metabolites	Overall Process Variability	11 %	9 %

4.4.2 There was some clustering observed with SMCSO-treated and MMTSO-treated samples, compared to controls

PCA plots were used to visualise clusters of samples based on their similarity to each other. To explore whether there was clustering between control and treatments, PCA plots were utilised. With the MMTSO cell treated samples, there was some clustering between control and treated samples in basal (Figure 4.2A) and high glucose conditions (Figure 4.2B). Likewise with the MMTSO supernatant treated samples, there was some clustering between the control and treated samples in basal (Figure 4.3A) and high glucose conditions (Figure 4.3B).

With the SMCSO treated samples, there was no distinct clustering compared to control samples in the basal glucose samples (Figure 4.4A and 4.5A) however there was some clustering demonstrated in the high glucose samples (Figure 4.4B and 4.5B).

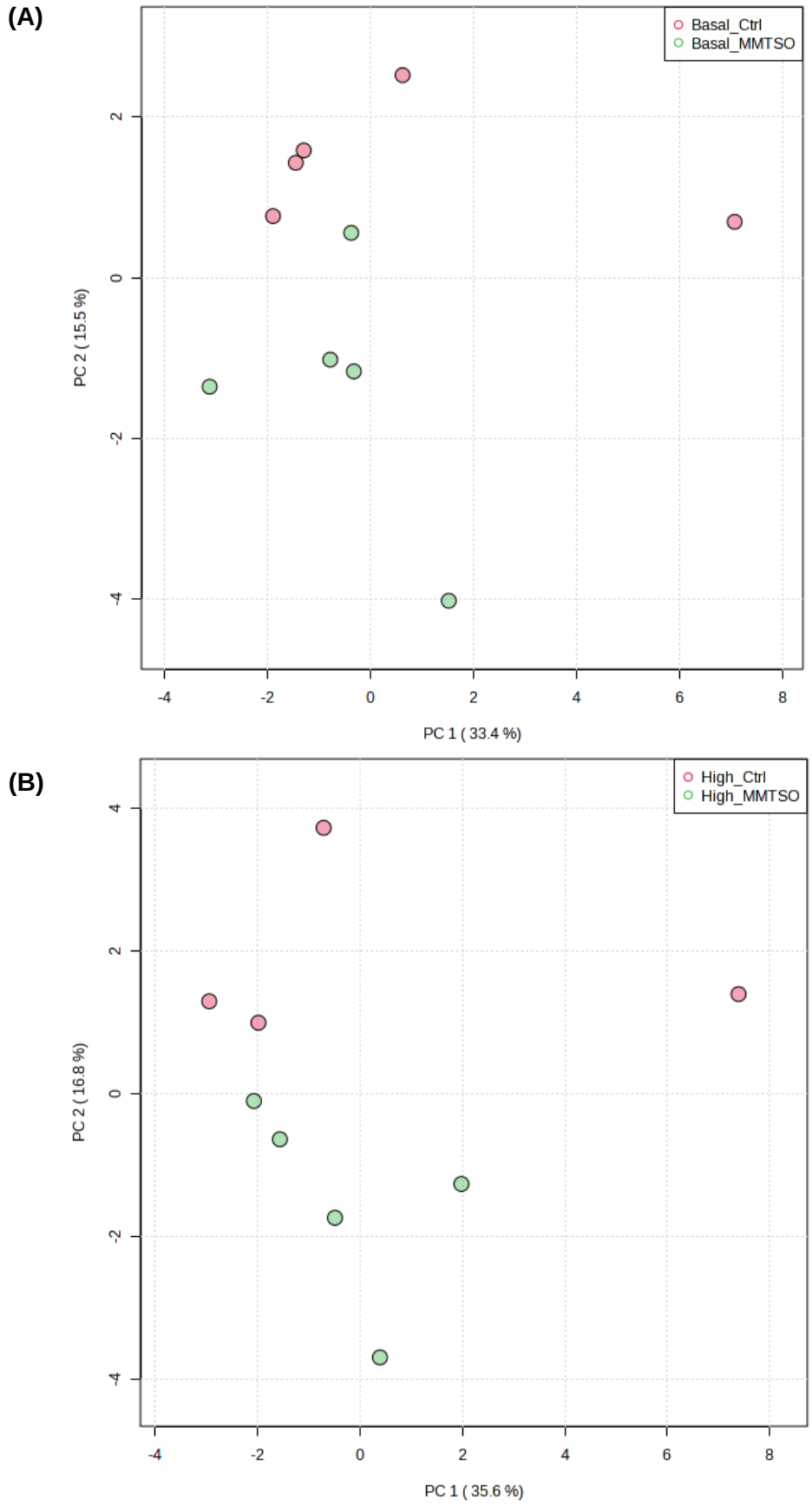

Figure 4.2. Principal component analysis (PCA) plots for control vs MMTSO in cell samples. Some clustering is demonstrated in the MMTSO treated samples (green circles) compared to control samples (red circles) samples in basal glucose (A) and high glucose (B) conditions.

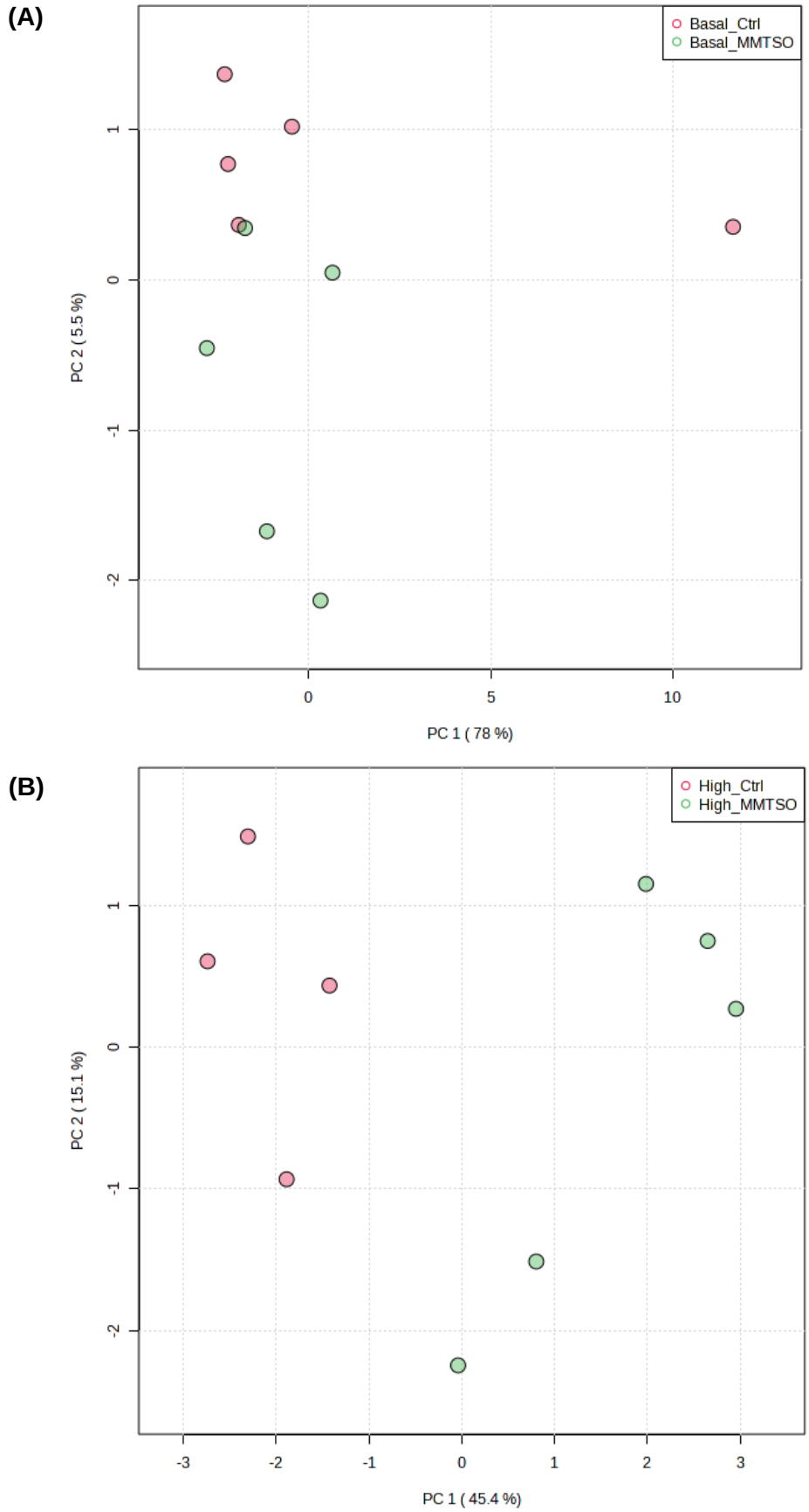

Figure 4.3. PCA plots for control vs MMTSO in supernatant samples. Some clustering is demonstrated in the MMTSO treated samples (green circles) compared to control samples (red circles) in basal glucose (A) and high glucose (B) conditions.

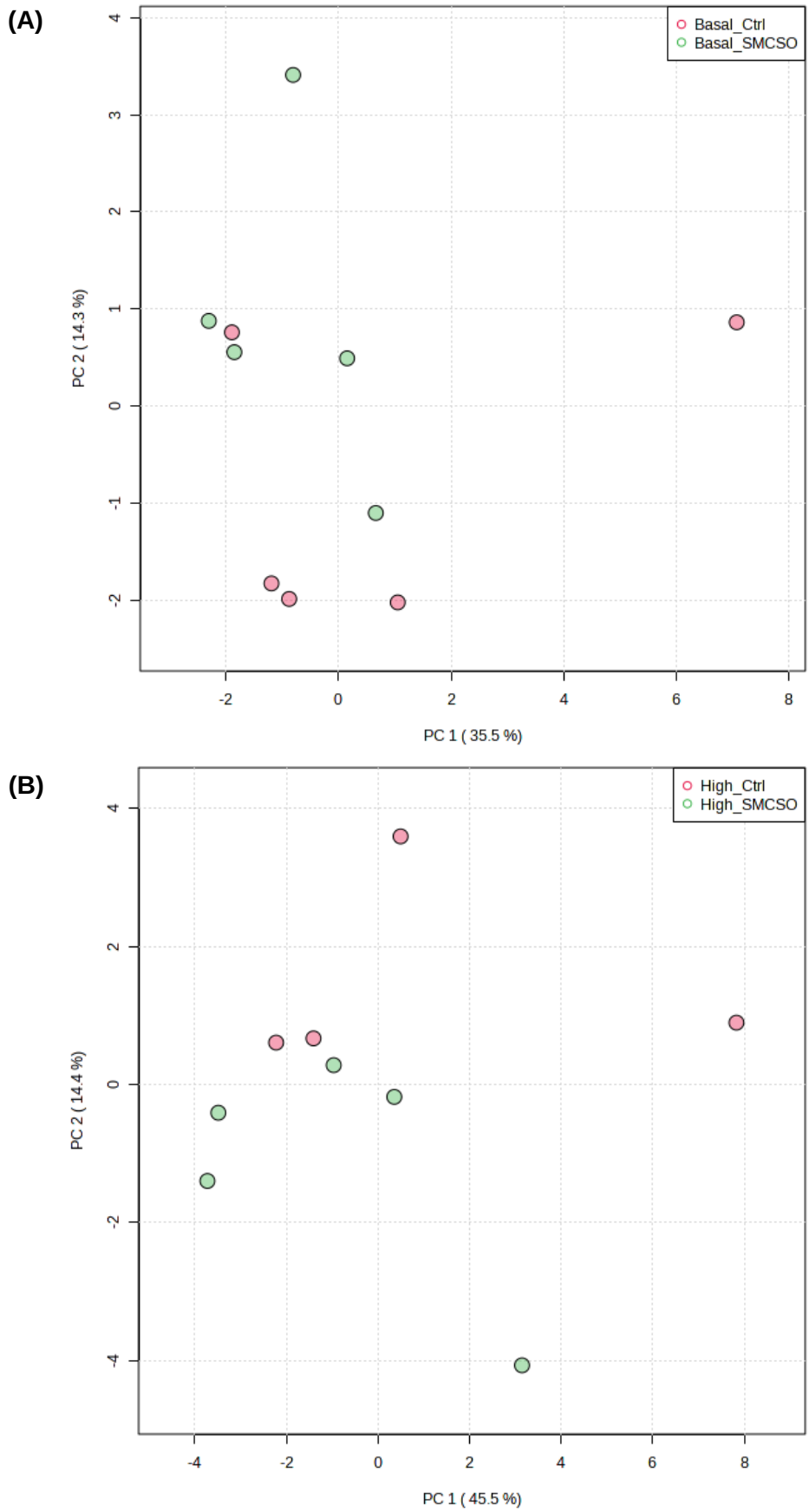

Figure 4.4. PCA plots for control vs SMCSO in cell samples. No clear clustering is demonstrated in the SMCSO treated samples (green circles) compared to control samples (red circles) in basal glucose (A); some clustering is demonstrated in the high glucose (B) conditions.

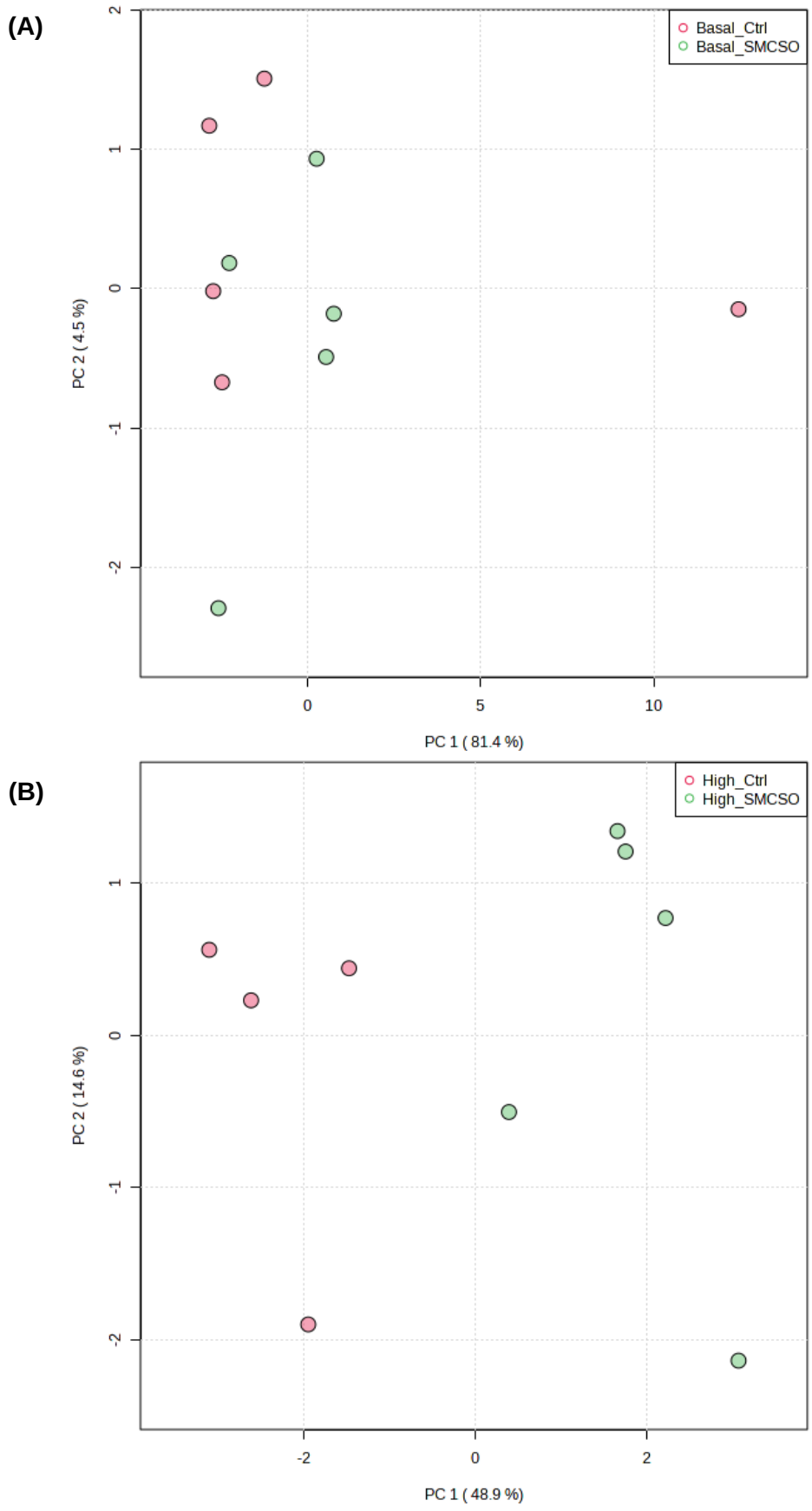

Figure 4.5. PCA plots for control vs SMCSO in supernatant samples. No clear clustering is demonstrated in the SMCSO treated samples (green circles) compared to control samples (red circles in basal glucose (A); some clustering is demonstrated in the high glucose (B) conditions.

4.4.3 More metabolites were detected in cell samples than in supernatant samples

The total number of compounds and the number of compounds per matrix detectable in each sample are shown in Table 4.2. A greater number of metabolites were detected in the cell samples compared to the supernatant samples.

Table 4.2. Number of compounds per matrix detected in each biological class by Metabolon

Biological Class	Number of compounds per matrix	
	Cell	Supernatant
Amino Acids	135	105
Carbohydrates	47	13
Vitamins	31	15
Tricarboxylic acid cycle	9	8
Lipids	325	49
Nucleotides	56	22
Peptides	41	9
Xenobiotics	19	18
Total	663	239

4.4.4 MMTSO significantly changed the abundance of metabolites from several different biological classes, especially in the high glucose environment

The number of significantly different compounds ($p < 0.05$) in cells for each treatment group compared to the relevant control, detailed in Table 4.3, indicated more compounds were significantly different from MMTSO exposure in basal glucose (75 in total) compared to MMTSO exposure in high glucose (43 in total). More tricarboxylic acid cycle compounds were significantly altered by MMTSO treatment (6 in basal glucose; 5 in high glucose). Regarding the supernatant number of significantly different compounds ($p < 0.05$) for each treatment group compared to the relevant control, detailed in Table 4.4, more compounds were significantly different in high glucose environment (53 in SMCSO; 66 in MMTSO). Fewer tricarboxylic acid cycle compounds were significant in MMTSO treated samples in the supernatant samples (1 in basal glucose; 2 in high glucose).

Table 4.3. Number of significantly different compounds in each biological class in cells

Biological Class	Number of significantly different compounds ($p < 0.05$)			
	SMCSO, Basal	SMCSO, High	MMTSO, Basal	MMTSO, High
Amino Acids	7	13	19	9
Carbohydrates	2	3	3	3
Vitamins	3	2	5	4
Tricarboxylic acid cycle	0	2	**6**	**5**
Lipids	16	5	32	8
Nucleotides	0	3	4	5
Peptides	4	4	4	6
Xenobiotics	0	3	2	3
Total	32	35	75	43

Table 4.4. Number of significantly different compounds in each biological class in supernatant

Biological Class	Number of significantly different compounds ($p < 0.05$)			
	SMCSO, Basal	SMCSO, High	MMTSO, Basal	MMTSO, High
Amino Acids	16	27	26	40
Carbohydrates	1	3	0	4
Vitamins	1	4	1	2
Tricarboxylic acid cycle	1	3	1	2
Lipids	1	2	1	3
Nucleotides	4	8	1	7
Peptides	3	1	1	1
Xenobiotics	2	5	2	7
Total	29	53	33	66

Regarding the cell samples, heatmaps of the z-scores of the number of significantly different compounds between each control and treatment ($p < 0.05$) were employed to explore the similarities and variance between control and treatment conditions. An increase was indicated by blue colour; a decrease was indicated by red colour and no change was indicated by no colour. Regarding the cell samples, in basal glucose there was a difference in the lipid and peptide compounds between the SMCSO and control samples (Figure 4.6), and no visual difference between MMTSO and control samples (Figure 4.7). However, in high glucose conditions, there was an increase in metabolites in samples treated with SMCSO compared to control (Figure 4.8) and with MMTSO compared to control (Figure 4.9). With closer investigation, key tricarboxylic acid compounds including fumaric acid and malic acid were seen to be increased following MMTSO treatment in basal and high glucose compared to controls (section 4 in Figure 4.7 and Figure 4.8).

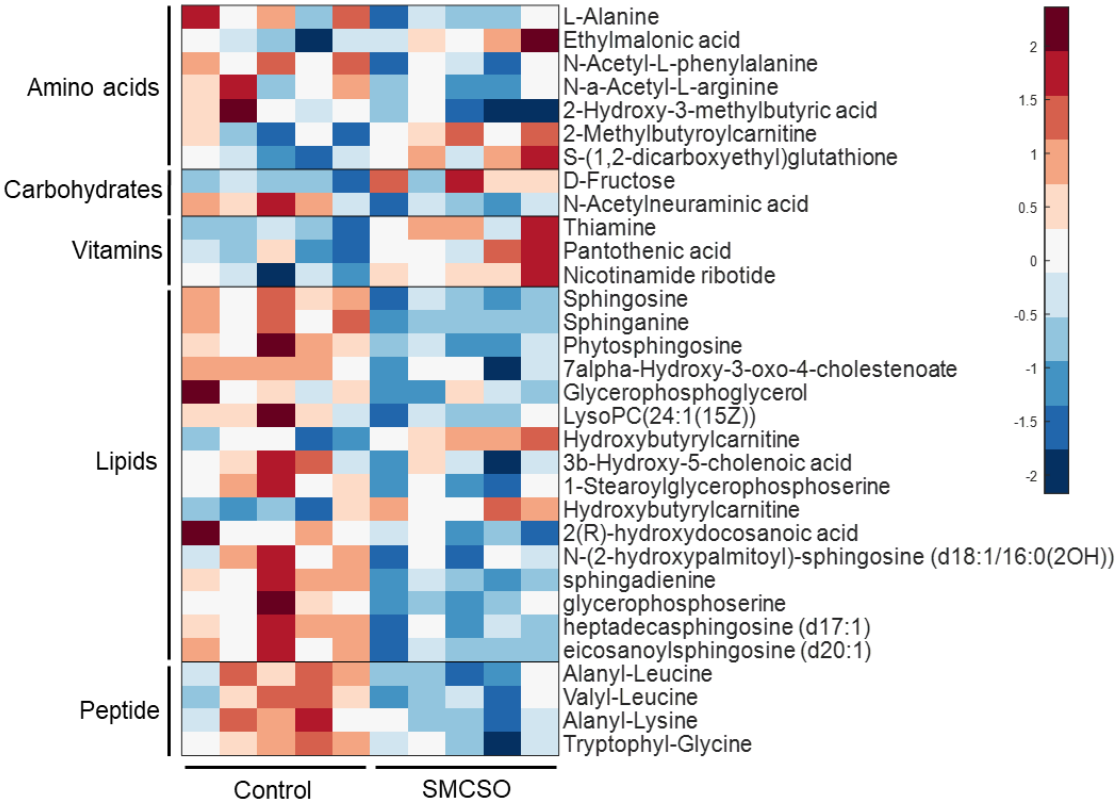

Figure 4.6. Heatmap analysis of significantly different metabolites ($p < 0.05$) detected by Metabolon within cells treated with SMCSO with respect to control in basal glucose. Plots were generated using z-scores using MatLab; metabolite change is scaled from -2 to 2 using a colour scale of red (decreased) to blue (increased) with no colour representing no change. There was no visual difference between SMCSO and control samples.

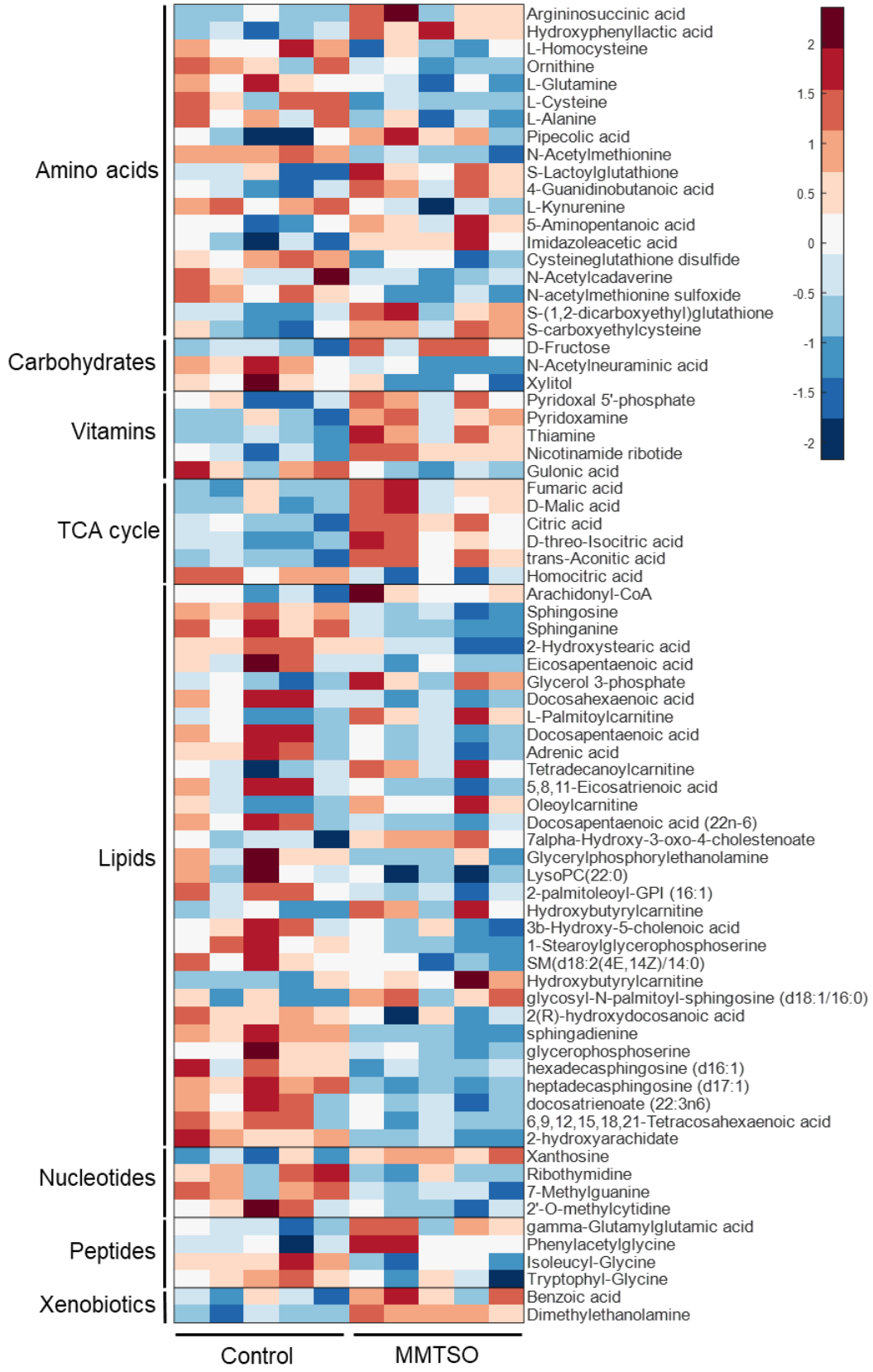

Figure 4.7. Heatmap analysis of significantly different metabolites ($p < 0.05$) detected by Metabolon within cells treated with MMTSO with respect to control in basal glucose. Plots were generated using z-scores using MatLab; metabolite change is scaled from -2 to 2 using a colour scale of red (decreased) to blue (increased) with no colour representing no change. There was no visual difference between MMTSO and control samples, although increased following MMTSO treatment in tricarboxylic acid (TCA) cycle biological class.

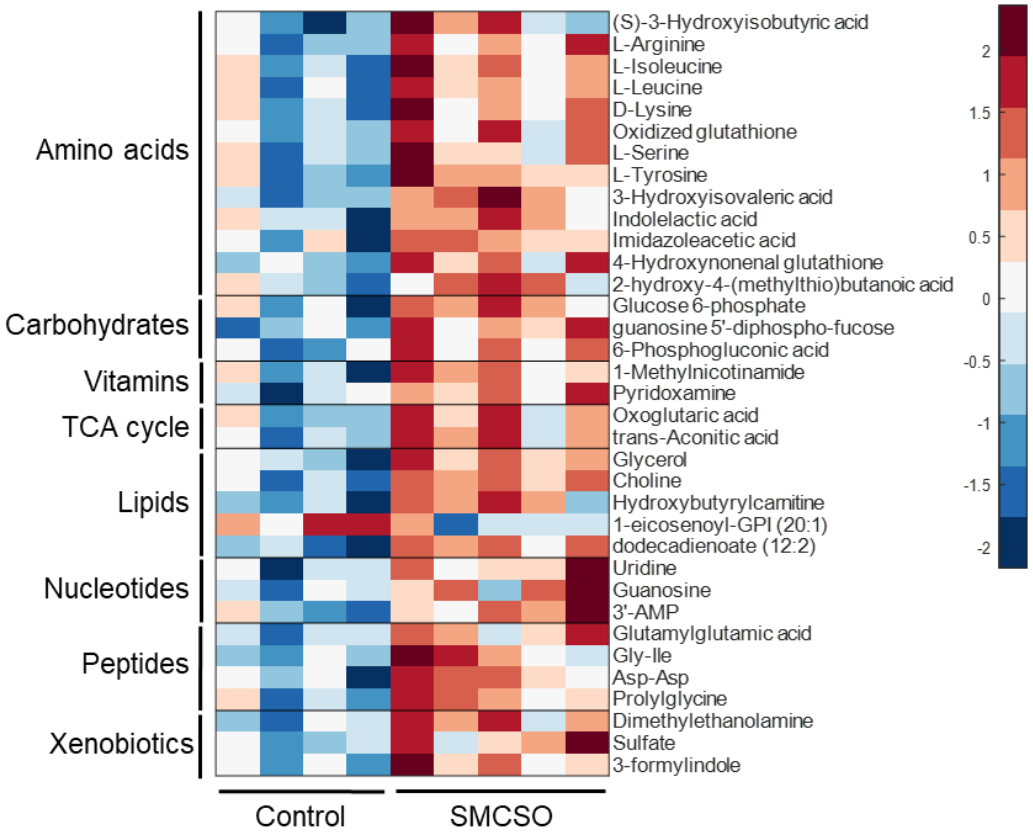

Figure 4.8. Heatmap analysis of significantly different metabolites ($p < 0.05$) detected by Metabolon within cells treated with SMCSO with respect to control in high glucose. Plots were generated using z-scores using MatLab; metabolite change is scaled from -2 to 2 using a colour scale of red (decreased) to blue (increased) with no colour representing no change. There was increased compounds following SMCSO treatment compared to control. TCA; tricarboxylic acid.

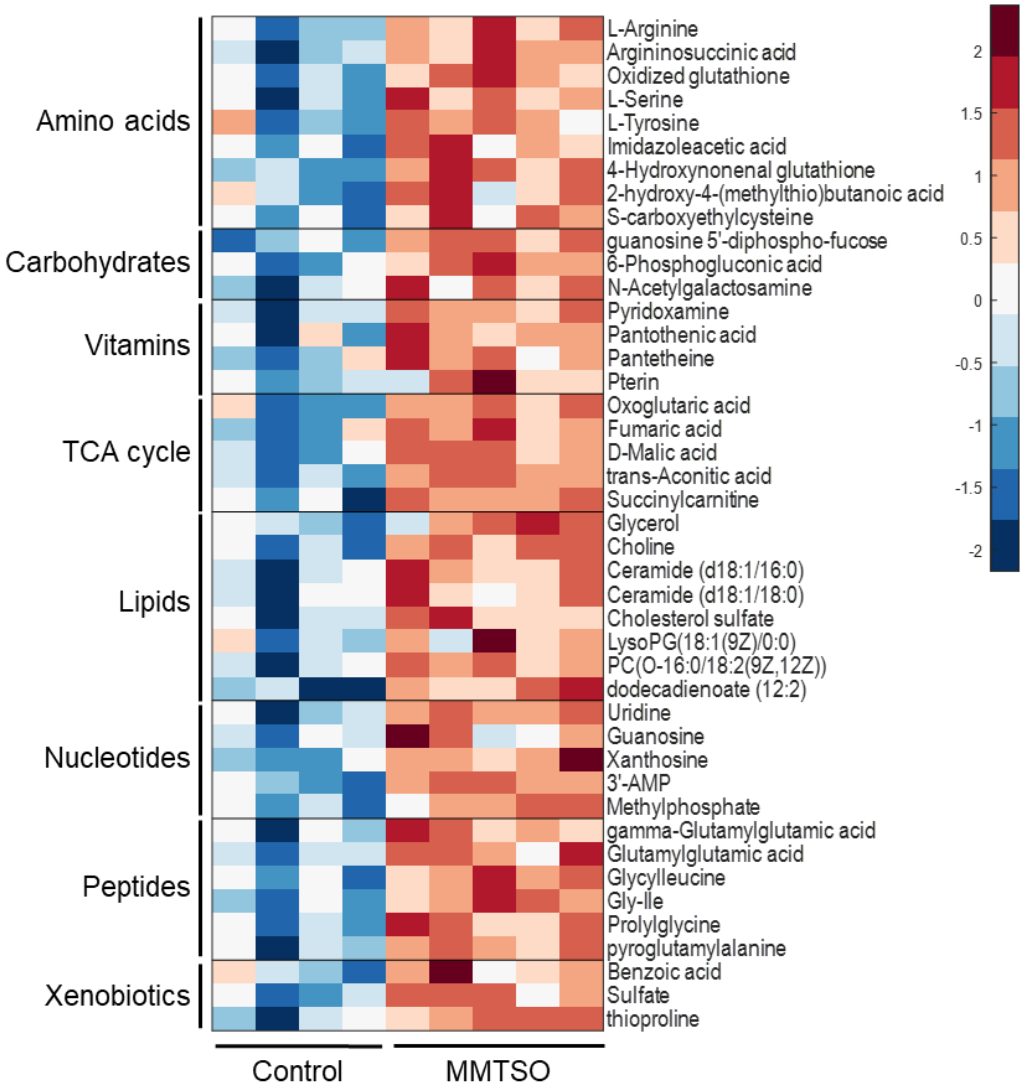

Figure 4.9. Heatmap analysis of significantly different metabolites ($p < 0.05$) detected by Metabolon within cells treated with MMTSO with respect to control in high glucose. Plots were generated using z-scores using MatLab; metabolite change is scaled from -2 to 2 using a colour scale of red (decreased) to blue (increased) with no colour representing no change. There was increased compounds following MMTSO treatment compared to control, highlighting increase in compounds in tricarboxylic acid (TCA) cycle biological class.

The proportion of significantly different metabolites compared to total metabolites in each biological class as a percentage was calculated followed by a hypergeometric comparison test to exam whether these biological classes were represented more than expected by chance in the set of compounds that were deemed to be different between control and treatment.

Regarding cells, the test indicated significance in amino acid biological class with SMCSO treatment in high glucose ($p = 0.0106$), detailed in Table 4.5. MMTSO treatment in high glucose reported significance in the peptide biological class ($p = 0.0483$), and interestingly high significance in tricarboxylic acid cycle biological class with MMTSO treatment both in basal and high glucose ($p = 0.0001$ for both), detailed in Table 4.6 and corresponding to the increased metabolites shown in Figure 4.7 and Figure 4.8.

With the supernatant, the test indicated no significance in SMCSO treated samples, detailed in Table 4.7, and only significance in amino acids biological class with MMTSO treatment in basal glucose ($p = 0.0003$), detailed in Table 4.8.

Table 4.5. Proportion of significantly different metabolites compared to total metabolites (%) and p-values in cell samples exposed to SMCSO

Biological Class	SMCSO, Basal		SMCSO, High	
	%	p-value	%	p-value
Amino Acids	5.51	0.4563	***10.4***	***0.0106***
Carbohydrates	4.26	0.6996	6.52	0.4760
Vitamins	10.0	0.1844	6.67	0.5045
Tricarboxylic acid cycle	0.00	1.0000	22.2	0.0837
Lipids	5.10	0.5284	1.61	1.0000
Nucleotides	0.00	1.0000	5.66	0.5762
Peptides	10.0	0.1319	10.0	0.1728
Xenobiotics	0.00	1.0000	15.8	0.0816

Table 4.6. Proportion of significantly different metabolites compared to total metabolites (%) and p-values in cell samples exposed to MMTSO

Biological Class	MMTSO, Basal		MMTSO, High	
	%	p-value	%	p-value
Amino Acids	15.0	0.1350	7.32	0.4800
Carbohydrates	6.52	0.9261	6.52	0.6307
Vitamins	17.2	0.2458	13.8	0.1307
Tricarboxylic acid cycle	***66.7***	***0.0001***	***55.6***	***0.0001***
Lipids	10.1	0.9199	2.61	1.0000
Nucleotides	7.55	0.8933	9.43	0.2960
Peptides	10.0	0.7146	***15.0***	***0.0483***
Xenobiotics	11.1	0.6452	16.7	0.1200

Table 4.7. Proportion of significantly different metabolites compared to total metabolites (%) and p-values in supernatant samples exposed to SMCSO

Biological Class	SMCSO, Basal		SMCSO, High	
	%	p-value	%	p-value
Amino Acids	15.7	0.3659	26.2	0.6008
Carbohydrates	7.69	0.8754	23.1	0.7193
Vitamins	6.67	0.9108	26.7	0.5979
Tricarboxylic acid cycle	12.5	0.7174	37.5	0.3582
Lipids	5.88	0.9364	12.5	0.9572
Nucleotides	19.0	0.3540	40.0	0.1217
Peptides	33.3	0.1229	11.1	0.9415
Xenobiotics	11.8	0.7365	31.3	0.4239

Table 4.8. Proportion of significantly different metabolites compared to total metabolites (%) and p-values in supernatant samples exposed to MMTSO

Biological Class	MMTSO, Basal		MMTSO, High	
	%	p-value	%	p-value
Amino Acids	***25.2***	***0.0003***	40.0	0.0534
Carbohydrates	0.00	1.0000	33.3	0.6370
Vitamins	6.67	0.9371	13.3	0.9864
Tricarboxylic acid cycle	12.5	0.7647	25.0	0.8244
Lipids	5.88	0.9573	18.8	0.9553
Nucleotides	4.76	0.9806	38.9	0.4203
Peptides	11.1	0.8045	11.1	0.9791
Xenobiotics	11.8	0.8019	46.7	0.2160

4.4.5 MMTSO significantly influenced compounds involved in the tricarboxylic acid cycle in cell samples

Interestingly, from the Metabolon analysis, the tricarboxylic acid (TCA) cycle compounds were significantly influenced following MMTSO exposure in basal and high glucose environment. Intriguingly, the TCA intermediates: citric acid (Figure 4.10A), aconitic acid (Figure 4.10B), isocitric acid (Figure 4.10C), fumaric acid (Figure 4.10D) and malic acid (Figure 4.10E) were significantly increased following MMTSO exposure in both basal and the high glucose environment. The TCA intermediate oxoglutaric acid (Figure 4.10F) was significantly increased following MMTSO exposure in high glucose conditions only. The TCA metabolite succinylcarnitine (Figure 4.10G) was significantly increased followed MMTSO exposure in high glucose conditions only.

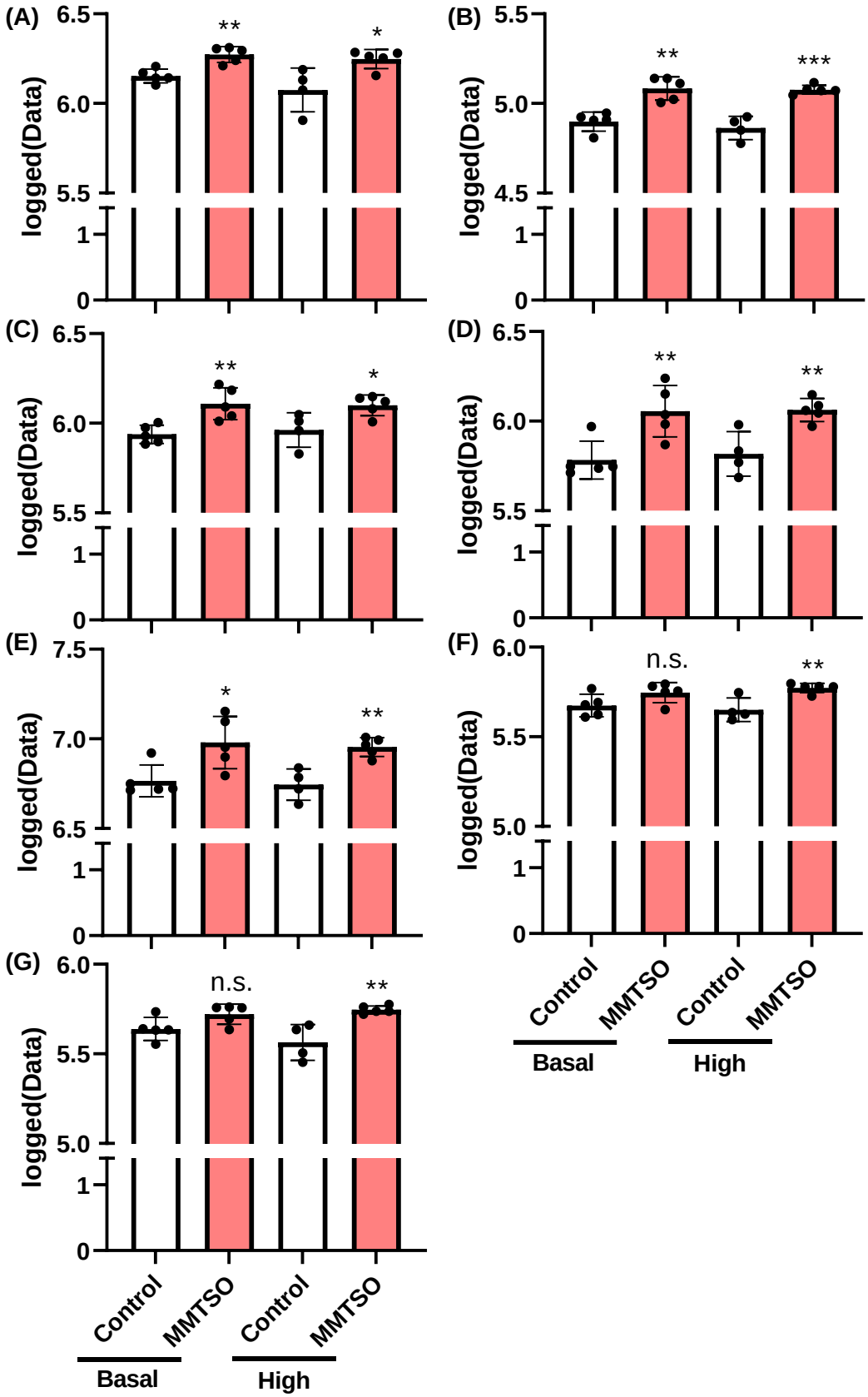

Figure 4.10. Tricarboxylic acid (TCA) compounds following MMTSO exposure in basal and high glucose. The log of peak area normalised to total protein (logged(Data)) was plotted. There was increased citric acid (A), aconitic acid (B), isocitric acid (C), fumaric acid (D) and malic acid (E) in both glucose; increased oxoglutaric acid (F) succinylcarnitine (G) in high glucose only. n.s. = not significant; * = p <0.1; ** = p < 0.01.

4.4.6 SMCSO and MMTSO significantly influenced the concentrations of amino acids in cell samples

Amino acids are key for cancer development. Using in house LC-MS/MS analysis, the concentration (μM) of seven of the non-essential and eight of the essential amino acids in the cell samples from high glucose conditions were analysed.

Following SMCSO treatment, four of the non-essential amino acids were significantly increased compared to control; alanine (Figure 4.11A), arginine (Figure 4.11B), serine (Figure 4.11C) and tyrosine (Figure 4.11D). Three non-essential amino acids had no significant difference following SMCSO exposure compared to the control; proline (Figure 4.11E), glycine (Figure 4.11F) and glutamate (Figure 4.11G) although a slight decrease was shown with glutamate. Of the essential amino acids following SMCSO exposure, six amino acids were significantly increased compared to control; isoleucine (Figure 4.12A), leucine (Figure 4.12B), lysine (Figure 4.12C), methionine (Figure 4.12D), threonine (Figure 4.12E) and valine (Figure 4.12F). Two essential amino acids although slightly increased had no significant difference following SMCSO exposure compared to the control; histidine (Figure 4.12G) and phenylalanine (Figure 4.12H).

Following MMTSO treatment, two of the non-essential amino acids amino acids were significantly reduced compared to control; glycine (Figure 4.13A) and glutamate (Figure 4.13B); five amino acids had no significant difference compared to control; alanine (Figure 4.13C), arginine (Figure 4.13D), proline (Figure 4.13E), serine (Figure 4.13F), tyrosine (Figure 4.13G). Of the essential amino acids following MMTSO exposure, all eight measured had no significant difference compared to control (Figure 4.14A – 4.14H).

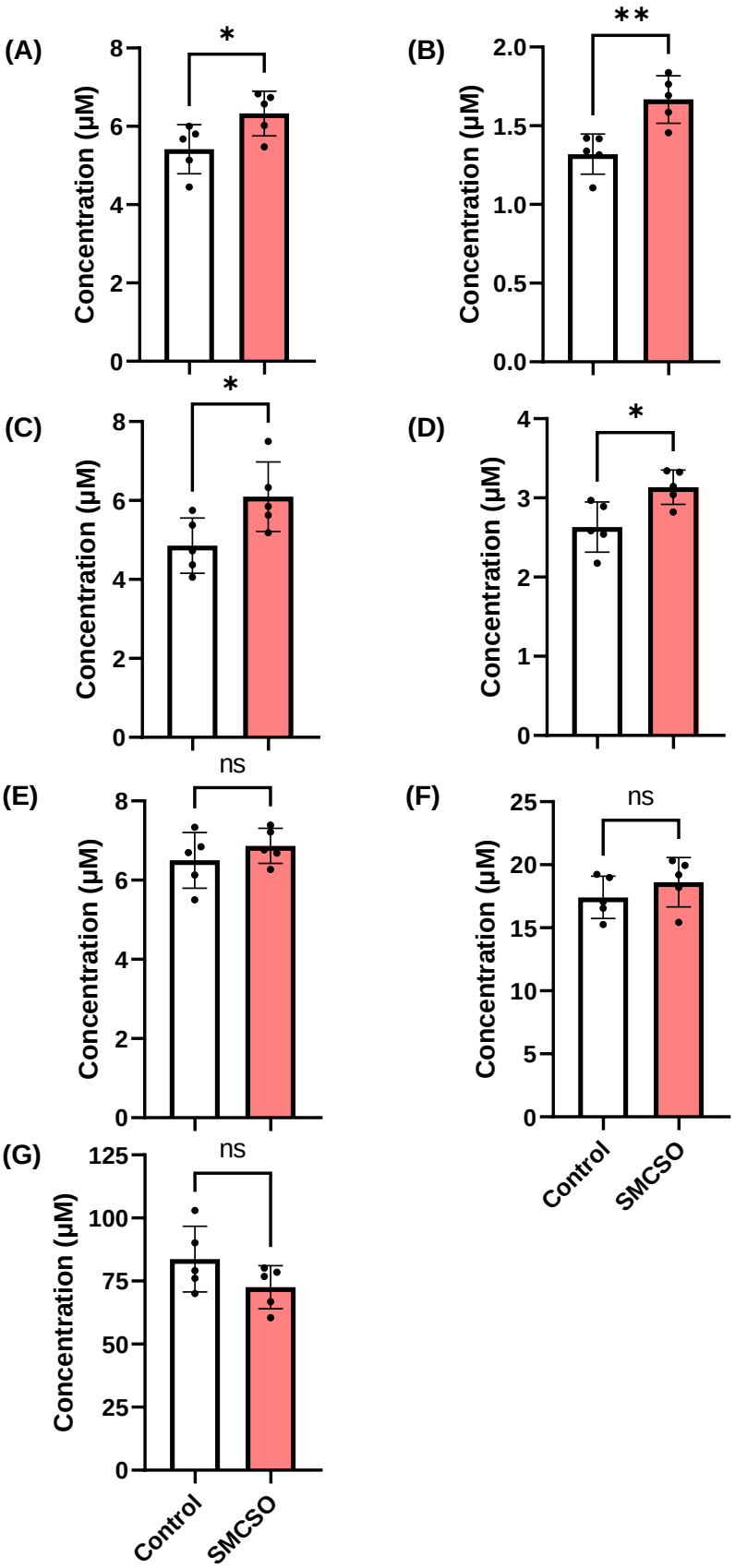

Figure 4.11. Non-essential amino acids following SMCSO exposure in high glucose in cell samples. The concentration (µM) of each was plotted. After 24-hour treatment with control and SMCSO, there was increased alanine (A), arginine (B), serine (C) and tyrosine (D) and no significant change in proline (E), glycine (F) and glutamate (G), although a slight decrease was shown with glutamate. n.s. = not significant; * = p <0.1; ** = p < 0.01.

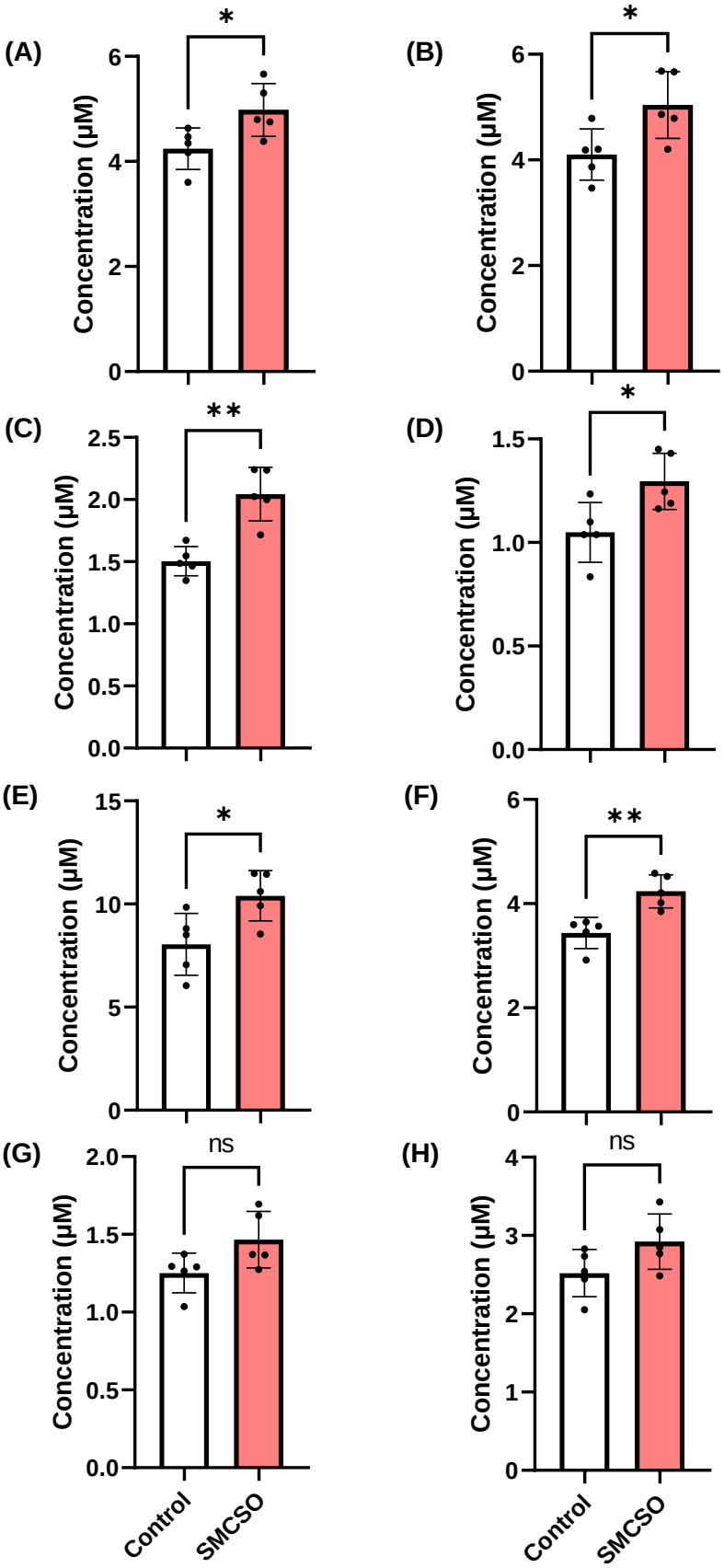

Figure 4.12. Essential amino acids following SMCSO exposure in high glucose in cell samples. The concentration (µM) of each was plotted. After 24-hour treatment with control and SMCSO, there was increased isoleucine (A), leucine (B), lysine (C), methionine (D), threonine (E) and valine (F) and no significant change in histidine (G) and phenylalanine (H), although these were slightly increased. n.s. = not significant; * = p <0.1; ** = p < 0.01.

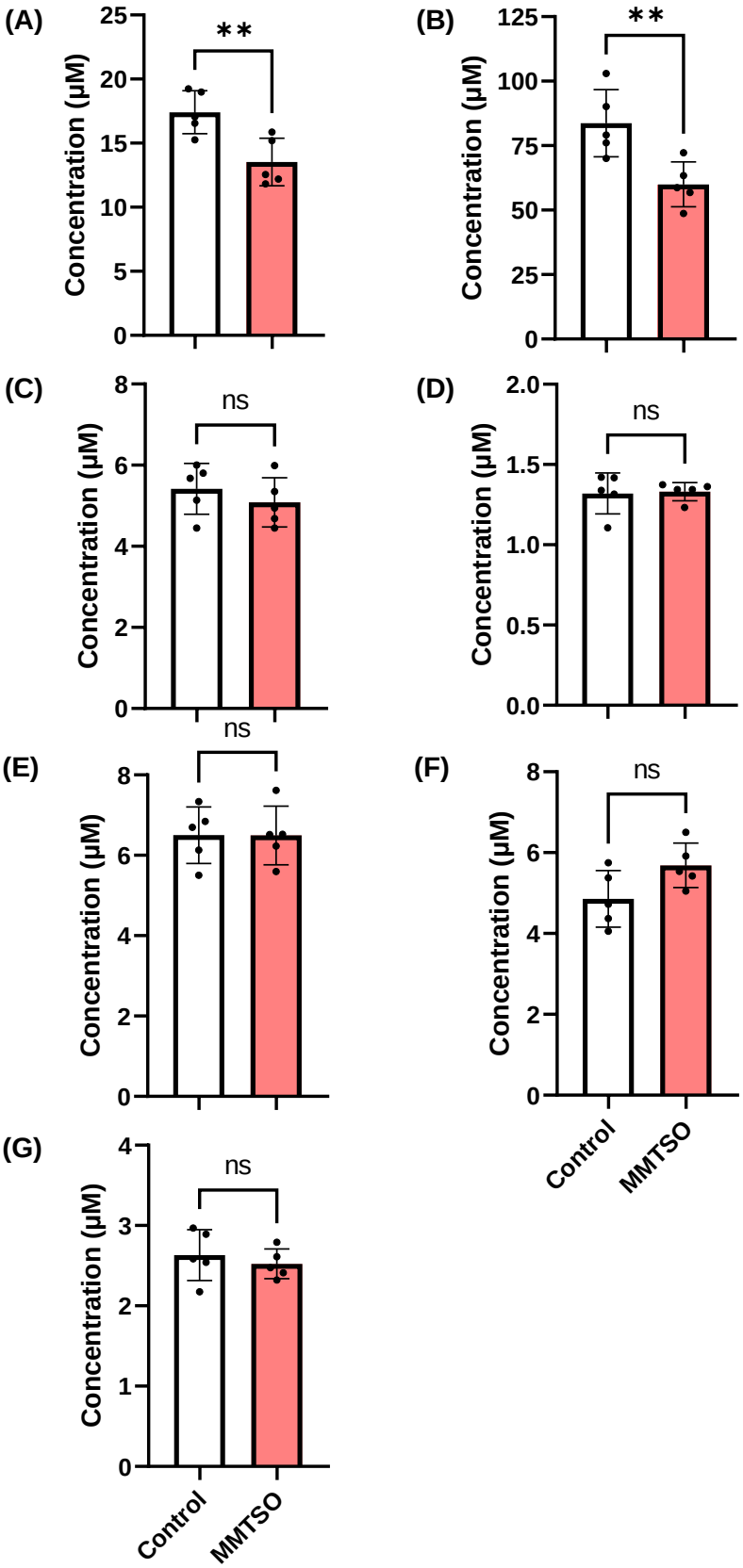

Figure 4.13. Non-essential amino acids following MMTSO exposure in high glucose in cell samples. The concentration (μM) of each was plotted. After 24-hour treatment with control and MMTSO, there was decreased glycine (A) and glutamate (B) and no significant change in alanine (C), arginine (D), proline (E), serine (F), tyrosine (G). n.s. = not significant; ** = $p < 0.01$.

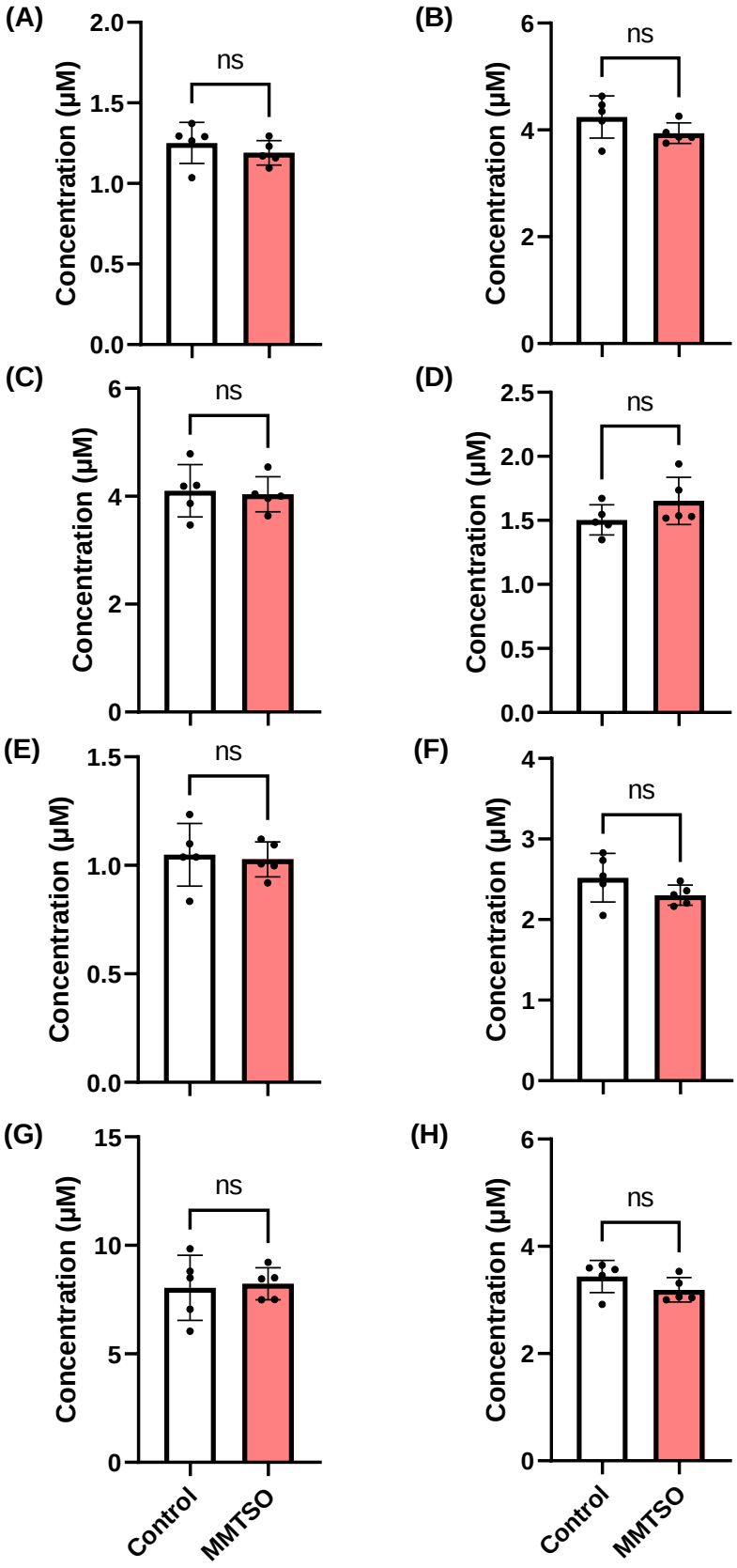

Figure 4.14. Essential amino acids following MMTSO exposure in high glucose in cell samples. The concentration (µM) of each was plotted. After 24-hour treatment with control and MMTSO, there was no significant change in all eight amino acids measured: histidine (A), isoleucine (B), leucine (C), lysine (D), methionine (E), phenylalanine (F), threonine (G) and valine (H). n.s. = not significant.

Serine-to-glycine conversion is a vital factor for cancer cell metabolism and development (252). Interestingly, the serine-to-glycine ratio was increased after SMCSO (Figure 4.15A) and MMTSO (Figure 4.15B) exposure in cells in high glucose conditions, with the increase greater in response to MMTSO exposure compared to SMCSO exposure.

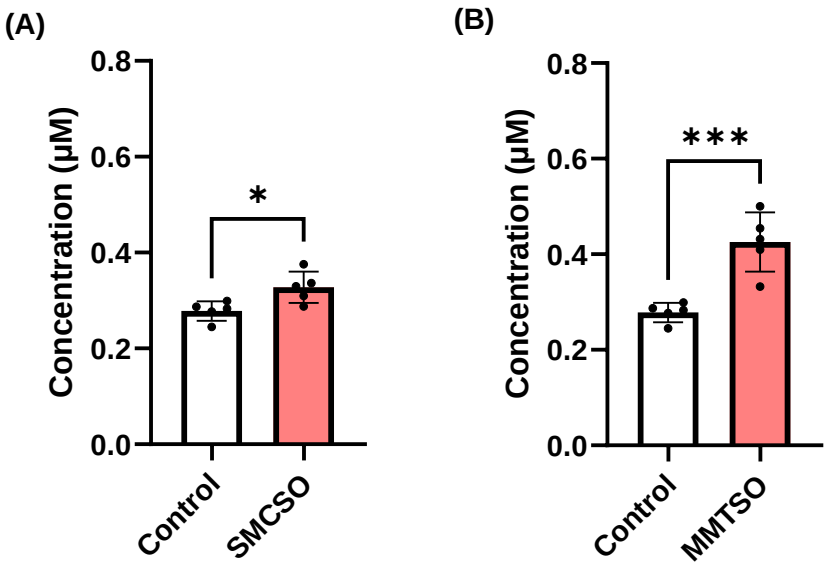

Figure 4.15. Serine-to-glycine ratio following SMCSO and MMTSO exposure in high glucose in cell samples. The concentration (µM) of each was plotted. After 24-hour treatment with control and treatment (SMCSO or MMTSO), there was significant increase in serine-to-glycine ratio; more with MMTSO exposure than SMCSO. * = $p < 0.1$; *** = $p < 0.001$.

4.4.7 DU145 cell pathway analysis showed significant differences in key metabolic pathways in response to SMCSO and MMTSO exposure

Using the Metaboanalyst online platform, pathway analysis was conducted, and the top 15 pathways were selected. The match status column indicated the number of identified compounds over the total number of compounds in the specific pathway; the match status and centrality within pathways confer higher pathway impact. DU145 cell exposure to SMCSO in basal glucose caused statistically significant differences in both fatty acid biosynthesis ($p = 0.017$) and butyrate metabolism ($p = 0.047$), with alpha linolenic acid and linoleic acid metabolism in the top 3 but not significant ($p = 0.176$), as detailed in Table 4.9 and Figure 4.16.

Table 4.9 Metabolic pathway differences in DU145 cell exposure to SMCSO in basal glucose. Pathways are ranked by p-value ($p < 0.05$ as significant); 15 highest-ranked pathways are shown.

Metabolic Pathway	Match Status	p-value	Impact
Fatty Acid Biosynthesis	**6/33**	**0.017**	**0.065**
Butyrate Metabolism	**6/16**	**0.047**	**0.359**
Alpha Linolenic Acid and Linoleic Acid Metabolism	7/16	0.176	0.481
Malate-Aspartate Shuttle	3/7	0.313	0.429
Glycerol Phosphate Shuttle	3/8	0.314	1.000
Carnitine Synthesis	8/16	0.323	0.388
Glucose-Alanine Cycle	3/9	0.324	0.563
Cardiolipin Biosynthesis	6/11	0.330	0.299
Catecholamine Biosynthesis	3/14	0.334	0.001
Histidine Metabolism	11/35	0.334	0.546
Porphyrin Metabolism	5/36	0.335	0.001
Tyrosine Metabolism	8/55	0.345	0.097
Betaine Metabolism	8/18	0.347	0.519
De Novo Triacylglycerol Biosynthesis	4/9	0.350	0.200
Phospholipid Biosynthesis	13/25	0.353	0.640

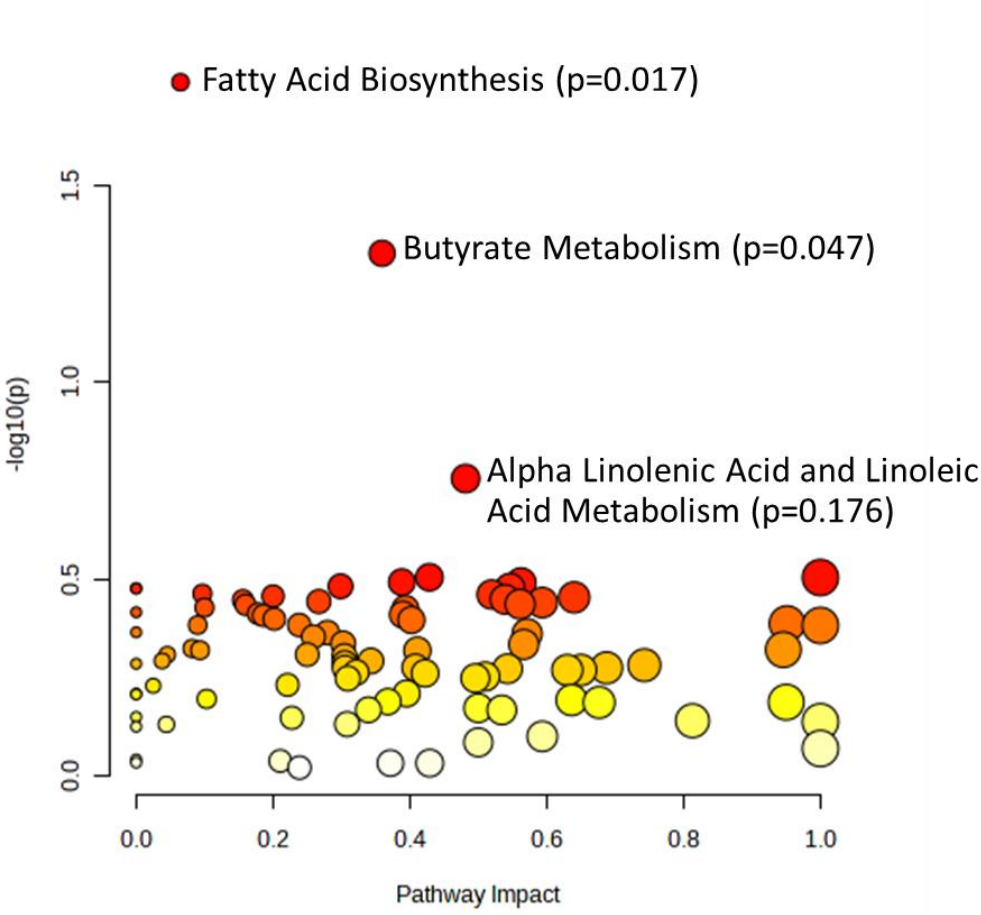

Figure 4.16. The pathway analysis metabolome view from DU145 cell exposure to SMCSO in basal glucose using Metaboanalyst. Y-axis values are presented as -log10(p) for graphical separation and X-axis values for pathway impact according to analysis and detailed in Table 4.8. The match status and centrality within pathways confer higher pathway impact. Fatty acid biosynthesis and butyrate metabolism are both significantly different ($p < 0.05$) between control and SMCSO treated samples. The alpha linolenic acid and linoleic acid metabolism is also highlighted although not significant ($p = 0.176$).

DU145 cell exposure to MMTSO in basal glucose revealed statistically significant differences in phenylalanine and tyrosine metabolism (p = 0.019), pyruvaldehyde degradation (p = 0.026) and alpha linolenic acid and linoleic acid metabolism (p = 0.034), as shown in Table 4.10 and Figure 4.17. Interestingly, the mitochondrial electron transport chain is ranked 9 out of 15, although not significant (p = 0.227).

Table 4.10 Metabolic pathway differences in DU145 cell exposure to MMTSO in basal glucose. Pathways are ranked by p-value (p < 0.05 as significant); 15 highest-ranked pathways are shown.

Metabolic Pathway	Match Status	p-value	Impact
Phenylalanine and Tyrosine Metabolism	**6/25**	**0.019**	**0.221**
Pyruvaldehyde Degradation	**2/7**	**0.026**	**0.001**
Alpha Linolenic Acid and Linoleic Acid Metabolism	**7/16**	**0.034**	**0.481**
Vitamin B6 Metabolism	6/15	0.072	0.339
Taurine and Hypotaurine Metabolism	2/9	0.073	0.001
Homocysteine Degradation	3/7	0.073	0.500
Urea Cycle	11/23	0.193	0.539
Aspartate Metabolism	13/34	0.223	0.946
Mitochondrial Electron Transport Chain	6/15	0.227	0.393
Plasmalogen Synthesis	6/16	0.292	0.001
Biotin Metabolism	1/7	0.335	0.001
Arginine and Proline Metabolism	16/48	0.338	0.593
Pyruvate Metabolism	10/37	0.344	0.395
Thiamine Metabolism	5/9	0.351	0.950
Purine Metabolism	24/63	0.382	0.322

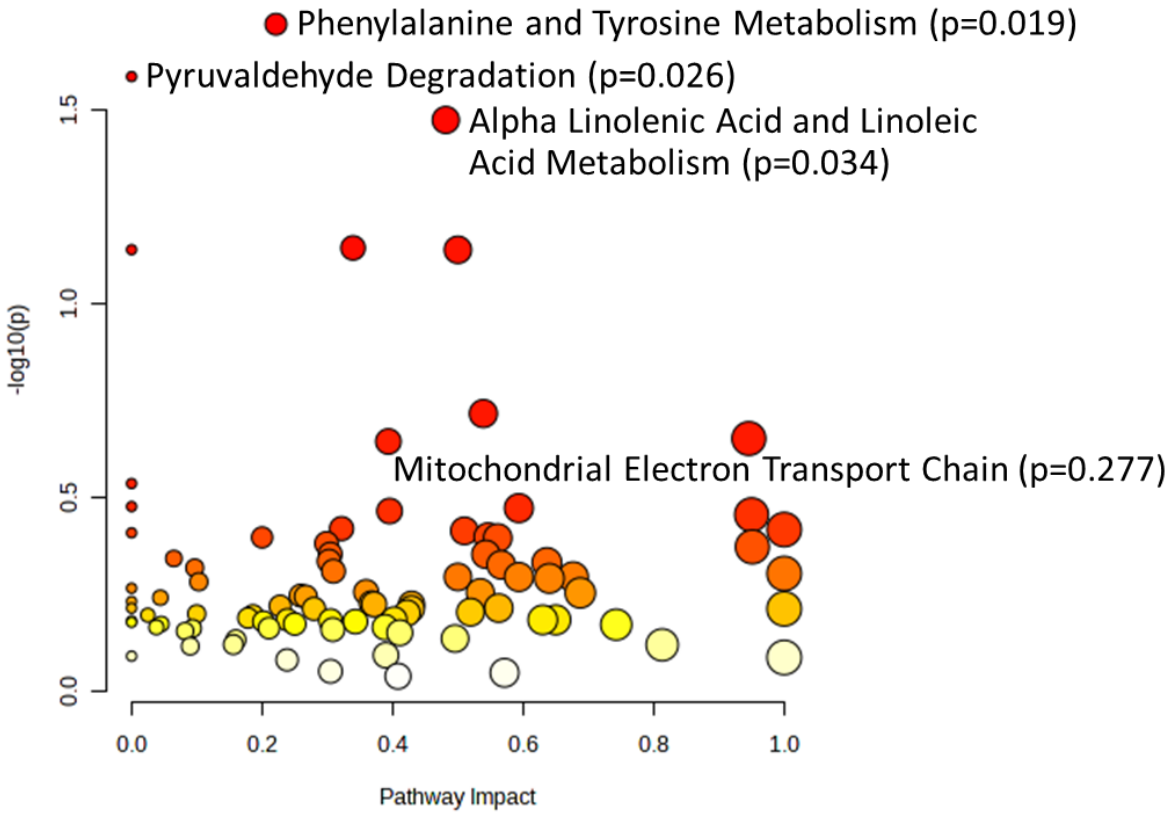

Figure 4.17. The pathway analysis metabolome view from DU145 cell exposure to MMTSO in basal glucose using Metaboanalyst. Y-axis values are presented as -log10(p) for graphical separation and X-axis values for pathway impact according to analysis and detailed in Table 4.9. The match status and centrality within pathways confer higher pathway impact. Phenylalanine and tyrosine metabolism, pyruvaldehyde degradation, and alpha linolenic acid and linoleic acid metabolism were significantly different ($p < 0.05$) between control and MMTSO treated samples. The mitochondrial electron transport chain is also highlighted although not significant ($p = 0.227$).

DU145 cell exposure to SMCSO in high glucose conditions caused no statistically significant differences according to the pathway analysis. Although not significant, the top three ranked pathways were phenylalanine and tyrosine metabolism (p = 0.096), vitamin B6 metabolism (p = 0.121) and pentose phosphate pathway (p = 0.198), as detailed in Table 4.11 and Figure 4.18.

Table 4.11 Metabolic pathway differences in DU145 cell exposure to SMCSO in high glucose. Pathways are ranked by p-value (p < 0.05 as significant); 15 highest-ranked pathways are shown.

Metabolic Pathway	Match Status	p-value	Impact
Phenylalanine and Tyrosine Metabolism	6/25	0.096	0.221
Vitamin B6 Metabolism	6/15	0.121	0.339
Pentose Phosphate Pathway	13/27	0.198	0.561
Inositol Metabolism	5/28	0.214	0.429
Inositol Phosphate Metabolism	5/22	0.214	0.372
Alpha Linolenic Acid and Linoleic Acid Metabolism	7/16	0.220	0.481
Phosphatidylethanolamine Biosynthesis	7/13	0.227	1.000
Arachidonic Acid Metabolism	5/65	0.228	0.302
Taurine and Hypotaurine Metabolism	2/9	0.232	0.001
Phosphatidylcholine Biosynthesis	11/18	0.239	0.951
Sulfate/Sulfite Metabolism	4/19	0.266	0.239
Phosphatidylinositol Phosphate Metabolism	6/14	0.270	0.813
Glutathione Metabolism	7/19	0.276	0.309
Homocysteine Degradation	3/7	0.283	0.500
Thiamine Metabolism	5/9	0.284	0.950

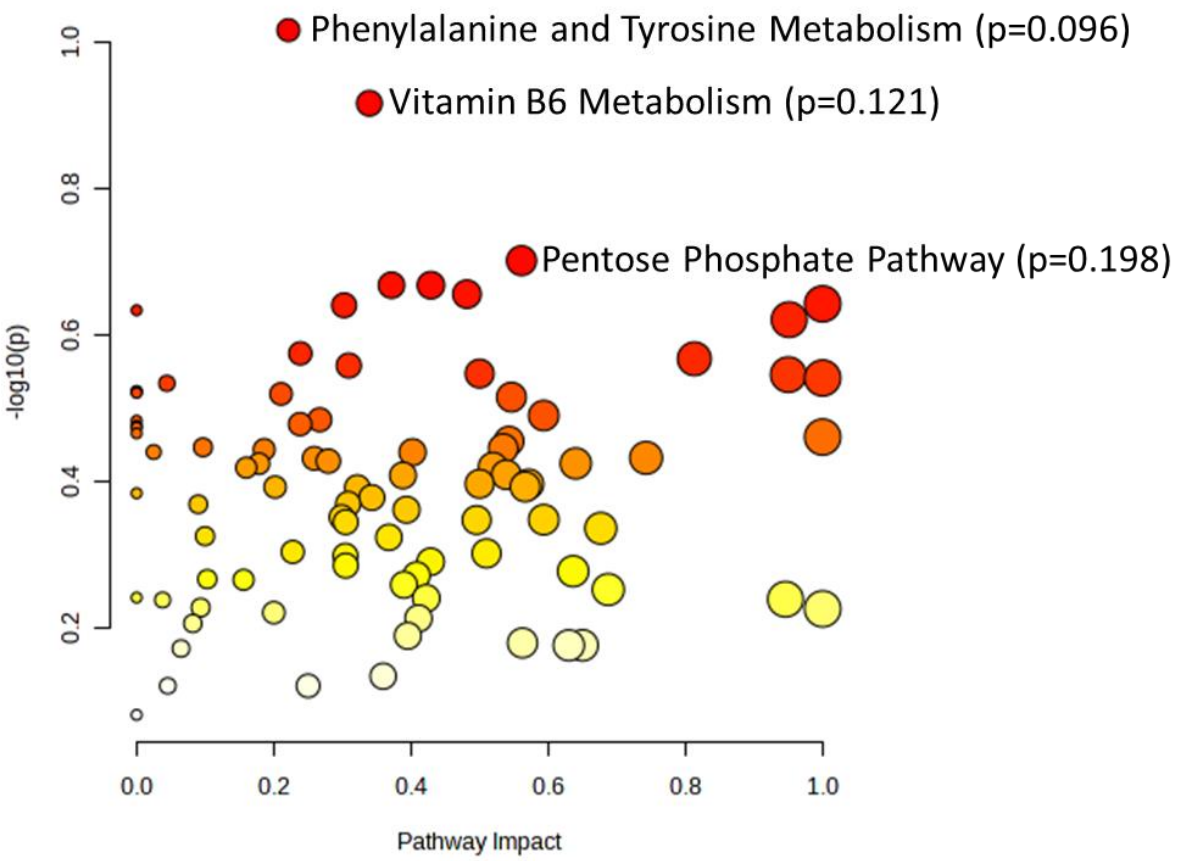

Figure 4.18. The pathway analysis metabolome view from DU145 cell exposure to SMCSO in high glucose using Metaboanalyst. Y-axis values are presented as -log10(p) for graphical separation and X-axis values for pathway impact according to analysis and detailed in Table 4.10. The match status and centrality within pathways confer higher pathway impact. No pathways were significantly different ($p < 0.05$) between control and SMCSO treated samples. The top three ranked pathways (phenylalanine and tyrosine metabolism, vitamin B6 metabolism and pentose phosphate pathway) are highlighted although not significant.

DU145 cell exposure to MMTSO in high glucose caused statistically significant differences in vitamin B6 metabolism (p = 0.022), phenylalanine and tyrosine metabolism (p = 0.025) and urea cycle (p = 0.045), as shown in Table 4.12 and Figure 4.19. Interestingly, the mitochondrial electron transport chain is ranked 6 out of 15, although not significant (p = 0.117).

Table 4.12 Metabolic pathway differences in DU145 cell exposure to MMTSO in high glucose. Pathways are ranked by p-value (p < 0.05 as significant); 15 highest-ranked pathways are shown.

Metabolic Pathway	Match Status	p-value	Impact
Vitamin B6 Metabolism	**6/15**	**0.022**	**0.339**
Phenylalanine and Tyrosine Metabolism	**6/25**	**0.025**	**0.221**
Urea Cycle	**11/23**	**0.045**	**0.539**
Glucose-Alanine Cycle	3/9	0.099	0.563
Malate-Aspartate Shuttle	3/7	0.111	0.429
Mitochondrial Electron Transport Chain	6/15	0.117	0.393
Glycerol Phosphate Shuttle	3/8	0.127	1.000
Ammonia Recycling	11/25	0.131	0.202
Phospholipid Biosynthesis	13/25	0.143	0.640
Porphyrin Metabolism	5/36	0.151	0.001
Cardiolipin Biosynthesis	6/11	0.173	0.299
Threonine and 2-Oxobutanoate Degradation	6/13	0.173	0.408
De Novo Triacylglycerol Biosynthesis	4/9	0.186	0.200
Arginine and Proline Metabolism	16/48	0.206	0.593
Pyruvaldehyde Degradation	2/7	0.211	0.001

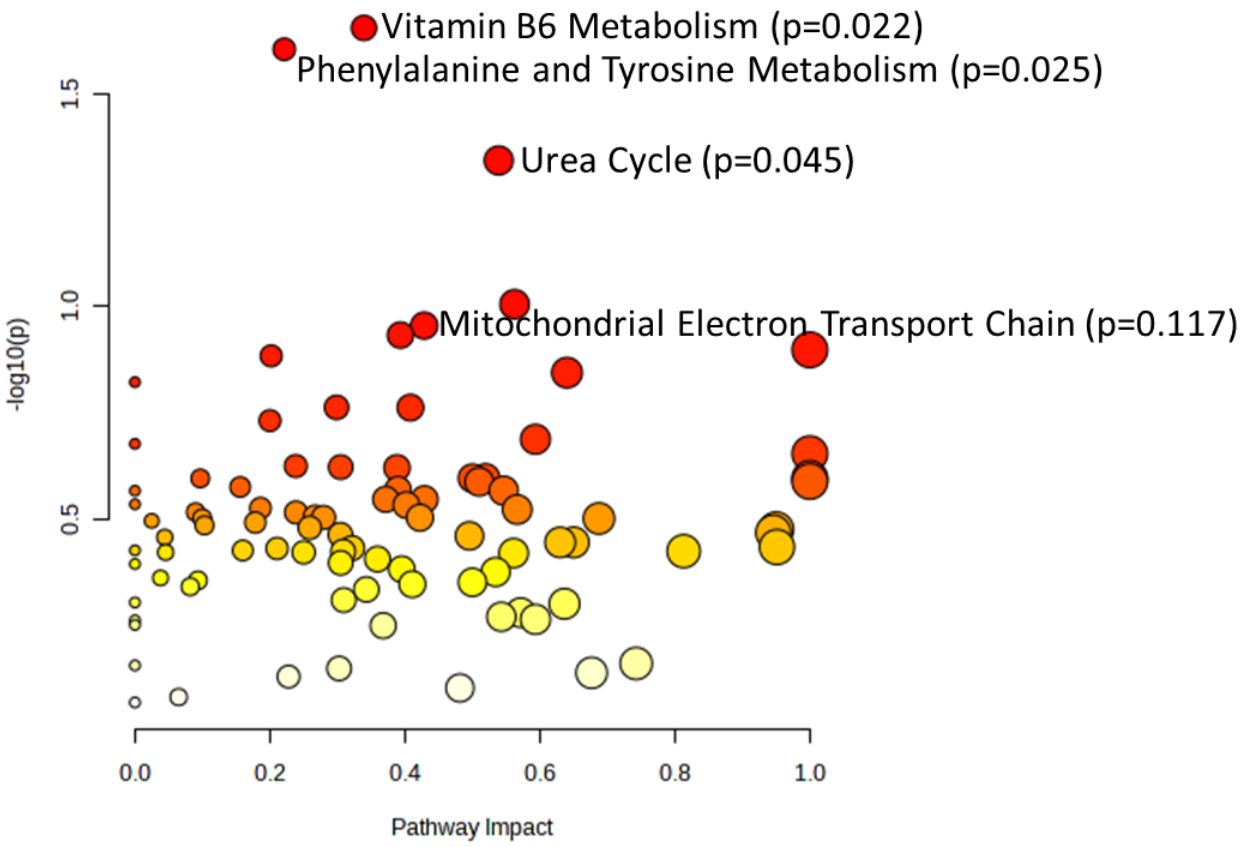

Figure 4.19. The pathway analysis metabolome view from DU145 cell exposure to MMTSO in high glucose using Metaboanalyst. Y-axis values are presented as -log10(p) for graphical separation and X-axis values for pathway impact according to analysis and detailed in Table 4.11. The match status and centrality within pathways confer higher pathway impact. Vitamin B6 metabolism, phenylalanine and tyrosine metabolism and urea cycle were significantly different ($p < 0.05$) between control and MMTSO treated samples. The mitochondrial electron transport chain is also highlighted although not significant ($p = 0.117$).

4.5 Discussion

In cancerous cells, it is typical for cellular metabolism to be substantially deregulated which enables cell proliferation and helps evade apoptosis through rewiring intracellular metabolism and adapting the tumour microenvironment (253, 254). Epidemiological studies have indicated a negative correlation between consumption of cruciferous vegetables and prostate cancer progression, which is thought to be due to the presence of sulfur-containing compounds, and potentially occurs via modulation of cancer-related genes and metabolites (24, 124). There is a growing abundance of data emerging from studies involving metabolomic profiling of cancer tissues including prostate, breast, lung and colorectal (242, 255), but until now there has been no evidence on the potential of the sulfur-containing compounds SMCSO and MMTSO, to affect metabolite profiles in prostate cancer cells. In this Chapter, the effects of treatment of DU145 prostate cancer cells with SMCSO and MMTSO on the metabolomic profile has been reported for the first time. In addition, the effects of these compounds on prostate cancer cell metabolism under different glucose environments has been reported which builds on the evidence presented in Chapters 2 and 3.

Previous metabolomic analyses of biological samples from individuals on a broccoli soup intervention have identified some metabolic changes including enhanced incorporation of fatty acid β-oxidation through the TCA cycle and effects on cellular redox capacity (24, 256, 257). One previous human intervention study explored the effect of broccoli-soup consumption on plasma metabolite profiles of volunteers with a mild to moderate risk of cardiovascular disease, using a three-arm soup intervention with varying levels of glucoraphanin: none, standard and high (256). The study detected 347 metabolites over numerous biological classes with most of the effects of treatment occurring in amino acid and lipid metabolites, TCA intermediates and acylcarnitines across both the standard and high broccoli interventions (256). From another human intervention in which prostate tissue from men recruited onto the ESCAPE study was analysed, it was reported that although there were no significant changes in metabolites across the three broccoli soup arms (24), there were increases in metabolites related to redox status and balance across all three broccoli soups (unpublished data). The evidence presented in this Chapter indicates clear increases in key amino acids and tricarboxylic acid (TCA) cycle metabolites following MMTSO treated cell samples, providing evidence that effects reported in these previous human studies may be unrelated to

glucoraphanin content and related to the other sulfur-containing compounds such as SMCSO and/or MMTSO present.

The high levels of citrate produced through the tricarboxylic acid (TCA) cycle is essential for the function of the prostate, giving the prostate a unique and unusual metabolomic profile compared to other organs (31). In malignant transformation of normal prostate epithelial cells, there is metabolic reprogramming which results in a shift of the TCA cycle from citrate accumulation to citrate oxidation to facilitate cancer growth and progression (40, 258), although the mechanisms remain unknown. Metabolomic analysis has highlighted TCA cycle dysregulation in prostate cancer tissues with increased fumarate and malate linked with tumour stage (40). In the current study reported here, there was increased fumaric acid and malic acid upon MMTSO exposure in both basal and high glucose environments, providing evidence that MMTSO exposure can modulate the TCA cycle.

Amino acids are vital for prostate cancer progression with deprivation of key amino acids now becoming a target in the development of cancer therapies (259-262). Through stable isotope tracer studies, glucose, glutamine and aspartate have been reported to increase citrate production in mouse prostate organoids restoring citrate levels through the TCA cycle and reprogramming the tumour environment to a normal prostate epithelial environment (31). This could provide evidence that the key TCA cycle metabolites were upregulated following MMTSO exposure in both glucose environments, but more so in the high glucose, and therefore could be modulating the tumour microenvironment differently to that observed in a normal environment. Glutamine conversion generates glutamate that can enter the TCA cycle at the α-ketoglutarate point for production of downstream intermediates and allowing mitochondrial respiration, and also feeds into the glutathione synthesis pathway which is involved in redox balance (263, 264). It has been reported that glutamate deprivation of prostate cancer cells reduced cell growth, invasion, migration and led to apoptotic-cell death (265). In the studies presented in this Chapter, following MMTSO exposure in high glucose conditions, glutamate was significantly reduced, suggesting that MMTSO could be modulating redox homeostasis in DU145 prostate cancer cells. Aspartate enters the TCA cycle at the malate entry point and influences the malate-aspartate shuttle (31). Interestingly, the malate-aspartate shuttle was ranked in the top 10 metabolic pathways in three of the four treatment environments. This alongside reduced

glutamate upon MMTSO exposure in high glucose, suggests these sulfur-containing compounds may act on the TCA cycle and thus modulate prostate cancer metabolism.

Serine and glycine are key in prostate tumourgenesis (252), refuelling one-carbon metabolism and affecting cellular antioxidative ability (266, 267). The serine to glycine ratio slightly increased with SMCSO exposure but significantly increased with MMTSO exposure. This is consistent with the evidence presented in this Chapter that SMCSO and MMTSO are affecting serine and glycine metabolism and suggests there is potential for serine and glycine to be investigated as possible biomarkers of prostatic cancer.

Previous studies have reported that dysregulated phenylalanine and tyrosine metabolism is associated with prostate cancer progression (268). One study undertook urine metabolomic analysis on 26 men diagnosed with stage 3 prostate cancer and 26 men with normal PSA levels; they reported aromatic amino acid metabolism was significantly altered in the prostate cancer urine samples compared to normal urine samples including phenylalanine, tyrosine and tryptophan biosynthesis, tyrosine metabolism and phenylalanine metabolism (269). Further, a report from cultured cells provided evidence that tyrosine and phenylalanine deprivation induced apoptosis in DU145 prostate cancer cells (270). In this Chapter, it was shown that DU145 exposure to SMCSO in high glucose, and MMTSO in both basal and high glucose, caused significant changes in phenylalanine and tyrosine metabolism compared to controls, suggesting that SMCSO and MMTSO may be able to interfere with prostate cancer progression affecting aromatic amino acid metabolism.

DU145 exposure to SMCSO and MMTSO in basal glucose caused significant changes in the alpha linoleic acid and linoleic acid metabolic pathway. Alpha linoleic acid is an omega-6 fatty acid acquired through diet that is essential for lipid metabolism (271). Reports from studies evaluating possible relationships between alpha linoleic acid and prostate cancer risk and progression have been inconsistent; some have suggested an association between alpha linoleic acid levels and elevated risk of prostate cancer (272-274), while others have observed the opposite, reduced risk and decreased tumour growth (275-278). Therefore, further studies are required, perhaps focussing on dietary interventions that can establish whether there is a cause and effect relationship as opposed to association studies.

Vitamin B6 intake has been inversely linked with prostate cancer risk and may improve prostate cancer survival (279, 280). One study suggested that vitamin B6 deficiency alongside hyperglycaemia could contribute to DNA damage and tumorigenesis (281). Here, DU145 exposure to SMCSO and MMTSO only in the high glucose environment gave significant differences in vitamin B6 metabolism, suggesting that in a high glucose environment SMCSO and MMTSO can modulate vitamin B6 metabolism in prostate cancer cells.

Prostate cancer exhibits dysregulated lipid and fatty acid metabolism (30, 282). Malignant prostate cancer tissues normally exhibit higher fatty acid uptake compared to benign tissue mediated through the fatty acid transporter CD36 which is linked with aggressive disease (283). DU145 prostate cancer cell exposure to SMCSO in basal glucose revealed statistically significant differences in fatty acid biosynthesis, providing evidence that SMCSO could be interfering with lipid metabolism in DU145 prostate cancer cells.

Mitochondria play a key role in tumorigenesis by regulating the energetic ability of the cells supporting malignant transformation and cell proliferation (77). Intriguingly, DU145 prostate cancer cell exposure to MMTSO in both basal and high glucose revealed the mitochondrial electron transport chain ranked in the top ten of the highest-ranked metabolic pathways (9 out of 15 in basal glucose and 6 out of 15 in the high glucose). This, alongside the evidence reported in Chapter 2, suggests a role of MMTSO in the mitochondrial energy metabolism of DU145 prostate cancer cells.

Global untargeted metabolomics can be very expensive and time-consuming depending on the sample size. In addition to this, the data analysis is limited by methods developed and devices available to detect metabolites, and how up to date the available tools and databases are (284). Regardless of this, metabolomics allows the quantification of intracellular metabolites within biological samples to distinguish between treatments (285). Metabolomics in combination with other omics analyses including proteomics and transcriptomics, is becoming a more widespread approach for assessing the impacts of treatments compared to appropriate controls (238).

Future work could use targeted tracer experiments and metabolic flux assessments with glucose and glutamine to observe the redirection of these energy sources under different treatment and glucose environments. Future work

could also explore the metabolic modelling of the data presented in this Chapter and in Chapter 2 and 3, in combination with the tracer and metabolic flux analyses, to give a more robust picture of the molecular pathways regulated by SMCSO and MMTSO exposure to prostate cancer cells. This could identify potential biomarkers for the development of targeted therapeutics to reduce cancer progression.

4.6 Conclusion

This Chapter provides evidence that MMTSO treatment and to a lesser extent SMCSO can affect the metabolomic profile of DU145 prostate cancer cells, with the most important changes observed in the tricarboxylic acid (TCA) cycle metabolites and amino acids, and in cellular metabolism pathways including fatty acid metabolism, phenylalanine and tyrosine metabolism, and the mitochondrial electron transport chain. These observations are consistent with the notion that SMCSO and/or its metabolite MMTSO are at least partially responsible for the beneficial effects of a cruciferous-rich diet on prostate cancer risk.

Chapter Five.

Evaluation of dietary products for the development of an SMCSO-rich product for use in cancer human trials

Chapter Five: Evaluation of dietary products for the development of an SMCSO-rich product for use in cancer human trials

5.1 Introduction

Collectively Chapters 2, 3 and 4 provide evidence towards a role of the sulfur metabolites SMCSO and MMTSO on prostate cancer metabolism in vitro. Thus, it would be reasonable to investigate this effect in a human intervention study with prostate cancer cohort. Currently, there is no commercially available product rich in SMCSO that could be used in a human study. This Chapter considers the best delivery and formulation of an SMCSO-rich product matched with a control product to be used in future cancer dietary interventions trials.

Cancer is a global burden with prostate cancer the most common cancer in men accounting for 26 % of all new male cancer cases in the UK (85). It is estimated that 30 – 50 % of all cancer cases are preventable through implementation of healthy eating and a physically active lifestyle (286). The chemopreventative properties associated with consumption of cruciferous vegetables, including broccoli, are largely attributed to the sulfur-containing secondary metabolites they contain (85, 88, 91, 287-289). Whilst much of the cancer human studies have focused on the benefits related to the sulfur-containing compound sulforaphane, there has been no human intervention assessing the bioactivity of the secondary metabolite S-methyl cysteine sulfoxide (SMCSO) or its metabolite S-methyl methanethiosulphonate (MMTSO). Data presented in Chapters 2, 3 and 4 of this thesis have provided evidence that the breakdown product of SMCSO, MMTSO, could also be responsible for the beneficial effects of a broccoli-rich diet on DU145 prostate cancer cells. To date, no isolated SMCSO supplement or SMCSO-rich food product has been developed and made commercially available. In light of the emerging evidence that SMCSO and its metabolites may be at least partly responsible for the health benefits associated with consumption of broccoli, it would be useful to develop or identify food-grade products that are rich in SMCSO that could be used to directly test in future cancer human trials.

The delivery of bioactive compounds to their biological targets in vivo, such as cancerous regions of the prostate, needs careful consideration of food processing to ensure they retain the bioactive compounds and can provide an effective concentration (290). With cultured cell based studies, specific doses of the

bioactives can be administered for a known length of treatment time to the biological target allowing for assessment of physiological changes including gene, protein and metabolite variations (291). In the case of human dietary intervention trials, the whole body is potentially exposed to the bioactive compound, but in addition there are multiple other processes that can take place and may affect the response(s); these include incomplete or partial absorption, changes in the chemical nature of the bioactive(s) as a consequence of gut microbial or human metabolism, bioactive effects on the structure, diversity and/or function of the gut microbiome which consequently affects the host. Such studies allow for bioactive exposure to the whole body and therefore multiple potential biological targets, giving a better representation of the effects of the bioactive which may be caused, for example, via the effects on the tumour microenvironment rather than the cancerous cells themselves (292). However, concentrations used in vitro are often far above what would be achievable in dietary interventions, thus careful consideration is warranted to ensure the delivery of an effective concentration in vivo (293). Understanding how a compound is metabolised and how quickly is also vital in the choosing the most appropriate delivery method. A report of a human pharmacokinetics study (the BOBS study) showed that the appearance of sulforaphane in plasma peaked at 6 to 8 hours, which suggested absorption from the distal gut, which was in contrast to SMCSO which peaked much earlier at 1.5 to 2 hours, which is almost certainly due to small intestinal absorption (99). This is because sulforaphane is a metabolic product that is only generated once the glucose of glucoraphanin has been removed by microbial thioglucosidases, whereas SMCSO can be directly absorbed (99).

Designing functional foods requires strategic and scientific consideration. Initial studies in cell and animal models could identify a potential bioactive that may have health benefits in vivo but may require processing to develop functional products. Whole food-based products such as a dried broccoli powder would contain a mixture of bioactive compounds and micronutrients including fibre. Alternatively, the compounds can be extracted, concentrated and/or isolated to generate supplements containing relatively high concentrations of the isolated compounds; an example is Broccomax, which is isolated sulforaphane obtained from broccoli seed extract. Previous human interventions with prostate cancer patients have used a variety of delivery methods such as a fresh soup product including the SAP, BOBS and ESCAPE studies (24, 25, 99), or supplements including the Norfolk

ADAPT study (26). Careful consideration is required when choosing the most appropriate approach for efficient delivery of the bioactive compounds.

Combination of a bioactive ingredient into an appropriate food matrix needs knowledge of their availability from the product, and an understanding of biological factors such as bioavailability, bioaccessibility, chemical stability, and dosage feasibility (292, 294). The optimal food matrix for delivery should be chosen to optimise for these factors. Once selected, further assessment of chemical and nutritional properties are needed to give analysis of the stability of bioactive within the functional food product, and the nutrient and microbiological profile of the product to prevent food spoilage (295). From this, additional processing may be required such as further heating or boiling of the product. If further processing is required, it is key to bear in mind the palatability of the product for clinical suitability, for example if the product is too chewy or too viscous, modifications can be made at this stage before taking the product to human clinical trials (296, 297). Once the final functional food product is carefully selected, large-scale production with appropriate food grade packaging for shelf stability and long term storage with appropriate temperature control may need to be considered, especially for long duration human studies (298). To ensure consistency between individuals in handling the product, detailed instructions and recording of the product consumption and background diet may be required (299, 300). The development of a functional product rich in SMCSO for use in a controlled human trial in a cancer cohort can help improve our understanding of SMCSO bioactivity and bioaccessibility, to potentially be used alongside current standard cancer prevention treatment.

5.2 Aims

Evaluation and formulation of a functional product for the appropriate delivery of a high dose of SMCSO for use in future cancer human trials:

- To assess fresh-broccoli soups, supplements and dried-broccoli soups to select the best source of SMCSO.
- To investigate the effects of cooking and heating such products on the levels of the sulfur metabolites including glucoraphanin, sulforaphane and SMCSO.
- To assess the colour and other characteristics of the broccoli and placebo powders and select a placebo that would facilitate blinding in future dietary interventions trials.

5.3 Materials and Methods

5.3.1 Fresh Soup Preparation

The fresh soup samples were produced by CRL FOODS (Gosforth Industrial Estate, Gosforth, Newcastle upon Tyne, NE3 1XD). For the development of the soup processing steps including pasteurisation and sterilisation was conducted by CRL FOODS. Approximately 300 g samples of each soup were packaged into plastic pouches and sent to the Quadram Institute Bioscience for analysis. Part of the fresh soup sample was accurately weighed and placed in a freeze drier for subsequent analysis of the metabolites. Freeze dried samples were stored at 4°C until analysis.

5.3.2 Broccoli Powders

A variety of broccoli powders were assessed for their sulfur metabolite profile as potential candidates. The broccoli cultivar 1086 that had elevated accumulation of glucosinolates was developed through introgression of a novel allele of *MYB28* from wild *Brassica villosa* and previously described in (98); this was made into a powder form and provided by Professor Richard Mithen. Commercially available broccoli powders were purchased from four different companies: Just Ingredients (https://justingredients.co.uk/products/broccoli-powder), Bulk Powders (https://www.bulk.com/uk/broccoli-powder.html), Buy Whole Foods Online (https://www.buywholefoodsonline.co.uk/organic-broccoli-powder.html), and Sussex Wholefoods (https://www.healthysupplies.co.uk/fd-broccoli-powder-sussex-wholefoods.html). Broccoli powder of the 1086 variety was subjected to various hydration, heating and cooking processes. Each broccoli powder provided was specified as *Brassica oleracea* by the company marketing the product. The samples were stored at -80 °C until analysis.

5.3.3 Hydration and Stability Preparation of 1086 Broccoli Powder

Studies of hydration on 1086 variety of broccoli powder involved addition of 50 ml of water at varying temperatures (ambient temperature, 40 °C, 60 °C, 80 °C and 90 °C) to 3 g samples of broccoli powder with maintenance of the temperature for 20 min. For heat treatment, 3 g samples of broccoli powder were dry heated at 60 °C for 20 min. Effects of heating and hydration were done by dry heating 3 g samples of broccoli powder at 60 °C for 20 min and then hydrating the samples at ambient temperature for 20 min. Effects of cooking were assessed by steaming 3

g samples of broccoli powder at 100 °C for 20 min. A small proportion of the freeze-dried broccoli powder was either kept freeze dried at ambient temperature or hydrated at ambient temperature for one week. The hydrated samples were freeze dried once more. All samples were stored at -80 °C until analysis.

5.3.4 Commercially Available Broccoli Powders

Each of the commercially available broccoli powders from Just Ingredients, Bulk Powders, Buy Whole Foods Online and Sussex Wholefoods, were assessed for their sulfur metabolite profile. The powder with the highest SMCSO content was selected for the dried soup product. An appropriate control that was similar in macronutrient profile and colour was selected for potential use as a placebo.

5.3.5 Dried Soup Preparations

The composition of the dried soup product was optimised and developed at Quadram Institute Bioscience with the support of Dr Jennifer Ahn-Jarvis. Each soup contained 20.5 g of a base golden vegetable soup (Batchelors) to which was added 16 g of a commercially available freeze-dried broccoli powder (Sussex Wholefoods) or 16 g of a commercially available freeze-dried courgette powder (Sussex Wholefoods).

5.3.6 Dried Soup Heating Evaluation

Briefly, the dried soups were either not treated or treated with 250 ml of 100 °C MilliQ water. The treated soups were freeze dried in an Edwards Vacuum and all samples were appropriately stored at -80 °C until analysis. A commercially available broccoli and stilton cup of soup was analysed as a positive control.

5.3.7 Commercially Available Supplements

Broccoli and garlic supplements were purchased from Broccomax® and Kwai Heartcare respectively. The supplements were received in sealed tubes. Once opened, supplements were stored at room temperature until analysis. Prior to analysis, supplements were ground with a mortar and pestle to give a fine powder.

5.3.8 S-methyl-L-cysteine sulfoxide (SMCSO) Extraction and Detection

To extract S-methyl cysteine sulphoxide (SMCSO), a 40–60 mg sample of freeze-dried powdered soup or supplement was measured. A 5 ml aliquot of 1.1 mg/ml O-

(carboxymethyl)hydroxylamine hemihydrochloride (OCMHA) in MilliQ water was prepared. All samples were vortexed thoroughly and shaken on a horizontal shaker at 1000 rpm for 10-minutes at 4 °C. After this incubation, the samples were centrifuged at 4000 *xg* for 10-minutes at 4 °C. The clear supernatant was removed and diluted 1:10 in HPLC-H_2O containing 0.1 % formic acid and placed into HPLC vials (Agilent®). Trideutromethyl $^{[34]}$S cysteine sulfoxide that was synthesised by Dr. Paul Needs (Quadram Institute Bioscience) was added as an isotopically-labelled reference standard (10 µg/ml in MilliQ water). Tubes were capped using a crimper, vortexed and stored at -20 °C until analysis.

A model Agilent 6490 Triple Quadrupole LC/MS/MS system equipped with a binary pump, cooled autosampler, degasser, column oven and diode array detector, was used. A mobile phase A of 10 mM ammonium acetate (Sigma-Aldrich®) and 0.05 % hetaflurobutyric acid (Sigma-Aldrich®) in MilliQ water, a mobile phase B of 10 mM ammonium acetate (Sigma-Aldrich®) and 0.05 % hetaflurobutyric acid (Sigma-Aldrich®) diluted in 10 % MilliQ water with the remaining volume made up with 100 % methanol. Initially, the flow rate was set at 0.1 ml/min to purge the binary pump, this was followed by loading the appropriate method. For analysis, the flow rate was set at 0.3 ml/min; the gradient started with 0 % mobile phase B, increased 3 % mobile phase B within 4 min, after washing for 2 min and equilibration was for another 2 min. The total run was 8 min. The column temperature and autosampler temperature maintained at 20 °C and 4 °C respectively. Samples were analysed using an Agilent SB-AQ 1.8 µM (100 x 2.1 mm) C18 column with an Agilent Zorbax guard column, using a programmed gradient mobile phase and ESI positive MRM. The injection volume was 2 µl per sample. The retention time of SMCSO was approx. 0.906. Quantification was performed by the use of calibration standards. Briefly, into separate vials SMCSO standard (Methiin, Abcam) was dissolved in MilliQ water to each give a 1 mg/ml stock. The stock was diluted in water from 0 µg/ml to the highest concentration of 500 µg/ml. All standards were made prior to each run.

5.3.9 Glucoraphanin Extraction and Detection

Reservoirs (Varian) with a frit (Varian) and a needle (P. Harris) were prepared and placed into a rack. To the reservoirs, 0.5 ml MilliQ water was added to the frit and left to pass through. This was followed by the addition of 0.5 ml of prepared A25 Sephadex (Amerersham Biosciences) to each reservoir which was left to settle to form an approx. 0.5 cm bed of ion exchange material. Each reservoir was washed

with 0.5 ml MilliQ water, and all liquid was left to pass through. For glucosinolates, a 40–60 mg sample of freeze-dried soup or supplement was weighed out and a 10 ml aliquot of 70 °C 70 % (v/v) aqueous methanol added followed by 50 µl of internal standard (16 mM sinigrin, Sigma-Aldrich®). All samples were vortexed thoroughly and incubated in a water-bath preheated at 70 °C for 30-minutes. During the incubation, the samples were vortexed twice. After being left to cool, the samples were centrifuged at 4000 *xg* for 10-minutes at 4 °C. Of each sample, three millilitres of liquid supernatant were collected and allowed to drip through slowly which allowed the glucosinolates to absorb to the ion exchange column. Once the liquid had all dripped through, the column was washed twice with 0.5 ml MilliQ water and 0.5 ml 0.02 M sodium acetate pH 5, to wash off any free interfering ionic components. Once no more liquid was remaining, collecting vials (Agilent®) were placed under the needles. The glucosinolates were desulfated by the addition of 75 µl purified sulphatase (Sigma-Aldrich®) to the column, which was left at room temperature overnight. Next day, the desulfated glucosinolates in the ion exchange column were eluted with 1.25 ml of MilliQ water. Once eluted, a cap (Agilent®) was crimped on top of the collecting vial and stored at -20 °C until analysis.

A model 1100 High Performance Liquid Chromatography (HPLC) system (Agilent®) including a binary pump, cooled autosampler, degasser, column oven and diode array detector, was used. A mobile phase A of MilliQ water and a mobile phase B of LC-MS grade acetonitrile (Sigma-Aldrich®) were used. Initially, the flow rate was set at 5 ml/min to flush the binary pump, this was followed by loading the appropriate method. For analysis, the flow rate was set at 1 ml/min with a maximum pressure 300 bar and a gradient of increasing mobile phase B from 5 % to 90 % over 32-minutes. This was reduced to 5 % for 14-minutes preceding re-equilibration. Samples were analysed using Waters Spherisorb ODS2 (4.6 x 250 mm id, 5 µm particle size) column (Waters) equipped with a Waters Spherisorb guard column (Waters), by positive ion atmospheric pressure chemical ionisation (APCI+) LC-MS. Quantification was conducted from the chromatogram data measured at the absorbance 229 nm, and the ratio comparison of the peak of interest and the internal standard (16 mM sinigrin).

5.3.10 Hydrolysis of Glucoraphanin and Detection of Isothiocyanates

For all freeze-dried materials (freeze-dried soup or supplement), 40–60 mg samples were taken. For ambient temperature samples, to each tube, 1 ml of 1x phosphate-buffered saline (PBS, Gibco®) was added. For 100 °C samples, 900 µl

of boiling water was added followed by the addition of 100 µl of 10x PBS stock (Gibco®) to achieve a 1:10 dilution. The tubes were sealed and vortexed. All samples were incubated on a 37 °C heating block for 2 hours; each sample was vortexed every 15-minutes to ensure optimal hydrolysis before the tubes were centrifuged at 13,000 rpm for 30-minutes at 4 °C. The clear liquid supernatant was taken undiluted for sulforaphane analysis into HPLC vials (Agilent®), followed by the addition of 100 µM sulforaphane-D8 internal standard (TRC) in MilliQ water. Sulforaphane-D8 internal standard was dissolved in dimethyl sulfoxide (DMSO, Sigma) to give a 5.395 mM stock and further diluted in MilliQ water to generate a working concentration of 100 µM. A cap (Agilent®) was crimped on top of the collecting vial, vortexed and samples stored at -20 °C until analysis.

A model Agilent 6490 Triple Quadrupole LC/MS/MS system equipped with a binary pump, cooled autosampler, degasser, column oven and diode array detector, was used. A mobile phase A of 0.1 % ammonium acetate (Sigma-Aldrich®), adjusted to a of pH 4 with 0.1 % acetic acid (Biosolve) in MilliQ water and a mobile phase B of 0.1 % acetic acid in LC-MS grade acetonitrile (Sigma-Aldrich®) were used. For analysis, the flow rate was set at 0.25 ml/min; the gradient started at 5 % mobile phase B increasing over 5 min to 30 % mobile phase B and finally re-equilibrated to 5% mobile phase B for 6 min. The column temperature and autosampler temperature maintained at 20 °C and 4 °C respectively. Samples were separated on Phenomenex Luna 3u C18(2) 100A (100 x 2.1 mm) column by multiple-reaction monitoring (MRM) mode. The injection volume was 2 µl per sample. Quantification was conducted through the identification of sulforaphane at retention time of approx. 7.294, to generate a standard curve. Briefly, sulforaphane (S8044, LKT Laboratories) was dissolved in DMSO to give a 100 mM stock solution and further diluted in MilliQ water to generate a working concentration of 1 mM. The stock was diluted in water from 0 mM to the highest concentration of 50 µM. All standards were made prior to each run.

5.3.11 Colorimetric analysis

To gain empirical values for the colour of freeze dried broccoli soup preparations, colorimetric analysis was performed. Briefly, images were taken of the powders using an Epson flatbed scanner, the image was transferred to photoshop where four L*a*b* readings could be taken. L* represents level of lightness where L*=0 is dark black and L*=100 is bright white. The a* axis represents the green to red component, with red in the positive direction and green in the negative direction.

The b* axis represents the yellow to blue component, with the yellow in the positive direction and blue in the negative direction. This is summarised in Figure 5.1.

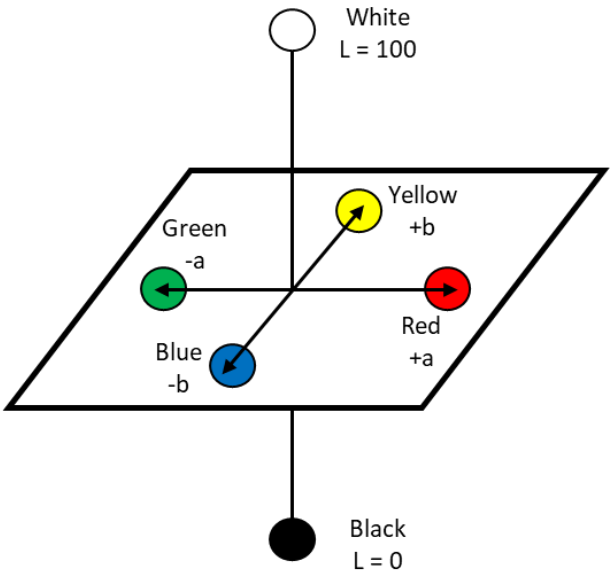

Figure 5.1. Colorimetric representation using L*a*b*. Briefly, L*=100 is white, L=0 is black, negative a* is green, positive a* is red, negative b* is blue and positive b* is yellow.

5.3.12 Statistical Analysis

All statistical analysis were performed in Prism using GraphPad Software. Where appropriate either one-way ANOVA followed by Tukey's honest statistical hypothesis test for multiple comparisons, or unpaired two-way T-test were used. A $p < 0.05$ with a 95 % confidence interval was defined to be statistically significant; n.s. $p > 0.05$; no significance present, *$p \leq 0.05$, **$p \leq 0.01$, ***$p \leq 0.001$, ****$p \leq 0.0001$. Data are expressed as mean ± standard deviation.

5.4 Results

5.4.1 Heating causes thermal degradation of glucoraphanin but not SMCSO in fresh broccoli soups

Evaluation of the appropriate delivery of high-SMCSO functional product for use in future cancer human trials was conducted assessing supplements, fresh-broccoli soup or dried-broccoli soup. Initially, fresh broccoli soups were produced at CRL foods and either not-treated, pasteurised (70 °C and 85 °C) or sterilised (100 °C, 105 °C, 110 °C and 115 °C). The soups were delivered, freeze-dried and the SMCSO and glucoraphanin content were assessed. Glucoraphanin content, but not SMCSO, was significantly reduced with increased temperature (Figure 5.2).

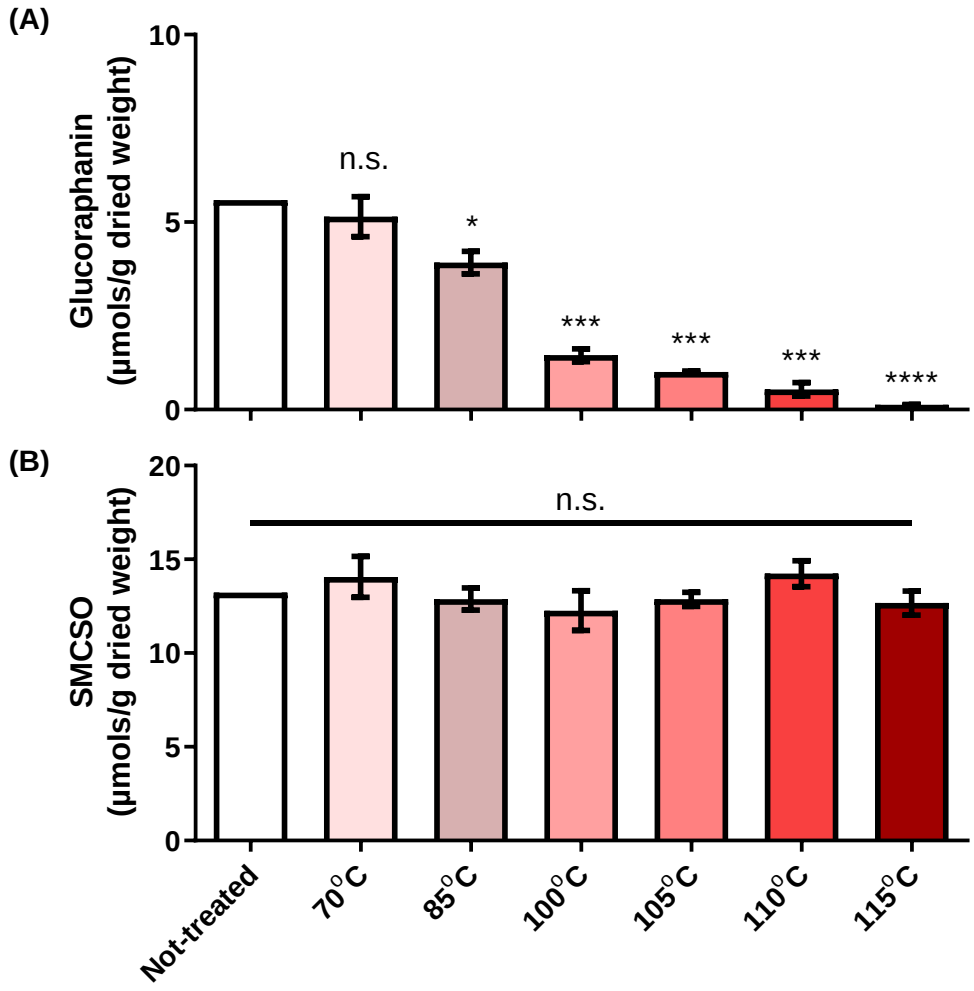

Figure 5.2: Thermal degradation of glucosinolates but not SMCSO. Fresh broccoli soups were either not-treated, pasteurised (70 °C and 85 °C) or sterilised (100 °C, 105 °C, 110 °C and 115 °C). Glucoraphanin content (A) was substantially and significantly decreased with increasing temperature, SMCSO content (B) was not altered with increased temperature. n.s. = not significant, * = $p < 0.01$, *** = $p < 0.001$, **** = $p < 0.0001$, compared to not-treated.

5.4.2 Evaluation of 1086 freeze dried broccoli powder as a potential candidate

As a potential contender for the broccoli soup, the 1086 broccoli variant used in the ESCAPE study was investigated under different cooking conditions. Briefly, the broccoli, in freeze dried powdered form, was either not-treated, hydrated under various temperatures, dry heated, dry heated and then hydrated or steamed. The cooking and heating preparations influenced the greenness of the broccoli powder (Figure 5.3), especially when steamed.

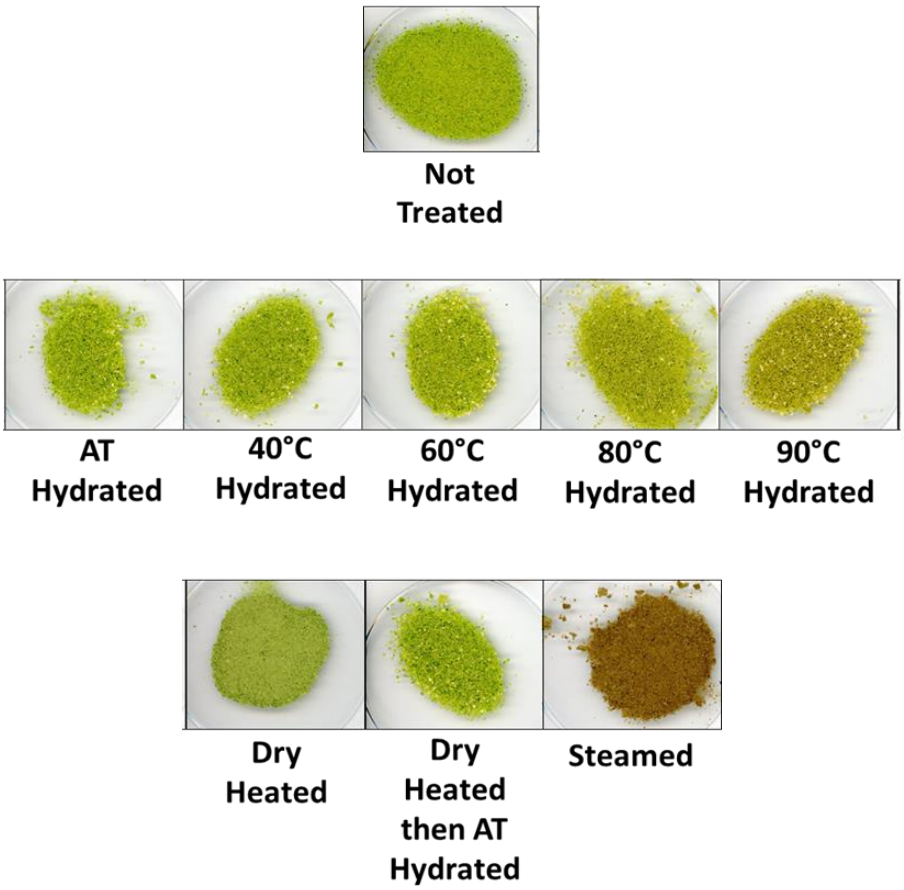

Figure 5.3. Images of 1086 broccoli powder samples under different cooking environments. The cooking method used influenced the greenness of the broccoli powders; especially steaming the broccoli powder. AT; ambient temperature.

To assess the sulfur metabolites, glucoraphanin and SMCSO, in the 1086 broccoli powder, LC-MS and LC-MS/MS was used. In the original preparations, the glucoraphanin content significantly decreased when hydrated at 80 °C and 90 °C, and completely disappeared when steamed (Figure 5.4A). SMCSO content was not influenced when hydrated at any temperature but reduced around to a third in value when steamed (Figure 5.4B).

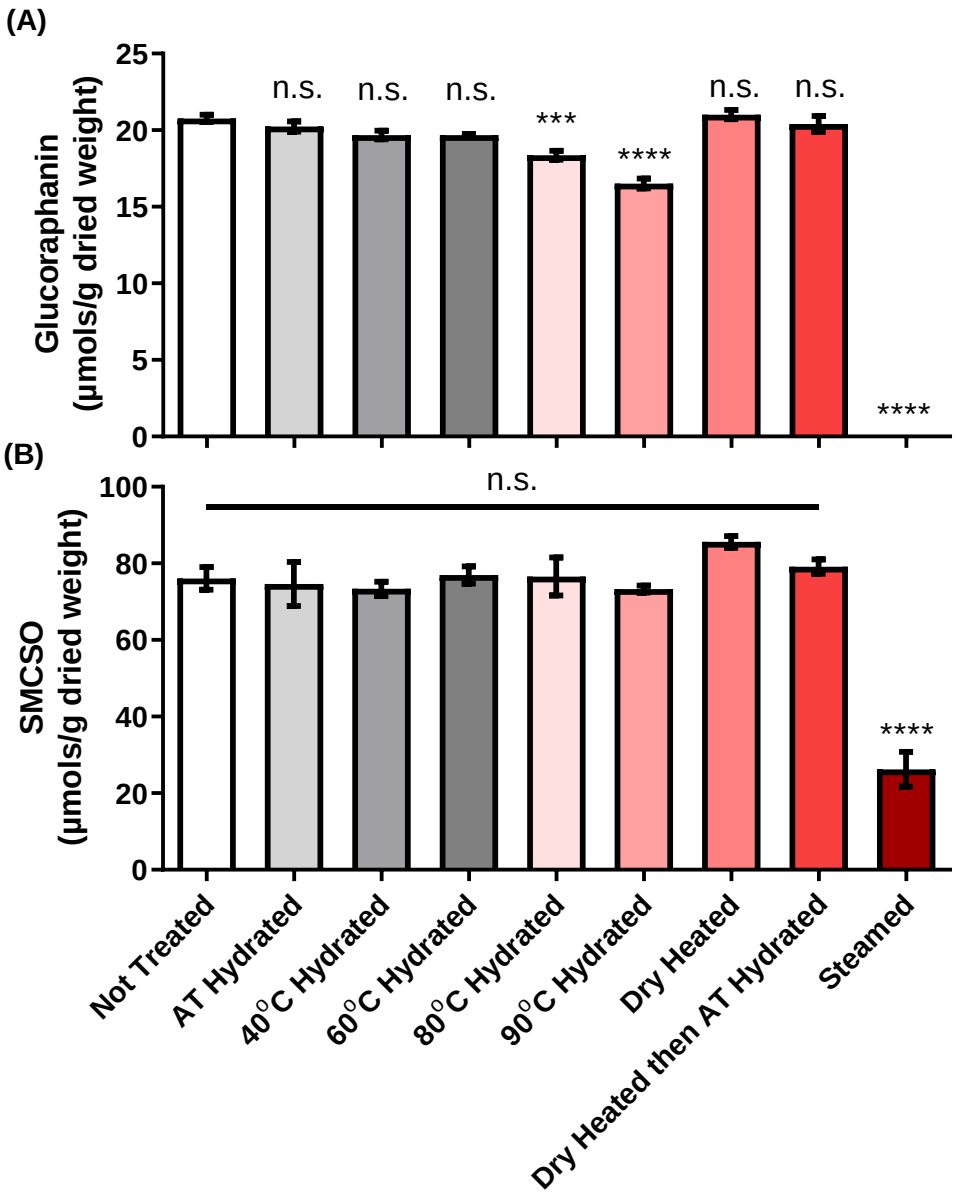

Figure 5.4. Sulfur compound content in original preparations of freeze-dried 1086 broccoli powder under different cooking environments. (A) Glucoraphanin content. (B) SMCSO content. The cooking method used influenced the glucoraphanin content of the broccoli powders; but did not with SMCSO, apart from steaming the broccoli powder. AT; ambient temperature. n.s. = not significant, *** = $p < 0.001$, **** = $p < 0.0001$, compared to not-treated.

The room temperature stability of the 1086 freeze-dried samples was assessed. Briefly, the freeze-dried powders were either kept at ambient temperature for 1 week or hydrated at ambient temperature for 1 week. The freeze-dried powders kept at ambient temperature for 1 week did not decrease in glucoraphanin nor SMCSO content (Figure 5.5A and 5.5B respectively). Glucoraphanin content, but not SMCSO content, significantly decreased when kept hydrated at ambient temperature for 1 week (Figure 5.6A and 5.6B respectively), especially at 40 °C.

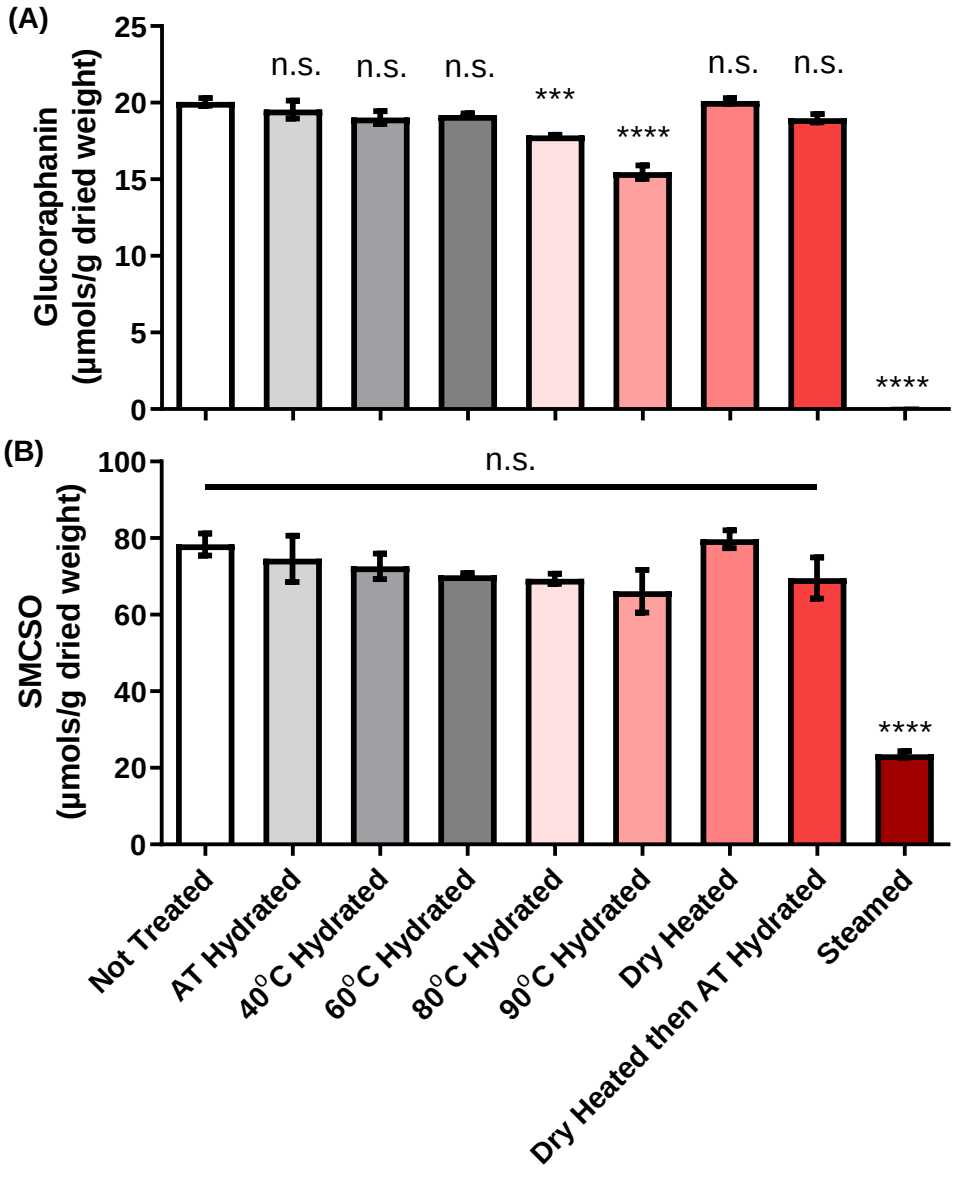

Figure 5.5. Sulfur compound content in freeze-dried 1086 broccoli powder preparations kept at ambient temperature for 1 week. (A) Glucoraphanin content. (B) SMCSO content. The freeze-dried powders kept at ambient temperature for 1 week did not decrease in glucoraphanin nor SMCSO. AT; ambient temperature. n.s. = not significant, *** = $p < 0.001$, **** = $p < 0.0001$, compared to not-treated.

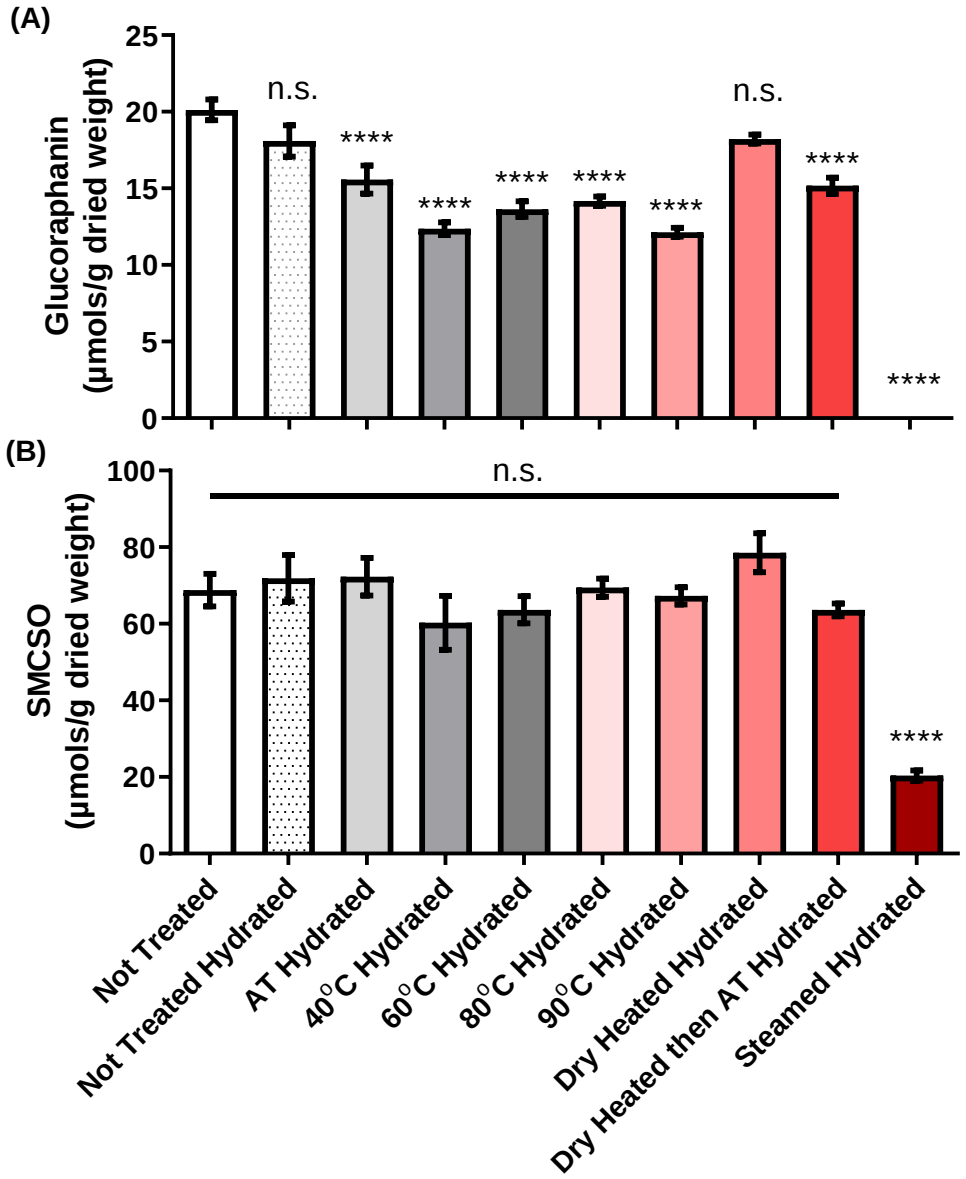

Figure 5.6. Sulfur compound content in freeze-dried 1086 broccoli powder preparations hydrated at ambient temperature for 1 week. (A) Glucoraphanin content. (B) SMCSO content. Glucoraphanin content, but not SMCSO, significantly decreased when kept hydrated at ambient temperature for 1 week. AT; ambient temperature. n.s. = not significant, **** = $p < 0.0001$, compared to not-treated.

5.4.3 Evaluation of commercially available freeze dried broccoli powders as potential candidates

Commercially available broccoli powders were considered as a possible source of a high SMCSO food product. Briefly, four commercially available powders were assessed for colour profile and sulfur-metabolite content. Even though all powders were *Brassica oleracea*, all the samples were different in green colour (Figure 5.7A). Bulk Powder broccoli powder was more olive than green; Sussex Wholefoods broccoli powder was a bright green which was the similar to the 1086 broccoli powder seen in Figure 5.3. Sussex Wholefoods broccoli powder contained the highest level of glucoraphanin (8 µmols/g dried weight) and SMCSO (79 µmols/g dried weight), when compared to the three other broccoli powders (Figure 5.7B and 5.7C). Buy Whole Foods Online contained moderately high levels of SMCSO (63 µmols/g dried weight) compared to glucoraphanin (4 µmols/g dried weight). Bulk powder and Just Ingredients contained low levels of both glucoraphanin and SMCSO.

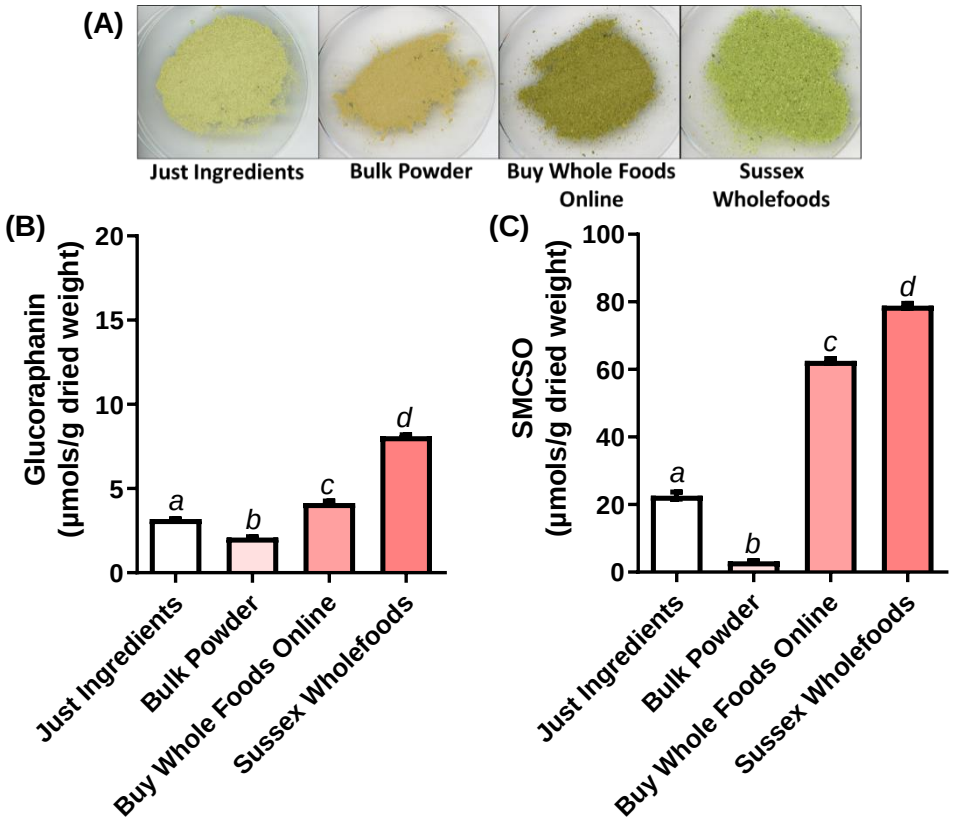

Figure 5.7. Sulfur compound content in commercially available freeze-dried broccoli powders. (A) Images of commercially available broccoli powders. (B) Glucoraphanin content. (C) SMCSO content. Bulk Powder broccoli powder was more olive than green; Sussex Wholefoods broccoli powder was a bright green Sussex Wholefoods contained the highest glucoraphanin and SMCSO content, Buy Whole Foods Online contained high levels of glucoraphanin and SMCSO and Bulk powder and Just Ingredients contained low levels of both glucoraphanin and SMCSO. a, b, c, d; denotes $p < 0.0001$ significance between each broccoli powder.

5.4.4 Evaluation of commercially available supplements as potential candidates

Two supplements were investigated for their sulfur-containing compound content: BroccoMax® (broccoli supplement) and Kwai Heartcare (garlic supplement). BroccoMax® had a very high content of glucoraphanin (22.7 mg/capsule, Figure 5.8), but glucoraphanin was not measured in the Kwai Heartcare product. Both Broccomax® and Kwai Heartcare products contained minimal SMCSO (0.17 and 0.71 mg/capsule respectively, Figure 5.9).

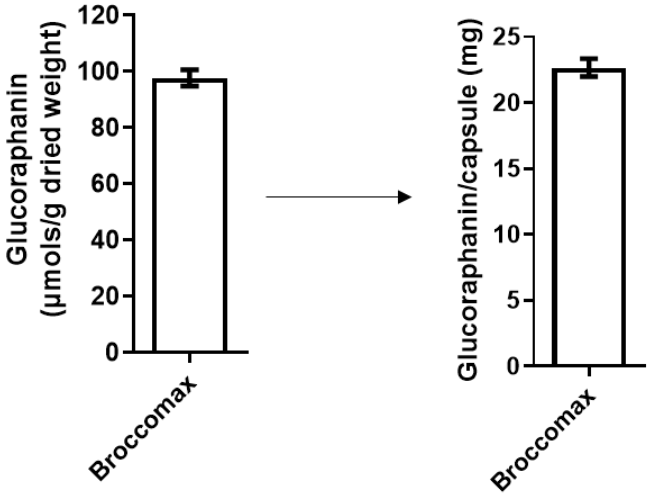

Figure 5.8. Glucoraphanin content in Broccomax. The Broccomax supplement contained huge levels of glucoraphanin with 22.7 mg/capsule. Glucoraphanin was not measured in Kwai Heartcare.

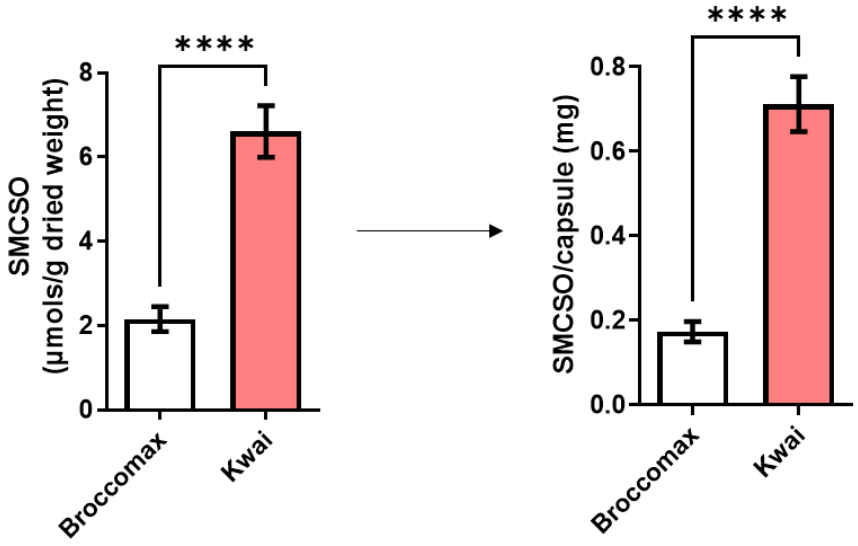

Figure 5.9. SMCSO content in supplements, Broccomax and Kwai Heartcare. Both Broccomax and Kwai Heartcare contained minimal levels of SMCSO (0.17 and 0.71 mg/capsule respectively). **** = $p < 0.0001$, compared between supplements.

5.4.5 Sussex Wholefoods broccoli powder could be a suitable high SMCSO material

This work aimed to develop a product to deliver a high content of the secondary metabolite SMCSO for use in future clinical intervention studies. Regarding the broccoli powders, Sussex Wholefoods gave the highest quantity, and 1086 variant broccoli powder gave second highest quantity of SMCSO, whereas the Bulk Powder product contained the lowest level of SMCSO. The Sussex Wholefoods broccoli powder appears to be a good candidate for delivery a high dose of SMCSO. Both supplements (Broccomax and Kwai Heartcare) contained only low levels of SMCSO. The data are summarised in Table 5.1.

Table 5.1. Sulfur metabolite analysis in all samples for highest delivery of SMCSO to participants

Broccoli Product	Glucoraphanin			SMCSO		
	µmols/g dried weight	mg/g	mg/capsule	µmols/g dried weight	mg/g	mg/capsule
1086	20.4	9.08	N/A	77.3	11.5	N/A
JI	3.18	1.39	N/A	22.7	3.43	N/A
Bulk	2.09	0.92	N/A	3.25	0.49	N/A
BWFO	4.13	1.81	N/A	62.5	9.45	N/A
Sussex	8.11	3.55	N/A	78.9	11.9	N/A
Broccomax	97.7	42.8	22.7	2.15	0.33	0.17
Kwai	NM	NM	NM	6.61	1.00	0.71

SMCSO, S-methyl cysteine sulfoxide; 1086; Variant of Broccoli Powder; JI, Just Ingredients; Bulk, Bulk Powder; BWFO, Buy Whole Foods Online; Sussex, Sussex Wholefoods; Kwai, Kwai Heartcare supplement; NM; not measured; N/A; not applicable.

5.4.6 Courgette powder could be an appropriate control to broccoli powder

Evaluation of potential control products for use alongside the broccoli product was conducted. Variables such as whether they contain sulfur compounds and whether they had similar fibre, starch and colouring to broccoli were considered and summarised in Table 5.2. From this analysis, courgette powder was identified as a suitable placebo control as it does not contain any sulfur compounds and has similar fibre and starch composition to that of broccoli.

Table 5.2. Evaluation of potential placebo products compared to broccoli powder

Potential Control Product	Contains sulfur compounds?	Fibre similar to broccoli?	Starch similar to broccoli?	Similar in colour?	Good Candidate? Why?
Cauliflower	Yes	Yes	Yes	No	No, contains sulfur compounds
Brussel Sprouts	Yes	No	No	No	No, contains sulfur compounds
Steamed Broccoli Powder	No glucoraphanin, Low SMCSO	Same	Same	No	No, control would still contain SMCSO and would be different in colour
Pea Powder	No	Yes	No	Yes	No, difference in starch could influence glucose metabolism of cancer
Courgette Powder	No	Yes	Yes	Yes	Yes, does not contain sulfur compounds and has similar fibre and starch to broccoli

SMCSO, S-methyl cysteine sulfoxide

5.4.7 The dried-broccoli soup product contained high levels of SMCSO

To make the Sussex Wholefoods broccoli powder and courgette powder palatable and to assist with blinding, it was decided to add the vegetable powders to a dried base vegetable soup. Of the base vegetable soups available, Batchelors Golden Vegetable Cup of Soup supplemented with either broccoli or courgette powder gave soups that were similar in consistency and tasted similar to each other. Even though the golden vegetable soup contained swede, leek and onion, it was shown by direct analysis that it contained very low quantities of sulfur compounds (0.00 ± 0.00 micromoles of glucoraphanin and 16.2 ± 1.11 micromoles of SMCSO).

The Batchelors golden vegetable cup of soup was supplemented with 16 g of either broccoli powder or courgette powder and either not-treated or treated as the participants would prepare the soup, with 250 ml of 100 °C boiling water. The broccoli soup contained high levels of SMCSO, moderate levels of glucoraphanin and low levels of sulforaphane, whereas the courgette soup contained no detectable quantities of any of these sulfur compounds (Figure 5.10). Not-treated broccoli soups contained 1768 ± 84.4 micromoles of SMCSO and 147 ± 7.39 micromoles of glucoraphanin, respectively (Figure 5.10A and 10C, respectively). Heat-treated (100 °C) soups contained 1816 ± 80.8 micromoles of SMCSO and 146 ± 1.85 micromoles of glucoraphanin, respectively (Figure 5.10B and 5.10D, respectively). Using in situ glucosinolate hydrolysis, it was shown that the glucoraphanin in the not-treated broccoli samples was converted to 0.22 ± 2.33 micromoles of sulforaphane (Figure 5.10E), and in the heat-treated soups it generated 0.16 ± 0.01 micromoles of sulforaphane (Figure 5.10F). There was a small increase in SMCSO levels in the not-treated soup samples compared to 100 °C treated samples (48 micromoles, Figure 5.10A and 5.10B respectively). There was a slight reduction in sulforaphane in not-treated samples compared to 100 °C treated samples (0.06 micromoles, Figure 5.10E and 5.10F respectively). The Co-op broccoli and stilton soup, a commercially available dried-broccoli soup used as a positive control, contained low levels of SMCSO, glucoraphanin and sulforaphane compared to the broccoli soups (Figure 5.10).

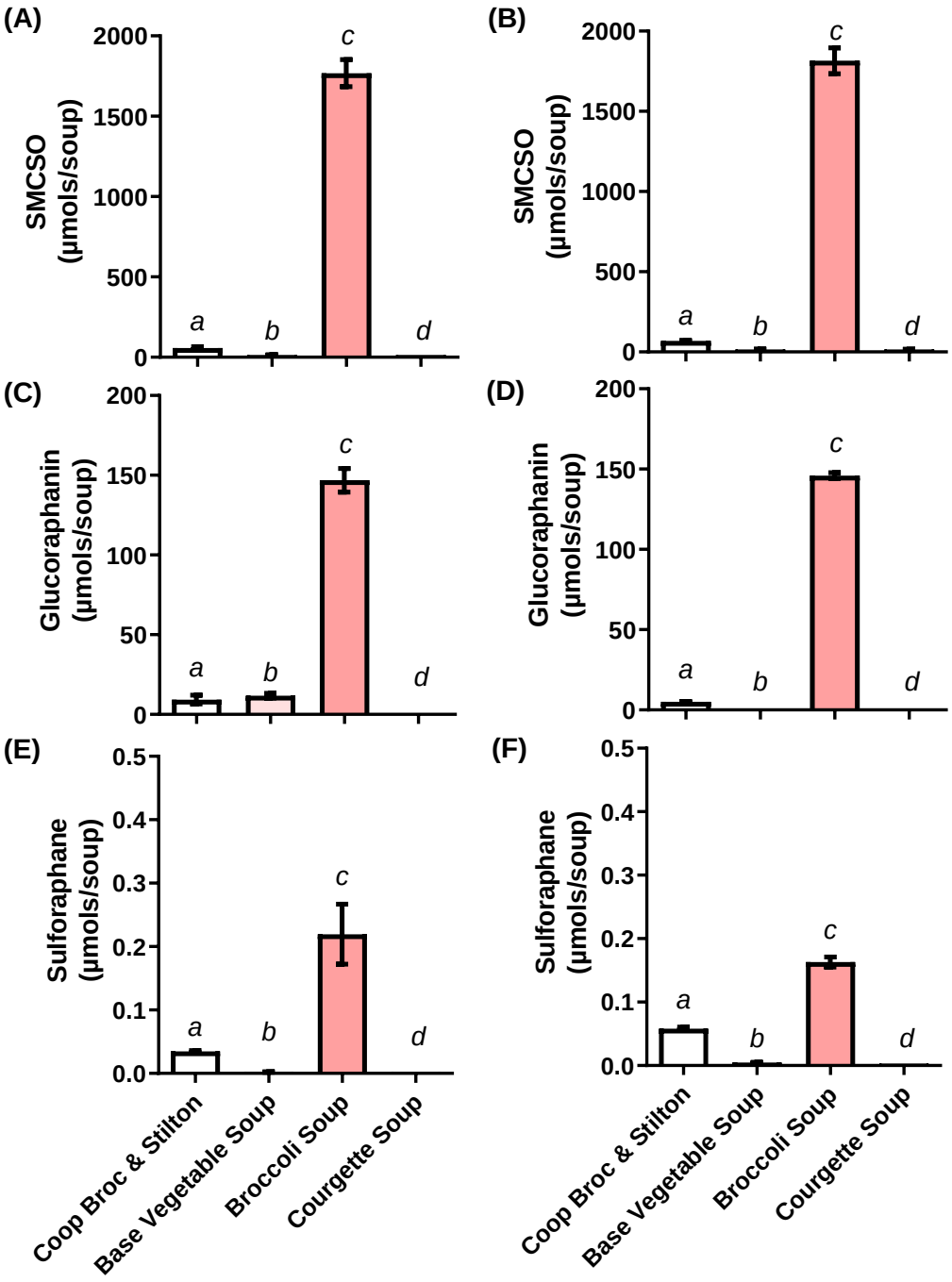

Figure 5.10. Sulfur metabolite analysis of vegetable soups to use in future cancer human trials. Briefly, the soups were either left not-treated (A, C and E) or treated with 100°C water (B, D and F) and analysed using LC-MS or LC-MS/MS to determine the µmols/soup of the following sulfur metabolites: SMCSO (A and B), glucoraphanin (C and D) and sulforaphane (E and F). Each broccoli soup contained high SMCSO and low sulforaphane from glucoraphanin hydrolysis. a, b, c, d; denotes $p < 0.0001$ significance between each soup.

For effective blinding of the broccoli and courgette soups, assessment of the colour of the not-treated dried soup (dried soup) and soup heat-treated at 100°C (fresh soup) was conducted using L*a*b* quantification. Briefly, images were taken of the soups and L*a*b* readings were taken using Adobe photoshop. The fresh soups appeared to be visually different in terms of greenness (Figure 5.11A) and when quantified there were significant differences in greenness (a*) and yellowness (b*) between the dried and fresh soups (Figure 5.11B), although there was no significant difference in lightness observed between the soups.

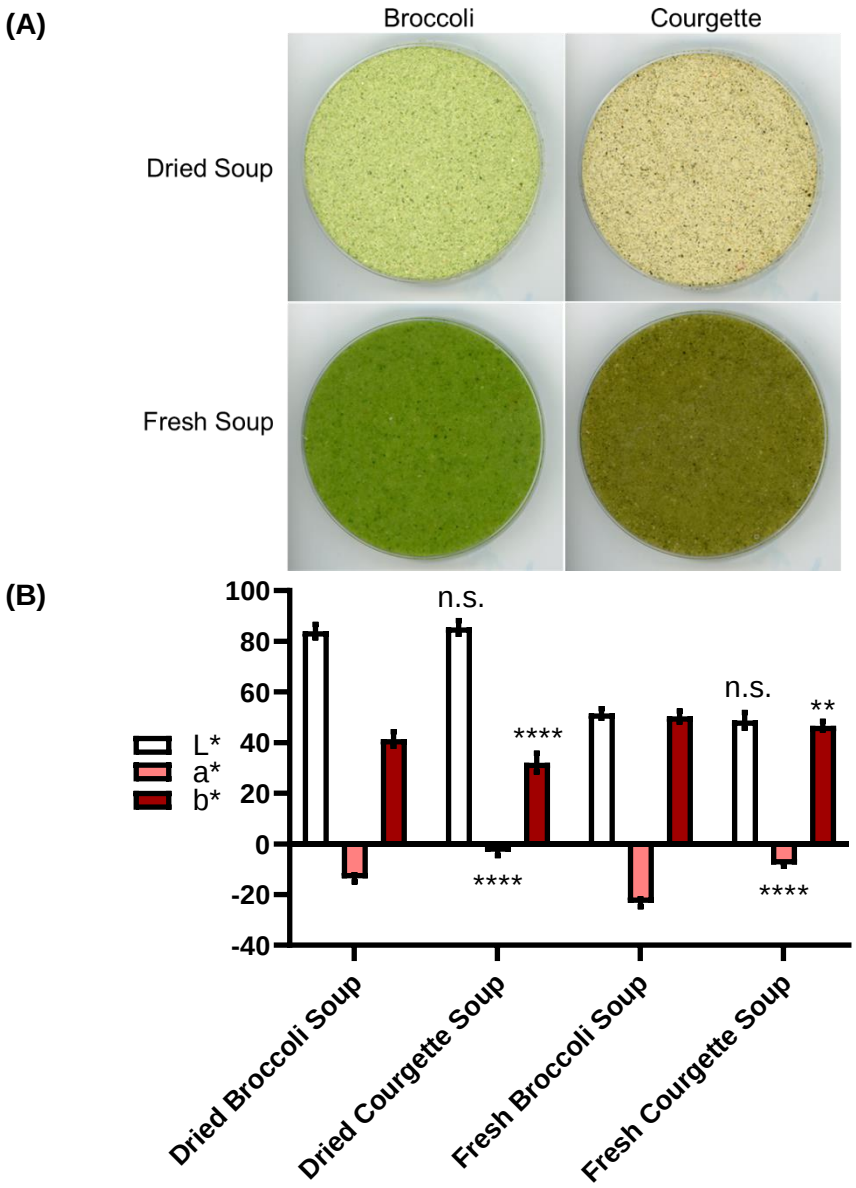

Figure 5.11. Colorimetric assessment of vegetable soups to use in future cancer human trials. (A) Images of the original dried product (dried soup) and 100°C treated soup (fresh soup) (B) L*a*b* quantification of the soups. Significant differences in greenness (a*) and yellowness (b*) between the dried soups, and the fresh soups, no significant differences in the lightness was observed. Statistical analysis on graph: dried broccoli soup compared to dried courgette soup, fresh broccoli soup compared to dried courgette soup, n.s = not significant, ** = $p < 0.01$, **** = $p < 0.0001$.

5.5 Discussion

Functional foods and components give health benefits more than nutrition of a balanced diet. Previous studies have reported substantial evidence between functional foods rich in bioactives such as polyphenols, flavonoids and sulfur-containing compounds and reduction of chronic diseases including cardiovascular disease, type 2 diabetes and cancer (85, 301-303). These studies have utilised both whole foods and supplement based products for delivery of bioactive compounds. One study developed and used an oral supplement product containing a mixture of pomegranate, green tea, broccoli and turmeric and matched with an identical placebo control; they recruited 199 men with localised prostate cancer for 6-months and reported the median rise in PSA was 14.7 % in supplement group compared to 78.5 % in the placebo group (90). This provides evidence that concentrated amounts of bioactives can be effectively delivered and display significant effects on prostate cancer. A recent systematic review looked at articles published from 2010 to 2020 focusing on whole functional foods and breast, liver and cervical cancers and reported various functional foods in the studies selected to influence cancer related metabolism including induction of apoptosis, modulation of signaling cascades, and ROS generation (304). It is clear from the published evidence that cancer prevention by functional foods could be a plausible method of delivery of high concentrations of bioactives.

Studies of efficacy of dietary interventions with sulfur bioactives in humans with cancer is essential for understanding their influence on disease progression. Successful delivery of the appropriate concentration of a bioactive to the target tissue in the body is key to achieving an effect. Broccoli contains several different sulfur-metabolites, and therefore it is important that a functional product that contains a high content of SMCSO contains relatively small amount of other sulfur compounds and is able to deliver the SMCSO in a bioavailable form in the final processed product. One option would be to provide SMCSO in the form of an isolated purified product, for example in a capsule or similar. However, this would be extremely difficult, time-consuming and costly because it would require extensive purification of SMCSO from a plant tissue and would likely also require evidence that such highly purified forms and doses are safe for human consumption. It is worth noting that overconsumption of polyphenols have previously been reported to cause harmful toxic effects (305). Even though the consumption of cruciferous vegetables is considered not toxic and not associated

with any serious adverse effects (306, 307), the careful consideration of the safe and beneficial levels of SMCSO is required for suitable development of a functional food product.

The cooking, heating and processing of the food product needs to be taken into account of when developing a functional food product (294). Assessment of a potential candidate for the delivery of high-SMCSO indicated thermal degradation and poor stability of glucoraphanin, but not SMCSO. Consistent with these findings, the effects of thermal degradation was reported by the heating of *Brassica* vegetables to 99 °C resulting in thermally-induced glucosinolate breakdown (308). Other cooking methods including steaming, microwaving and boiling have different effects on glucosinolate profile; steaming of broccoli preserved total glucosinolates and enhanced sulforaphane (309) but boiling and microwaving led to complete loss within 1-minute (310). This could be explained by the breakdown of plant tissues and inactivation of myrosinase, needed for the conversion of glucoraphanin to sulforaphane under high heat conditions (311). Interestingly, certain processing methods can apparently increase the yields of glucosinolates including high pressure processing and pulsed electric field; high pressure processing of broccoli led to the breakdown of glucosinolates but the recovery of isothiocyanates such as sulforaphane (312), and pulsed electric field processing of broccoli led to increased aliphatic glucosinolate contents (313). The observed thermal degradation of the glucoraphanin but not SMCSO, would be beneficial for a designing a product rich in SMCSO. If designing a food product high in glucosinolates, to retain nutritional values at highest level, careful consideration of the cooking preparation is needed.

Of the commercially available supplements and broccoli powders, Broccomax was shown to contain a large quantity of glucoraphanin and both supplements contained very low amounts of SMCSO; Sussex Wholefoods broccoli powder contained high-SMCSO and moderate glucosinolate content. Supplements are easily administered and allow for the evaluation of specific isolated bioactives (314). However, with a food-based approach such as soup, the whole food ingredients containing multiple bioactive compounds and micronutrients can be assessed (292). Therefore, for a product high in SMCSO, Broccomax and Kwai Heartcare supplements would not be suitable. Instead, the Sussex Wholefoods commercially available broccoli powder was considered a good candidate to deliver sufficiently high doses of SMCSO.

The strategy used to make the Sussex Wholefoods dried-broccoli powder palatable and to assist with development of an appropriate placebo was to add it to a dried base vegetable soup. When supplemented with the broccoli powder, the broccoli soup treated with 100 °C water contained moderate glucoraphanin (146 ± 1.85 micromoles) and high SMCSO (1816 ± 80.8 micromoles). This is a slightly higher amount of glucoraphanin to what would be consumed in a standard broccoli portion (315) and would be safe for consumption. This is comparable to the broccoli soup used in the SAP human study in which one portion of broccoli soup contained 280 ± 8.8 micromoles of glucoraphanin and 1513 ± 36.8 micromoles of SMCSO (25), and the accumulation of SMCSO was observed in the prostate tissue in this previously reported human study (25). Thus, the soup developed in this Chapter could potentially deliver more SMCSO to the biological target tissue compared to the broccoli soup used in the SAP study.

The broccoli soup generated only a small quantity of sulforaphane when the soup was hydrated to allow any residual broccoli myrosinase enzyme to hydrolyse the glucoraphanin and generate sulforaphane. The low level of sulforaphane observed suggests that the thermally unstable myrosinase enzyme had been already inactivated, presumably during processing in the preparation of the broccoli powder (310, 316). The product would therefore rely on the human microbiota for the thioglucosidase activity required to hydrolyse the glucoraphanin. It is known that gut microbiota-dependent generation of sulforaphane from glucoraphanin is quite variable between individuals and is relatively low, certainly much less efficient than generation of sulforaphane through the action of endogenous broccoli myrosinase (100, 317). However, the consequence is a product that is high in SMCSO but low in sulforaphane, which is ideal. The other advantages of a dried soup as a potential food product for use in a long-term dietary intervention in humans is its relatively long shelf-life. Use of fresh products such as wet broccoli soups brings additional requirements in terms of storage space, and appropriate storage temperature. If fresh broccoli soups were to be used, this would be even more demanding in terms of maintaining a constant supply of fresh broccoli and storing it but would also introduce a significant level of variation in the food product that would be difficult to control. For example, fresh broccoli is sourced from different geographical locations across the world during different seasons of the year (318).

Selecting an appropriate control containing no sulfur metabolites for comparison to the functional treatment product containing high-SMCSO, the macronutrients, colour, taste and texture should be matched to ensure that the response seen is most likely due to the bioactive of interest and to successfully blind individuals between the interventions if a cross-over design is employed (292, 319). One human intervention study (the ESCAPE study) investigated the influence of once-a-week consumption of broccoli soup in a prostate cancer cohort on active surveillance. The study investigated the effect of broccoli variants with increasing glucoraphanin but similar SMCSO content (98), and reported changes in gene expression and pathways associated with prostate cancer development (24). However, since there was no comparison group not supplemented with SMCSO, future human studies with an appropriately selected control product are needed. In a supplementation study, a control supplement not containing any component being test, would be comparatively easy to use. With a food product, it is much harder to develop an appropriate control product that has identical properties to the treatment product and much more difficult to blind (320). In this case, courgette powder would be an appropriate control as it contained no sulfur metabolites and had a similar macronutrient content (starch and fibre) to broccoli. However, there were significant differences in greenness (a*) and yellowness (b*) between the broccoli and courgette supplemented dried and fresh soups, suggesting that if used in a human intervention, some colour modifications such as adding a food dye would be required to appropriately blind the soups.

A 12-step straightforward protocol for developing novel functional products was recently reported (297). The protocol led to the design of a new functional snack with the selected properties and high nutritional value that remains stable when stored at room temperature, had good sensory qualities and was amenable to large-scale production. The protocol initially identifies target consumer group(s), evaluates the problem, how this is caused and whether a food product would solve the issue. If the problem can be somewhat resolved with the design of a novel product, the food product concept is assessed and proposed. If the food product meets the requirements and contains the selected properties, such as high in a particular bioactive, preliminary products are prepared, produced and tested for functional properties, quality, consumer palatability and feasibility. If modifications are needed such as making the product less salty, these can be made at this stage. Once the product is decided, key testing on nutritional value, microbiological assessment, shelf-life and storage conditions are required to determine the final

attributes of the product (297). This protocol can be employed by researchers who are inexperienced in designing a functional product for a clinical trial.

There are key phases in developing and managing a dietary human intervention trial with the vegetable soups developed in this Chapter. These include the design phase, followed by the conduct phase and final the analysis and interpretation phase (320-322). It is key to explicitly describe each phase to ensure consistency throughout the human study, especially if it is conducted at multiple study sites.

The design phase considers the hypothesis and outcomes of the study, the study intervention and duration, eligibility of the participants, randomisation, blinding and study size. Careful consideration is needed to ensure a clear hypothesis is proposed along with an appropriate study design, such as selecting parallel or crossover, with clear primary and secondary outcome measures and suitably matched treatment and control products (323), such as the vegetable soups developed in this Chapter. The consumption of these products throughout the study period should be determined based on study outcome. For example, a minimum of 3 soups a week over an extended period of time should be considered in this case to gain long intermittent exposure to SMCSO. Clear description of randomisation and concealment is needed for effective blinding, and how the study size was determined through the power calculation should be clearly reported in the study protocol so that the study team can refer to ensure standardisation throughout the intervention. The roles and responsibilities of the study team should also be clearly described in the study protocol to confirm they are competent to conduct the human study and to declare any potential conflicts of interests, especially if the funding for the study is provided by a company they are employed by, that could lead to scientific bias (320).

With the conduct phase, the study protocol alongside appropriately selected appendices such as relevant questionnaires included in the study such as weekly consumption of cruciferous and alliaceous vegetables. These will be submitted for ethical approval to the national research ethics committee and registered on the appropriate websites including clinicaltrials.gov (324). After a favourable opinion is given and full ethical approval is obtained, recruitment can begin with an appropriate strategy to recruit the study size required. Once a participant is recruited and informed consent is gained, study packs including the food product can be given followed by sample collection according with the study protocol. Depending on the consent given, this could be biological samples such as biopsies,

urine, blood and faecal (325) Appropriate human sample management should be employed if biological samples are taken including correct storage and disposal (326). Questionnaires could also be given postal or electronically including food frequency questionnaires that assess habitual diet, and sensory questionnaires that assess factors such as taste and texture of the food product for palatability and satiety (327). Record sheets on when the food product was consumed, alongside any food products, could also be given. This will evaluate cause and effect from consumption of the food product and any other products that might influence the data. For example, if the participants consumed a high abundance of cruciferous and alliaceous vegetables whilst on the study with a high-SMCSO soup this could skew and affect the data.

The conduct phase is followed by the analysis and interpretation phase that uses the data collected and statistical analysis to determine whether the outcomes of the study were achieved, and a clear appropriate conclusion of the study is given. The hypothesis are evaluated, and clear distinctions are made between the primary and secondary outcomes proposed in the study protocol (320). For example, in a study assessing the effect of the high-SMCSO product developed in this Chapter on prostate cancer progression in individuals on active surveillance, a primary outcome could be to assess the effect of high-SMCSO product on gene expression profile from prostatic tissue, while a secondary outcome could be to assess PSA levels from blood samples. At this stage, the data is distributed appropriately to the study participants and through peer-reviewed publications to give a clear comparison between the intervention groups. Limitations and generalisability of the findings should also be discussed. Limitations may include if there was insufficient recruitment for an effectively powered intervention or missing data points due to participant dropout. Collectively, sensible consideration of human study design coupled with appropriate functional food products such as that developed in this Chapter are required to ensure reliability and validity of the data collected and disseminated.

5.6 Conclusion

This Chapter evaluated various approaches to design a product that was rich in SMCSO for use in future cancer human trials, it was demonstrated that commercially available broccoli powders contain high levels of SMCSO but low levels of glucoraphanin and sulforaphane and are therefore suitable for use as an SMCSO-rich treatment. It was also shown that the broccoli powder was suitably masked by adding it to a base vegetable soup, and that a courgette powder was suitable for use in the placebo control. These products could be used in future human studies to test the causal effects of high-SMCSO on cancer progression.

Chapter Six.

General Discussion

Chapter Six: General Discussion

6.1 General summary and main findings of this thesis

Of all the cancer cases diagnosed, between 30-50 % are preventable through lifestyle changes including increased exercise, not smoking and a balanced diet high in fruit and vegetables (328, 329). Prostate cancer is a global burden (330). It is the most common malignancy in men and ranked fifth worldwide and second in the UK for most common cause of death related to cancer in men (9, 19). Prostate cancers that are localised to the prostate, that are low-risk and have a tendency to grow slowly are manageable through active surveillance (331). Although if the cancer metastasises, other therapies including chemotherapy and radiation can be used with survival rate dependent on extent of the cancer spread (332). Thus, there is a growing need for targeted therapies alongside dietary and lifestyle intervention for low-risk prostate cancer to reduce the cancer metastasis.

The chemopreventative properties linked to consumption of cruciferous and alliaceous vegetables are hugely supported by epidemiological studies (7, 24-26, 85, 91). However, many factors remain unknown: whether this beneficial effect is linked to other secondary sulfur-containing compounds such as S-methyl-L-cysteine sulfoxide (SMCSO) or S-methyl methanethiosulphonate (MMTSO) as well as sulforaphane; whether SMCSO and MMTSO are contributing to gene and metabolite regulation in cancer as seen with sulforaphane, and whether this effect is linked directly with the sulfur-containing compounds alone or from the whole food delivery. Investigating these further will deepen our knowledge of the molecular mechanisms influenced by sulfur-containing compound exposure and give an insight into how these compounds could be acting in prostate cancer progression.

The evidence presented in this thesis has made a significant contribution to the current understanding of the biological activity of sulfur-containing compounds, SMCSO and MMTSO, on the prostate, and their mechanistic links to prostate cancer metabolism including:

- MMTSO not SMCSO exposure significantly reduced mitochondrial metabolism, mitochondrial ATP and glycolytic rate, and increased fatty acid dependency in DU145 prostate cancer cell line, particularly in the high glucose environment.
- MMTSO, and to a lesser extent SMCSO, is capable of altering the transcriptional profile of DU145 prostate cancer cells with MMTSO exposure gave rise to more differentially expressed genes, particularly in the high glucose environment.
- MMTSO, not SMCSO, exposure to DU145 prostate cancer cells influenced key immune and regulatory signalling pathways including IL-2-STAT5 and IL-6-JAK-STAT3, and key antioxidant including NQO1, and apoptotic-related genes including BAK1.
- MMTSO, and to a lesser extent SMCSO, is able to change the metabolomic profile of DU145 prostate cancer cells, including metabolite changes relating to the tricarboxylic acid (TCA) cycle and non-essential and essential amino acids.
- SMCSO and MMTSO exposure to DU145 prostate cancer cells influenced key metabolic pathways in cellular metabolism including fatty acid metabolism, phenylalanine and tyrosine metabolism, and the mitochondrial electron transport chain.

This thesis reported the novel findings of the effects of the sulfur-containing compounds, SMCSO and its metabolite MMTSO, on prostate cancer metabolism, expression of genes and metabolite profiles involved in energy metabolism and metabolic pathways which was investigated using cultured DU145 prostate cancer cells. The results are summarised in Figure 6.1.

This thesis has also reported the development and characterisation of a product rich in SMCSO and an appropriate SMCSO-free placebo product suitable for use in future cancer human trials, since there have been no randomised controlled trials that have specifically investigated the potential effects of SMCSO consumption on prostate cancer progression. These can be used investigate how SMCSO and/or MMTSO act in vivo on prostate cancer risk and progression.

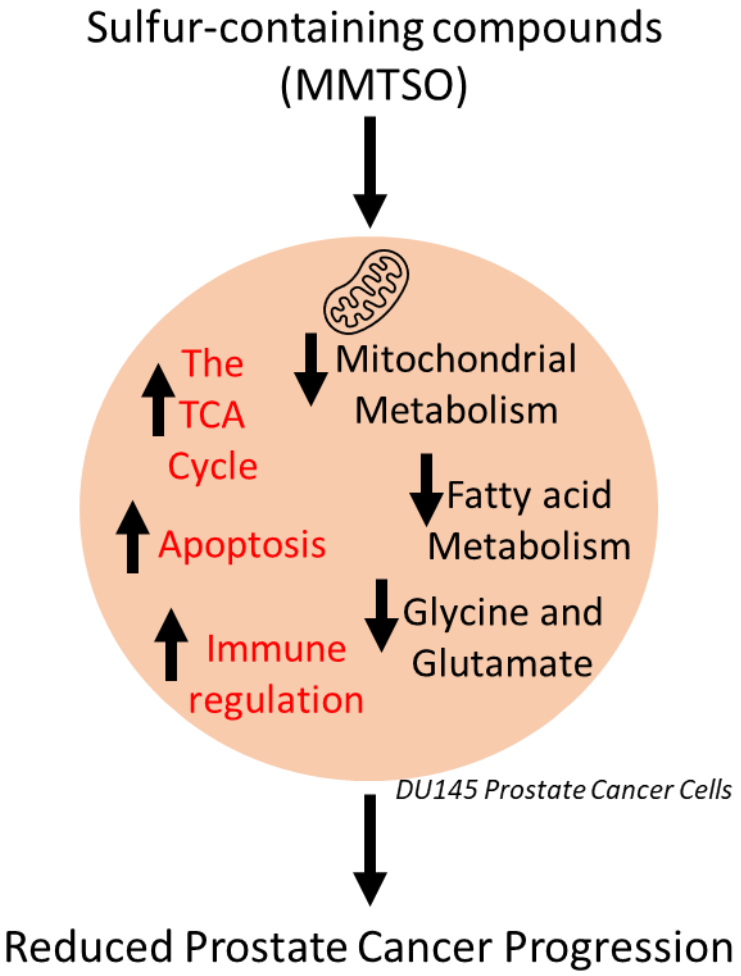

Figure 6.1: Summary of findings of this thesis. The sulfur-containing compounds such as MMTSO influenced various metabolic pathways within the DU145 prostate cancer cells including increased apoptosis and immune regulation and decreased mitochondrial metabolism, leading to reduced prostate cancer progression.

6.2 Discussion Points

6.2.1 How does the evidence presented in this thesis compare to previously published literature?

Whilst much of the current reports have focused on the glycaemic reducing effects of S-methyl cysteine sulfoxide (SMCSO) in diabetic rats, the role of SMCSO and its metabolite S-methyl methanethiosulphonate (MMTSO) in prostate cancer metabolism has been virtually disregarded.

The evidence presented in Chapter 2, 3 and 4 provided evidence that MMTSO, and to a lesser extent SMCSO, reduced mitochondrial metabolism and modulated key metabolic pathways including the mitochondrial electron transport chain in DU145 prostate cancer cells. This evidence is in agreement with the small number of in vitro and in vivo studies using cell lines including human liver cancer cells (123) and other human prostate cancer cells (124), animal models including mice (125) and rats (126). Interestingly, Chapter 3 reported dysregulated key immune and potential oncogenic pathways in DU145 prostate cancer cells. A few human studies are in agreement with the evidence including the Norfolk ADaPt study (26) and ESCAPE study (24) that conducted transcriptomic analysis of prostate tissue from individuals who consumed a product rich in sulfur-containing compounds and reported immune response and inflammatory pathways along with cancer-related pathways were dysregulated. Both Chapter 2 and 4 highlight upregulation and increased dependency of tricarboxylic acid (TCA) cycle and Chapter 3 highlights downregulation of key antioxidant genes following MMTSO exposure. This is in agreement with the evidence from previous human broccoli soup interventions that have indicated enhanced incorporation of fatty acid β-oxidation through the TCA cycle and influencing cellular redox capacity and glutathione regulation (24, 256, 257).

The current literature on normal prostate epithelial cell exposure to SMCSO and MMTSO reported no significant changes to mitochondrial, glycolytic function or transcriptomic profile (123, 124), suggesting potential cancer specific energy metabolism changes from the treatment of SMCSO and MMTSO. Interestingly, thiosulphinates isolated from the garlic chive, including S-methyl methanethiosulfinate (MMTSI, the precursor compound before disproportionation to MMTSO), were reported to encourage apoptosis through both caspase-dependent and caspase independent pathways in human prostate and colon cancer cell lines (121, 122). The data presented in Chapter 3 supports that MMTSO

could also promote apoptosis through the upregulation of key apoptotic genes including BAK1 and FADD. With the evidence presented in this thesis and the published evidence, it clear that in cancer cells energy metabolism evaluation alongside omics assessment should be considered more widely to assess target function in cancer progression and prevention.

6.2.2 How may in vitro studies of SMCSO and MMTSO translate in vivo?

Much of the anti-carcinogenic activity of cruciferous vegetable consumption has concerned the glucosinolates and sulforaphane, with limited evidence relating to SMCSO effect. From the discovery of SMCSO and its breakdown product MMTSO, there has been a rapid increase in publications, summarised in Figure 6.2. Although, much of this has focused on the beneficial effects of SMCSO and its breakdown products on glucose metabolism through administration to diabetic rats (129-131, 141), with a very few cell-based studies showing promise in inhibiting proliferation of human prostate and colon cancer cell lines (121, 122, 333).

Only a few human studies that have reported accumulation and excretion of SMCSO, there has been no human intervention has explored the role of SMCSO specifically on prostate cancer metabolism or progression. The ESCAPE not only provided evidence that sulfur-containing compounds consumption led to suppression of potential oncogenic related pathways in prostate cancer progression but also provided evidence that consumption of the cruciferous vegetables is inversely correlated with WHO prostate cancer grade with the most substantial correlation related with consumption of SMCSO (24). Although this finding was not-significant, as not effectively powered to assess this outcome, this finding indicates that SMCSO may be able to elicit an impact in vivo. However, up until this point it was uncertain as to whether the effect was due to indirect or direct exposure to the metabolites to the prostate tissue, as no study had reported the accumulation of sulfur-containing compounds within the prostatic tissue. It wasn't until the SAP study was conducted that demonstrated that SMCSO accumulated within the prostate tissue of individuals on active surveillance (25) and more recently the Norfolk ADaPt study that provided evidence that other sulfur-containing compounds including sulforaphane also accumulated within the prostate tissue (26). These studies provide evidence that the biological effects of sulfur-containing compounds are likely due to the direct accumulation within the prostate tissue.

The next rational step to develop our understanding of the impact of SMCSO and its breakdown products on the development of prostate cancer, was to conduct cell-based analysis asses the direct exposure of the compounds to prostate cancer cells. In this thesis, the cell-based evidence presented in Chapter 2, 3 and 4 provided an insight into the mitochondrial, transcriptomic and metabolomic modulation of SMCSO and MMTSO exposure to DU145 prostate cancer cells. This deepens our mechanistic understanding of the biological effect of these compounds on prostate cancer progression. Although it is worth noting that these analysis were conducted in vitro and so may not translate directly to humans in vivo. Further dietary human studies are warranted to test this further with a product rich or pure in SMCSO to directly test the effect in vivo on prostate cancer progression.

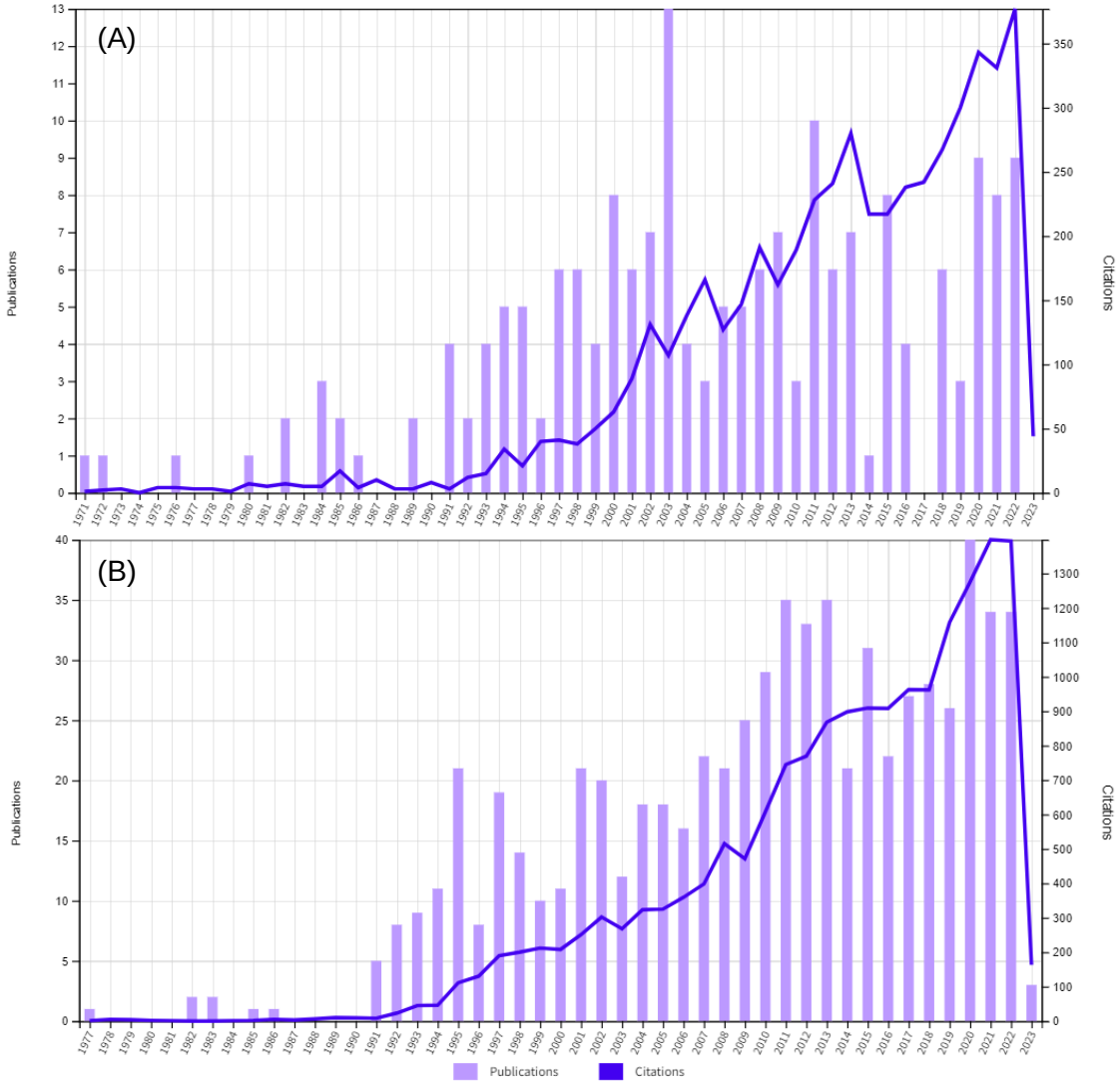

Figure 6.2: Citations and publications from of SMCSO and of MMTSO produced using Web of Science. (A) SMCSO publications from 1971 to present; keywords searched: S-methyl cysteine sulfoxide, S-methyl-L-cysteine sulfoxide, SMCSO and methiin. (B) MMTSO publications from 1977 to present; keywords searched: S-methyl methanethiosulfonate, methyl methanethiosulfonate, MMTSO and MMTS. Accessed March 2023.

6.2.3 How the current models could be used to evaluate SMCSO and MMTSO on prostate cancer metabolism?

The cellular progression of prostate cancer is complex and not completely defined. The use of in vitro and in vivo models of prostate cancer have reported evidence that dietary compounds could have chemopreventive properties through modulation on multiple signalling and metabolic properties (334, 335). Research relies strongly on in vitro and in vivo models to examine functional analysis at a molecular level deepening understanding of gene and pathway regulation in a preclinical environment. Several useful model systems have been developed that can be easily used under controlled experimental environment and help towards our understanding of prostate cancer. These include numerous prostate cell lines, several animal models, and more recently xenograft and 3D culture models (336).

Prostate cell line models both non-cancerous and cancerous have been established from patients from various zones of the prostate or from metastatic forms. They are vital research models for functional, molecular and mechanistic understanding. Non-cancerous prostate epithelial cells lines include PNT1A (337) and RWPE-1 (338), and represent normal prostate cells that can be used to understand the normal prostate metabolism and could be used to compare to the cancerous cell lines. Prostate cancer cell lines can be divided into two groups: hormone sensitive including LNCaP (339) and VCaP (340), and castration resistant including DU145 (340) and PC3 (341). Depending on the outcome of the study with dependent on which cell line is investigated. Each cell line has different doubling time, different phenotypes of prostate cancer such as androgen-dependent or androgen-independent and may have mutations such as PTEN or p53 loss (336). The work presented in this thesis (Chapter 2, 3 and 4) utilised cell lines to deepen our understanding of the mechanistic consequences of SMCSO and MMTSO exposure before further analysis could be conducted in animal and organoid models, and future human intervention trials.

A few animal models have been established that develop on cell-based studies and provide direct in vivo evidence for oncogenic function and regulation. The transgenic adenocarcinoma of the mouse prostate (TRAMP) mouse model, developed in 1996, is an extremely useful model for studying the pathology and evolution of prostate cancer (342). The LADY prostate cancer mouse model, developed in 1998, is similar to the TRAMP model and allows for evaluation of metastases to other organs such as the liver, lymph nodes and bone (343).

More recently, xenografts and 3D culture models have been developed to mimic human tumours to support preclinical research. Patient- derived xenografts include the androgen-dependent prostate cancer xenograft model developed in 1977 (344); the 3D culture models include the 3D organoid culture model from patient derived tumour developed in 2014 (345). These model mirror the tumour microenvironment, and carry intrinsic and growth factors involved in prostate cancer progression whilst ensuring heterogeneity and genetic profile of the tumour (336). However, these models are time-consuming, expensive, and have shown success in only aggressive prostate cancer specimens (346, 347).

Selecting the appropriate models for the research with bioactive compounds such as SMCSO and MMTSO needs careful concern of outcomes and hypothesis being tested. For example, to test cell viability of exposure to a bioactive compound, a cell line should initially be selected to highlight any cytotoxic effects of high concentrations of the compound, as shown in Chapter 2 with MMTSO. These high concentrations would then not be used in future animal and human based studies.

6.2.4 How can multi-omics analysis to assess SMCSO and MMTSO on prostate cancer metabolism?

The application of next generation sequencing technologies such as RNA-sequencing and metabolomic profiling analysis is hugely shifting our understanding of the mechanistic links with prostate cancer metabolism and diet (245, 246, 348-350). This application allows in-depth gene and metabolic analysis of any cell, tissue or body fluid collected. Whilst they have become a useful tool of exploring the gene and metabolite profiles under different treatment environments, it can be costly, time-consuming and limited by the databases and tools available (237). Thus, careful consideration is needed when selecting the most appropriate omics analysis within the research.

The ESCAPE study utilised RNA-sequencing technology of prostate tissue, and demonstrated that sulfur-containing compounds within the broccoli soups were able to in a dose-dependent manner suppress immune genes and potentially oncogenic pathways related to prostate cancer development including apoptosis and inflammatory response (24). The data demonstrated in Chapter 3 and 4 could provide evidence that the transcriptomic results seen in the ESCAPE study may also be due to the presence of SMCSO and/or MMTSO within the broccoli soups given. The SAP study utilised global metabolomic profiling of prostate tissue and demonstrated key metabolic pathways including caffeine metabolism and steroid

hormone biosynthesis was significantly different between the study arms, potentially due to the participants' habitual diet (124). Further metabolomic profiling of other human samples from the SAP study, indicated differences in the dietary coffee metabolites trigonelline, quinate and tryptophan betaine between study arms with higher abundance in the prostate (124), suggesting a role of systemic and potentially urinary reflux in exposure of these compounds to the prostate tissue.

6.2.5 How could the development of functional products for use in human cancer trials be useful?

Dietary interventions are becoming an attractive approach for cancer mitigation (351), however the development of a functional product for delivery of bioactive compounds for use in human trials can be challenging. It requires careful consideration of the delivery, absorption and matrix of the product for the highest concentration of the compounds. This could be through whole food product such as a soup or supplementation such as a capsule. Previous human intervention studies investigating the role of sulfur-containing compounds on human health and disease have used both whole food products in the broccoli soups (24, 25, 99, 256, 257), whilst others have used supplement delivery (26). Most of the studies that used whole food products in the form of a soup for the delivery of the sulfur-containing compounds, lacked a suitable control product without sulfur-containing compounds for comparison. This was explored in Chapter 5 through the development of a whole functional food product rich in SMCSO to be used in future human studies matched with an appropriate control product.

The delivery would depend on with bioactive compound was being explored. The BOBS pharmacokinetic study demonstrated in plasma samples the levels of sulforaphane peaked from 6 to 8 hours compared to the levels of SMCSO that peaked from 1.5 to 2 hours (99). Sulforaphane itself is unstable so the delivery of glucoraphanin would be more appropriate; whereas SMCSO is stable, but the breakdown products MMTSI and MMTSO are less stable so delivery of SMCSO would be most suitable. To add, the Norfolk ADaPt study that used supplements (Broccomax) reported much higher concentrations of sulforaphane in the prostate tissue compared to those on the SAP study that used whole food broccoli soup. The Broccomax supplements contained a much higher dosage, suggesting that higher dosage leads to more accumulation in the prostate tissue. Although it still remains uncertain to whether the compounds are localised to the primary tissue,

systemic exposure to the metabolites or if there is microbial influence or a mixture of all three processes in the delivery of the compounds to specific tissues such as the prostate (352). Thus, regard to the delivery method is required when developing a functional product.

Very few dietary interventions have scientifically proven to alleviate cancer progression, however there is promising evidence that dietary intervention modulate potential oncogenic pathways (24), and more recently when combined with targeted cancer therapies increase therapeutic effectiveness. This has been highlighted with the sulfur-containing compound, sulforaphane, in enhancing the effects of several chemotherapy drugs including doxorubicin and cisplatin and reducing toxic side effects (353, 354). Given this evidence, it could be plausible that the sulfur-containing compound, SMCSO, could also give similar outcomes. Thus, given the evidence discussed in this thesis of SMCSO and MMTSO exposure in DU145 prostate cancer cells, it is essential to design, administer and investigate a novel SMCSO-rich product to be used in future cancer human interventions to test if there is a casual effect of high-SMCSO consumption and cancer progression. This work may give evidence that the beneficial effects of a cruciferous and alliaceous-rich diet could also be due the SMCSO and MMTSO present within the vegetables.

6.3 Strengths and Limitations of the Research

The work presented in this thesis provided several new insights into the role of sulfur-containing compounds in prostate cancer metabolism and progression, with a number of strengths in the way the research was conducted. One strength was as there is very limited in vitro studies on the biological effects of SMCSO and MMTSO on prostate cancer progression, the use of prostate cancer cell lines gives the ability to explore the mechanistic effects of the compounds under controlled and known concentrations and treatment times. Another strength of the research was high concentrations of SMCSO and MMTSO could be administered in vitro to the prostate cancer cells and this indicated high concentrations of MMTSO reduced cell viability; if this concentration was administered in vivo in the form of a supplement this could have serious toxic side effects, thus in vitro viability assays would need to be conducted before in vivo analysis was performed. A further strength was that highly purified SMCSO and MMTSO were used, which provides strong evidence that the effects observed are due to these compounds and not the other components such as dietary fibre, or other sulfur-containing compounds such as sulforaphane commonly found in cruciferous and alliaceous vegetables.

There are several limitations in the way this research was conducted. One limitation was all the work conducted was undertaken using in vitro cell lines. Although cell based studies are easy to setup, much cheap that animal models and give molecular and mechanistic understanding of how the bioactive compound influences cellular processes and pathways, the evidence from in vitro studies are somewhat difficult to translate to in vivo situations. This is due to the fact that the cells are isolated and grown as a monolayer in culture medium and the in vitro cells would not be exposed to certain growth factors and cell-to-cell interactions especially with considering the tumour microenvironment.

Another limitation of this research regarding the use of in vitro cell lines is passage number; each time the cells are passaged, it could act slightly differently from previous, thus it is recommended when using cell lines that narrow passage numbers are used. The DU145 prostate cancer cells were used from passage 10 to passage 20 and passaged twice a week to avoid creating anomalies in the data.

A further limitation of the work carried out in this thesis was the constant intermediate or high glucose concentration for the whole treatment time. In vivo an individual would experience peaks and troughs in blood glucose concentration, and

although they may be exposed to high blood glucose on a regular basis such as pre-diabetes or diabetes level, they would not constantly be exposed to an intermediate or high glucose environment (355). It is worth noting that the consistency of the cell-based observations in this thesis and those from previous animal studies suggest that in vitro cell analysis is an excellent initial model for studying the biological effects of sulfur-containing compounds on prostate cancer metabolism.

The significant limitations of using transcriptomics and metabolomics technologies are they are time-consuming for extraction, running and data analysis, can be costly, and limited to the databases and tools available (237, 284). This being said transcriptomics and metabolomics allow the study of gene expression and metabolite regulation to give a snapshot of the metabolic rewiring under different treatment environments.

6.4 Recommendations for Future Work

The work presented in this thesis has provided new insights into the role of SMCSO and MMTSO on prostate cancer metabolism and has made new observations of the transcriptomic and metabolomic consequences of exposure to these compounds. These findings have generated new objectives to be investigated in future experiments and work.

- From the evidence presented in this thesis, it is clear that MMTSO is capable of modulating energy metabolism and key metabolic pathways. With the evidence from a previous study that reported modified MMTSO bound to STAT3 transcription factor (175), identification of new biomarkers would put context to the evidence in this thesis and provide evidence of specific targets involved in energy regulation of prostate cancer cells.
- Presented in chapter 3, the transcriptomic analysis demonstrated that SMCSO and MMTSO exposure influenced expression at a gene level in several pathways, however whether this influence is translated at a protein level was not explored. Thus, it would be vital to conduct assessment at a protein level to delineate functional downstream consequences of these gene expression changes.
- The evidence presented in Chapter gave a single snapshot of the metabolic consequences of SMCSO and MMTSO in DU145 prostate cancer cells, however the production and consumption rates of specific metabolites over different time-points was not investigated. Hence, it would be crucial to explore this further using metabolic flux experiments and ^{13}C-labelled glucose tracers to give an insight into the metabolic modifications in the prostate cancer cells.
- The evidence presented in this thesis was only investigated in one prostate cancer cell line (DU145) which are brain metastatic, castration resistant and androgen-independent (336). It would be beneficial to explore if the same effect is observed in other prostate cancer cell lines that are hormone sensitive such as LNCaP that are lymph node metastatic and androgen-responsive (336).
- The design and development of a functional food product rich in SMCSO with appropriate control product, presented in Chapter 5, could be used in a future human dietary intervention study with prostate cancer patients. Careful consideration on the study design would be needed although a 12-

week two-arm crossover intervention with a washout period could be suitable to assess the impact of dietary intake of SMCSO on prostate cancer metabolism. Longer studies such as 1 to 2 years would be needed to evaluate the effect of SMCSO on prostate cancer progression. The evidence from the human study would give a better insight into the metabolic regulation in vivo.

- SMCSO administered to diabetic rats was reported to reduce glycemia and lipids, advocate immunomodulation and mitigate oxidative stress in numerous animal studies (129-131, 141), however, this effect has not been explored in humans. Using the dietary product developed in Chapter 5, a human intervention could be conducted initially with individuals that have hyperglycaemia and/or diabetes, before a further study recruiting with prostate cancer patients with hyperglycaemia and/or diabetes. For both, an 8 to 12-week two-arm crossover intervention with a 12-week washout to minimise the presence of a carry-over effect, would be sufficient to evaluate the effect of SMCSO on blood glucose markers including glycated haemoglobin (HbA1c). HbA1c is typically measured over a period of 8 to 12 weeks and is diagnosed through measuring fasting plasma glucose and/or HbA1c through a fasting blood test and/or oral glucose tolerance test (356).
- The breakdown of SMCSO to MMTSO is facilitated by cysteine conjugate β lyases. A previous human study reported that the gut microbiota, particularly *E. coli*, could play a role in the conversion of SMCSO to the reduced analogue, S-methyl cysteine (119). It would be beneficial isolate candidate genes for the specific cysteine conjugate β lyase to generate a knock-out strain of *E. coli*. This knock-out strain of *E. coli* could be cultured with SMCSO and if it is no longer metabolised, will give an insight into the specific lyases in SMCSO metabolism.

6.5 Conclusion

The evidence in this thesis reported the unique mitochondrial, transcriptomic and metabolomic profiles of DU145 prostate cancer cells, and demonstrated that SMCSO and MMTSO are capable of modulating these signatures. Future research should consider the effect of these sulfur-containing compounds on individuals with prostate cancer with and without hyperglycaemia and/or diabetes to give an insight into how these compounds could mitigate prostate cancer progression in vivo. The work presented in this thesis has made a significant contribution to the current knowledge of the biological activity of SMCSO and MMTSO on prostate metabolism, and their metabolic and mechanistic links to prostate cancer prevention adding to the field of cancer and nutrition.

References

References

1. McNeal JE. The zonal anatomy of the prostate. Prostate. 1981;2(1):35-49.
2. Butel R, Ball R. The distribution of BCG prostatitis: A clue for pathogenetic processes? Prostate. 2018;78(15):1134-9.
3. Huggins C, Neal W. Coagulation and Liquefaction of Semen: Proteolytic Enzymes and Citrate in Prostatic Fluid. J Exp Med. 1942;76(6):527-41.
4. Kaler J, Hussain A, Haque A, Naveed H, Patel S. A Comprehensive Review of Pharmaceutical and Surgical Interventions of Prostate Cancer. Cureus. 2020;12(11):e11617.
5. Balk SP, Ko YJ, Bubley GJ. Biology of prostate-specific antigen. J Clin Oncol. 2003;21(2):383-91.
6. Adhyam M, Gupta AK. A Review on the Clinical Utility of PSA in Cancer Prostate. Indian J Surg Oncol. 2012;3(2):120-9.
7. Rawla P. Epidemiology of Prostate Cancer. World J Oncol. 2019;10(2):63-89.
8. Smith J, Dodd RH, Gainey KM, Naganathan V, Cvejic E, Jansen J, et al. Patient-Reported Factors Associated With Older Adults' Cancer Screening Decision-making: A Systematic Review. JAMA Netw Open. 2021;4(11):e2133406.
9. UK CR. Prostate Cancer Statistics [Available online: https://www.cancerresearchuk.org/health-professional/cancer-statistics/statistics-by-cancer-type/prostate-cancer#heading-Zero].
10. Taitt HE. Global Trends and Prostate Cancer: A Review of Incidence, Detection, and Mortality as Influenced by Race, Ethnicity, and Geographic Location. Am J Mens Health. 2018;12(6):1807-23.
11. Gann PH. Risk factors for prostate cancer. Rev Urol. 2002;4 Suppl 5(Suppl 5):S3-s10.
12. Ekman P. Genetic and environmental factors in prostate cancer genesis: identifying high-risk cohorts. Eur Urol. 1999;35(5-6):362-9.
13. Wilson KM, Giovannucci EL, Mucci LA. Lifestyle and dietary factors in the prevention of lethal prostate cancer. Asian J Androl. 2012;14(3):365-74.
14. Marshall JR. Diet and prostate cancer prevention. World J Urol. 2012;30(2):157-65.
15. Ambrosini GL, Fritschi L, de Klerk NH, Mackerras D, Leavy J. Dietary patterns identified using factor analysis and prostate cancer risk: a case control study in Western Australia. Ann Epidemiol. 2008;18(5):364-70.
16. Mandair D, Rossi RE, Pericleous M, Whyand T, Caplin ME. Prostate cancer and the influence of dietary factors and supplements: a systematic review. Nutr Metab (Lond). 2014;11:30.
17. Lozano-Lorca M, Rodríguez-González M, Salcedo-Bellido I, Vázquez-Alonso F, Arrabal M, Martín-Castaño B, et al. Dietary Patterns and Prostate Cancer: CAPLIFE Study. Cancers (Basel). 2022;14(14).
18. Carlsson S, Assel M, Ulmert D, Gerdtsson A, Hugosson J, Vickers A, et al. Screening for Prostate Cancer Starting at Age 50-54 Years. A Population-based Cohort Study. Eur Urol. 2017;71(1):46-52.
19. Leslie SW, Soon-Sutton TL, R IA, Sajjad H, Siref LE. Prostate Cancer. StatPearls. Treasure Island (FL): StatPearls Publishing
Copyright © 2022, StatPearls Publishing LLC.; 2022.
20. Albertsen PC. Prostate cancer screening with prostate-specific antigen: Where are we going? Cancer. 2018;124(3):453-5.
21. Leal J, Welton NJ, Martin RM, Donovan J, Hamdy F, Neal D, et al. Estimating the sensitivity of a prostate cancer screening programme for different PSA cut-off levels: A UK case study. Cancer Epidemiol. 2018;52:99-105.

22. Power J, Murphy M, Hutchinson B, Murphy D, McNicholas M, O'Malley K, et al. Transperineal ultrasound-guided prostate biopsy: what the radiologist needs to know. Insights Imaging. 2022;13(1):77.
23. Shill DK, Roobol MJ, Ehdaie B, Vickers AJ, Carlsson SV. Active surveillance for prostate cancer. Transl Androl Urol. 2021;10(6):2809-19.
24. Traka MH, Melchini A, Coode-Bate J, Al Kadhi O, Saha S, Defernez M, et al. Transcriptional changes in prostate of men on active surveillance after a 12-mo glucoraphanin-rich broccoli intervention-results from the Effect of Sulforaphane on prostate CAncer PrEvention (ESCAPE) randomized controlled trial. Am J Clin Nutr. 2019;109(4):1133-44.
25. Coode-Bate J, Sivapalan T, Melchini A, Saha S, Needs PW, Dainty JR, et al. Accumulation of Dietary S-Methyl Cysteine Sulfoxide in Human Prostate Tissue. Mol Nutr Food Res. 2019;63(20).
26. Livingstone TL, Saha S, Bernuzzi F, Savva GM, Troncoso-Rey P, Traka MH, et al. Accumulation of Sulforaphane and Alliin in Human Prostate Tissue. Nutrients. 2022;14(16).
27. Costello LC, Franklin RB. Concepts of citrate production and secretion by prostate. 1. Metabolic relationships. Prostate. 1991;18(1):25-46.
28. Eidelman E, Twum-Ampofo J, Ansari J, Siddiqui MM. The Metabolic Phenotype of Prostate Cancer. Front Oncol. 2017;7:131.
29. Costello LC, Franklin RB. The clinical relevance of the metabolism of prostate cancer; zinc and tumor suppression: connecting the dots. Mol Cancer. 2006;5:17.
30. Sena LA, Denmeade SR. Fatty Acid Synthesis in Prostate Cancer: Vulnerability or Epiphenomenon? Cancer Res. 2021;81(17):4385-93.
31. Frégeau-Proulx L, Lacouture A, Berthiaume L, Weidmann C, Harvey M, Gonthier K, et al. Multiple metabolic pathways fuel the truncated tricarboxylic acid cycle of the prostate to sustain constant citrate production and secretion. Mol Metab. 2022;62:101516.
32. Lin C, Salzillo TC, Bader DA, Wilkenfeld SR, Awad D, Pulliam TL, et al. Prostate Cancer Energetics and Biosynthesis. Adv Exp Med Biol. 2019;1210:185-237.
33. Schiliro C, Firestein BL. Mechanisms of Metabolic Reprogramming in Cancer Cells Supporting Enhanced Growth and Proliferation. Cells. 2021;10(5).
34. Zhang Y, Yang JM. Altered energy metabolism in cancer: a unique opportunity for therapeutic intervention. Cancer Biol Ther. 2013;14(2):81-9.
35. Wanjari UR, Mukherjee AG, Gopalakrishnan AV, Murali R, Dey A, Vellingiri B, et al. Role of Metabolism and Metabolic Pathways in Prostate Cancer. Metabolites. 2023;13(2).
36. Ahmad F, Cherukuri MK, Choyke PL. Metabolic reprogramming in prostate cancer. Br J Cancer. 2021;125(9):1185-96.
37. Twum-Ampofo J, Fu DX, Passaniti A, Hussain A, Siddiqui MM. Metabolic targets for potential prostate cancer therapeutics. Curr Opin Oncol. 2016;28(3):241-7.
38. Lasorsa F, di Meo NA, Rutigliano M, Ferro M, Terracciano D, Tataru OS, et al. Emerging Hallmarks of Metabolic Reprogramming in Prostate Cancer. Int J Mol Sci. 2023;24(2).
39. Wang Y, Ma S, Ruzzo WL. Spatial modeling of prostate cancer metabolic gene expression reveals extensive heterogeneity and selective vulnerabilities. Scientific Reports. 2020;10(1):3490.
40. Shao Y, Ye G, Ren S, Piao HL, Zhao X, Lu X, et al. Metabolomics and transcriptomics profiles reveal the dysregulation of the tricarboxylic acid cycle and related mechanisms in prostate cancer. Int J Cancer. 2018;143(2):396-407.
41. Chaplin DD. Overview of the immune response. J Allergy Clin Immunol. 2010;125(2 Suppl 2):S3-23.

42. Gonzalez H, Hagerling C, Werb Z. Roles of the immune system in cancer: from tumor initiation to metastatic progression. Genes Dev. 2018;32(19-20):1267-84.
43. Kim SK, Cho SW. The Evasion Mechanisms of Cancer Immunity and Drug Intervention in the Tumor Microenvironment. Front Pharmacol. 2022;13:868695.
44. Beatty GL, Gladney WL. Immune escape mechanisms as a guide for cancer immunotherapy. Clin Cancer Res. 2015;21(4):687-92.
45. Vitkin N, Nersesian S, Siemens DR, Koti M. The Tumor Immune Contexture of Prostate Cancer. Front Immunol. 2019;10:603.
46. Lin D, Wang X, Choi SYC, Ci X, Dong X, Wang Y. Immune phenotypes of prostate cancer cells: Evidence of epithelial immune cell-like transition? Asian J Urol. 2016;3(4):195-202.
47. Choi SY, Gout PW, Collins CC, Wang Y. Epithelial immune cell-like transition (EIT): a proposed transdifferentiation process underlying immune-suppressive activity of epithelial cancers. Differentiation. 2012;83(5):293-8.
48. Wu SQ, Su H, Wang YH, Zhao XK. Role of tumor-associated immune cells in prostate cancer: angel or devil? Asian J Androl. 2019;21(5):433-7.
49. Palano MT, Gallazzi M, Cucchiara M, Dehò F, Capogrosso P, Bruno A, et al. The tumor innate immune microenvironment in prostate cancer: an overview of soluble factors and cellular effectors. Explor Target Antitumor Ther. 2022;3(5):694-718.
50. Bou-Dargham MJ, Sha L, Sang QA, Zhang J. Immune landscape of human prostate cancer: immune evasion mechanisms and biomarkers for personalized immunotherapy. BMC Cancer. 2020;20(1):572.
51. Risk M, Corman JM. The role of immunotherapy in prostate cancer: an overview of current approaches in development. Rev Urol. 2009;11(1):16-27.
52. Russo M, Nastasi C. Targeting the Tumor Microenvironment: A Close Up of Tumor-Associated Macrophages and Neutrophils. Front Oncol. 2022;12:871513.
53. Lin Y, Xu J, Lan H. Tumor-associated macrophages in tumor metastasis: biological roles and clinical therapeutic applications. Journal of Hematology & Oncology. 2019;12(1):76.
54. Takeya M, Komohara Y. Role of tumor-associated macrophages in human malignancies: friend or foe? Pathol Int. 2016;66(9):491-505.
55. Lanciotti M, Masieri L, Raspollini MR, Minervini A, Mari A, Comito G, et al. The role of M1 and M2 macrophages in prostate cancer in relation to extracapsular tumor extension and biochemical recurrence after radical prostatectomy. Biomed Res Int. 2014;2014:486798.
56. Maillard M, Cadot B, Ball RY, Sethia K, Edwards DR, Perbal B, et al. Differential expression of the ccn3 (nov) proto-oncogene in human prostate cell lines and tissues. Mol Pathol. 2001;54(4):275-80.
57. Chen PC, Cheng HC, Wang J, Wang SW, Tai HC, Lin CW, et al. Prostate cancer-derived CCN3 induces M2 macrophage infiltration and contributes to angiogenesis in prostate cancer microenvironment. Oncotarget. 2014;5(6):1595-608.
58. Fridlender ZG, Sun J, Kim S, Kapoor V, Cheng G, Ling L, et al. Polarization of tumor-associated neutrophil phenotype by TGF-beta: "N1" versus "N2" TAN. Cancer Cell. 2009;16(3):183-94.
59. Masucci MT, Minopoli M, Carriero MV. Tumor Associated Neutrophils. Their Role in Tumorigenesis, Metastasis, Prognosis and Therapy. Front Oncol. 2019;9:1146.
60. Costanzo-Garvey DL, Keeley T, Case AJ, Watson GF, Alsamraae M, Yu Y, et al. Neutrophils are mediators of metastatic prostate cancer progression in bone. Cancer Immunol Immunother. 2020;69(6):1113-30.
61. Ohue Y, Nishikawa H. Regulatory T (Treg) cells in cancer: Can Treg cells be a new therapeutic target? Cancer Sci. 2019;110(7):2080-9.

62. Takeuchi Y, Nishikawa H. Roles of regulatory T cells in cancer immunity. Int Immunol. 2016;28(8):401-9.
63. Nardone V, Botta C, Caraglia M, Martino EC, Ambrosio MR, Carfagno T, et al. Tumor infiltrating T lymphocytes expressing FoxP3, CCR7 or PD-1 predict the outcome of prostate cancer patients subjected to salvage radiotherapy after biochemical relapse. Cancer Biol Ther. 2016;17(11):1213-20.
64. Davidsson S, Andren O, Ohlson AL, Carlsson J, Andersson SO, Giunchi F, et al. FOXP3(+) regulatory T cells in normal prostate tissue, postatrophic hyperplasia, prostatic intraepithelial neoplasia, and tumor histological lesions in men with and without prostate cancer. Prostate. 2018;78(1):40-7.
65. Mohr A, Malhotra R, Mayer G, Gorochov G, Miyara M. Human FOXP3(+) T regulatory cell heterogeneity. Clin Transl Immunology. 2018;7(1):e1005.
66. Groth C, Hu X, Weber R, Fleming V, Altevogt P, Utikal J, et al. Immunosuppression mediated by myeloid-derived suppressor cells (MDSCs) during tumour progression. Br J Cancer. 2019;120(1):16-25.
67. Beury DW, Parker KH, Nyandjo M, Sinha P, Carter KA, Ostrand-Rosenberg S. Cross-talk among myeloid-derived suppressor cells, macrophages, and tumor cells impacts the inflammatory milieu of solid tumors. J Leukoc Biol. 2014;96(6):1109-18.
68. Jachetti E, Cancila V, Rigoni A, Bongiovanni L, Cappetti B, Belmonte B, et al. Cross-Talk between Myeloid-Derived Suppressor Cells and Mast Cells Mediates Tumor-Specific Immunosuppression in Prostate Cancer. Cancer Immunol Res. 2018;6(5):552-65.
69. Chi N, Tan Z, Ma K, Bao L, Yun Z. Increased circulating myeloid-derived suppressor cells correlate with cancer stages, interleukin-8 and -6 in prostate cancer. Int J Clin Exp Med. 2014;7(10):3181-92.
70. Lopez-Bujanda Z, Drake CG. Myeloid-derived cells in prostate cancer progression: phenotype and prospective therapies. J Leukoc Biol. 2017;102(2):393-406.
71. Culig Z, Puhr M. Interleukin-6 and prostate cancer: Current developments and unsolved questions. Mol Cell Endocrinol. 2018;462(Pt A):25-30.
72. Mao C, Ding Y, Xu N. A Double-Edged Sword Role of Cytokines in Prostate Cancer Immunotherapy. Front Oncol. 2021;11:688489.
73. Bostwick DG, Burke HB, Djakiew D, Euling S, Ho SM, Landolph J, et al. Human prostate cancer risk factors. Cancer. 2004;101(10 Suppl):2371-490.
74. Schieber M, Chandel NS. ROS function in redox signaling and oxidative stress. Curr Biol. 2014;24(10):R453-62.
75. Di Meo S, Reed TT, Venditti P, Victor VM. Role of ROS and RNS Sources in Physiological and Pathological Conditions. Oxid Med Cell Longev. 2016;2016:1245049.
76. Khandrika L, Kumar B, Koul S, Maroni P, Koul HK. Oxidative stress in prostate cancer. Cancer Lett. 2009;282(2):125-36.
77. Vayalil PK. Mitochondrial oncobioenergetics of prostate tumorigenesis. Oncol Lett. 2019;18(5):4367-76.
78. Han C, Wang Z, Xu Y, Chen S, Han Y, Li L, et al. Roles of Reactive Oxygen Species in Biological Behaviors of Prostate Cancer. Biomed Res Int. 2020;2020:1269624.
79. Schöpf B, Weissensteiner H, Schäfer G, Fazzini F, Charoentong P, Naschberger A, et al. OXPHOS remodeling in high-grade prostate cancer involves mtDNA mutations and increased succinate oxidation. Nat Commun. 2020;11(1):1487.
80. Singh AN, Sharma N. Quantitative SWATH-Based Proteomic Profiling for Identification of Mechanism-Driven Diagnostic Biomarkers Conferring in the Progression of Metastatic Prostate Cancer. Front Oncol. 2020;10:493.

81. Lee B, Mahmud I, Marchica J, Dereziński P, Qi F, Wang F, et al. Integrated RNA and metabolite profiling of urine liquid biopsies for prostate cancer biomarker discovery. Scientific Reports. 2020;10(1):3716.
82. Song Z, Yang Y, Wu Y, Zheng M, Sun D, Li H, et al. Glutamic oxaloacetic transaminase 1 as a potential target in human cancer. Eur J Pharmacol. 2022;917:174754.
83. Bagheri A, Nachvak SM, Rezaei M, Moravridzade M, Moradi M, Nelson M. Dietary patterns and risk of prostate cancer: a factor analysis study in a sample of Iranian men. Health Promot Perspect. 2018;8(2):133-8.
84. Parsons JK, Pierce JP, Mohler J, Paskett E, Jung SH, Humphrey P, et al. A randomized trial of diet in men with early stage prostate cancer on active surveillance: rationale and design of the Men's Eating and Living (MEAL) Study (CALGB 70807 [Alliance]). Contemp Clin Trials. 2014;38(2):198-203.
85. Livingstone TL, Beasy G, Mills RD, Plumb J, Needs PW, Mithen R, et al. Plant Bioactives and the Prevention of Prostate Cancer: Evidence from Human Studies. Nutrients. 2019;11(9):2245.
86. Hao Q, Wu Y, Vadgama JV, Wang P. Phytochemicals in Inhibition of Prostate Cancer: Evidence from Molecular Mechanisms Studies. Biomolecules. 2022;12(9).
87. Patra S, Nayak R, Patro S, Pradhan B, Sahu B, Behera C, et al. Chemical diversity of dietary phytochemicals and their mode of chemoprevention. Biotechnology Reports. 2021;30:e00633.
88. Ağagündüz D, Şahin T, Yılmaz B, Ekenci KD, Duyar Özer Ş, Capasso R. Cruciferous Vegetables and Their Bioactive Metabolites: from Prevention to Novel Therapies of Colorectal Cancer. Evid Based Complement Alternat Med. 2022;2022:1534083.
89. Khoo HE, Azlan A, Tang ST, Lim SM. Anthocyanidins and anthocyanins: colored pigments as food, pharmaceutical ingredients, and the potential health benefits. Food Nutr Res. 2017;61(1):1361779.
90. Thomas R, Williams M, Sharma H, Chaudry A, Bellamy P. A double-blind, placebo-controlled randomised trial evaluating the effect of a polyphenol-rich whole food supplement on PSA progression in men with prostate cancer--the U.K. NCRN Pomi-T study. Prostate Cancer Prostatic Dis. 2014;17(2):180-6.
91. Connolly EL, Sim M, Travica N, Marx W, Beasy G, Lynch GS, et al. Glucosinolates From Cruciferous Vegetables and Their Potential Role in Chronic Disease: Investigating the Preclinical and Clinical Evidence. Frontiers in Pharmacology. 2021;12.
92. Hill CR, Shafaei A, Balmer L, Lewis JR, Hodgson JM, Millar AH, et al. Sulfur compounds: From plants to humans and their role in chronic disease prevention. Crit Rev Food Sci Nutr. 2022:1-23.
93. Traka MH, Saha S, Huseby S, Kopriva S, Walley PG, Barker GC, et al. Genetic regulation of glucoraphanin accumulation in Beneforté broccoli. New Phytol. 2013;198(4):1085-95.
94. Soundararajan P, Kim JS. Anti-Carcinogenic Glucosinolates in Cruciferous Vegetables and Their Antagonistic Effects on Prevention of Cancers. Molecules. 2018;23(11).
95. Ishida M, Hara M, Fukino N, Kakizaki T, Morimitsu Y. Glucosinolate metabolism, functionality and breeding for the improvement of Brassicaceae vegetables. Breed Sci. 2014;64(1):48-59.
96. Steinbrecher A, Linseisen J. Dietary intake of individual glucosinolates in participants of the EPIC-Heidelberg cohort study. Ann Nutr Metab. 2009;54(2):87-96.
97. Mithen R, Faulkner K, Magrath R, Rose P, Williamson G, Marquez J. Development of isothiocyanate-enriched broccoli, and its enhanced ability to

induce phase 2 detoxification enzymes in mammalian cells. Theor Appl Genet. 2003;106(4):727-34.
98. Neequaye M, Steuernagel B, Saha S, Trick M, Troncoso-Rey P, van den Bosch F, et al. Characterisation of the Introgression of Brassica villosa Genome Into Broccoli to Enhance Methionine-Derived Glucosinolates and Associated Health Benefits. Front Plant Sci. 2022;13:855707.
99. Sivapalan T, Melchini A, Saha S, Needs PW, Traka MH, Tapp H, et al. Bioavailability of Glucoraphanin and Sulforaphane from High-Glucoraphanin Broccoli. Mol Nutr Food Res. 2018;62(18):e1700911.
100. Traka M, Mithen R. Glucosinolates, isothiocyanates and human health. Phytochem Rev. 2009;8(1):269-82.
101. Barba FJ, Nikmaram N, Roohinejad S, Khelfa A, Zhu Z, Koubaa M. Bioavailability of Glucosinolates and Their Breakdown Products: Impact of Processing. Front Nutr. 2016;3:24.
102. Sikorska-Zimny K, Beneduce L. The Metabolism of Glucosinolates by Gut Microbiota. Nutrients. 2021;13(8).
103. Nelson CP, Kidd LC, Sauvageot J, Isaacs WB, De Marzo AM, Groopman JD, et al. Protection against 2-hydroxyamino-1-methyl-6-phenylimidazo[4,5-b]pyridine cytotoxicity and DNA adduct formation in human prostate by glutathione S-transferase P1. Cancer Res. 2001;61(1):103-9.
104. Singh SV, Singh K. Cancer chemoprevention with dietary isothiocyanates mature for clinical translational research. Carcinogenesis. 2012;33(10):1833-42.
105. Kaiser AE, Baniasadi M, Giansiracusa D, Giansiracusa M, Garcia M, Fryda Z, et al. Sulforaphane: A Broccoli Bioactive Phytocompound with Cancer Preventive Potential. Cancers (Basel). 2021;13(19).
106. Mandrich L, Caputo E. Brassicaceae-Derived Anticancer Agents: Towards a Green Approach to Beat Cancer. Nutrients. 2020;12(3).
107. Kyriakou S, Trafalis DT, Deligiorgi MV, Franco R, Pappa A, Panayiotidis MI. Assessment of Methodological Pipelines for the Determination of Isothiocyanates Derived from Natural Sources. Antioxidants (Basel). 2022;11(4).
108. Matusheski NV, Jeffery EH. Comparison of the bioactivity of two glucoraphanin hydrolysis products found in broccoli, sulforaphane and sulforaphane nitrile. J Agric Food Chem. 2001;49(12):5743-9.
109. Hanschen FS, Schreiner M. Isothiocyanates, Nitriles, and Epithionitriles from Glucosinolates Are Affected by Genotype and Developmental Stage in Brassica oleracea Varieties. Front Plant Sci. 2017;8:1095.
110. Sturm C, Wagner AE. Brassica-Derived Plant Bioactives as Modulators of Chemopreventive and Inflammatory Signaling Pathways. Int J Mol Sci. 2017;18(9).
111. Huang Y, Li W, Su ZY, Kong AN. The complexity of the Nrf2 pathway: beyond the antioxidant response. J Nutr Biochem. 2015;26(12):1401-13.
112. Dinkova-Kostova AT, Fahey JW, Kostov RV, Kensler TW. KEAP1 and Done? Targeting the NRF2 Pathway with Sulforaphane. Trends Food Sci Technol. 2017;69(Pt B):257-69.
113. Singh KB, Hahm ER, Rigatti LH, Normolle DP, Yuan JM, Singh SV. Inhibition of Glycolysis in Prostate Cancer Chemoprevention by Phenethyl Isothiocyanate. Cancer Prev Res (Phila). 2018;11(6):337-46.
114. Lin JF, Tsai TF, Yang SC, Lin YC, Chen HE, Chou KY, et al. Benzyl isothiocyanate induces reactive oxygen species-initiated autophagy and apoptosis in human prostate cancer cells. Oncotarget. 2017;8(12):20220-34.
115. Beaver LM, Löhr CV, Clarke JD, Glasser ST, Watson GW, Wong CP, et al. Broccoli Sprouts Delay Prostate Cancer Formation and Decrease Prostate Cancer Severity with a Concurrent Decrease in HDAC3 Protein Expression in Transgenic Adenocarcinoma of the Mouse Prostate (TRAMP) Mice. Current Developments in Nutrition. 2017;2(3).

116. Marks HS, Hilson JA, Leichtweis HC, Stoewsand GS. S-Methylcysteine sulfoxide in Brassica vegetables and formation of methyl methanethiosulfinate from Brussels sprouts. J Agric Food Chem. 1992;40(11):2098-101.
117. Edmands WMB, Gooderham NJ, Holmes E, Mitchell SC. S-Methyl-l-cysteine sulphoxide: the Cinderella phytochemical? Toxicology Research. 2013;2(1):11-22.
118. Kellingray L, Tapp HS, Saha S, Doleman JF, Narbad A, Mithen RF. Consumption of a diet rich in Brassica vegetables is associated with a reduced abundance of sulphate-reducing bacteria: A randomised crossover study. Mol Nutr Food Res. 2017;61(9).
119. Kellingray L, Le Gall G, Doleman JF, Narbad A, Mithen RF. Effects of in vitro metabolism of a broccoli leachate, glucosinolates and S-methylcysteine sulphoxide on the human faecal microbiome. European Journal of Nutrition. 2021;60(4):2141-54.
120. Kim S-Y, Park K-W, Kim J-Y, Jeong I-Y, Byun M-W, Park J-E, et al. Thiosulfinates from Allium tuberosum L. induce apoptosis via caspase-dependent and -independent pathways in PC-3 human prostate cancer cells. Bioorganic & medicinal chemistry letters. 2008;18(1):199-204.
121. Kim SY, Park KW, Kim JY, Shon MY, Yee ST, Kim KH, et al. Induction of apoptosis by thiosulfinates in primary human prostate cancer cells. Int J Oncol. 2008;32(4):869-75.
122. Lee JH, Yang HS, Park KW, Kim JY, Lee MK, Jeong IY, et al. Mechanisms of thiosulfinates from Allium tuberosum L.-induced apoptosis in HT-29 human colon cancer cells. Toxicol Lett. 2009;188(2):142-7.
123. Prosolek S. The Effect of Broccoli-Derived Sulfur-Containing Bioactives On Cellular Metabolism: Doctoral Thesis, University of East Anglia; 2020.
124. Coode-Bate J. Effects of Broccoli-Derived Sulphur Compounds on the Prostate Microenvironment: Doctoral Thesis, University of East Anglia; 2017.
125. Marks HS, Anderson JA, Stoewsand GS. Effect of S-methyl cysteine sulphoxide and its metabolite methyl methane thiosulphinate, both occurring naturally in Brassica vegetables, on mouse genotoxicity. Food Chem Toxicol. 1993;31(7):491-5.
126. Kawamori T, Tanaka T, Ohnishi M, Hirose Y, Nakamura Y, Satoh K, et al. Chemoprevention of azoxymethane-induced colon carcinogenesis by dietary feeding of S-methyl methane thiosulfonate in male F344 rats. Cancer Res. 1995;55(18):4053-8.
127. Reddy BS, Kawamori T, Lubet R, Steele V, Kelloff G, Rao CV. Chemopreventive effect of S-methylmethane thiosulfonate and sulindac administered together during the promotion/progression stages of colon carcinogenesis. Carcinogenesis. 1999;20(8):1645-8.
128. Sugie S, Okamoto K, Ohnishi M, Makita H, Kawamori T, Watanabe T, et al. Suppressive effects of S-methyl methanethiosulfonate on promotion stage of diethylnitrosamine-initiated and phenobarbital-promoted hepatocarcinogenesis model. Jpn J Cancer Res. 1997;88(1):5-11.
129. Kumari K, Mathew BC, Augusti KT. Antidiabetic and hypolipidemic effects of S-methyl cysteine sulfoxide isolated from Allium cepa Linn. Indian J Biochem Biophys. 1995;32(1):49-54.
130. Kumari K, Augusti KT. Antidiabetic and antioxidant effects of S-methyl cysteine sulfoxide isolated from onions (Allium cepa Linn) as compared to standard drugs in alloxan diabetic rats. Indian J Exp Biol. 2002;40(9):1005-9.
131. Sheela CG, Kumud K, Augusti KT. Anti-diabetic effects of onion and garlic sulfoxide amino acids in rats. Planta Med. 1995;61(4):356-7.
132. Liberti MV, Locasale JW. The Warburg Effect: How Does it Benefit Cancer Cells? Trends Biochem Sci. 2016;41(3):211-8.

133. Li W, Zhang X, Sang H, Zhou Y, Shang C, Wang Y, et al. Effects of hyperglycemia on the progression of tumor diseases. Journal of Experimental & Clinical Cancer Research. 2019;38(1):327.
134. Duan W, Shen X, Lei J, Xu Q, Yu Y, Li R, et al. Hyperglycemia, a neglected factor during cancer progression. Biomed Res Int. 2014;2014:461917.
135. Gonzalez-Menendez P, Hevia D, Alonso-Arias R, Alvarez-Artime A, Rodriguez-Garcia A, Kinet S, et al. GLUT1 protects prostate cancer cells from glucose deprivation-induced oxidative stress. Redox Biol. 2018;17:112-27.
136. Sarkar PL, Lee W, Williams ED, Lubik AA, Stylianou N, Shokoohmand A, et al. Insulin Enhances Migration and Invasion in Prostate Cancer Cells by Up-Regulation of FOXC2. Front Endocrinol (Lausanne). 2019;10:481.
137. Feng X, Song M, Preston MA, Ma W, Hu Y, Pernar CH, et al. The association of diabetes with risk of prostate cancer defined by clinical and molecular features. Br J Cancer. 2020;123(4):657-65.
138. Axelsson AS, Tubbs E, Mecham B, Chacko S, Nenonen HA, Tang Y, et al. Sulforaphane reduces hepatic glucose production and improves glucose control in patients with type 2 diabetes. Sci Transl Med. 2017;9(394).
139. Tian S, Li X, Wang Y, Lu Y. The protective effect of sulforaphane on type II diabetes induced by high-fat diet and low-dosage streptozotocin. Food Sci Nutr. 2021;9(2):747-56.
140. Jo ES, Sp N, Kang DY, Rugamba A, Kim IH, Bae SW, et al. Sulfur Compounds Inhibit High Glucose-Induced Inflammation by Regulating NF-κB Signaling in Human Monocytes. Molecules. 2020;25(10).
141. Lemos LIC, Medeiros MA, Lima J, Teixeira TO, Figueiredo CA, Farias NBS, et al. S-methyl cysteine sulfoxide mitigates histopathological damage, alleviate oxidative stress and promotes immunomodulation in diabetic rats. J Complement Integr Med. 2021;18(4):719-25.
142. Castro VMD, Medeiros KCP, Lemos LIC, Pedrosa LFC, Ladd FVL, Carvalho TG, et al. S-methyl cysteine sulfoxide ameliorates duodenal morphological alterations in streptozotocin-induced diabetic rats. Tissue Cell. 2021;69:101483.
143. Rose P, Moore PK, Whiteman M, Zhu YZ. An Appraisal of Developments in Allium Sulfur Chemistry: Expanding the Pharmacopeia of Garlic. Molecules. 2019;24(21).
144. Liu B, Mao Q, Cao M, Xie L. Cruciferous vegetables intake and risk of prostate cancer: a meta-analysis. Int J Urol. 2012;19(2):134-41.
145. Alumkal JJ, Slottke R, Schwartzman J, Cherala G, Munar M, Graff JN, et al. A phase II study of sulforaphane-rich broccoli sprout extracts in men with recurrent prostate cancer. Invest New Drugs. 2015;33(2):480-9.
146. Zhang Z, Garzotto M, Davis EW, 2nd, Mori M, Stoller WA, Farris PE, et al. Sulforaphane Bioavailability and Chemopreventive Activity in Men Presenting for Biopsy of the Prostate Gland: A Randomized Controlled Trial. Nutr Cancer. 2020;72(1):74-87.
147. Waring RH, Harris RM, Steventon GB, Mitchell SC. Degradation to sulphate of S-methyl-L-cysteine sulphoxide and S-carboxymethyl-L-cysteine sulphoxide in man. Drug Metabol Drug Interact. 2003;19(4):241-55.
148. Lee J, Giovannucci E, Jeon JY. Diabetes and mortality in patients with prostate cancer: a meta-analysis. Springerplus. 2016;5(1):1548.
149. Kasper JS, Liu Y, Giovannucci E. Diabetes mellitus and risk of prostate cancer in the health professionals follow-up study. Int J Cancer. 2009;124(6):1398-403.
150. Murtola TJ, Vihervuori VJ, Lahtela J, Talala K, Taari K, Tammela TL, et al. Fasting blood glucose, glycaemic control and prostate cancer risk in the Finnish Randomized Study of Screening for Prostate Cancer. Br J Cancer. 2018;118(9):1248-54.

151. Nagata M, Iwasaki K, Akazawa K, Komaki M, Yokoyama N, Izumi Y, et al. Conditioned Medium from Periodontal Ligament Stem Cells Enhances Periodontal Regeneration. Tissue Eng Part A. 2017;23(9-10):367-77.
152. Teng AM, Jones AC, Mizdrak A, Signal L, Genç M, Wilson N. Impact of sugar-sweetened beverage taxes on purchases and dietary intake: Systematic review and meta-analysis. Obes Rev. 2019;20(9):1187-204.
153. Cancel-Tassin G, Ondet V, Gaffory C, Orsoni C, Efstathiou T, Cussenot O. Effets pharmacogénomique du Prostaphane® sur des cellules cancéreuses de prostate. Progrès en Urologie. 2015;25(13):837-9.
154. Bahadoran Z, Tohidi M, Nazeri P, Mehran M, Azizi F, Mirmiran P. Effect of broccoli sprouts on insulin resistance in type 2 diabetic patients: a randomized double-blind clinical trial. Int J Food Sci Nutr. 2012;63(7):767-71.
155. Kirby RS, Lowe D, Bultitude MI, Shuttleworth KE. Intra-prostatic urinary reflux: an aetiological factor in abacterial prostatitis. Br J Urol. 1982;54(6):729-31.
156. Persson BE, Ronquist G. Evidence for a mechanistic association between nonbacterial prostatitis and levels of urate and creatinine in expressed prostatic secretion. J Urol. 1996;155(3):958-60.
157. Balasar M, Doğan M, Kandemir A, Taskapu HH, Cicekci F, Toy H, et al. Investigation of granulomatous prostatitis incidence following intravesical BCG therapy. Int J Clin Exp Med. 2014;7(6):1554-7.
158. Bilhim T, Tinto HR, Fernandes L, Martins Pisco J. Radiological anatomy of prostatic arteries. Tech Vasc Interv Radiol. 2012;15(4):276-85.
159. Gasper AV, Al-Janobi A, Smith JA, Bacon JR, Fortun P, Atherton C, et al. Glutathione S-transferase M1 polymorphism and metabolism of sulforaphane from standard and high-glucosinolate broccoli. Am J Clin Nutr. 2005;82(6):1283-91.
160. Javier-DesLoges J, McKay RR, Swafford AD, Sepich-Poore GD, Knight R, Parsons JK. The microbiome and prostate cancer. Prostate Cancer Prostatic Dis. 2022;25(2):159-64.
161. Miyake M, Tatsumi Y, Ohnishi K, Fujii T, Nakai Y, Tanaka N, et al. Prostate diseases and microbiome in the prostate, gut, and urine. Prostate Int. 2022;10(2):96-107.
162. Hurst R, Meader E, Gihawi A, Rallapalli G, Clark J, Kay GL, et al. Microbiomes of Urine and the Prostate Are Linked to Human Prostate Cancer Risk Groups. Eur Urol Oncol. 2022;5(4):412-9.
163. Makarov VA, Tikhomirova NK, Savvateeva LV, Petushkova AI, Serebryakova MV, Baksheeva VE, et al. Novel applications of modification of thiol enzymes and redox-regulated proteins using S-methyl methanethiosulfonate (MMTS). Biochim Biophys Acta Proteins Proteom. 2019;1867(11):140259.
164. Wang X, Sun B, Wei L, Jian X, Shan K, He Q, et al. Cholesterol and saturated fatty acids synergistically promote the malignant progression of prostate cancer. Neoplasia. 2022;24(2):86-97.
165. Tang NT, R DS, Brown MD, Haines BA, Ridley A, Gardner P, et al. Fatty-Acid Uptake in Prostate Cancer Cells Using Dynamic Microfluidic Raman Technology. Molecules. 2020;25(7).
166. Agilent. Agilent Seahorse XFp Cell Mito Stress Test Kit - User Guide. 2019.
167. Agilent. Agilent Seahorse XFp Glycolysis Test Kit - User Guide. 2019.
168. Agilent. Agilent Seahorse XF Real-Time ATP Rate Assay Kit - User Guide. 2018.
169. Agilent. Agilent Seahorse XF Mito Fuel Flex Test Kit - User Guide. 2019.
170. Higdon JV, Delage B, Williams DE, Dashwood RH. Cruciferous vegetables and human cancer risk: epidemiologic evidence and mechanistic basis. Pharmacol Res. 2007;55(3):224-36.

171. Morrison MEW, Joseph JM, McCann SE, Tang L, Almohanna HM, Moysich KB. Cruciferous Vegetable Consumption and Stomach Cancer: A Case-Control Study. Nutr Cancer. 2020;72(1):52-61.
172. Wu QJ, Yang Y, Wang J, Han LH, Xiang YB. Cruciferous vegetable consumption and gastric cancer risk: a meta-analysis of epidemiological studies. Cancer Sci. 2013;104(8):1067-73.
173. Association AD. Postprandial blood glucose. American Diabetes Association. Diabetes Care. 2001;24(4):775-8.
174. Ohishi T, Abe H, Sakashita C, Saqib U, Baig MS, Ohba SI, et al. Inhibition of mitochondria ATP synthase suppresses prostate cancer growth through reduced insulin-like growth factor-1 secretion by prostate stromal cells. Int J Cancer. 2020;146(12):3474-84.
175. Gabriele E, Ricci C, Meneghetti F, Ferri N, Asai A, Sparatore A. Methanethiosulfonate derivatives as ligands of the STAT3-SH2 domain. J Enzyme Inhib Med Chem. 2017;32(1):337-44.
176. Bader DA, Hartig SM, Putluri V, Foley C, Hamilton MP, Smith EA, et al. Mitochondrial pyruvate import is a metabolic vulnerability in androgen receptor-driven prostate cancer. Nat Metab. 2019;1(1):70-85.
177. Patra S, Pradhan B, Nayak R, Behera C, Panda KC, Das S, et al. Apoptosis and autophagy modulating dietary phytochemicals in cancer therapeutics: Current evidences and future perspectives. Phytother Res. 2021;35(8):4194-214.
178. Hong M, Tao S, Zhang L, Diao LT, Huang X, Huang S, et al. RNA sequencing: new technologies and applications in cancer research. J Hematol Oncol. 2020;13(1):166.
179. Wang D, Wan X, Zhang Y, Kong Z, Lu Y, Sun X, et al. A novel androgen-reduced prostate-specific lncRNA, PSLNR, inhibits prostate-cancer progression in part by regulating the p53-dependent pathway. Prostate. 2019;79(12):1362-77.
180. Beaver LM, Löhr CV, Clarke JD, Glasser ST, Watson GW, Wong CP, et al. Broccoli Sprouts Delay Prostate Cancer Formation and Decrease Prostate Cancer Severity with a Concurrent Decrease in HDAC3 Protein Expression in Transgenic Adenocarcinoma of the Mouse Prostate (TRAMP) Mice. Curr Dev Nutr. 2018;2(3):nzy002.
181. Agyeman AS, Chaerkady R, Shaw PG, Davidson NE, Visvanathan K, Pandey A, et al. Transcriptomic and proteomic profiling of KEAP1 disrupted and sulforaphane-treated human breast epithelial cells reveals common expression profiles. Breast Cancer Res Treat. 2012;132(1):175-87.
182. Traka M, Gasper AV, Smith JA, Hawkey CJ, Bao Y, Mithen RF. Transcriptome analysis of human colon Caco-2 cells exposed to sulforaphane. J Nutr. 2005;135(8):1865-72.
183. Arcidiacono P, Ragonese F, Stabile A, Pistilli A, Kuligina E, Rende M, et al. Antitumor activity and expression profiles of genes induced by sulforaphane in human melanoma cells. Eur J Nutr. 2018;57(7):2547-69.
184. Li Y, Buckhaults P, Li S, Tollefsbol T. Temporal Efficacy of a Sulforaphane-Based Broccoli Sprout Diet in Prevention of Breast Cancer through Modulation of Epigenetic Mechanisms. Cancer Prev Res (Phila). 2018;11(8):451-64.
185. Livingstone TL. Accumulation of Sulphur-Containing Dietary Bioactives and the Impact on the Transcriptional Signature of the Prostate: Doctoral Thesis, University of East Anglia; 2022.
186. Sivapalan T. The bioavailability and biological activity of sulphur-containing compounds from broccoli: Doctoral Thesis, University of East Anglia; 2017.
187. Baumgart SJ, Nevedomskaya E, Haendler B. Dysregulated Transcriptional Control in Prostate Cancer. Int J Mol Sci. 2019;20(12).
188. Barbieri CE, Bangma CH, Bjartell A, Catto JW, Culig Z, Grönberg H, et al. The mutational landscape of prostate cancer. Eur Urol. 2013;64(4):567-76.

189. Poluri RTK, Audet-Walsh É. Genomic Deletion at 10q23 in Prostate Cancer: More Than PTEN Loss? Front Oncol. 2018;8:246.
190. Park S, Kim YS, Kim DY, So I, Jeon JH. PI3K pathway in prostate cancer: All resistant roads lead to PI3K. Biochim Biophys Acta Rev Cancer. 2018;1870(2):198-206.
191. Karala AR, Ruddock LW. Does s-methyl methanethiosulfonate trap the thiol-disulfide state of proteins? Antioxid Redox Signal. 2007;9(4):527-31.
192. Stancato LF, Hutchison KA, Chakraborti PK, Simons SS, Jr., Pratt WB. Differential effects of the reversible thiol-reactive agents arsenite and methyl methanethiosulfonate on steroid binding by the glucocorticoid receptor. Biochemistry. 1993;32(14):3729-36.
193. Mitchell AR, Yuan M, Morgan HP, McNae IW, Blackburn EA, Le Bihan T, et al. Redox regulation of pyruvate kinase M2 by cysteine oxidation and S-nitrosation. Biochem J. 2018;475(20):3275-91.
194. Pertea M, Kim D, Pertea GM, Leek JT, Salzberg SL. Transcript-level expression analysis of RNA-seq experiments with HISAT, StringTie and Ballgown. Nature Protocols. 2016;11(9):1650-67.
195. http://cis.nbi.ac.uk/. NBIsCIfSCAa.
196. Love MI, Huber W, Anders S. Moderated estimation of fold change and dispersion for RNA-seq data with DESeq2. Genome Biology. 2014;15(12):550.
197. Jolliffe IT, Cadima J. Principal component analysis: a review and recent developments. Philos Trans A Math Phys Eng Sci. 2016;374(2065):20150202.
198. Witten DM. Classification and clustering of sequencing data using a Poisson model. The Annals of Applied Statistics. 2011;5(4):2493-518, 26.
199. Plaisier SB, Taschereau R, Wong JA, Graeber TG. Rank-rank hypergeometric overlap: identification of statistically significant overlap between gene-expression signatures. Nucleic Acids Res. 2010;38(17):e169.
200. Subramanian A, Tamayo P, Mootha VK, Mukherjee S, Ebert BL, Gillette MA, et al. Gene set enrichment analysis: a knowledge-based approach for interpreting genome-wide expression profiles. Proc Natl Acad Sci U S A. 2005;102(43):15545-50.
201. Liberzon A, Birger C, Thorvaldsdóttir H, Ghandi M, Mesirov JP, Tamayo P. The Molecular Signatures Database (MSigDB) hallmark gene set collection. Cell Syst. 2015;1(6):417-25.
202. Townsend BE, Johnson RW. Sulforaphane induces Nrf2 target genes and attenuates inflammatory gene expression in microglia from brain of young adult and aged mice. Exp Gerontol. 2016;73:42-8.
203. Han J, Zhang L, Guo H, Wysham WZ, Roque DR, Willson AK, et al. Glucose promotes cell proliferation, glucose uptake and invasion in endometrial cancer cells via AMPK/mTOR/S6 and MAPK signaling. Gynecol Oncol. 2015;138(3):668-75.
204. Rahmoon MA, Elghaish RA, Ibrahim AA, Alaswad Z, Gad MZ, El-Khamisy SF, et al. High Glucose Increases DNA Damage and Elevates the Expression of Multiple DDR Genes. Genes. 2023;14(1):144.
205. Marei HE, Althani A, Afifi N, Hasan A, Caceci T, Pozzoli G, et al. p53 signaling in cancer progression and therapy. Cancer Cell International. 2021;21(1):703.
206. Lukin DJ, Carvajal LA, Liu WJ, Resnick-Silverman L, Manfredi JJ. p53 Promotes cell survival due to the reversibility of its cell-cycle checkpoints. Mol Cancer Res. 2015;13(1):16-28.
207. Villalobos-Hernandez A, Bobbala D, Kandhi R, Khan MGM, Mayhue M, Dubois CM, et al. SOCS1 inhibits migration and invasion of prostate cancer cells, attenuates tumor growth and modulates the tumor stroma. Prostate Cancer and Prostatic Diseases. 2017;20(1):36-47.

208. Olshavsky NA, Groh EM, Comstock CE, Morey LM, Wang Y, Revelo MP, et al. Cyclin D3 action in androgen receptor regulation and prostate cancer. Oncogene. 2008;27(22):3111-21.
209. Wang Q, Wu W, Gao Z, Li K, Peng S, Fan H, et al. GADD45B Is a Potential Diagnostic and Therapeutic Target Gene in Chemotherapy-Resistant Prostate Cancer. Front Cell Dev Biol. 2021;9:716501.
210. Singal R, Ramachandran K, Gopisetty G, Navarro L, Gordian E, Manoharan M. Role of GADD45α as a potential therapeutic target for prostate cancer. Journal of Clinical Oncology. 2007;25(18_suppl):10566-.
211. Loh CY, Arya A, Naema AF, Wong WF, Sethi G, Looi CY. Signal Transducer and Activator of Transcription (STATs) Proteins in Cancer and Inflammation: Functions and Therapeutic Implication. Front Oncol. 2019;9:48.
212. Lin J, Tang H, Jin X, Jia G, Hsieh JT. p53 regulates Stat3 phosphorylation and DNA binding activity in human prostate cancer cells expressing constitutively active Stat3. Oncogene. 2002;21(19):3082-8.
213. Whiteside TL. The tumor microenvironment and its role in promoting tumor growth. Oncogene. 2008;27(45):5904-12.
214. Cao Z, Kyprianou N. Mechanisms navigating the TGF-β pathway in prostate cancer. Asian J Urol. 2015;2(1):11-8.
215. Jones E, Pu H, Kyprianou N. Targeting TGF-beta in prostate cancer: therapeutic possibilities during tumor progression. Expert Opin Ther Targets. 2009;13(2):227-34.
216. Roberts AB, Tian F, Byfield SD, Stuelten C, Ooshima A, Saika S, et al. Smad3 is key to TGF-beta-mediated epithelial-to-mesenchymal transition, fibrosis, tumor suppression and metastasis. Cytokine Growth Factor Rev. 2006;17(1-2):19-27.
217. Guo Y, Kyprianou N. Overexpression of transforming growth factor (TGF) beta1 type II receptor restores TGF-beta1 sensitivity and signaling in human prostate cancer cells. Cell Growth Differ. 1998;9(2):185-93.
218. Massagué J, Blain SW, Lo RS. TGFbeta signaling in growth control, cancer, and heritable disorders. Cell. 2000;103(2):295-309.
219. Chen H, Zhu B, Zhao L, Liu Y, Zhao F, Feng J, et al. Allicin Inhibits Proliferation and Invasion in Vitro and in Vivo via SHP-1-Mediated STAT3 Signaling in Cholangiocarcinoma. Cell Physiol Biochem. 2018;47(2):641-53.
220. Berraondo P, Sanmamed MF, Ochoa MC, Etxeberria I, Aznar MA, Pérez-Gracia JL, et al. Cytokines in clinical cancer immunotherapy. Br J Cancer. 2019;120(1):6-15.
221. Doersch KM, Moses KA, Zimmer WE. Synergistic immunologic targets for the treatment of prostate cancer. Exp Biol Med (Maywood). 2016;241(17):1900-10.
222. Nobrega OT E-CW, Avelar GG, Tonet-Furioso AC, Perez DIV, Moraes CF Serum levels of interleukin-2 differ between prostate cancer and benign prostatic hyperplasia. J Bras Patol Med Lab. 2022;58.
223. Dieli F, Vermijlen D, Fulfaro F, Caccamo N, Meraviglia S, Cicero G, et al. Targeting human {gamma}delta} T cells with zoledronate and interleukin-2 for immunotherapy of hormone-refractory prostate cancer. Cancer Res. 2007;67(15):7450-7.
224. Schäfer G, Kaschula CH. The immunomodulation and anti-inflammatory effects of garlic organosulfur compounds in cancer chemoprevention. Anticancer Agents Med Chem. 2014;14(2):233-40.
225. Freitas M, Baldeiras I, Proença T, Alves V, Mota-Pinto A, Sarmento-Ribeiro A. Oxidative stress adaptation in aggressive prostate cancer may be counteracted by the reduction of glutathione reductase. FEBS Open Bio. 2012;2:119-28.

226. Kumar B, Koul S, Khandrika L, Meacham RB, Koul HK. Oxidative stress is inherent in prostate cancer cells and is required for aggressive phenotype. Cancer Res. 2008;68(6):1777-85.
227. Sun J, Zhou C, Ma Q, Chen W, Atyah M, Yin Y, et al. High GCLC level in tumor tissues is associated with poor prognosis of hepatocellular carcinoma after curative resection. J Cancer. 2019;10(15):3333-43.
228. Traverso N, Ricciarelli R, Nitti M, Marengo B, Furfaro AL, Pronzato MA, et al. Role of glutathione in cancer progression and chemoresistance. Oxid Med Cell Longev. 2013;2013:972913.
229. Zhang P, Singh A, Yegnasubramanian S, Esopi D, Kombairaju P, Bodas M, et al. Loss of Kelch-like ECH-associated protein 1 function in prostate cancer cells causes chemoresistance and radioresistance and promotes tumor growth. Mol Cancer Ther. 2010;9(2):336-46.
230. Thapa D, Meng P, Bedolla RG, Reddick RL, Kumar AP, Ghosh R. NQO1 suppresses NF-κB-p300 interaction to regulate inflammatory mediators associated with prostate tumorigenesis. Cancer Res. 2014;74(19):5644-55.
231. Traka M, Gasper AV, Melchini A, Bacon JR, Needs PW, Frost V, et al. Broccoli consumption interacts with GSTM1 to perturb oncogenic signalling pathways in the prostate. PLoS One. 2008;3(7):e2568.
232. Khan N, Adhami VM, Mukhtar H. Apoptosis by dietary agents for prevention and treatment of prostate cancer. Endocr Relat Cancer. 2010;17(1):R39-52.
233. Vrânceanu M, Galimberti D, Banc R, Dragoş O, Cozma-Petruţ A, Hegheş SC, et al. The Anticancer Potential of Plant-Derived Nutraceuticals via the Modulation of Gene Expression. Plants (Basel). 2022;11(19).
234. McKenzie S, Kyprianou N. Apoptosis evasion: the role of survival pathways in prostate cancer progression and therapeutic resistance. J Cell Biochem. 2006;97(1):18-32.
235. Wanner E, Thoppil H, Riabowol K. Senescence and Apoptosis: Architects of Mammalian Development. Front Cell Dev Biol. 2020;8:620089.
236. Shi XB, Xue L, Yang J, Ma AH, Zhao J, Xu M, et al. An androgen-regulated miRNA suppresses Bak1 expression and induces androgen-independent growth of prostate cancer cells. Proc Natl Acad Sci U S A. 2007;104(50):19983-8.
237. Alpern D, Gardeux V, Russeil J, Mangeat B, Meireles-Filho ACA, Breysse R, et al. BRB-seq: ultra-affordable high-throughput transcriptomics enabled by bulk RNA barcoding and sequencing. Genome Biology. 2019;20(1):71.
238. Resurreccion EP, Fong K-w. The Integration of Metabolomics with Other Omics: Insights into Understanding Prostate Cancer. Metabolites. 2022;12(6):488.
239. Gómez-Cebrián N, Rojas-Benedicto A, Albors-Vaquer A, López-Guerrero JA, Pineda-Lucena A, Puchades-Carrasco L. Metabolomics Contributions to the Discovery of Prostate Cancer Biomarkers. Metabolites. 2019;9(3):48.
240. Lodi A, Saha A, Lu X, Wang B, Sentandreu E, Collins M, et al. Combinatorial treatment with natural compounds in prostate cancer inhibits prostate tumor growth and leads to key modulations of cancer cell metabolism. NPJ Precis Oncol. 2017;1.
241. Kdadra M, Höckner S, Leung H, Kremer W, Schiffer E. Metabolomics Biomarkers of Prostate Cancer: A Systematic Review. Diagnostics. 2019;9(1):21.
242. Zhang A, Yan G, Han Y, Wang X. Metabolomics Approaches and Applications in Prostate Cancer Research. Appl Biochem Biotechnol. 2014;174(1):6-12.
243. Lima AR, Pinto J, Amaro F, Bastos ML, Carvalho M, Guedes de Pinho P. Advances and Perspectives in Prostate Cancer Biomarker Discovery in the Last 5 Years through Tissue and Urine Metabolomics. Metabolites. 2021;11(3).
244. Wang X, Liu H, Ni Y, Shen P, Han X. Lactate shuttle: from substance exchange to regulatory mechanism. Human Cell. 2022;35(1):1-14.

245. Trock BJ. Application of metabolomics to prostate cancer. Urol Oncol. 2011;29(5):572-81.
246. Guertin KA, Moore SC, Sampson JN, Huang WY, Xiao Q, Stolzenberg-Solomon RZ, et al. Metabolomics in nutritional epidemiology: identifying metabolites associated with diet and quantifying their potential to uncover diet-disease relations in populations. Am J Clin Nutr. 2014;100(1):208-17.
247. Huang J, Mondul AM, Weinstein SJ, Derkach A, Moore SC, Sampson JN, et al. Prospective serum metabolomic profiling of lethal prostate cancer. Int J Cancer. 2019;145(12):3231-43.
248. Huang J, Zhao B, Weinstein SJ, Albanes D, Mondul AM. Metabolomic profile of prostate cancer-specific survival among 1812 Finnish men. BMC Medicine. 2022;20(1):362.
249. Frolkis A, Knox C, Lim E, Jewison T, Law V, Hau DD, et al. SMPDB: The Small Molecule Pathway Database. Nucleic Acids Res. 2010;38(Database issue):D480-7.
250. Jewison T, Su Y, Disfany FM, Liang Y, Knox C, Maciejewski A, et al. SMPDB 2.0: big improvements to the Small Molecule Pathway Database. Nucleic Acids Res. 2014;42(Database issue):D478-84.
251. Perez-Moral N, Saha S, Pinto AM, Bajka BH, Edwards CH. In vitro protein bioaccessibility and human serum amino acid responses to white bread enriched with intact plant cells. Food Chem. 2023;404:134538.
252. Amelio I, Cutruzzolá F, Antonov A, Agostini M, Melino G. Serine and glycine metabolism in cancer. Trends Biochem Sci. 2014;39(4):191-8.
253. Schmidt DR, Patel R, Kirsch DG, Lewis CA, Vander Heiden MG, Locasale JW. Metabolomics in cancer research and emerging applications in clinical oncology. CA Cancer J Clin. 2021;71(4):333-58.
254. Hammoudi N, Ahmed KB, Garcia-Prieto C, Huang P. Metabolic alterations in cancer cells and therapeutic implications. Chin J Cancer. 2011;30(8):508-25.
255. Wishart D. Metabolomics and the Multi-Omics View of Cancer. Metabolites. 2022;12(2).
256. Armah CN, Traka MH, Dainty JR, Defernez M, Janssens A, Leung W, et al. A diet rich in high-glucoraphanin broccoli interacts with genotype to reduce discordance in plasma metabolite profiles by modulating mitochondrial function. Am J Clin Nutr. 2013;98(3):712-22.
257. Armah CN, Derdemezis C, Traka MH, Dainty JR, Doleman JF, Saha S, et al. Diet rich in high glucoraphanin broccoli reduces plasma LDL cholesterol: Evidence from randomised controlled trials. Mol Nutr Food Res. 2015;59(5):918-26.
258. Mamouni K, Kallifatidis G, Lokeshwar BL. Targeting Mitochondrial Metabolism in Prostate Cancer with Triterpenoids. Int J Mol Sci. 2021;22(5).
259. Butler M, van der Meer LT, van Leeuwen FN. Amino Acid Depletion Therapies: Starving Cancer Cells to Death. Trends Endocrinol Metab. 2021;32(6):367-81.
260. Wei Z, Liu X, Cheng C, Yu W, Yi P. Metabolism of Amino Acids in Cancer. Front Cell Dev Biol. 2020;8:603837.
261. Dereziński P, Klupczynska A, Sawicki W, Pałka JA, Kokot ZJ. Amino Acid Profiles of Serum and Urine in Search for Prostate Cancer Biomarkers: a Pilot Study. Int J Med Sci. 2017;14(1):1-12.
262. Wang Q, Bailey CG, Ng C, Tiffen J, Thoeng A, Minhas V, et al. Androgen receptor and nutrient signaling pathways coordinate the demand for increased amino acid transport during prostate cancer progression. Cancer Res. 2011;71(24):7525-36.
263. Aggarwal V, Tuli HS, Varol A, Thakral F, Yerer MB, Sak K, et al. Role of Reactive Oxygen Species in Cancer Progression: Molecular Mechanisms and Recent Advancements. Biomolecules. 2019;9(11).

264. Lieu EL, Nguyen T, Rhyne S, Kim J. Amino acids in cancer. Experimental & Molecular Medicine. 2020;52(1):15-30.
265. Koochekpour S. Glutamate, a metabolic biomarker of aggressiveness and a potential therapeutic target for prostate cancer. Asian J Androl. 2013;15(2):212-3.
266. Pan S, Fan M, Liu Z, Li X, Wang H. Serine, glycine and one-carbon metabolism in cancer (Review). Int J Oncol. 2021;58(2):158-70.
267. Ganini C, Amelio I, Bertolo R, Candi E, Cappello A, Cipriani C, et al. Serine and one-carbon metabolisms bring new therapeutic venues in prostate cancer. Discov Oncol. 2021;12(1):45.
268. Zhang X, Xia B, Zheng H, Ning J, Zhu Y, Shao X, et al. Identification of characteristic metabolic panels for different stages of prostate cancer by 1H NMR-based metabolomics analysis. Journal of Translational Medicine. 2022;20(1):275.
269. Akbari Z, Dijojin RT, Zamani Z, Hosseini RH, Arjmand M. Aromatic amino acids play a harmonizing role in prostate cancer: A metabolomics-based cross-sectional study. Int J Reprod Biomed. 2021;19(8):741-50.
270. Fu YM, Yu ZX, Li YQ, Ge X, Sanchez PJ, Fu X, et al. Specific amino acid dependency regulates invasiveness and viability of androgen-independent prostate cancer cells. Nutr Cancer. 2003;45(1):60-73.
271. Burdge GC. Metabolism of alpha-linolenic acid in humans. Prostaglandins Leukot Essent Fatty Acids. 2006;75(3):161-8.
272. Gann PH, Hennekens CH, Sacks FM, Grodstein F, Giovannucci EL, Stampfer MJ. Prospective study of plasma fatty acids and risk of prostate cancer. J Natl Cancer Inst. 1994;86(4):281-6.
273. Newcomer LM, King IB, Wicklund KG, Stanford JL. The association of fatty acids with prostate cancer risk. Prostate. 2001;47(4):262-8.
274. Azrad M, Zhang K, Vollmer RT, Madden J, Polascik TJ, Snyder DC, et al. Prostatic alpha-linolenic acid (ALA) is positively associated with aggressive prostate cancer: a relationship which may depend on genetic variation in ALA metabolism. PLoS One. 2012;7(12):e53104.
275. Chavarro JE, Stampfer MJ, Hall MN, Sesso HD, Ma J. A 22-y prospective study of fish intake in relation to prostate cancer incidence and mortality. Am J Clin Nutr. 2008;88(5):1297-303.
276. Crowe FL, Allen NE, Appleby PN, Overvad K, Aardestrup IV, Johnsen NF, et al. Fatty acid composition of plasma phospholipids and risk of prostate cancer in a case-control analysis nested within the European Prospective Investigation into Cancer and Nutrition. Am J Clin Nutr. 2008;88(5):1353-63.
277. Park SY, Wilkens LR, Henning SM, Le Marchand L, Gao K, Goodman MT, et al. Circulating fatty acids and prostate cancer risk in a nested case-control study: the Multiethnic Cohort. Cancer Causes Control. 2009;20(2):211-23.
278. Li J, Gu Z, Pan Y, Wang S, Chen H, Zhang H, et al. Dietary supplementation of α-linolenic acid induced conversion of n-3 LCPUFAs and reduced prostate cancer growth in a mouse model. Lipids in Health and Disease. 2017;16(1):136.
279. Weinstein SJ, Stolzenberg-Solomon R, Pietinen P, Taylor PR, Virtamo J, Albanes D. Dietary factors of one-carbon metabolism and prostate cancer risk. The American Journal of Clinical Nutrition. 2006;84(4):929-35.
280. Kasperzyk JL, Fall K, Mucci LA, Håkansson N, Wolk A, Johansson J-E, et al. One-carbon metabolism–related nutrients and prostate cancer survival. The American Journal of Clinical Nutrition. 2009;90(3):561-9.
281. Merigliano C, Mascolo E, Burla R, Saggio I, Vernì F. The Relationship Between Vitamin B6, Diabetes and Cancer. Front Genet. 2018;9:388.
282. Wu X, Daniels G, Lee P, Monaco ME. Lipid metabolism in prostate cancer. Am J Clin Exp Urol. 2014;2(2):111-20.

283. Watt MJ, Clark AK, Selth LA, Haynes VR, Lister N, Rebello R, et al. Suppressing fatty acid uptake has therapeutic effects in preclinical models of prostate cancer. Sci Transl Med. 2019;11(478).
284. Gertsman I, Barshop BA. Promises and pitfalls of untargeted metabolomics. J Inherit Metab Dis. 2018;41(3):355-66.
285. Saoi M, Britz-McKibbin P. New Advances in Tissue Metabolomics: A Review. Metabolites. 2021;11(10).
286. Lampe JW. Diet and Cancer Prevention Research: From Mechanism to Implementation. J Cancer Prev. 2020;25(2):65-9.
287. Higdon JV, Delage B, Williams DE, Dashwood RH. Cruciferous vegetables and human cancer risk: epidemiologic evidence and mechanistic basis. Pharmacol Res. 2007;55(3):224-36.
288. Miękus N, Marszałek K, Podlacha M, Iqbal A, Puchalski C, Świergiel AH. Health Benefits of Plant-Derived Sulfur Compounds, Glucosinolates, and Organosulfur Compounds. Molecules. 2020;25(17):3804.
289. Ramirez D, Abellán-Victorio A, Beretta V, Camargo A, Moreno DA. Functional Ingredients From Brassicaceae Species: Overview and Perspectives. International Journal of Molecular Sciences. 2020;21(6):1998.
290. Kurek M, Benaida-Debbache N, Elez Garofulić I, Galić K, Avallone S, Voilley A, et al. Antioxidants and Bioactive Compounds in Food: Critical Review of Issues and Prospects. Antioxidants. 2022;11(4):742.
291. Pokimica B, García-Conesa MT. Critical Evaluation of Gene Expression Changes in Human Tissues in Response to Supplementation with Dietary Bioactive Compounds: Moving Towards Better-Quality Studies. Nutrients. 2018;10(7).
292. Ahn-Jarvis JH, Parihar A, Doseff AI. Dietary Flavonoids for Immunoregulation and Cancer: Food Design for Targeting Disease. Antioxidants (Basel). 2019;8(7).
293. Lévesque S, Pol JG, Ferrere G, Galluzzi L, Zitvogel L, Kroemer G. Trial watch: dietary interventions for cancer therapy. Oncoimmunology. 2019;8(7):1591878.
294. Galanakis CM. Functionality of Food Components and Emerging Technologies. Foods. 2021;10(1).
295. Brul S, Schuren F, Montijn R, Keijser BJ, van der Spek H, Oomes SJ. The impact of functional genomics on microbiological food quality and safety. Int J Food Microbiol. 2006;112(3):195-9.
296. Esmaeili M, Ajami M, Barati M, Javanmardi F, Houshiarrad A, Mousavi Khaneghah A. The significance and potential of functional food ingredients for control appetite and food intake. Food Sci Nutr. 2022;10(5):1602-12.
297. Tkaczewska J, Kulawik P, Morawska-Tota M, Zając M, Guzik P, Tota Ł, et al. Protocol for Designing New Functional Food with the Addition of Food Industry By-Products, Using Design Thinking Techniques-A Case Study of a Snack with Antioxidant Properties for Physically Active People. Foods. 2021;10(4).
298. Brown L, Caligiuri SPB, Brown D, Pierce GN. Clinical trials using functional foods provide unique challenges. Journal of Functional Foods. 2018;45:233-8.
299. AbuMweis SS, Jew S, Jones PJ. Optimizing clinical trial design for assessing the efficacy of functional foods. Nutr Rev. 2010;68(8):485-99.
300. Lichtenstein AH, Petersen K, Barger K, Hansen KE, Anderson CAM, Baer DJ, et al. Perspective: Design and Conduct of Human Nutrition Randomized Controlled Trials. Adv Nutr. 2021;12(1):4-20.
301. Williamson G. The role of polyphenols in modern nutrition. Nutr Bull. 2017;42(3):226-35.
302. Kumar S, Pandey AK. Chemistry and biological activities of flavonoids: an overview. ScientificWorldJournal. 2013;2013:162750.

303. Aghajanpour M, Nazer MR, Obeidavi Z, Akbari M, Ezati P, Kor NM. Functional foods and their role in cancer prevention and health promotion: a comprehensive review. Am J Cancer Res. 2017;7(4):740-69.
304. Teibo JO, Ayinde, K.S., Olaoba, O.T., Adelusi, T.I., Teibo, T.K.A., Bamikunle, M.V., et al. . Functional foods' bioactive components and their chemoprevention mechanism in cervical, breast, and liver cancers: A systematic review. . Functional Foods in Health and Disease. 2021;11(11):559-85.
305. Cory H, Passarelli S, Szeto J, Tamez M, Mattei J. The Role of Polyphenols in Human Health and Food Systems: A Mini-Review. Front Nutr. 2018;5:87.
306. Swegarden H, Stelick A, Dando R, Griffiths PD. Bridging Sensory Evaluation and Consumer Research for Strategic Leafy Brassica (Brassica oleracea) Improvement. J Food Sci. 2019;84(12):3746-62.
307. Shapiro TA, Fahey JW, Dinkova-Kostova AT, Holtzclaw WD, Stephenson KK, Wade KL, et al. Safety, tolerance, and metabolism of broccoli sprout glucosinolates and isothiocyanates: a clinical phase I study. Nutr Cancer. 2006;55(1):53-62.
308. Hanschen FS, Kühn C, Nickel M, Rohn S, Dekker M. Leaching and degradation kinetics of glucosinolates during boiling of Brassica oleracea vegetables and the formation of their breakdown products. Food Chem. 2018;263:240-50.
309. Abukhabta S, Khalil Ghawi S, Karatzas KA, Charalampopoulos D, McDougall G, Allwood JW, et al. Sulforaphane-enriched extracts from glucoraphanin-rich broccoli exert antimicrobial activity against gut pathogens in vitro and innovative cooking methods increase in vivo intestinal delivery of sulforaphane. Eur J Nutr. 2021;60(3):1263-76.
310. Wang GC, Farnham M, Jeffery EH. Impact of thermal processing on sulforaphane yield from broccoli (Brassica oleracea L. ssp. italica). J Agric Food Chem. 2012;60(27):6743-8.
311. Vallejo F, Tomás-Barberán F, García-Viguera C. Glucosinolates and vitamin C content in edible parts of broccoli florets after domestic cooking. Eur Food Res Technol. 2002;215(4):310-6.
312. Butz P, Edenharder R, García AF, Fister H, Merkel C, Tauscher B. Changes in functional properties of vegetables induced by high pressure treatment. Food Res Int. 2002;35(2):295-300.
313. Frandsen HB, Markedal KE, Martin-Belloso O, Sanchez-Vega R, Soliva-Fortuny R, Sorensen H, et al. Effects of Novel Processing Techniques on Glucosinolates and Membrane Associated Myrosinases in Broccoli. Polish Journal of Food and Nutrition Sciences. 2014;64(1):17-25.
314. Floyd ZE, Ribnicky DM, Raskin I, Hsia DS, Rood JC, Gurley BJ. Designing a Clinical Study With Dietary Supplements: It's All in the Details. Frontiers in Nutrition. 2022;8.
315. Fahey JW, Zhang Y, Talalay P. Broccoli sprouts: an exceptionally rich source of inducers of enzymes that protect against chemical carcinogens. Proc Natl Acad Sci U S A. 1997;94(19):10367-72.
316. Ghawi SK, Methven L, Niranjan K. The potential to intensify sulforaphane formation in cooked broccoli (Brassica oleracea var. italica) using mustard seeds (Sinapis alba). Food Chem. 2013;138(2-3):1734-41.
317. Barba FJ, Nikmaram N, Roohinejad S, Khelfa A, Zhu Z, Koubaa M. Bioavailability of Glucosinolates and Their Breakdown Products: Impact of Processing. Frontiers in Nutrition. 2016;3.
318. Ilahy R, Tlili I, Pék Z, Montefusco A, Siddiqui MW, Homa F, et al. Pre- and Post-harvest Factors Affecting Glucosinolate Content in Broccoli. Front Nutr. 2020;7:147.
319. Weaver CM, Miller JW. Challenges in conducting clinical nutrition research. Nutr Rev. 2017;75(7):491-9.

320. Welch RW, Antoine JM, Berta JL, Bub A, de Vries J, Guarner F, et al. Guidelines for the design, conduct and reporting of human intervention studies to evaluate the health benefits of foods. Br J Nutr. 2011;106 Suppl 2:S3-15.
321. Pallmann P, Bedding AW, Choodari-Oskooei B, Dimairo M, Flight L, Hampson LV, et al. Adaptive designs in clinical trials: why use them, and how to run and report them. BMC Medicine. 2018;16(1):29.
322. Lichtenstein AH, Petersen K, Barger K, Hansen KE, Anderson CAM, Baer DJ, et al. Perspective: Design and Conduct of Human Nutrition Randomized Controlled Trials. Advances in Nutrition. 2020;12(1):4-20.
323. Nair B. Clinical Trial Designs. Indian Dermatol Online J. 2019;10(2):193-201.
324. Weaver CM, Hodges JK. Designing, Conducting, and Documenting Human Nutrition Plant-Derived Intervention Trials. Front Nutr. 2021;8:782703.
325. Grady C, Eckstein L, Berkman B, Brock D, Cook-Deegan R, Fullerton SM, et al. Broad Consent for Research With Biological Samples: Workshop Conclusions. Am J Bioeth. 2015;15(9):34-42.
326. Redrup MJ, Igarashi H, Schaefgen J, Lin J, Geisler L, Ben M'Barek M, et al. Sample Management: Recommendation for Best Practices and Harmonization from the Global Bioanalysis Consortium Harmonization Team. Aaps j. 2016;18(2):290-3.
327. Edwards P. Questionnaires in clinical trials: guidelines for optimal design and administration. Trials. 2010;11(1):2.
328. Kushi LH, Doyle C, McCullough M, Rock CL, Demark-Wahnefried W, Bandera EV, et al. American Cancer Society Guidelines on nutrition and physical activity for cancer prevention: reducing the risk of cancer with healthy food choices and physical activity. CA Cancer J Clin. 2012;62(1):30-67.
329. Kerschbaum E, Nüssler V. Cancer Prevention with Nutrition and Lifestyle. Visc Med. 2019;35(4):204-9.
330. Wang L, Lu B, He M, Wang Y, Wang Z, Du L. Prostate Cancer Incidence and Mortality: Global Status and Temporal Trends in 89 Countries From 2000 to 2019. Frontiers in Public Health. 2022;10.
331. Hagmann S, Ramakrishnan V, Tamalunas A, Hofmann M, Vandenhirtz M, Vollmer S, et al. Two Decades of Active Surveillance for Prostate Cancer in a Single-Center Cohort: Favorable Outcomes after Transurethral Resection of the Prostate. Cancers (Basel). 2022;14(2).
332. Chen FZ, Zhao XK. Prostate cancer: current treatment and prevention strategies. Iran Red Crescent Med J. 2013;15(4):279-84.
333. Oh M, Kim SY, Park S, Kim KN, Kim SH. Phytochemicals in Chinese Chive (Allium tuberosum) Induce the Skeletal Muscle Cell Proliferation via PI3K/Akt/mTOR and Smad Pathways in C2C12 Cells. Int J Mol Sci. 2021;22(5).
334. Salehi B, Fokou PVT, Yamthe LRT, Tali BT, Adetunji CO, Rahavian A, et al. Phytochemicals in Prostate Cancer: From Bioactive Molecules to Upcoming Therapeutic Agents. Nutrients. 2019;11(7).
335. Rahman MA, Hannan MA, Dash R, Rahman MH, Islam R, Uddin MJ, et al. Phytochemicals as a Complement to Cancer Chemotherapy: Pharmacological Modulation of the Autophagy-Apoptosis Pathway. Front Pharmacol. 2021;12:639628.
336. Saranyutanon S, Deshmukh SK, Dasgupta S, Pai S, Singh S, Singh AP. Cellular and Molecular Progression of Prostate Cancer: Models for Basic and Preclinical Research. Cancers (Basel). 2020;12(9).
337. Avancès C, Georget V, Térouanne B, Orio F, Cussenot O, Mottet N, et al. Human prostatic cell line PNT1A, a useful tool for studying androgen receptor transcriptional activity and its differential subnuclear localization in the presence of androgens and antiandrogens. Mol Cell Endocrinol. 2001;184(1-2):13-24.

338. Bello D, Webber MM, Kleinman HK, Wartinger DD, Rhim JS. Androgen responsive adult human prostatic epithelial cell lines immortalized by human papillomavirus 18. Carcinogenesis. 1997;18(6):1215-23.
339. Horoszewicz JS, Leong SS, Kawinski E, Karr JP, Rosenthal H, Chu TM, et al. LNCaP model of human prostatic carcinoma. Cancer Res. 1983;43(4):1809-18.
340. Korenchuk S, Lehr JE, L MC, Lee YG, Whitney S, Vessella R, et al. VCaP, a cell-based model system of human prostate cancer. In Vivo. 2001;15(2):163-8.
341. Kaighn ME, Narayan KS, Ohnuki Y, Lechner JF, Jones LW. Establishment and characterization of a human prostatic carcinoma cell line (PC-3). Invest Urol. 1979;17(1):16-23.
342. Gingrich JR, Barrios RJ, Morton RA, Boyce BF, DeMayo FJ, Finegold MJ, et al. Metastatic prostate cancer in a transgenic mouse. Cancer Res. 1996;56(18):4096-102.
343. Klezovitch O, Chevillet J, Mirosevich J, Roberts RL, Matusik RJ, Vasioukhin V. Hepsin promotes prostate cancer progression and metastasis. Cancer Cell. 2004;6(2):185-95.
344. Hoehn W, Schroeder FH, Reimann JF, Joebsis AC, Hermanek P. Human prostatic adenocarcinoma: some characteristics of a serially transplantable line in nude mice (PC 82). Prostate. 1980;1(1):95-104.
345. Gao D, Vela I, Sboner A, Iaquinta PJ, Karthaus WR, Gopalan A, et al. Organoid cultures derived from patients with advanced prostate cancer. Cell. 2014;159(1):176-87.
346. Yada E, Wada S, Yoshida S, Sasada T. Use of patient-derived xenograft mouse models in cancer research and treatment. Future Sci OA. 2018;4(3):Fso271.
347. Zhou L, Zhang C, Zhang Y, Shi C. Application of Organoid Models in Prostate Cancer Research. Front Oncol. 2021;11:736431.
348. Kamps R, Brandão RD, Bosch BJ, Paulussen AD, Xanthoulea S, Blok MJ, et al. Next-Generation Sequencing in Oncology: Genetic Diagnosis, Risk Prediction and Cancer Classification. Int J Mol Sci. 2017;18(2).
349. Ho E, Beaver LM, Williams DE, Dashwood RH. Dietary Factors and Epigenetic Regulation for Prostate Cancer Prevention. Advances in Nutrition. 2011;2(6):497-510.
350. Labbé DP, Zadra G, Ebot EM, Mucci LA, Kantoff PW, Loda M, et al. Role of diet in prostate cancer: the epigenetic link. Oncogene. 2015;34(36):4683-91.
351. Morita M, Kudo K, Shima H, Tanuma N. Dietary intervention as a therapeutic for cancer. Cancer Sci. 2021;112(2):498-504.
352. Gabriel D, Dvir T, Kohane DS. Delivering bioactive molecules as instructive cues to engineered tissues. Expert Opin Drug Deliv. 2012;9(4):473-92.
353. Calcabrini C, Maffei F, Turrini E, Fimognari C. Sulforaphane Potentiates Anticancer Effects of Doxorubicin and Cisplatin and Mitigates Their Toxic Effects. Front Pharmacol. 2020;11:567.
354. Saavedra-Leos MZ, Jordan-Alejandre E, Puente-Rivera J, Silva-Cázares MB. Molecular Pathways Related to Sulforaphane as Adjuvant Treatment: A Nanomedicine Perspective in Breast Cancer. Medicina (Kaunas). 2022;58(10).
355. Yari Z, Behrouz V, Zand H, Pourvali K. New Insight into Diabetes Management: From Glycemic Index to Dietary Insulin Index. Curr Diabetes Rev. 2020;16(4):293-300.
356. Khan RMM, Chua ZJY, Tan JC, Yang Y, Liao Z, Zhao Y. From Pre-Diabetes to Diabetes: Diagnosis, Treatments and Translational Research. Medicina (Kaunas). 2019;55(9).